LÉKAŘSKÁ FAKULTA MASARYKOVY UNIVERZITY
V BRNĚ

Trojrozměrné rentgenové zobrazovací metody v podpoře katétrových ablací srdečních arytmií

(SOUBOR PUBLIKACÍ)

MUDr. Zdeněk Stárek, Ph.D.

HABILITAČNÍ PRÁCE

BRNO 2020

Pokládám za milou povinnost poděkovat

Svým učitelům:

prof. MUDr. Karlovi Zemanovi, doc. MUDr. Josefovi Šumberovi, CSc. a **doc. MUDr. Miroslavovi Novákovi, Ph.D.** za uvedení do srdeční elektrofyziologie, odborné podněty, cenné rady a velkou trpělivost při konzultacích

přednostům I. Interní kardio-angiologické kliniky:

prof. MUDr. Miloši Štejfovi, DrSc, prof. MUDr. Jiřímu Tomanovi, CSc, prof. MUDr. Jiřímu Vítovcovi, CSc a **prof. MUDr. Lence Špinarové, Ph.D.** za vytváření prostředí pro vědeckou práci

svým kolegům:

MUDr. Františkovi Leharovi, Ph.D., MUDr. Jiřímu Ježovi, Ph.D., MUDr. Martinovi Pešlovi, Ph.D. a Ing. Jiřímu Wolfovi a **celému týmu biomedicínských inženýrů elektrofyziologické skupiny** za pomoc při vyšetřování nemocných a při zpracování získaných dat

OBSAH

1 KOMENTÁŘ

1.1 Úvod

Katétrová ablace srdečních arytmií je zavedená metoda kurativní léčby těchto onemocnění. Katétrová ablace má výrazně vyšší úspěšnost než léčba farmakologická a není zatížena řadou komplikací a vedlejších účinků související s podáváním antiarytmické a antikoagulační léčby. Úspěšnost této metody je významně závislá na orientaci v srdečních dutinách, které jsou anatomicky komplikované, a navíc interindividuálně vysoce variabilní. Vzhledem k intervenčnímu charakteru těchto výkonů je nefarmakologická terapie spojena s řadou specifických komplikací, a to zejména u katétrových ablací komplexních síňových a komorových arytmií. Jen namátkou zmíním perforaci stěny srdeční s následnou tamponádou srdeční či atrioventrikulární blokádu vyššího stupně. Těsný vztah zadní stěny levé síně a jícnu může vést ke vzniku ojedinělé, nicméně většinou fatální, atrioesofageální píštěle. Pro zlepšení orientace při katétrových ablacích je klíčové trojrozměrné (3D) zobrazení srdce pomocí různých zobrazovacích metod a užití těchto 3D modelů pro zvýšení účinnosti a bezpečnosti katétrových ablací. Na našem pracovišti standardně používáme komputerovou tomografii (CT) srdce a 3D rotační angiografii (3DRA) levé síně a jícnu v podpoře katétrových ablací arytmií a v uplynulých letech jsme publikovali řadu prací týkajících se použití těchto metod v různých aspektech katétrových ablací arytmií.

1.2 Cíle

Habilitační práce je komentářem souboru publikací, obsahujících problematiku podpory katétrových ablací komplexních síňových a komorových arytmií 3D rentgenovými zobrazovacími metodami, kde je uchazeč prvním autorem nebo spoluautorem. Práce jsou seřazeny do 5 kapitol podle cílů.

<u>Cíl 1</u>. Zjistit variabilitu anatomie síní srdečních a detailní anatomickou souvislost levé síně a jícnu.

<u>Cíl 2</u>. Zjistit efektivitu použití periprocedurálního 3D zobrazení levé síně a jícnu pomocí 3DRA těchto struktur při katétrové ablaci fibrilace síní.

<u>Cíl 3</u>. Zjistit radiační zátěž při zobrazení levé síně pomocí 3DRA a srovnat s jinými metodami.

Cíl 4. Zjistit efektivitu použití periprocedurálního 3D zobrazení pravé a levé komory srdeční pomocí 3DRA těchto struktur při katétrové ablaci komorových arytmií.

Cíl 5. Zjistit variabilitu polohy (mobilitu) jícnu vůči levé síni pomocí komputerové tomografie srdce a 3D zobrazení levé síně a jícnu pomocí 3DRA u pacientů podstupujících katétrovou ablaci fibrilace síní.

1.3 Metody

Cíl 1. Tohoto cíle se týkají dvě práce - retrospektivní vyhodnocení polohy jícnu vůči levé síni u 293 pacientů podstupujících katétrovou ablaci fibrilace síní s podporou 3DRA levé síně a jícnu a detailní analýza variability levé síně a jícnu z CT vyšetření hrudníku u 56 pacientů podstupujících katétrovou ablaci fibrilace síní s podporou CT srdce.

Cíl 2. Tohoto cíle se týkají tři originální práce – retrospektivní srovnání různých akvizičních protokolů 3DRA levé síně a jícnu u 547 konsekutivních pacientů podstupujících katétrovou ablaci fibrilace síní, prospektivní srovnání kvality 3D modelů levé síně získaných z 3DRA a CT levé síně u 65 pacientů podstupujících katétrovou ablaci fibrilace síní vyšetřených oběma modalitami a retrospektivní klinické srovnání účinnosti katétrové ablace fibrilace síní navigované s podporou buď 3DRA levé síně nebo CT levé síně u 125 pacientů podstupující katétrovou ablaci fibrilace síní.

Cíl 3. Retrospektivní srovnání radiační zátěže vyšetření CT srdce a 3DRA levé síně u 157 pacientů podstupujících katétrovou ablaci fibrilace síní vyšetřených pomocí 3DRA a/nebo CT srdce.

Cíl 4. Tohoto cíle se týkají dvě originální práce – retrospektivní vyhodnocení katétrové ablace 13 pacientů podstupujících katétrovou ablaci levokomorových arytmií s podporou 3DRA levé komory a retrospektivní vyhodnocení katétrových ablací arytmií z pravé i levé komory řešených s podporou 3DRA levé či pravé komory u 35 pacientů,

Cíl 5. Tohoto cíle se týkají dvě originální práce – prospektivní hodnocení dlouhodobé mobility jícnu vůči levé síni u 56 pacientů referovaných k ablaci fibrilace síní z preprocedurálně získaných CT dat a periprocedurálně získaných dat z 3DRA levé síně a jícnu a prospektivní hodnocení krátkodobé mobility jícnu během několikahodinové katétrové ablace u 33 pacientů podstupujících katétrovou ablaci fibrilace síní z opakovaných stanovení polohy jícnu pomocí 3DRA levé síně a jícnu a kontrastních esofagografií.

1.4 Výsledky

Cíl 1. Vyhodnocením velkého množství vyšetření analyzujících polohu jícnu vůči levé síni jsme zjistili, že poloha jícnu vůči levé síni je vysoce variabilní a nejčastěji se jícen vyskytuje za levou částí zadní stěny levé síně. Detailní analýza topografické anatomie levé síně a okolních struktur potvrdila, že nejčastější poloha jícnu je za levou částí zadní stěny levé síně a jícen je v těsném kontaktu s levou síní (tzn. oddělený méně jak 4 mm svaloviny bez vmezeřené tukové tkáně od dutiny levé síně) v horní části zadní stěny levé síně, a to na ploše cca 2/3 délky a 1/3 šířky zadní stěny levé síně.

Cíl 2. Vyhodnocení více jak 500 3DRA levé síně a jícnu jsme zjistili, že 3DRA levé síně je spolehlivá a bezpečná metoda, periprocedurální zobrazení jícnu je jednoduché a bezpečné a jako nejspolehlivější se jeví přímý levosíňový protokol. Prokázali jsme, že 3D modely levé síně vytvořené na podkladě 3DRA jsou srovnatelné s modely levé síně vytvořenými z CT dat a výsledky katétrové ablace fibrilace síní s podporou 3D modelů levé síně z CT dat a z 3DRA jsou srovnatelné.

Cíl 3. Srovnáním radiační zátěže pacientů podstupujících 3DRA levé síně a CT srdce jsme zjistili, že radiační zátěž při 3DRA je statisticky významně nižší než při CT srdce.

Cíl 4. Retrospektivním vyhodnocením soboru pacientů podstupujících katétrovou ablaci komorových arytmií s podporou 3DRA levé či pravé komory jsme zjistili, že použití 3D modelů levé či pravé komory vytvořené pomocí 3DRA je jednoduché a bezpečné a usnadňuje katétrovou ablaci komorových arytmií. Zároveň jsme ověřili, že nejvhodnější pro tyto účely je přímý levokomorový protokol.

Cíl 5. Prospektivním vyhodnocením rozdílu polohy jícnu před ablací (v řádech týdnů dle preprocedurálního zobrazení srdce a jícnu pomocí CT) a na počátku ablace (dle periprocedurálního zobrazení levé síně a jícnu pomocí 3DRA) jsme zjistili, že jícen je v horizontu několika týdnů velmi variabilní struktura a jeho preprocedurální zobrazení neodpovídá poloze jícnu na počátku ablace. Naopak krátkodobá mobilita jícnu v horizontu několika hodin trvajícího výkonu (verifikovaná vstupní 3DRA levé síně a jícnu a opakovanými kontrastními esofagografiemi během výkonu) je statisticky nevýznamná a zobrazení jícnu na počátku výkonu dostatečně spolehlivě určuje jeho polohu i během výkonu.

1.5 Závěr

Naše práce podpořily význam 3DRA srdce a CT srdce pro podporu katétrových ablací srdeční arytmií. Naše analýza topografické anatomie srdce a přiléhajících struktur přispěla ke znalostem o anatomii této oblasti. Analýzou velkého množství 3DRA srdečních síní i komor jsme ověřili nejvhodnější akviziční protokol pro jednotlivé srdeční oddíly. Ověřili jsme výrazně vyšší radiační zátěž CT srdce oproti 3DRA srdce. Ověřili jsme, že 3DRA srdečních komor je jednoduše a bezpečně proveditelná metoda použitelná v podpoře katétrových ablací komorových arytmií. Ověřili jsme, že dlouhodobá mobilita jícnu v horizontu několika týdnů před katétrovou ablací je významná a preprocedurální zobrazení jícnu tudíž nemá smysl. Naopak krátkodobá mobilita jícnu (změna polohy jícnu během několik hodin trvajícího výkonu) je nevýznamná a zobrazení jícnu na počátku výkonu umožní jeho lokalizaci během celého výkonu.

1.6 Klíčová slova

katétrová ablace srdečních arytmií; katétrová ablace fibrilace síní; katétrová ablace komorových arytmií; trojrozměrná rotační angiografie; komputerová tomografie; trojrozměrné zobrazení síní; trojrozměrné zobrazení komor; trojrozměrné zobrazení jícnu

2 COMMENTARY

2.1 Introduction

Catheter ablation of cardiac arrhythmias is an established method of curative treatment of these diseases. Catheter ablation has a significantly higher success rate than pharmacological treatment and is not burdened by a number of complications and side effects associated with the administration of antiarrhythmic and anticoagulant therapy. The success of this method is significantly dependent on the orientation in the heart cavities, which are anatomically complicated and, in addition, interindividually highly variable. Due to the interventional nature of these procedures, non-pharmacological therapy is associated with a number of specific complications, especially in catheter ablation of complex atrial and ventricular arrhythmias. As an example, I can mention the perforation of the heart wall with a subsequent cardiac tamponade or high-grade atrioventricular block. The close relationship between the posterior wall of the left atrium and the esophagus can lead to a rare, but mostly fatal, atrioesophageal fistula. To improve orientation during catheter ablations, three-dimensional (3D) imaging of the heart using various imaging methods and the use of these 3D models to increase the efficiency and safety of catheter ablations is key. At our workplace, we standardly use computed tomography (CT) of the heart and 3D rotational angiography (3DRA) of the left atrium and esophagus to support catheter ablation of arrhythmias, and in recent years we have published a number of papers on the use of these methods in various aspects of catheter ablation of arrhythmias.

2.2 Aims

The habilitation thesis is a commentary on a set of publications containing the issue of supporting catheter ablations of complex atrial and ventricular arrhythmias by 3D X-ray imaging methods, where the applicant is the first author or co-author. The works are organized into 5 chapters according to aims.

Aim 1. To determine the variability of the anatomy of the atria of the heart and the detailed anatomical connection of the left atrium and esophagus.

Aim 2. To determine the effectiveness of using periprocedural 3D imaging of the left atrium and esophagus using 3DRA of these structures in catheter ablation of atrial fibrillation.

Aim 3. To determine the radiation exposure when imaging the left atrium using 3DRA and compare with other methods.

Aim 4. To determine the effectiveness of using periprocedural 3D imaging of the right and left ventricles of the heart using 3DRA of these structures in catheter ablation of ventricular arrhythmias.

Aim 5. To determine the variability of the position (mobility) of the esophagus to the left atrium using computer tomography of the heart and 3D imaging of the left atrium and esophagus using 3DRA in patients undergoing catheter ablation of atrial fibrillation.

2.3 Methods

Aim 1. Two works are related to this aim – retrospective evaluation of the position of the esophagus relative to the left atrium in 293 patients undergoing catheter ablation of atrial fibrillation with 3DRA support of the left atrium and esophagus, and detailed analysis of left atrial and esophageal variability from CT examination of the chest in 56 patients undergoing catheter ablation of atrial fibrillation with support of the CT of the heart.

Aim 2. Three original works relate to this objective - a retrospective comparison of different left atrial and esophageal 3DRA acquisition protocols in 547 consecutive patients undergoing atrial fibrillation catheter ablation, a prospective comparison of 3D left atrial models obtained from 3DRA and left atrial CT in 65 patients undergoing catheter ablation of atrial fibrillation examined by both modalities and a retrospective clinical comparison of the efficacy of catheter ablation of atrial fibrillation navigated with support of either left atrial 3DRA or left atrial CT in 125 patients undergoing catheter ablation of atrial fibrillation.

Aim 3. Retrospective comparison of radiation exposure of CT of the heart and 3DRA of left atrium in 157 patients undergoing catheter ablation of atrial fibrillation examined with 3DRA and / or CT of the heart.

Aim 4. Two original works relate to this objective - retrospective evaluation of catheter ablation of 13 patients undergoing catheter ablation of left ventricular arrhythmias with left ventricular 3DRA support, and retrospective evaluation of catheter ablation of right and left ventricular arrhythmias treated with support of left or right ventricular 3DRA in 35 patients.

Aim 5. Two original works relate to this objective - prospective evaluation of long-term mobility of the esophagus towards the left atrium in 56 patients referred to ablation of atrial fibrillation from preprocedural CT data and data from periprocedural 3DRA of the left atrium and esophagus, and prospective evaluation of short-term mobility of the esophagus during several hours of catheter ablation in 33 patients undergoing catheter ablation of atrial fibrillation from repeated determination of position of the esophagus using 3DRA of left atrium and esophagus and contrast esophagography.

2.4 Results

Aim 1. By evaluating a large number of examinations analyzing the position of the esophagus relative to the left atrium, we found that the position of the esophagus relative to the left atrium is highly variable and the esophagus most often occurs behind the left posterior wall of the left atrium. A detailed analysis of the topographic anatomy of the left atrium and surrounding structures confirmed that the most common position of the esophagus is behind the left posterior wall of the left atrium and the esophagus is in close contact with the left atrium (i.e. separated by less than 4 mm atrium musculature without intervening fat pad on the left atrial cavity) in the upper part of the posterior wall of the left atrium on an area of approximately 2/3 of the length and 1/3 of the width of the posterior wall of the left atrium.

Aim 2. By evaluation of more than 500 3DRAs of the left atrium and esophagus, we found that 3DRA of the left atrium is a reliable and safe method, periprocedural esophageal imaging is simple and safe, and the direct left atrial protocol appears to be the most reliable. We have shown that 3D models of the left atrium created on the basis of 3DRA are comparable with models of the left atrium created from CT data and the results of catheter ablation of atrial fibrillation with support of 3D models of the left atrium from CT data and from 3DRA are comparable.

Aim 3. By comparing the radiation exposure of patients undergoing 3DRA of the left atria and CT of the heart, we found that the radiation exposure of 3DRA is statistically significantly lower than cardiac CT.

Aim 4. By retrospective evaluation of the group of patients undergoing catheter ablation of ventricular arrhythmias with support of 3DRA of left or right ventricle, we found that the use of 3D models of left or right ventricles created by 3DRA is simple and safe and facilitates catheter ablation of ventricular arrhythmias. At the same time, we verified that the direct left ventricular protocol is the most suitable for these purposes.

Aim 5. By prospective evaluation of the difference between the position of the esophagus before ablation (in weeks according to preprocedural imaging of the heart and esophagus by CT) and at the beginning of ablation (according to periprocedural imaging of the left atrium and esophagus by 3DRA) we found that the esophagus is very variable over several weeks and its preprocedural imaging does not correspond to its position at the beginning of ablation. In contrast, short-term esophageal mobility over several hours of procerude (verified initial 3DRA of the left atrium and esophagus and repeated contrast esophagographies during procedure) is statistically insignificant, and imaging of the esophagus at the beginning of procedure determines its position sufficiently reliably also during procedure.

2.5 Conclusion

Our works supported the importance of 3DRA of the heart and of cardiac CT for the support of catheter ablations of cardiac arrhythmias. Our analysis of the topographic anatomy of the heart and adjacent structures has contributed to the knowledge of the anatomy of this area. By analyzing a large number of 3DRA of atria and ventricles, we verified the most suitable acquisition protocol for individual compartments of the heart. We verified a significantly higher radiation exposure of the CT of the heart compared to the 3DRA of the heart. We have verified that 3DRA of ventricle is a simple and safe method to support catheter ablation of ventricular arrhythmias. We verified that the long-term mobility of the esophagus in the horizon of several weeks before catheter ablation is significant and therefore preprocedural imaging of the esophagus does not make sense. On the contrary, the short-term mobility of the esophagus (change of the position of the esophagus during several hours of the procedure) is insignificant and the display of the esophagus at the beginning of the procedure will allow its localization during the whole procedure.

2.6 Key words

catheter ablation of cardiac arrhythmias; catheter ablation of atrial fibrillation; catheter ablation of ventricular arrhythmias; three-dimensional rotational angiography; computer tomography; three-dimensional representation of the atria; three-dimensional imaging of the ventricles; three-dimensional imaging of the esophagus

3 ÚVOD A CÍLE

3.1 Farmakologická a nefarmakologická léčba srdečních arytmií

Srdeční arytmie jsou velmi častým onemocněním jak na úrovni České republiky, tak i na úrovni celosvětové. Jedná se o heterogenní, velmi širokou skupinu poruch rytmu, postihující pacienty všech věkových skupin (1), (2), (3). Může se jednat o arytmie primární, idiopatické, bez organického postižení srdce, či o velkou skupinu arytmií sekundárních, provázejících organické onemocnění srdce, jako je ischemická choroba srdeční, dilatační kardiomyopatie a řada dalších. Mnoho arytmií, zvláště ze skupiny idiopatických, je relativně benigních, ale velká část arytmií je prognosticky závažná a je jednou z příčin vysoké mortality a morbidity kardiovaskulárních chorob.

Co mají všechny arytmie společné, je jejich většinou nedostatečná a leckdy rozporuplná odpověď na farmakologickou terapii. Již od objevu účinku digitalisu počátkem 19. st. probíhá intenzivní výzkum a rozsáhlé klinické používání léků potlačujících arytmie, tzv. antiarytmik. Zlaté období antiarytmické farmakoterapie poruch srdečního rytmu byla druhá polovina 20. st., kdy s bouřlivým rozvojem chemie a chemického a farmaceutického průmyslu vzniklo obrovské množství nových molekul, z nichž řada byla použita jako antiarytmika. V 70. a 80. letech 20. století byla používána v léčbě nejen idiopatických, ale i sekundárních, substrátových, arytmií celá škála antiarytmik všech tříd dle Vaughana Williamse (4). Od počátku bylo zřejmé, že řada arytmií, zejména komplexních arytmií síňových a komorových, je k léčbě antiarytmiky více či méně rezistentní a úspěšnost této terapie je velmi nízká s vysokým rizikem recidiv. Například v léčbě fibrilace síní je dlouhodobá efektivita i nejúčinnějších antiarytmik jako je amiodaron pouze kolem 50% v závislosti na typu arytmie a přidružených onemocněních (5), (6). Další negativní stránkou užívání antiarytmik je nutnost dlouhodobého, resp. trvalého, doživotního, užívání léků. To je limitující zejména u mladých pacientů s perspektivou mnoha desetiletí užívání potenciálně nebezpečných a finančně nákladných léků. Nepříznivý dopad na dominantní postavení farmakoterapie měly i výsledky řady randomizovaných studií, zahájené studií CAST v 80. letech 20. století, sledující vliv antiarytmik na mortalitu pacientů se strukturálním onemocněním srdce a arytmiemi (7) (8). Původní předpoklad, že potlačení arytmií antiarytmiky povede ke zlepšení prognózy pacientů se nejen nepotvrdil, naopak se ukázalo, že pacienti léčení antiarytmiky měli výrazně horší prognózu, vyšší mortalitu i morbiditu, a to zejména na podkladě maligních arytmií indukovaných antiarytmickou terapií.

Od 90. let 20. st. se vývoj nových terapeutických postupů v léčbě arytmií orientoval jiným směrem. Jako nejnadějnější se jevila intervenční katétrová diagnostika a terapie arytmií, prováděná metodami a technikami srdeční elektrofyziologie. Tato metoda se v rámci rozvoje technologií koncem 20. st. začala bouřlivě rozvíjet a rychle se stala metodou volby u řady arytmií.

Prvopočátky srdeční elektrofyziologie spadají do devatenáctého a počátku dvacátého století, kdy byly publikovány takové převratné objevy jako první anatomický popis vodivé soustavy srdce (J.E.Purkyně, 1845), objev anatomických struktur spojujících síně a komory (Kent a His, 1893), objev sinoatriálního uzlu (Gaskel, 1900) či objev atrioventrikulárního uzlu (Aschoff, Tawara, 1906). S rozvojem snímání povrchových elektrokardiografických záznamů a jejich použití v diagnostice srdečních onemocnění došlo v druhé polovině 20. století k rozvoji klinické intrakardiální katétrové elektrofyziologie. Klíčovou událostí na tomto poli byla první úspěšná registrace potenciálu Hisova svazku u lidí (Sherlag, 1969 (9)). Zajímavostí je, že prvenství na tomto poli patří brněnskému kardiologovi prof. Vítkovi, který provedl tento výkon již v roce 1962 (dle svědectví pamětníků), bohužel vzhledem k tehdejší politické situaci se tomuto klíčovému objevu nedostalo náležité publicity. Druhá polovina 20. století se nese v duchu bouřlivého rozvoje diagnostických elektrofyziologických metod. Již v roce 1967 popsal Durrer možnost indukce arymií pomocí programované elektrické stimulace srdce (10). Další rozvoj diagnostiky srdečních arytmií pomocí programované elektrické stimulace srdce pomocí několika simultánně zavedených intrakardiálních elektrod (11) udělalo z elektrofyziologického vyšetření klinicky použitelnou rutinní diagnostickou metodu pomáhající při léčbě arytmií.

Nefarmakologické terapeutické možnosti v léčbě arytmií v 60. a 70. letech byly značně omezené a jedinou možností byla kardiochirurgická léčba. Nejčastějšími výkony bylo chirurgické přerušení AV uzlu (12), selektivní přerušení akcesorní dráhy (13) nebo excise zdroje fokální síňové tachykardie (14). První zkušenosti s katétrovým přerušením vedení AV uzlem výbojem jednosměrného elektrického proudu byly získány v roce 1981 náhodou při aplikaci standardního defibrilačního výboje do katétru zavedeného na AV uzel. Po testování této metody na animálním modelu (15) byla v roce 1982 publikována první série pacientů s farmakorezistentními supraventrikulárními tachykardiemi léčených touto metodou (16). Tato metoda byla používána i pro léčbu arytmií souvisejících s přídatnými drahami (17), (18).

Katétrová ablace výbojem stejnosměrného proudu byla zatížena řadou rizik a negativních vedlejších účinků. Výboj proudu o vysokém napětí byl obtížně kontrolovatelný a vedl k rozsáhlému poškození tkáně, což limitovalo běžné klinické použití této metody. Teprve použití radiofrekvenční energie při katétrové ablaci srdečních arytmií umožnil na přelomu 80. a 90. let raketový rozvoj katétrové ablace arytmií. Tento vývoj byl odstartován prvním úspěšným klinickým použitím radiofrekvenční energie při přerušení akcesorní dráhy dr. Borggrefem v roce 1987 (19). Radiofrekvenční ablace spočívá v aplikaci sinusoidálního vysokofrekvenčního elektrického proudu (500 – 750 Hz) na hrot ablačního katétru vytvářející ablační léze na podkladě termálního poškození myokardu. Princip je stejný jako u chirurgického kauteru. Radiofrekvenční energie umožňuje bezpečné vytvoření dobře ohraničených, dobře kontrolovatelných, přiměřeně velikých termálních ablačních lézí (20). Radiofrekvenční ablace se stala metodou volby pro většinu supraventrikulárních arytmií (21). V dalších letech došlo k dalším vylepšením, zvyšující účinnost a bezpečnost katétrových ablací, jako bylo zavedení teplotně řízené ablace (22), zavedení katétrů s prodlouženým či s chlazeným hrotem (23) (24), Velkou výhodou katétrové radiofrekvenční ablace je fakt, že je léčbou kauzální, s vysokou úspěšností, což zvláště vynikne ve srovnání s farmakologickou léčbou arytmií, která je zatížena řadou vedlejších účinků a proarytmogenním efektem při nedostatečné účinnosti. Nicméně ani radiofrekvenční ablace nemá 100% úspěšnost a je zatížena řadou specifických rizik související s tímto intervenčním katétrovým výkonem. Pro vytvoření dostatečně velké a hluboké, transmurální, nekrózy pomocí radiofrekvenční ablace je zapotřebí dosáhnout optimální rovnováhy mezi teplotou v místě kontaktu hrotu katétru s tkání (50 °C a více), množství dodané energie, plochou hrotu katétru, tlakem katétru na stěnu srdeční a mírou chlazení hrotu během ablace (prouděním krve a aktivním chlazením u katétrů s chlazeným proplachovaným hrotem) (20). Akutní radiofrekvenční koagulační nekróza je obklopena lemem reverzibilně poškozené tkáně s pouze přechodně vymizelými vodivými schopnostmi. V případě neadekvátně malých lézí vede hojení této oblasti k obnovení vedení v buňkách myokardu a k recidivám arytmií. Recidiva arytmie může dosáhnout dle typu arytmie od 5 až do 50% (25). Pokud naopak teplota na hrotu katétru dosáhne 100 °C, dojde k náhlé přeměně tekutin v plyn s následnou „explozí“ v této oblasti označované jako „pop“ fenomén. Následkem je mechanické poškození tkáně až s možností perforace stěny srdeční a tvorba příškvaru a koagula na hrotu katétru, což snižuje účinnost aplikace radiofrekvenční energie a zvyšuje riziko trombembolických komplikací (20), (26) Katétrové ablace arytmií jsou prováděny na elektrofyziogickém sále vybaveném speciálním vybavením nezbytným pro diagnostiku a následnou katétrovou ablaci arytmií. Diagnostické a ablační katétry jsou zaváděny perkutánně většinou cestou femorálních žil. Zavádění cestou v. subclavia či v. jugularis je dnes výjimečné. Katétry umístěné s srdečních dutinách umožňují snímání intrakardiálních potenciálů a stimulaci klíčových oblastí - pravá síň, oblast AV uzlu, pravá komora, koronární sinus (jeho poloha mezi levou síní a levou komorou umožňuje snímání záznamu z obou těchto dutin) (18), (20). V případě potřeby lze katétry zavést do levostranných srdečních dutin a to buď „antegrádně“ transseptální punkcí z pravé síně do levé síně a eventuelně až do levé komory nebo „retrográdně“ přes femorální tepnu, aortu a aortální chlopeň přímo do levé komory. Typickou sestavu katétrů zavedených do srce během elektrofyziologického vyšetření a katétrové ablace přídatné dráhy viz obr. 1. Poté, co je identifikován substrát arytmie, místo vzniku arytmie, aplikací energie pomocí ablačního katétru (většinou 7F katétr s hrotem o délce 4 mm) dojde k vytvoření nekrotické léze o hloubce 5-7 mm, což je dostačující pro řešení většiny síňových arytmií (20)

3.2 Katétrová ablace komplexních arytmií a trojrozměrné rentgenové zobrazovací metody

Katétrová ablace arytmií se nyní, na počátku 3. tisíciletí stala uznávanou metodou volby pro velkou část arytmií (27). Invazivní léčba arytmií pomocí katétrové radiofrekvenční ablace se stala nejúčinnější terapeutickou metodou u většiny supraventrikulárních arytmií (28). To bylo dáno relativní jednoduchostí výkonů v pravé síni, jejich velmi vysoké úspěšnosti a zároveň i bezpečnosti. V terapii arytmií jako je atrioventrikulární nodální reentry tachykardie, akcesorní dráhy či typický flutter síní je katétrová, radiofrekvenční ablace metodou první volby. Podobné postavení má dnes katétrová ablace i v léčbě idiopatických komorových arytmií z výtokového traktu levé a pravé komory (29). Rozvoj katétrových ablací v léčbě komorových arytmií při strukturálním onemocnění srdce následoval s jistým odstupem vzhledem ke komplexnímu charakteru těchto arytmií a obtížím plynoucím z těžko předvídatelného účinku ablační terapie na prevenci náhlé srdeční smrti (29).

V prvním desetiletí 21. století došlo k rychlému rozvoji katétrových ablací komplexních síňových arytmií, a to zejména fibrilace síní. Jistá prodleva v rozvoji nefarmakologické katétrové léčby komplexních síňových arytmií oproti jednodušším formám supraventrikulárních arytmií byla dána komplexním charakterem arytmie a složitou anatomickou strukturou intervenované oblasti – u fibrilace síní je to v prvé řadě levá síň. Nicméně v posledních deseti letech se vůbec nejčastěji ablovanou arytmií stala právě fibrilace síní, nejčastěji její paroxyzmální forma (27). V roce 2018 bylo pouze v České republice řešeno celkem 7464 pacientů s arytmiemi pomocí katétrové ablace. Ve 47,9% se jednalo o ablaci v levé síni pro fibrilaci síní, přičemž 66,7% tvořili pacienti s paroxyzmální fibrilací síní (Registr katetrizačních ablací pro arytmie, Česká republika, 2018).

Katétrová ablace fibrilace síní je založena na vytváření soustav cirkulárních a lineárních radiofrekvenčních ablačních lézí nejčastěji v levé síni modifikujících vznik a šíření vzruchu. Tyto léze jsou v drtivé většině případů vytvářeny bod po bodu vytvářením řady jednotlivých, navzájem se dotýkajících, ložiskových ablačních lézí, které ve svém souhrnu vytváří lézi lineární, resp. cirkulární. Tato strategie vede k náročným, dlouhotrvajícím výkonům, které jsou potenciálně nebezpečné a s vyšším rizikem komplikací než výkony „klasické“ (30). Přesto jsou tyto metody natolik efektivní, že vzhledem k nízké účinnosti farmakologických terapeutických metod a s nimi spojenými riziky začala být katetrizační ablace doporučována u určitých skupin pacientů jako metoda první volby (31). Katétrová ablace fibrilace síní má významně vyšší účinnost v udržení sinusového rytmu (32) a vede jednoznačně ke zlepšení kvality života u pacientů s fibrilací síní léčených katetrizační ablací ve srovnání s farmakoterapií (33), (34). Některé práce prokázaly i snížení mortality a morbidity (33), nicméně poslední studie prokázaly pouze trend ke snížení mortality a morbidity pacientů léčených katétrovou ablací (32).

Rozhodujícím faktorem jak z hlediska úspěšnosti výkonu, tak i s ohledem na riziko komplikací je orientace v srdečních dutinách během ablace. Již od prvních pionýrských dob srdeční elektrofyziologie byl hlavním, základním, a po dlouhou dobu taky jediným zobrazovacím systémem rentgenová skiaskopie. Katetrizující až do nedávné doby pracovali v přítmí katetrizačních sálů a jediným anatomickým vodítkem, umožňující prostorovou lokalizaci zavedených katétrů a tím i účinnost a bezpečnost výkonu byly stíny vyznačující srdeční kontury a stíny zavedených katétrů, viz obr. 1. Z těchto prostorových informací a z intrakardiálního EKG byl elektrofyziolog schopen určit polohu katétrů v srdci během ablace. Tento postup zůstával po desetiletí stejný a pro řadu supraventrikulárních arytmií jsou tyto informace zcela dostačující a zkušený elektrofyziolog je schopen s minimálními komplikacemi a vysokou úspěšností řešit arytmie jako je atrioventrikulární nodální reentry tachykardie, akcesorní dráhy či typický flutter síní.

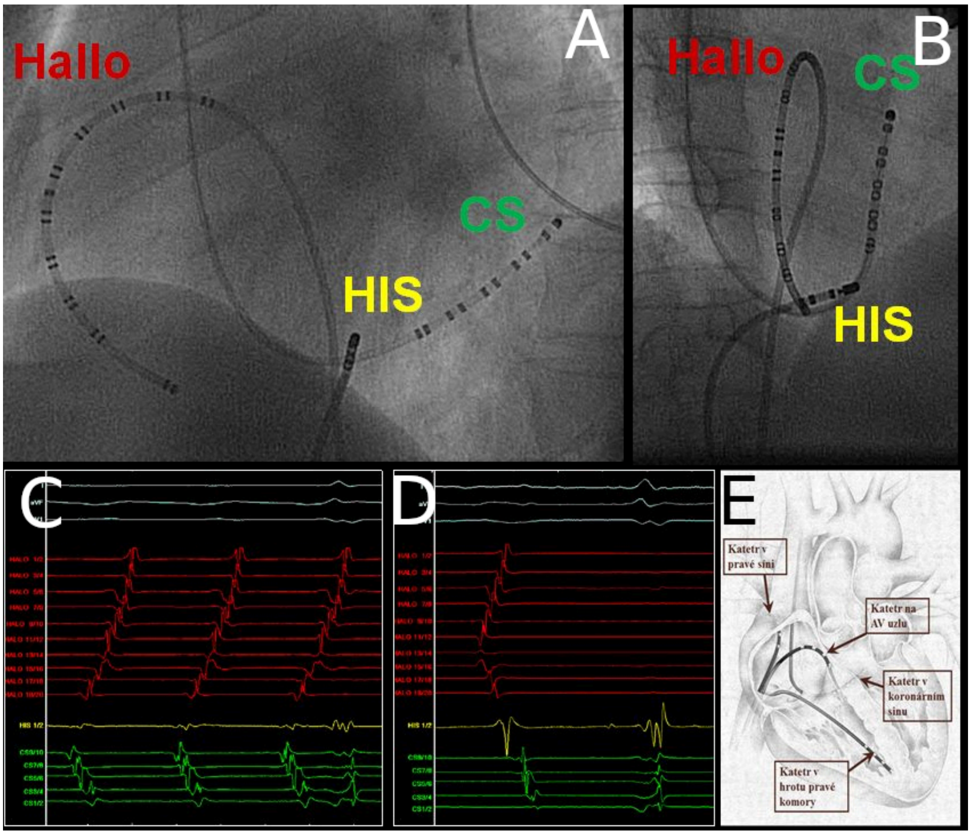

Obr. 1 Katétrová ablace za podpory skiaskopie a intrakardiálních elektrogramů. A, B - rentgenový skiaskopický obraz katétrů zavedených do srdečních síní. 20 polární „Halo“ katétr zavedený do pravé síně, 10 polární „CS“ katétr zavedený do koronárního sinu a mapovací/ablační katétr zavedený do oblasti atrioventrikulárního uzlu – „HIS“. A – levá šikmá projekce, B – pravá šikmá projekce. C, D – intrakardiální záznam srdeční aktivace u téhož pacienta při typickém flutteru síní (C) a při sinusovém rytmu (D). E – přehledný nákres katétrů zavedených do srdečních dutin.

U katétrových ablací komplexních arytmií je poněkud odlišná situace. Mapování a ablace v anatomicky složitých strukturách jako je levá síň a strategie vytváření komplikovaných systémů lineárních a cirkulárních lézí vede k výrazně vyšším nárokům na navigaci katétru a orientaci katetrizujícího lékaře. I tyto výkony lze provádět pouze za skiaskopické kontroly, celková délka takových výkonů a radiační zátěž je však značná a nároky na katetrizujícího lékaře jsou obrovské. Vývoj se ubíral cestou usnadnění navigace katétrů v srdečních dutinách pomocí 3D mapovacích elektroanatomických systémů (35). V současnosti se nejčastěji používají systém CARTO 3, Biosense Webster a systém EnSite Precision, Abbott. Tyto systémy dokážou lokalizovat polohu katétrů v srdečních dutinách a vytvářet trojrozměrné nonfluoroskopické mapy srdečních dutin. Trojrozměrné modely srdečních dutin jsou vytvářeny offline postupně mapováním dutiny srdeční mapovacím katétrem. Do takto vytvořených anatomických modelů (model zobrazující pouze anatomii srdeční dutiny bez dalších informací) mohou být zaznačeny i informace o šíření vzruchu (aktivační mapa znázorňující mechanizmus arytmie) nebo údaje o amplitudě lokálních potenciálů (voltážová mapa znázorňující změny ve voltáži myokardu názorně ukazující např. jizvu po infarktu myokardu). Stejně mohou být zaznamenána i místa aplikace radiofrekvenční energie při ablaci, místa pozdních či frakcionovaných potenciálů a tím zjednodušit a usnadnit ablační výkon. Příklad 3D modelů srdečních síní a komor viz obr. 2.

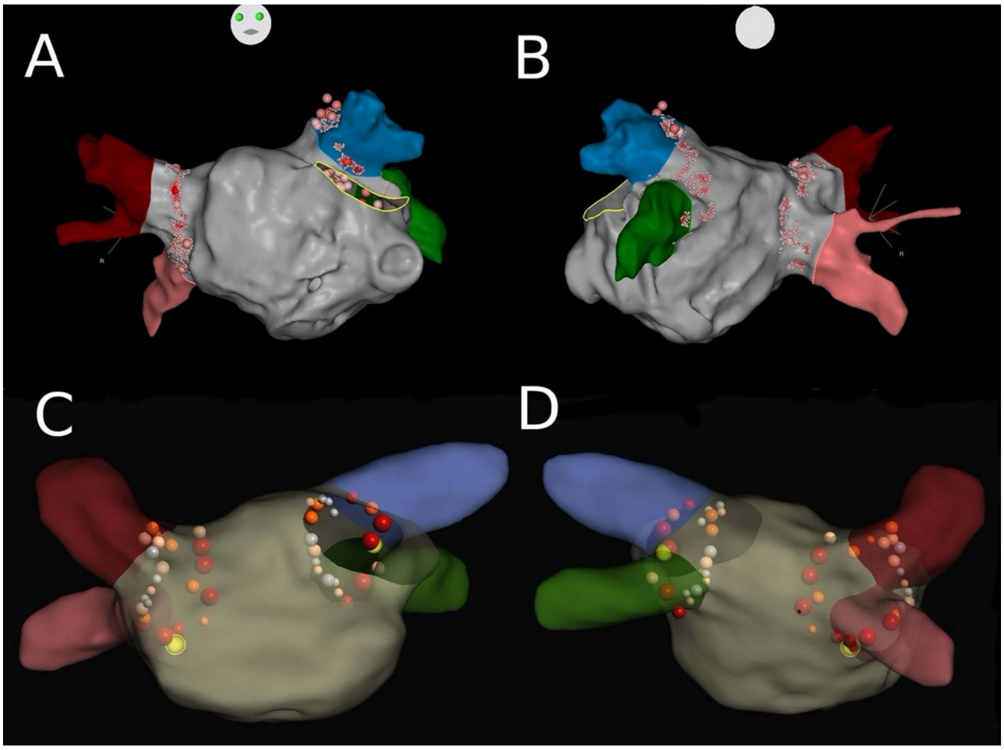

Obr. 2 Trojrozměrná elektroanatomická mapa levé síně při katétrové ablaci fibrilace síní. A, B - mapa vytvořená systémem CARTO. Jednotlivé plicní žíly jsou barevně zvýrazněny – modrá levá horní plicní žíla, zelená levá dolní plicní žíla, hnědá pravá horní plicní žíla, růžová pravá dolní plicní žíla. Ouško zvýrazněné žlutě není pro větší přehlednost zobrazeno (žlutá linie před levostrannými plicními žilami). Body v odstínech

růžové až červené jsou znázorněny jednotlivé ablace vytvářející cirkulární ablační léze kolem levostranných a pravostranných plicních žil. C a D - mapa vytvořená systémem EnSite Precision. Barevné kódování plicních žil je stejné, ouško levé síně není pro větší přehlednost zobrazeno, body v odstínech bílé až červené znázorňují jednotlivé ablace vytvářející cirkulární ablační léze kolem levostranných a pravostranných plicních žil. Obě mapy jsou znázorněny ve stejných projekcích – obr. A a C je pohled zepředu (předozadní projekce), obr. C a D je pohled zezadu (zadopřední projekce).

I když 3D elektroanatomické mapovací systémy urychlily a zjednodušily katétrovou ablaci komplexních arytmií, zůstaly tyto výkony mezi těmi nejsložitějšími v kardiologii. Už samotné vytváření 3D elektroanatomické mapy levé síně je potenciálně rizikové vzhledem ke značné variabilitě anatomie levé síně (36), (37). Počet plicních žil může kolísat, jejich velikost, úhel odstupu a větvení je velmi variabilní, stejně jako velikost ouška levé síně a jeho napojení na síň. Vzhledem k riziku poškození síně s možností vzniku perikardiálního výpotku až s obrazem srdeční tamponády je znalost anatomie srdeční dutiny, zejména levé síně, klíčová pro bezpečnost výkonu. Riziko poškození síně může být minimalizováno a celý výkon může být urychlen a zjednodušen použitím trojrozměrných preprocedurálně získaných modelů srdce, které nás objektivně informují o skutečné anatomii. Podobný přínos má zobrazení srdečních komor před a při ablaci, kde kromě čistě anatomických informací můžeme použít i zobrazení jizev a dalších patologií komorového myokardu.

3.3 Počítačová tomografie srdce v podpoře katétrových ablací srdečních arytmií

Nejčastěji používaným systémem pro zobrazení srdce před samotným ablačním výkonem je počítačová tomografie (CT). Dnes se již standardně užívá angio CT vyšetření srdce pomocí multidetektorového CT (multi-detector computed tomography - MDCT). Počítačový tomograf byl vynalezen sirem Godfrey Hounsfieldem a doktorem Allanem Cormackem v roce 1972 (38), (39). CT přístroj vytváří 2D řezy skenovanou tkání a z velkého počtu takových řezů je přístroj schopen vytvořit 3D rekonstrukci dané oblasti. Ačkoli počítačová tomografie dosáhla velkých úspěchů v zobrazení statických struktur jako je mozek či břišní orgány, zobrazení srdce bylo obtížnější. První přístroje nebyly pro zobrazení srdečních struktur vhodné pro malé časové a prostorové rozlišení a pohybové artefakty dané kontrakcemi srdečních dutin. Tyto problémy byly postupně vyřešeny. Zejména došlo ke zvýšení počtu řad detektorů z původních 2 až na dnes běžných 64-128 (40). Pohybové artefakty byly výrazně omezeny zvýšením rychlosti rotace prstence se soustavou detektorů a rentgenky (gantry) a zavedením časového gatování/trigeringu (rekonstrukce obrazu srdce ze scanů vždy z jedné fáze srdečního cyklu) (41).

Takto vylepšené CT přístroje byly od počátku 3. tisíciletí používány i v kardiologii. Jedním z důležitých použití bylo vyšetřování koronárních tepen (42). MDCT umožňuje také detailní zhodnocení srdečních dutin, myokardu i perikardu. Pomocí této metody jsme schopni velmi přesně a objektivně posuzovat myokard a funkci srdečních komor (43). Stejně tak se dá posuzovat i morfologie chlopní (44), vrozené srdeční vady (45), či postižení perikardu (46).

CT zobrazení srdce je v dnešní době etablovaná zobrazovací metoda v kardiologii. Vzhledem k naprosto převažujícím endokardiálním ablacím srdečních arytmií jsou pro použití při katetrizačních ablacích důležité rekonstrukce srdečních dutin. Velmi kvalitní obrazy s vysokým prostorovým rozlišením získáváme preprocedurálně pomocí angio CT srdečních dutin. 3D obraz srdečních dutin je získáván pomocí multidetektorového CT přístroje po intravenózní aplikaci kontrastní látky. Pro omezení pohybových artefaktů je prováděno EKG spouštěným protokolem (přístroj snímkuje pouze v určité fázi srdečního cyklu). Výsledkem CT srdce je řada „řezů" tímto orgánem. Na jednotlivých řezech jsme schopni sledovat anatomii srdečních dutin a dalším softwarovým zpracováním, tzv. segmentací jsme schopni z velkého množství dvojrozměrných řezů vytvořit 3D modely srdečních dutin, nejčastěji levé síně. Tyto 3D modely pak mohou být použity k navigaci katétrové ablace např. při ablaci fibrilace síní. U srdečních komor s větší tloušťkou svaloviny jsme schopni detekovat i strukturální změny myokardu. Současné multidetektorové CT je schopno vytvářet obrazy s vysokým rozlišením, umožňující velmi přesnou anatomickou rekonstrukci levé komory včetně aortální chlopně, epikardiálního tuku a koronárních tepen (47). S pomocí zobrazení ztenčení stěny levé komory či detekce pozdního sycení myokardu kontrastní látkou (CT scan s odstupem 10 min. po aplikaci kontrastní látky) je přístroj schopen zobrazit patologické změny myokardu, poruchy perfúze myokardu a přítomnost fibrózy či jizvy (48). Metoda pozdního sycení bývá nejčastěji používána u arytmií při strukturálním onemocnění srdce (typicky ischemická choroba srdeční či dilatační kardiomyopatie), ale byla použita i pro diagnostiku strukturálních změn myokardu u jiných diagnóz, např. ke kvantifikaci fibrózy u pacientů s hypertrofickou obstrukční kardiomyopatií (49).

Obdobně jako u anatomických 3D modelů je systém schopen vytvořit 3D modely srdečních komor se strukturálními změnami myokardu (48), které jsou používány při navigaci ablací komorových arytmií. I když zlatým standardem pro diagnostiku strukturálních změn myokardu je magnetická rezonance srdce (50), (51), u skupiny pacientů podstupujících katétrovou ablaci komorových arytmií při strukturálním onemocnění srdce je CT srdce s pozdním sycením v řadě případů jedinou možností. Většina těchto pacientů má implantovaný kardioverter defibrilátor, jehož přítomnost výrazně zhoršuje kvalitu a použitelnost magnetické rezonance (52).

Segmentace 3D modelů srdečních dutin z 2D řezů může být provedena na pracovní stanici CT přístroje, nebo přímo na pracovní stanici angiolinky na elektrofyziologickém sále. Druhá možnost je výrazně operativnější a umožňuje pružnější zpracování, úpravu a použití takto získaných obrazů. Příklad segmentace 3D modelu levé síně vidíme na obrázku 3.

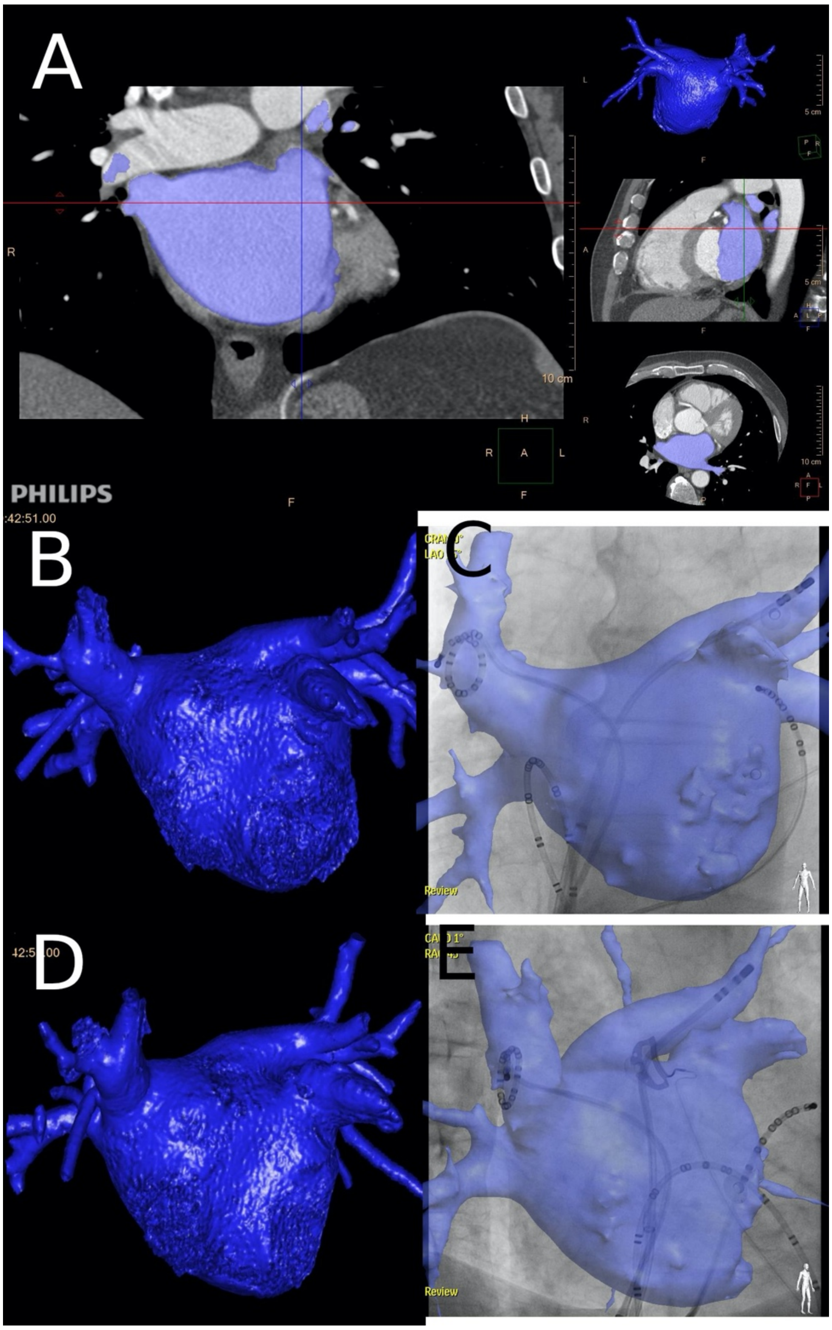

Obr. 3 Trojrozměrná rekonstrukce levé síně z angioCT dat. A – Segmentace 3D modelu na pracovní stanici CT přístroje. Vlevo frontální řez CT daty s modře zvýrazněnou dutinou levé síně a plicních žil, vpravo odshora výsledný 3D model levé síně v zadopřední projekci, sagitální řez a transverzální řez CT daty, v obou řezech je modře zvýrazněna levá síň a plicní žíly. B, D – výsledný rendrovaný 3D model levé síně, B předozadní projekce, D pravá šikmá projekce, C, E – 3D model levé síně fúzovaný s live skiaskopií, stejné projekce jako B a D, v 3D modelu levé síně vidíme Lasso katétr v pravé horní plicní žíle a ablační katétr v levé horní plicní žíle, katétr v koronárním sinu kopírující mitrání anulus a Halo katétr v pravé síni.

Jak napovídá způsob získávání těchto dat, je nutno provádět CT srdce preprocedurálně, na CT pracovišti několik hodin až několik dní před samotným elektrofyziologickým výkonem. Vhledem k sofistikovaným technologiím jsou CT rekonstrukce srdečních dutin velmi kvalitní s vysokým rozlišením a jsou standardně používána při katétrových ablacích zejména v levé síni.

Informace získané pomocí CT srdce se dají využít několika způsoby. Velmi přesné anatomické zobrazení levé síně a přiléhajících struktur (zejména jícnu) nám umožňuje kvantifikovat variabilitu této oblasti. Řada prací hodnotících anatomii levé síně většinou z CT dat prokázala, že velikost plicních žil je silně variabilní. Ukázalo se též, že standardní anatomie levé síně (dvě levostranné a dvě pravostranné plicní žíly) je spíše výjimkou. Levostranné plicní žíly mají zhruba ve 30% společné ústí, u pravostranných plicních žil byla zhruba u 30% pacientů zjištěna přítomnost přídatné, akcesorní, pravostranné plicní žíly (36), (37). Stejně jako variabilita anatomie plicních žil i poloha jícnu vůči zadní stěně levé síně je vysoce variabilní. Nejčastější poloha je ve střední části zadní stěny levé síně (31,9%), naopak nejméně často se jícen vyskytuje v oblasti pravostranných plicních žil (9,4%) (53). Stejně tak i charakter kontaktu zadní stěny levé síně s jícnem je vysoce variabilní a plocha bezprostředního kontaktu mezi zadní stěnou a jícnem se může velmi výrazně lišit (54), (53). Velmi úzká prostorová souvislost mezi jícnem a zadní stěnou levé síně vede k riziku poškození jícnu při ablaci se vznikem atrioesofageání píštěle (55). Její incidence je naštěstí velmi nízká (0,04% všech ablací pro fibrilaci síní) (30) nicméně mortalita dosahuje 70-80% (56) a je příčinou 16% úmrtí spojených s katétrovou ablací fibrilace síní (56). Variabilita plicních žil a jícnu viz obr. 4

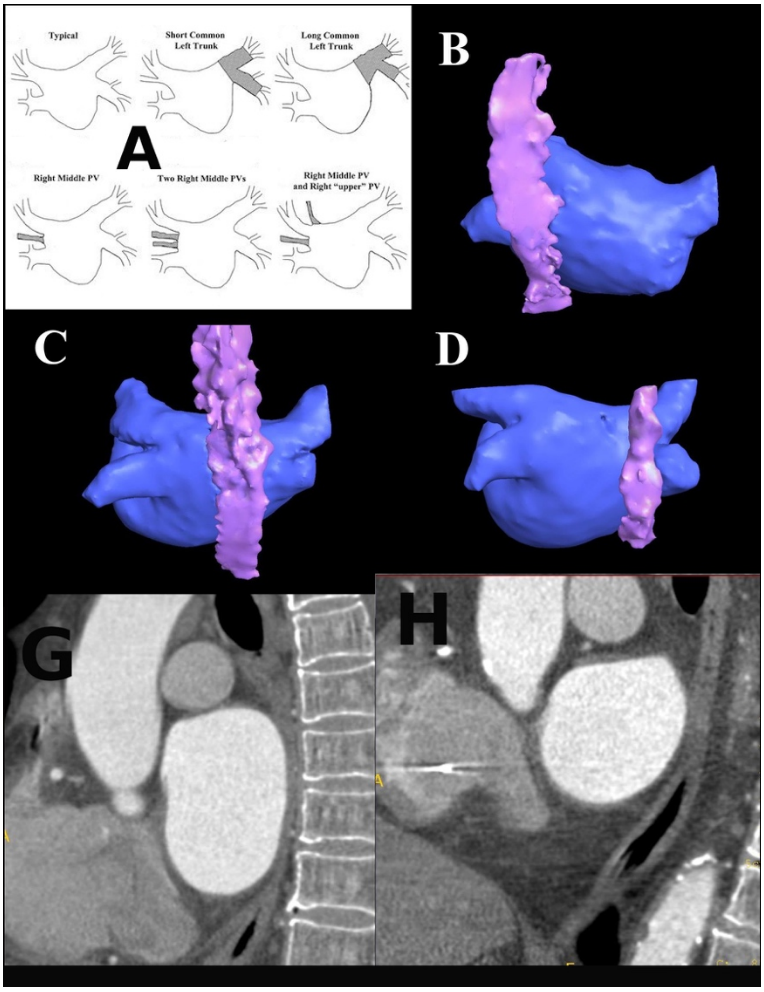

Obr. 4 Variabilita anatomie plicních žil a polohy jícnu vůči levé síni. A – nejčastější varianty anatomie levostranných a pravostranných plicních žil, viz popis. B, C, D – polohy jícnu vůči levé síni ve frontální rovině z 3D rotační angiografie levé síně a jícnu, extrémně levostranná poloha za levostrannými plicními žilami (B), střední poloha za zadní stěnou levé síně (C), extrémně pravostranná poloha za pravostrannými plicními žilami (D), zadopřední projekce. G, H - variabilita kontaktu zadní stěny levé síně a jícnu v sagitální rovině. G – maximální kontakt, kdy většina jícnu těsně naléhá na zadní stěnu levé síně. H – limitovaný kontakt, jícen těsně naléhá na zadní stěnu levé síně pouze v malé části zadní stěny, zbytek jícnu je od levé síně oddělen klínovitými oblastmi vmezeřené tukové tkáně.

Při katétrové ablaci fibrilace síní řada center standardně používá CT levé síně. Již pouhý pohled na segmentovanou levou síň nás informuje o anatomii levé síně a zejména zadní stěny a plicních žil. K optimálnímu periprocedurálnímu použití CT modelů srdečních dutin je potřeba určitá forma integrace 3D modelu a elektroanatomického mapovacího systému. Nejjednodušší metodou využití 3D rekonstrukcí srdce je synchronizované zobrazení 3D rekonstrukce a 3D elektroanatomické mapy, které je možno vidět na obr. 5. Na obrazovce elektroanatomického mapovacího systému vidíme vedle sebe oba modely s možností natočení do libovolné projekce, přičemž obě struktury se pohybují synchronně. Tím vidíme neustále ve shodné projekci skutečnou anatomii levé síně při vytváření anatomie virtuální. Zároveň se na vytvářenou mapu i na 3D rekonstrukci síně můžeme dívat z pohledu, který je v danou chvíli pro nás nejvýhodnější, nejpřehlednější. Tím se proces vytváření 3D elektroanatomické mapy urychluje a zjednodušuje a snižuje se riziko poškození stěny síně manipulací katétry.

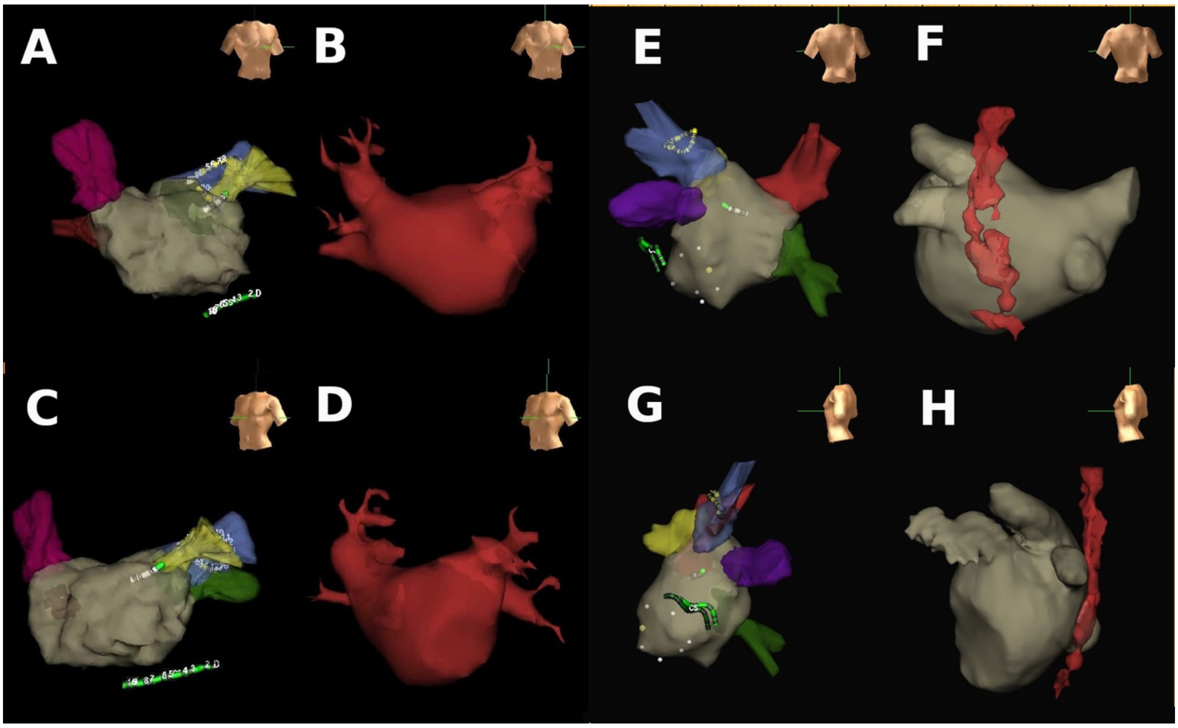

Obr. 5 Synchronizované zobrazení 3 RTG zobrazení levé síně a 3D elektroanatomického modelu levé síně během mapování A, C, E, G – 3D elektroanatomická mapa levé síně, mapovací systém EnSite Velocity, B, D – 3D model levé síně z CT dat, F, H – 3D model levé síně z 3D rotační angiografie levé síně se zobrazením polohy jícnu, A, B – pravá šikmá projekce, C, D – levá šikmá projekce, na CT modelu je vidět přídatná pravostranná střední plicní žíla, E, F – zadopřední projekce, G, H – levá bočná projekce, jícen je na typickém místě za levou částí zadní stěny levé síně.

Výsledkem tohoto postupu je nakonec opět „jen“ elektroanatomická mapa se svými limitacemi a nedostatky, viz obr. 5. Zejména u CARTO systémů starších verzí není tento obraz, a zejména samotné plicní žíly, příliš „anatomický“. U systému EnSite Velocity je obraz bližší skutečné anatomii s věrnějším vyobrazením detailů síňových struktur, ale dosáhnout anatomické věrnosti srovnatelné s 3D prostorovou rekonstrukcí levé síně z CT je složité a časově náročné. Řešením je další stupeň integrace obrazů, kterým je přímá fúze 3D CT modelu levé síně s elektroanatomickou mapou. Cílem této integrace je umístit 3D rekonstrukci levé síně do virtuálního prostředí 3D elektroanatomického mapovacího systému natolik přesně, že se její poloha shoduje s polohou levé síně s přesností na 1-2mm a můžeme pak navigovat katétry přímo ve fúzované 3D rekonstrukci, viz obr. 6. Praktické provedení fúze spočívá ve vytvoření jednoduché 3D elektroanatomické mapy ve které se definují klíčové integrační body odpovídající styčným bodům 3D modelu. Po definování těchto styčných anatomických bodů na obou strukturách dojde softwarově k fúzi obou modelů s proložením map podle těchto bodů. Po skrytí elektroanatomické mapy můžeme provádět ablace ve virtuální 3D rekonstrukci levé síně. Snahou je co nejjednodušší určení styčných bodů a minimalizace potřebného elektroanatomického mapování. Určité úskalí této technologie je nutnost precizního určení styčných bodů pro co nejpřesnější fúzi modelů. V každém případě je fúze 3D RTG modelu levé síně a elektroanatomické mapy spolehlivou a bezpečnou metodou usnadňující katetrizační ablaci v levé síni (57), (58). Některé práce prokázaly, že ablace paroxysmální fibrilace síní prováděné za podpory mapovacího systému s použitím technologie integrace obrazů (v tomto případě CARTO MERGE) mají statisticky vyšší úspěšnost při vyšší bezpečnosti (nižší riziko vzniku stenózy plicní žíly) (59).

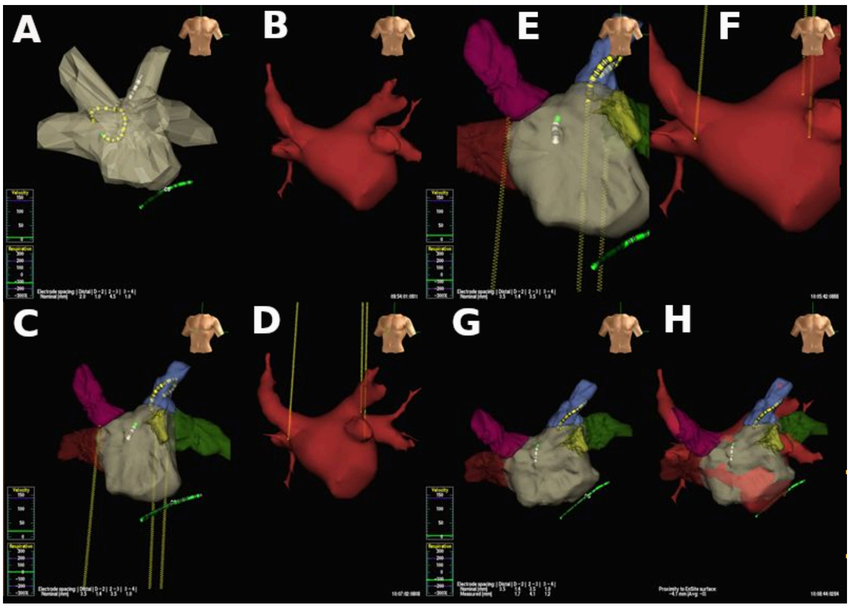

Obr. 6 Fúze CT modelu levé síně a 3D elektroanatomické mapy levé síně během mapování. A - 3D elektroanatomický model levé síně před finální úpravou, C, E, G – výsledný 3D elektroanatomický model levé síně, B, F, D – 3D model levé síně z CT dat, E, F, G, H –

modely s definovanými integračními body na obou modelech (žluté body s „pružinkami“), H – fúzovaný CT model a 3D elektroanatomický model.

Stejně široké využití jako při ablaci fibrilace síní mají CT modely i při ablaci komorových arytmií. Podobně jako u síňových ablací, základním modelem je anatomický 3D model srdeční komory, a to většinou komory levé. CT srdce vzhledem k vysoké prostorové rozlišovací schopnosti umožňuje vytvářet extrémně přesné modely komor se všemi detaily a usnadňovat orientaci operatéra. Použití 3D modelů je stejné jako u katétrové ablace levé síně – synchronizované zobrazení CT modelu a 3D elektroanatomické mapy nebo jejich přímá fúze. Fůze 3D modelu s elektroanatomickou mapou je prováděna stejným způsobem, pomocí klíčových integračních bodů, nejčastěji se jedná o bulbus aorty s odstupy koronárních arterií a hrot levé komory.

Při ablaci komorových arytmií u pacientů se strukturálním onemocněním srdce je pro úspěch výkonu důležitá objektivizace a zobrazení arytmogenního substrátu - organického postižení myokardu, nejčastěji jizvení či fibrotizace svaloviny. Tyto informace získáme při 3D elektroanatomickém mapování, nicméně tento proces je poměrně zdlouhavý a neumožní nám zachytit změny uložené intramurálně či epikardiálně (při standardním endokardiálním mapování). Proto nezávislé preprocedurálně získané informace o strukturálních změnách myokardu jsou klíčové. Zlatým standardem je v tomto případě magnetická rezonance srdce (MR). Late gadolinium-enhancement MR umožňuje přesně charakterizovat rozsah, lokalizaci a transmuralitu postižení stěny srdečních komor jizvením a fibrózou, nejčastěji u pacientů s ischemickou chorobou srdeční či dilatační kardiomyopatií (60), (61). Pomocí MR srdce lze diagnostikovat i zánětlivé postižení myokardu či různé střádavé choroby (62), (63). Takto získaná data lze segmentovat do 3D modelů použitelných v podpoře katétrových arytmií komorových arytmií. Použití těchto modelů umožňuje přesně lokalizovat arytmogenní substrát komorových tachykardií, nejčastěji reentry okruhy související s jizvami v komorovém myokardu a tím umožňuje zjednodušit a zkrátit jinak náročné a zdlouhavé mapování substrátu v levé komoře (48), (61), (64). (65)

CT srdečních komor může též přispět k zobrazení arytmogenního substrátu, byť s nižším přesností než srdeční MR. Vysoká rozlišovací schopnost srdečního CT umožňuje detekovat oblasti jizvy pomocí analýzy ztenčení stěny levé komory u pacientů s ischemickou kardiomyopatií. CT srdce umožňuje měřit tloušťku stěny LK s přesností pod 1mm. Ztenčení stěny levé komory pod 5mm velmi přesně korelovalo s oblastmi abnormálních komorových potenciálů typických pro oblast jizvy a přilehlých oblastí myokardu (66). Stejně dopadlo i srovnání 3D modelů z počítačové tomografie levé komory s pozdním sycením kontrastní látkou (67). Byla prokázána velmi těsná korelace mezi oblastmi jizvy prokázanými pozdním sycením a oblastmi jizvy detekovanými při elektroanatomickém mapování. Použití CT ke kvantifikaci a zobrazení arytmogenního substrátu v době masového použití srdečního MR se může zdát okrajové, nicméně vzhledem k velmi častému použití implantabilních kardioverterů defibrilátorů a pacientů s maligními arytmiemi, které prakticky znemožňují hodnocení strukturálních změn pomocí MR (52) je použití CT jedinou možností.

Kromě lokalizace substrátu arytmie, který vizualizují CT modely s pozdním sycením či analýzou lokálního ztenčení stěny levé komory existuje řada faktorů ovlivňujících účinnost a bezpečnost katétrové ablace komorových arytmií. Přítomnost epikardiálních ložisek tuku výrazně snižuje přesnost epikardiálního elektrofyziologického mapování (68) a snižuje účinnost aplikace radiofrekvenční energie epikardiálním přístupem (68). Nevýhodou epikardiálního přístupu při ablaci komorových arytmií je riziko aplikace radiofrekvenční energie v těsné blízkosti koronárních tepen s rizikem vzniku infarktu myokardu. K vyloučení této komplikace je nutno před každou aplikací kontrolovat polohu koronárních arterií pomocí nástřiků kontrastní látky. V rámci zjednodušení a urychlení výkonu lze k přesnému znázornění koronárních tepen a ložisek epikardiálního tuku při katétrové ablaci lze s úspěchem použit 3D CT model levé komory (47).

Jednou z výhod CT oproti jiným zobrazovacím systémům je vysoká rozlišovací schopnost. Pro maximalizaci prostorového rozlišení a pro zobrazení maxima informací o patologických změnách myokardu lze provést simultánní fúzi 3D elektroanatomického mapovacího systému s 3D CT modelem a 3D modelem z funkčních dat z magnetické rezonance (69). Nevýhodou je pracnost a vyšší cena daná použitím dvou 3D zobrazovacích systémů. Jinou variantou je současná fúze 3D elektroanatomické mapy, 3D modelu z CT srdce a modelu z pozitronové emisní tomografie (70). I v tomto případě se podařilo zobrazit excelentní anatomii arytmogenního substrátu zároveň se zobrazením lokální fibrózy. Kromě vysoké ceny se k negativům v tomto případě přidává ještě zvýšená radiační zátěž pacienta.

Kromě preprocedurálního použití má CT srdce nezastupitelné místo i postprocedurálně v managementu stenóz plicních žil jako komplikací katétrové ablace v levé síni. Stenóza plicní žíly po radiofrekvenční ablaci je vzácná a často asymptomatická komplikace a zlatým standardem v diagnostice je angioCT vyšetření srdce (71)

3.4 Trojrozměrná rotační angiografie levé síně v podpoře katétrové ablace fibrilace síní

Alternativou k CT obrazu srdce, k jejímuž rozvoji došlo v posledních deseti letech, je trojrozměrná rotační angiografie (3 DRA) srdce. Principem této metody je vytvoření řady snímků srdečních dutin naplněných kontrastní látkou při rotaci C ramene standardní angiolinky a jejich následné softwarové zpracování do trojrozměrného obrazu. V podstatě se jedná o rotační angiografii, používanou standardně při vyšetření periferních cév, aplikovanou na srdce. V současnosti existují tři výrobci, jejichž rentgenové systémy jsou vybaveny touto technologii. Jednou z nich je společnost Philips, jejichž angiolinka Alura FD je vybavena technologií s názvem 3 D Rotační Atriografie (72). Druhou společností je společnost Siemens, jejichž přístroj Artis je vybaven technologií Syngo DynaCT Cardiac (73). Třetí je firma General Electrics jejíž přístroj Innova je vybaven technologií EP Vision 3D. Všechny systémy jsou primárně stavěny pro zobrazení levé síně, s čímž souvisí limitace a potenciální nevýhody této metody.

3D modely vytvořené pomocí 3D rotační angiografie srdce jsou srovnatelné s modely vytvořenými pomocí CT (72), (74). Použití 3DRA modelů je zcela shodné s periprocedurálním použitím CT modelů srdečních dutin při katétrové ablaci arytmií. Výhoda rotační angiografie srdce je v možnosti operativního periprocedurálního vytvoření 3D rekonstrukce levé síně. Nezanedbatelná je i menší radiační zátěž (2.1 +/- 0.3 mSv vs. 13.8 +/- 2.4 mSv, P <.001) (75), (76). Stejně tak i dávka kontrastní látky je nižší (75), (76). Zcela zásadní výhoda je možnost periprocedurálního vytvoření 3D rekonstrukce srdeční dutiny, zjednodušující management pacientů referovaných ke katetrizační ablaci. Celé provedení rotační angiografie srdce včetně fúze se skiaskopií a přenesení do 3D mapovacích systémů netrvá déle než 15 min a vzhledem k možnosti paralelního průběhu katetrizace a vytváření a úpravy 3D obrazu ze surových dat se ablační výkon prodlužuje jen minimálně (vlastní zkušenosti se systémem EP Navigátor, Philips).

Základem této metody je nástřik kontrastní látky do srdečních síní. Provádí se injektorem standardně dodávaným s angiolinkou. Nástřik je prováděn buď do pravé síně (pravostranný či indirektní přístup), nebo přímo do levé síně (přístup levostranný či direktní). S určitým zpožděním, daným místem nástřiku a dobou průchodu kontrastní látka do levé síně, proběhne rotace C ramene se zaznamenáním řady snímků levé síně z různých úhlů pořízených během rotace. U levostranného přístupu se snažíme dosáhnout co nejlepší náplně levé síně zástavou komorové akce chvilkovou asystolií podáním Adenosinu či rychlou stimulací komor (77), (78), (79). Získaná surová data jsou poté automaticky zpracována pracovní stanicí (na našem pracovišti EP Navigator, Philips,) a výsledkem je 3D obraz levé síně ekvivalentní CT rekonstrukci srdeční síně. Zpracování je velmi rychlé, jde o „one click" technologii. V případě potřeby lze do segmentace zasáhnout a upravit rekonstrukci manuálně. Srovnání surových dat a výsledné rekonstrukce je vidět na obr. 7 Vzhledem k tomu, že tato technologie je používána relativně krátkou dobu, existuje řada odchylek mezi jednotlivými pracovišti, jak co se týče konkrétního protokolu podání kontrastní látky, tak i dalších detailů, jako je příprava pacienta, poloha pacienta, způsob dýchání při snímání surových dat, použité katétry atd.

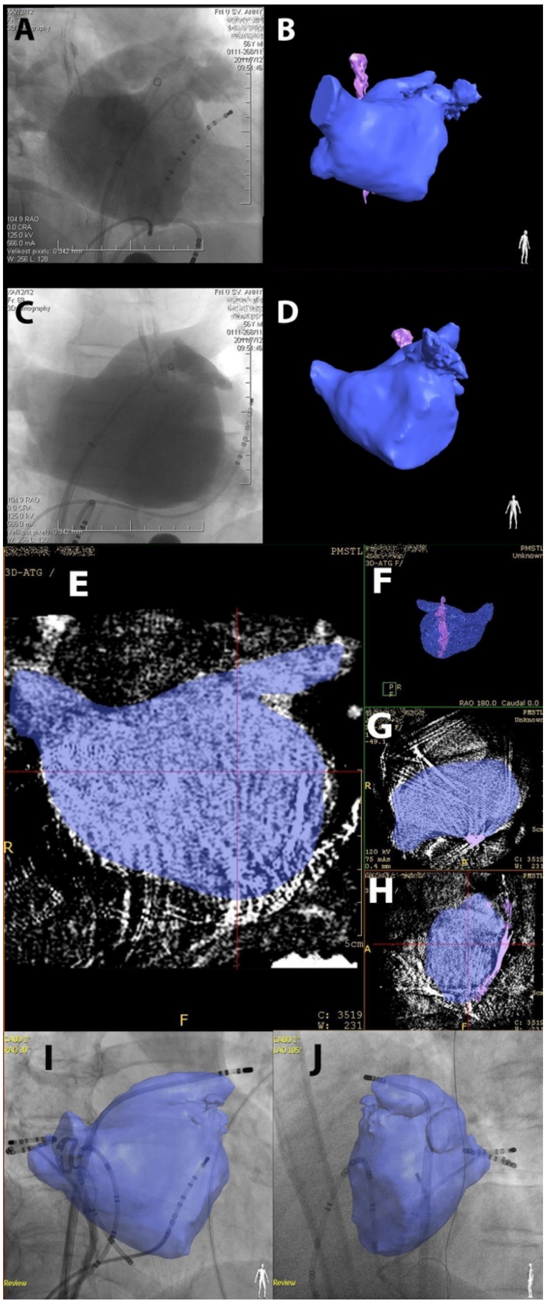

Obr. 7 Trojrozměrná rotační angiografie levé síně (3DRA). A, C – rotační angiografie levé síně, přímý nástřik levé síně pomocí pigtail katétru viditelného v levé síni. Za levou síní vidíme stopy kontrastní látky v jícnu, který je zobrazen jako fialová struktura v rendrovaném modelu. Zároveň vidíme i další katétry (10 polární katétr v koronárním sinu a čtyřpolární katétr v pravé komoře) a transeptální sheathy zavedené do levé síně. B, D – rendrovaný model levé síně a jícnu segmentovaný z rotační angiografie z obr. A a B. A, B – pravá šikmá projekce, C, D – levá šikmá projekce. A – H - Segmentace 3D modelu z rotační angiografie levé síně na pracovní stanici EP Navigator. E - frontální řez 3DRA daty s modře zvýrazněnou dutinou levé síně a plicních žil, F - výsledný 3D model

levé síně a jícnu v zadopřední projekci, G - transverzální řez 3DRA daty, H - sagitální řez 3DRA daty, v obou řezech je modře zvýrazněna levá síň a plicní žíly, fialově dutina jícnu. I, J – 3D model levé síně fúzovaný s live skiaskopií. Vidíme Lasso v pravé dolní plicní žíle a ablační katétr v levé horní plicní žíle. I – pravá šikmá projekce, J – levá boční projekce.

Nejčastěji používanou 3D rekonstrukcí srdeční dutiny je rekonstrukce levé síně. Tento model se dá použít v nefarmakologické terapii srdečních arytmií dvěma základními způsoby. První metodou je použití tohoto obrazu v podpoře vytváření nonfluoroskopické 3D elektroanatomické mapy používané při katétrové ablaci arytmií, nejčastěji systém EnSite Precision a CARTO 3. Druhá možnost, používaná u posledních generací výše zmiňovaných angiografických zobrazovacích systémů, je přímá fúze 3D modelu levé síně se skiaskopií.

Již pouhá segmentace 3D modelu levé síně přináší katetrizujícímu řadu důležitých informací. Jednoznačně se ukáže, kolik plicních žil konkrétní síň má, zda levostranné žíly nemají společné ústí, nebo naopak vpravo není akcesorní plicní žíla, což jsou nejčastější anomálie (37), (36), (80). Důležitý je také směr odstupu jednotlivých plicních žil, jejich diametr, velikost a morfologie ouška levé síně atd. Výsledný 3D model lze použít stejně jako modely vytvořené preprocedurálně pomocí MDCT. Základní a nejjednodušší formou je export modelu do 3D elektroanatomického mapovacího systému a jeho synchronní zobrazení s 3D elektroanatomickým modelem. Další úrovní je přímá fúze obou modelů, 3DRA modelu a 3D elektroanatomického modelu a provádění ablace v detailním 3 DRA modelu levé síně. Blíže viz kapitola 1.3 a obr. 4, 5 a 6.

Další cestou, unikátní pro 3D rotační angiografii srdce, jak usnadnit orientaci katetrizujícího lékaře v levé síni, je přímá integrace 3DRA modelů s live skiaskopií. Spočívá v softwarovém proložení 3D modelu levé síně a 2D skiaskopie na obrazovce RTG přístroje. 3D model je zobrazen na skiaskopické obrazovce angiolinky a pohyb 3D modelu je synchronizovaný s C ramenem, tudíž při jakékoli změně RTG projekce vidíme ve 2D skiaskopii shodně orientovaný 3D model viz obr. 7. Při této integraci je výhodou periprocedurálně získaný 3DRA model levé síně. Periprocedurálně získaná 3D rekonstrukce levé síně je automaticky umístěna přesně v místě skutečné levé síně a je správně orientovaná. Tím odpadá nutnost fúze 3D modelu s live skiaskopií pomocí definovaných klíčových styčných bodů. Pokud nedojde k pohybu pacienta mezi provedením 3DRA a fúzí 3D modelu s live skiaskopií, není třeba jakýchkoli úprav a korekcí polohy 3D obrazu. Jinak je tomu u CT rekonstrukce, která je získaná preprocedurálně, na jiném přístroji a jiném pracovišti. V tomto případě je zapotřebí provést fúzi 3D rekonstrukce s live skiaskopií podle styčných anatomických bodů podobně jako při integraci s elektroanatomickou mapou. Nejčastěji se používá trachea, jejíž 3D rekonstrukci lze vytvořit jak z CT, tak z 3DRA dat a stín trachey je dobře vidět i při prosté skiaskopii. V případě pohybu pacienta během výkonu můžeme fúzi 3DRA modelu s live skiaskopií opakovat a dosáhnout opět optimální integrace. Oproti zcela automatické fúzi 3DRA modelu vede fúze CT modelu s live skiaskopií k určitému zdržení. Na většině pracovišť používající CT modely v podpoře katétrové ablace fibrilace síní se provádí pouze fúze 3D modelů a 3D elektroanatomickým mapovacím systémem.

3D model levé síně integrovaný s live skiaskopií se nejčastěji používá ke zlepšení orientace při vytváření klasické elektroanatomické mapy. Umožňuje při sledování live skiaskopie vidět katétry přímo v 3D modelu levé síně což umožňuje trojrozměrnou orientaci i v rámci rentgenového přístroje. Toto zobrazení je natolik kvalitní, že se dá použít i jako jediná orientace při katetrizační ablaci fibrilace síní, přičemž nebyl prokázán rozdíl v trvání, RTG časech ani okamžitých či dlouhodobých výsledcích mezi navigací pomocí 3D rotační angiografie srdce a standardní navigací pomocí systému CARTO (81).

Další úrovní využití těchto 3D RTG modelů levé síně je možnost zaznamenávat informace přímo do 3D obrazu srdeční dutiny integrovaného do live skiaskopie (EP Navigátor, technologie Point Tagging, Philips, Dyna CT Cardiac, Siemens, EP Vision, General Electrics). Tato technologie umožňuje do 3D modelu zaznamenávat např. místa aplikace radiofrekvenční energie při katétrové ablaci fibrilace síní, ale i jakékoli jiné informace - místa dobrého pacemappingu, zajímavých lokálních potenciálů a podobně. Implementací dodatečných informací do 3D modelu se tato technologie přibližuje elektroanatomickým mapovacím systémům, neboť kromě navigace katétrů umožňuje i záznam důležitých prostorových bodů a je do určité míry ekvivalentní tzv. anatomické mapě srdeční dutiny vytvořené pomocí elektroanatomického mapovacího systému. Anatomická mapa je model srdeční dutiny vytvořený pomocí 3D elektroanatomického systému, do něhož nejsou zanesena data o potenciálech na povrchu srdeční dutiny, zobrazuje pouze prostorové uspořádání srdeční dutiny. Využívá se pro anatomické elektrofyziologické procedury či pro procedury, jejichž efekt je kontrolován jiným systémem, nejčastěji pomocí analýzy signálů z intrakardiálně zavedených katétrů. Pro RFA fibrilace síní se většinou používají právě tyto anatomické mapy s možností zaznamenání jednotlivých ablačních bodů, tedy míst aplikace radiofrekvenční energie, což umožňuje vytvářet z těchto jednotlivých bodových lézí souvislé, kontinuální, linie.

Nevýhodou Point Taggingu a ekvivalentních technologií jsou vysoké nároky kladené na operátora systému, elektrofyziologického technika a značná míra subjektivity daná touto vazbou na lidský faktor. Vkládání anatomických bodů do mapy vytvořené 3D elektroanatomickým mapovacím systémem je prováděno operátorem, prostorová lokalizace těchto bodů je však dána automaticky aktuální polohou hrotu ablačního katétru v srdeční dutině, která je detekována online 3D mapovacím systémem, jedná se o tzv. prostorové, neboli 3D body. Druhá možnost je pak automatická projekce aktuální polohy hrotu ablačního katétru na nejbližší stěnu virtuální 3D mapy srdeční dutiny, tyto body pak nazýváme dvojrozměrné, 2D body. Vzhledem k tomu, že při Point Taggingu nemá RTG přístroj aktuální prostorovou informaci o poloze hrotu ablačního katétru v prostoru, nahrazuje tuto funkci operátor, který manuálně umisťuje prostorové body na stěnu 3D modelu levé síně či jiné srdeční dutiny fúzované s live skiaskopií do místa, kde se při skiaskopii zobrazuje hrot ablačního katétru. V některých projekcích může být umísťování bodů poměrně obtížné a vyžaduje od operátora systému a katetrizujícího lékaře velmi dobrou znalost srdeční anatomie a RTG projekcí.

Od roku 2008 prováděla firma Philips ve spolupráci s firmou Bard vývoj další úrovně těchto 3D RTG aplikací. Pod názvem ElectroView a posléze ElectroNav vyvíjeli aplikaci, umožňující vynášet na povrch 3D RTG modelů, ať už vytvořených pomocí CT či 3DRA, nejen anatomická data, ale též data elektrofyziologická (82). V podstatě se jednalo o stejný proces, jako když se na anatomickou mapu vytvořenou pomocí 3D elektroanatomického mapovacího systému (typicky systém EnSite Velocity) vynášejí informace o amplitudě a šíření signálu. Tím vznikají mapy principiálně shodné a mapami z 3D elektroanatomických systémů umožňující analýzu intrakardiálních systémů a s tím související diagnostiku arytmií. Výsledkem mohou být voltážové mapy, které pomocí barevného kódování znázorňují amplitudu lokálního potenciálu a tzv. LAT mapy znázorňující šíření potenciálu, vzruchu, po srdeční dutině. Nicméně tento vývoj byl koncem roku 2011 ukončen vzhledem k trendu omezení dávek ionizujícího záření během katétrových ablací a k výše popsaným nevýhodám technologie Point Tagging, na kterou tato technologie navazovala.

3.5 Použití 3D rotační angiografie srdečních komor při katétrové ablaci komorových arytmií

Doposud byla řeč o vytváření a použití 3D rekonstrukcí levé síně při katetrizační ablaci pro fibrilaci síní. Všechny systémy 3D rotační angiografie srdce jsou primárně konstruovány na zobrazení levé síně, neboť levosíňové ablace pro fibrilaci síní jsou v současnosti nejčastějším ablačním výkonem. Např. v roce 2018 dle Českého registru katétrových ablací tvořily polovinu všech provedených ablací.

3D modely levé síně však nejsou jedinou možností využití RTG zobrazovacích systémů. Jak jsem zmínil v kapitole 1.3, 3D modely srdečních komor vytvořených pomocí CT srdce jsou běžně používány při katétrové ablaci komorových arytmií. Nesporné výhody periprocedurálního získávání 3D obrazů pomocí rotační angiografie srdce je možno použít i při zobrazení srdečních komor. Jsme zde však značně limitováni systémem, který je vytvořen a primárně určen pro zobrazení srdečních síní. Základní limitací je velikost detektoru (flat panelu) rentgenového přístroje, který je u kardiologické verze velikosti 10x10 palců. Takto omezená velikost flat panelu výrazně znesnadňuje vycentrování srdečních komor. Správné centrování neboli umístění rekonstruované dutiny do ohniska C ramene, je bezpodmínečně nutné pro vytvoření kvalitního obrazu, ze kterého se vytváří 3D model. Dalším problém jsou srdeční kontrakce, které zhoršují kvalitu dosaženého obrazu. To platí zejména u levé komory, jejíž kontrakce jsou nejvýraznější. Všechny problémy byly v posledních letech vyřešeny a 3DRA komor je klinicky použitelná.

Vzhledem k technickým obtížím byla jako první klinicky použitelná rotační angiografie komor vyzkoušena rotační angiografie výtokového traktu pravé komory (RVOT). Orlov a kol. v roce 2011 poprvé publikovali zobrazení RVOT u skupiny 8 pacientů indikovaných ke katétrové ablaci komorové ektopie z RVOT. Při použití indirektního protokolu (aplikace kontrastní látky do dolní části pravé síně) byla úspěšnost 88% a takto získané 3D modely byly úspěšně použity při radiofrekvenční katétrové ablaci komorových tachykardií z RVOT (82). Ve stejné době jsme i na našem pracovišti začali s 3DRA pravé komory. Celkem jsem provedli dvacet 3D rotačních angiografií pravé komory direktním protokolem (aplikace kontrastní látky přímo do pravé komory při rychlé stimulaci ke snížení kontrakcí komory) s celkovou úspěšností 95% a dobrým až excelentním výsledkem. 3D modely byly použity při podpoře katétrové ablace komorových arytmií jednak fúzí modelu s live fluoroskopií a jednak integrací modelu do 3D elektroanatomického mapovacího systému (83).

Vzhledem k dobrým zkušenostem s 3DRA pravé komory jsme v roce 2011 na našem pracovišti zahájili i program 3D rotačních angiografií levé komory. Celkem jsme provedli 13 vyšetření se zobrazením levé komory s úspěšností 100%. Všechny modely byly v dobré či excelentní kvalitě a byly s úspěchem použity podobně jako u 3D modelů RVOT – přímou fúzí modelu s live fluoroskopií a fúzí modelu s 3D elektroanatomickým mapovacím systémem (84). Příklady 3D modelů pravé a levé komory a jejich použití viz obr. 8 a 9.

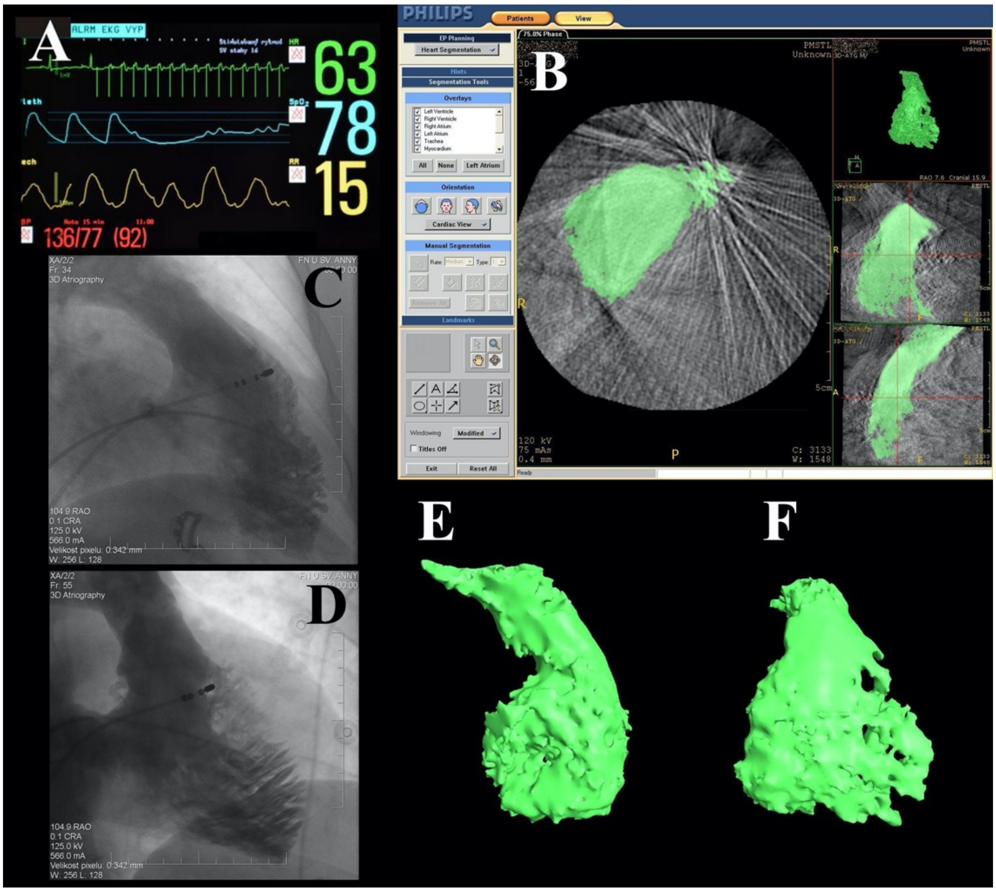

Obr. 8 Trojrozměrná rotační angiografie pravé komory. A – Snížení srdečního výdeje během aplikace kontrastní látky pomocí rychlé stimulace srdečních komor dokumentovaná poklesem saturace. B – Segmentace 3D modelu pravé komory ze surových dat. Vidíme 3 na sebe kolmé řezy surovými daty s dutinou pravé komory zvýrazněnou zelenou barvou a výsledný rendrovaný model pravé komory. C, D – Rotační angiografie pravé komory, RAO 104 (C), RAO 10 (D). E, F – výsledný rendrovaný model pravé komory, RAO 100 (E), RAO 40 (F). LAO – levá šikmá projekce, RAO – pravá šikmá projekce.

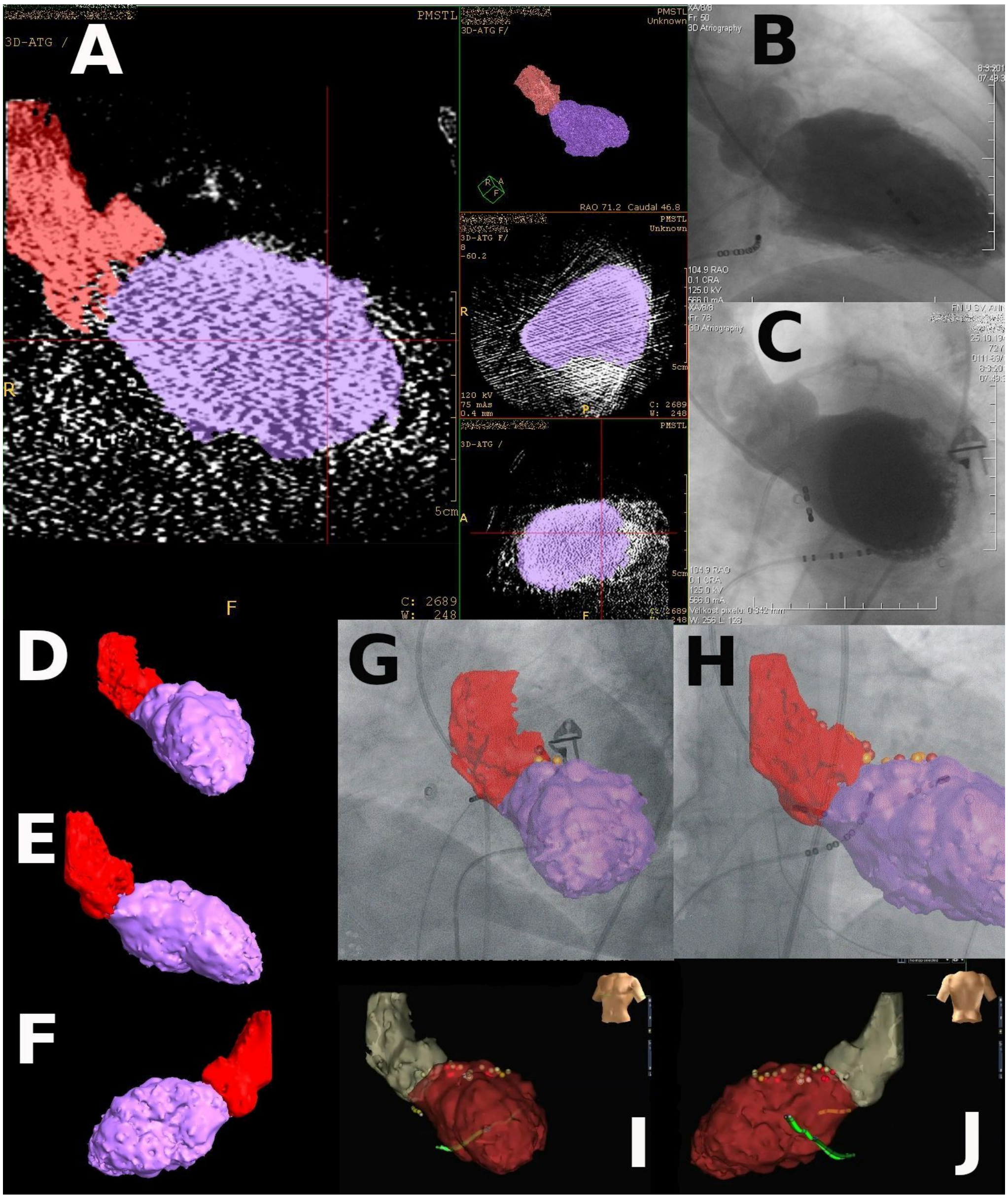

Obr. 9 Trojrozměrná rotační angiografie levé komory. A – Segmentace 3D modelu levé komory ze surových dat. Vidíme 3 na sebe kolmé řezy surovými daty s dutinou levé komory zvýrazněnou fialovou barvou a aortou zvýrazněnou červenou barvou a výsledný rendrovaný model levé komory. B, C – Rotační angiografie levé komory, AP (B), LAO (C). D, E, F – výsledný rendrovaný model levé komory, fialově je znázorněna dutina levé komory, červeně bulbus aorty, LAO (D), AP (E), PA (F). G, H – model levé komory s body znázorňující ablace v oblasti výtoku levé komory a bulbu aorty (point tagging) fúzovaný s live skiaskopií, LAO (G), AP (H). I, J – 3D model levé komory s body znázorňující ablace v oblasti výtoku a summitu levé komory (point tagging) fúzovaný s 3D elektroanatomickým mapovacím systémem EnSite Velocity, LAO (I), PA (J). LAO – levá šikmá projekce, AP – předozadní projekce, PA – zadopřední projekce.

Modely srdečních komor jsou anatomicky srovnatelné s modely vytvořenými pomocí CT (85), (84). Nicméně nemožnost zobrazení perfúze myokardu, přítomnost fibrózy a jizvení či jiných intramyokardiálních procesů výrazně limituje klinickou použitelnost těchto modelů. Vzhledem k velkému rozvoji funkčního zobrazení pomocí počítačové tomografie a magnetické rezonance jsou při ablaci komorových arytmií v dnešní době používány výhradně tyto modality.

3.6 3D zobrazení jícnu při katétrové ablaci fibrilace síní

Další důležitou strukturou, kterou jsme schopni znázornit pomocí 3D RTG zobrazovacích metod a použít v podpoře katétrových ablací srdečních arytmií, je jícen. Zobrazení této struktury nabylo na významu v posledních letech, kdy se v rámci bouřlivého rozvoje katétrových ablací v levé síni objevila vzácná, nicméně velmi závažná komplikace, atrioesofageální píštěl. Tato velmi obávaná komplikace je způsobena velmi těsným anatomickým vztahem jícnu a zadní stěny levé síně. Poloha jícnu vůči levé síni je velmi variabilní, nejčastější poloha je za střední či levou částí zadní stěny levé síně. Jícen je ve většině případů v těsném kontaktu s dlouhým úsekem zadní stěny levé síně, svalovina jícnu přímo naléhá na svalovinu levé síně a vzdálenost dutiny levé síně a lumen jícnu je pouhých několik milimetrů (53), (80), (54), (86). Dle naší analýzy topografických vztahů v této oblasti je průměrně 5 cm délky jícnu v těsném kontaktu a průměrná vzdálenost lumen levé síně a jícnu je 4.8 ± 1.6 mm, ve střední části, kde je kontakt nejtěsnější dokonce jen 3.63 ± 0.95 mm (80). Vztah mezi levou síní a jícnem viz obr. 10. Vzhledem k faktu, že základní strategie ablace fibrilace síní je izolace plicních žil cirkulárními liniemi v levé síni doplněné eventuálně o další lineární léze (87), (88) je riziko poškození jícnu poměrně značné.

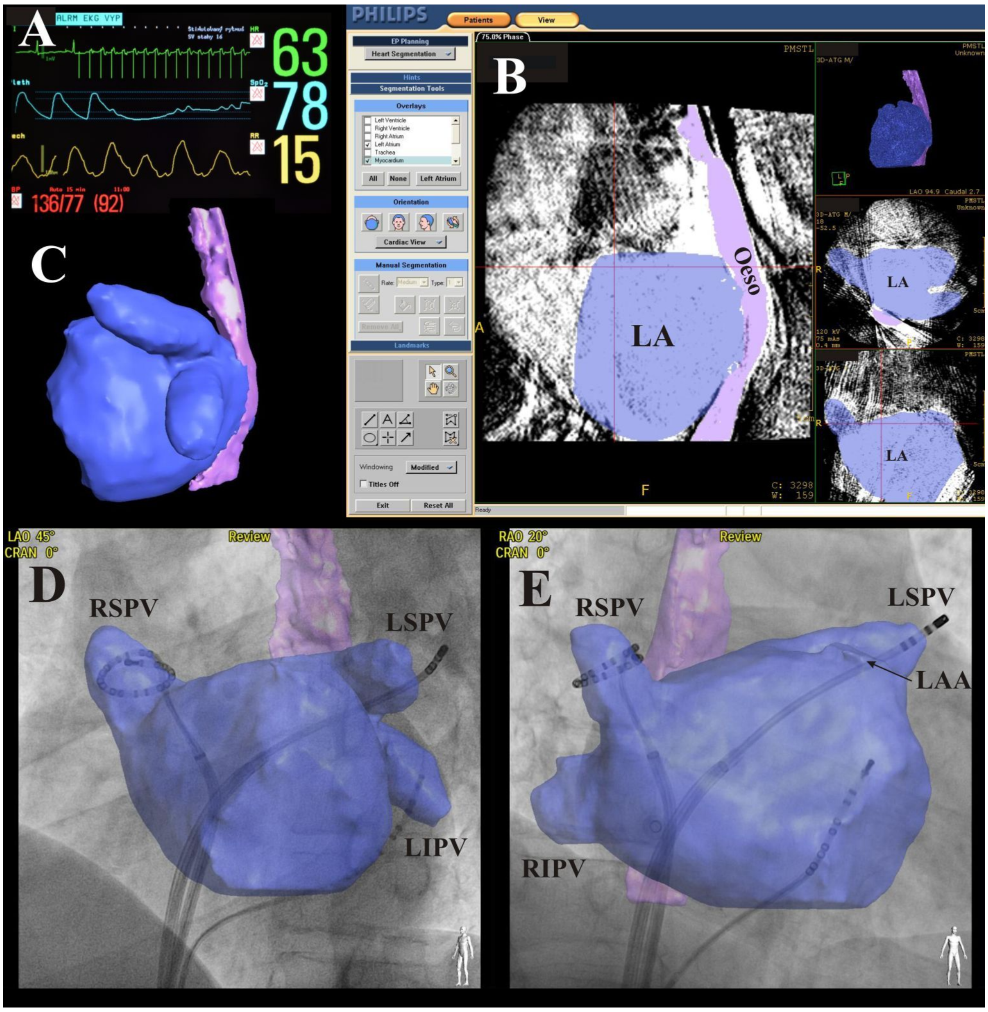

Obr. 10 Vztah mezi levou síní a jícnem na rotační angiografii levé síně a jícnu. A – Snížení srdečního výdeje během aplikace kontrastní látky pomocí rychlé stimulace srdečních komor dokumentovaná poklesem saturace. B – Segmentace 3D modelu levé síně a jícnu ze surových dat. Vidíme 3 na sebe kolmé řezy surovými daty s dutinou levé síně zvýrazněnou modrou barvou, dutinu jícnu zvýrazněnou fialovou barvou a výsledný rendrovaný model levé síně a jícnu v levé bočné projekci. C - rendrovaný model levé síně a jícnu v levé bočné projekci. Dobře je vidět těsná souvislost jícnu a zadní stěny levé síně na surových datech (největší obrázek B) a na rendrovaném modelu v levé bočné projekci (C). D, E – variabilita polohy jícnu, 3D model levé síně a jícnu fúzovaný s live skiaskopií v předozadní projekci. Vidíme Lasso katétr v RSPV, ablační katétr v LSPV a desetipolární katétr zavedený do koronárního sinu. D – jícen za levou částí zadní stěny levé síně, E – jícen za pravou částí zadní stěny levé síně. RSPV – pravá horní plicní žíla, RIPV – pravá dolní plicní žíla, LSPV – levá horní plicní žíla, LIPV – levá dolní plicní žíla, LAA – ouško levé síně, LA – levá síň, oeso - jícen

Atrioezofageální píštěl je patologická komunikace mezi levou síní a jícnem vedoucí k rozvoji sepse, kardioembolizačním příhodám, neurologické symptomatologii a v řadě případů k fatálnímu konci. Atrioezofageální píštěl je naštěstí velmi vzácná tvoří méně než 0,1% všech komplikací katétrové ablace fibrilace síní (30), nicméně v 70 – 80% končí úmrtím pacienta (89) a je příčinou 16% všech úmrtí spojených s katétrovou ablací fibrilace síní (56).

Vzhledem k závažnosti této komplikace existuje řada metod, jak ochránit jícen před vedlejšími účinky radiofrekvenční ablace a snížit riziko této komplikace. Principiálně nejjednodušší možností je omezení množství aplikované energie v místě kontaktu zadní stěny levé síně a plicních žil s jícnem k minimalizaci poškození jícnu (90). Předpokladem úspěchu tohoto opatření je znalost polohy jícnu. Základní metodou pro zobrazení vztahu jícnu a levé síně je CT srdce. 3D model levé síně a jícnu je možno fúzovat s elektroanatomickým mapovacím systémem a použít při katétrové ablaci (58), (90). Přesnost zobrazení jícnu je omezeno mobilitou této struktury. Jícen je v prostoru za levou síní uložen volně a vůči levé síni se poměrně volně pohybuje. Preprocedurální zobrazení jícnu je výrazně limitováno dlouhodobou mobilitou této struktury. Studie zabývající se dlouhodobou stabilitou jícnu přinesly rozporuplné výsledky. Některé studie prokázaly relativně stabilní polohu jícnu v dlouhodobém horizontu (55), (91), (92), (93) naopak jiné studie prokázaly velmi špatnou korelaci mezi preprocedurálním zobrazením jícnu a aktuální polohou jícnu při ablaci (94), (95). Naše práce srovnávající preprocedurální CT levé síně a jícnu s 3D rotační angiografií levé síně a jícnu na počátku výkonu prokázala statisticky významnou dlouhodobou mobilitu jícnu (96). Zdá se, že preprocedurálně získané zobrazení jícnu je pro orientaci při ablaci omezeně použitelné.

Naopak s výhodou se dá použít periprocedurálně vytvořený 3DRA model levé síně a jícnu. Toto zobrazení lze s minimální časovou ztrátou provést na začátku výkonu. Polknutí malého množství kontrastní látky před provedení rotační angiografie levé síně umožňuje s velkou přesností a spolehlivostí znázornit jícen a jeho polohu vůči levé síni (97), viz obr. 4 a 9. Vzhledem k mobilitě jícnu v prostoru za levou síní i v tomto případě vzniká otázka, zda je poloha jícnu dostatečně stabilní během několikahodinového výkonu. I v tomto případě nepřinesly povedené studie jasný závěr. Sherzer et al (98) prokázal stabilní polohu jícnu během několikahodinového výkonu v celkové anestezii, zatímco Good et al. (99) and Daoud et al. (94) naopak prokázali signifikantní krátkodobou mobilitu jícnu u pacientů řešených v analgosedaci. Naše práce srovnávající polohu jícnu opakovaně během výkonu vůči vstupní 3DRA levé síně a jícnu neprokázala významný posun jícnu během dvouhodinového výkonu u analgosedovaných pacientů (100). Průměrný posun jícnu byl 2.7 ± 2.2 až 3.8 ± 3.4 mm. Zároveň jsme prokázali velmi dobrou stabilitu fúzovaného modelu levé síně s live fluoroskopií, kdy průměrný posun modelu během výkonu byl v pravolevém směru 1.4 ± 1.8 to 3.3 ± 3.0 mm a v kraniokaudálním směru 0.9 ± 1.2 to 2.2 ± 1.3 mm.

Provedené práce prokázaly, že jícen je velmi variabilní struktura jak co do polohy vůči levé síni, tak co do změn této polohy v čase v dlouhodobém horizontu. Ochrana jícnu při katétrové ablaci v levé síni pomocí jeho vizualizace je možná, nicméně pouze v krátkodobém časovém horizontu pomocí periprocedurálního zobrazení této struktury. Co se RTG metod týče, lze s úspěchem použít prostou ezofagografii či 3DRA levé síně a jícnu. Preprocedurální zobrazení jícnu pomocí CT či MR srdce a hrudníku má limitovanou hodnotu vzhledem k signifikantní mobilitě jícnu v dlouhodobém časovém horizontu.

3.7 Závěr

Závěrem lze říct, že moderní 3D rentgenové zobrazovací metody zjednodušují a usnadňují katetrizační ablace komplexních arytmií a jsou běžně používány při těchto výkonech. Zlatým standardem jsou 3D modely vytvářené pomocí MDCT srdce. Klinicky je nejčastěji používaný 3D model levé síně. V naprosté většině případů je používán při katétrové ablaci fibrilace síní. Tyto preprocedurálně vytvářené modely mají vysoké prostorové rozlišení a mohou být využívány různými způsoby v podpoře těchto výkonů. Je několik možností integrace modelů do 3D elektroanatomických mapovacích systémů od synchronizovaného zobrazení po úplnou fúzi těchto modalit. Zároveň se 3D modely dají fúzovat s live skiaskopií a tím dál usnadnit orientaci v srdečních dutinách.

3D rotační angiografie srdce, v naprosté většině případů levé síně, je nová metoda umožňující vytvoření 3D modelu srdeční dutiny přímo na elektrofyziologickém sále pomocí standardní angiolinky. Tyto modely se dají získat periprocedurálně a jejich kvalita je srovnatelná s CT modely srdce. Výhodou 3DRA je větší flexibilita při managementu pacientů vzhledem k možnosti vytvoření 3D modelu přímo na elektrofyziologickém sále, v neposlední řadě pak i nižší dávka RTG záření a kontrastní látky. V těchto parametrech jde vývoj dopředu ve smyslu neustálého snižování zátěže pacienta kontrastní látkou a RTG zářením a nové generace CT přístrojů mají tyto parametry srovnatelné.

Užitečnou vlastností je možnost záznamu informací na povrch vytvořeného a fúzovaného modelu. Tím se 3D RTG modely blíží anatomickým mapám vytvářeným pomocí 3D elektroanatomických systémů. I když se 3D modely levé síně fúzované s live skiaskopií svou kvalitou blíží těmto anatomickým mapám, nahrazení 3D elektroanatomických mapovacích systémů CT či 3DRA modely fúzovanými s live skiaskopií se nejeví pravděpodobným. Příčinou je jejich ofline charakter. Byť poskytují excelentní prostorovou informaci o stavbě a utváření srdeční dutiny, chybí online informace o aktuální poloze katétrů v této dutině. Z tohoto důvodu jakékoli dodatečné informace mohou být zaznamenány pouze na povrchu 3D modelu a do hry vstupuje značný subjektivní faktor operátora tohoto systému. Dle našeho názoru je současná role těchto systémů coby velmi užitečných, leč pouze pomocných metod, usnadňujících katétrovou ablaci komplexních arytmií za pomoci 3D elektroanatomických mapovacích systémů.

Vytvoření 3D modelů dalších srdečních dutin je možné a použitelné v podpoře katétrových ablací srdečních arytmií. Z dat získaných pomocí CT jsme schopni segmentovat a použít jakoukoli srdeční dutinu. Pomocí 3D rotační angiografie srdce se dají jednoduše a efektivně vytvořit modely srdečních komor použitelné v podpoře katétrových ablací srdečních arytmií. Tato fakta jsme ověřili experimentální prací na našem pracovišti.

Z nesrdečních struktur má význam zobrazení jícnu. Zobrazení jícnu je jednoduché, spolehlivé a bezpečné a umožňuje nám udělat si představu o lokalizaci jícnu vzhledem k levé síni při plánování ablačních linií. Pokud pacient podstupuje 3DRA levé síně před katétrovou ablací komplexní arytmie, dá se doporučit zobrazení jícnu jako jednoduchá a bezpečná metoda k jeho lokalizaci.

Kontrastní CT vyšetření srdce s vytvořením 3D modelů srdečních dutin je dnes standardní součástí špičkových CT přístrojů renomovaných světových výrobců. Co se týče technologie 3D rotační angiografie srdce, v současnosti touto technologií disponují tři největší výrobci rentgenových přístrojů, společnost Philips, Siemens a General Electrics. Jejich produkty se liší spíše detaily a jsou navzájem srovnatelné.

Budoucnost 3D RTG modelů srdečních dutin je spojena s dalším vývojem RTG zobrazovacích systémů a jejich propojením s dalšími elektrofyziologickými technologiemi. Dlouhodobým trendem je vývoj nových generací přístrojů s nižší dávkou záření i kontrastní látky, a to jak v případě CT, tak v případě 3D rotační angiografie srdce. Snahou je maximálně zvýšit rozlišení u 3DRA a maximálně zjednodušit a zefektivnit protokol těchto vyšetření. Pro spokojenost uživatele je klíčová co nejjednodušší a pokud možno zcela automatická segmentace jednotlivých obrazů. Snahou je dosažení opravdu „one click" segmentace s maximální kvalitou obrazu při minimální nutnosti manuálně zasahovat do procesu segmentace. Stejně tak důležitá je snaha o co nejrychlejší vytvoření a následné použití 3D modelu, neboť katétrové ablace jsou samy o sobě časově náročnými výkony a každé zkrácení doby výkonu je vítané.

V oblasti fúze 3D modelů s live skiaskopií, která je klíčová pro co nejefektivnější použití těchto modelů, se jeví jako důležitý směr dalšího vývoje automatická korekce dýchacích pohybů, srdečních kontrakcí a pohybu pacienta během vyšetření. Vzhledem k tomu, že většina vyšetření neprobíhá v celkové anestezii, mohou tyto faktory vést k nutnosti opakovaných repozic polohy 3D modelu v live skiaskopii, což vede k prodloužení výkonu.

3D modely srdečních dutin vytvářené pomocí RTG zobrazovacích systémů se v posledních letech staly nedílnou součástí elektrofyziologických výkonů, kde slouží k podpoře katétrových ablací komplexních arytmií, nejčastěji ablaci fibrilace síní. Technologie umožňující vytváření a použití těchto modelů jsou v současnosti běžnou výbavou elektrofyziologických pracovišť zabývajících se řešením komplexních arytmií. Na poli vytváření, segmentace a použití těchto modelů došlo v posledních letech k obrovskému rozvoji, který zdaleka nekončí a bude pokračovat i v budoucnosti.

3.8 Cíle habilitační práce

1. Detailně popsat anatomii levé síně a okolních struktur, zejména jícnu, z dat získaných pomocí MDCT a 3DRA.
2. Najít optimální akviziční protokol a optimální použití výsledného modelu pro 3D rotační angiografii levé síně a jícnu.
3. Srovnat kvalitu a klinickou použitelnost 3D modelů levé síně a jícnu vytvořených pomocí MDCT a 3DRA v podpoře katétrových ablací fibrilace síní

4. Srovnat efektivitu a bezpečnost katétrové ablace fibrilace síní s podporou 3D modelů získaných pomocí MDCT a 3D rotační angiografie levé síně.
5. Prokázat proveditelnost, bezpečnost a efektivitu 3D rotační angiografie pravé a levé komory v podpoře katétrových ablací komorových arytmií.
6. Ověřit efektivitu preprocedurálního a intraprocedurálního zobrazení polohy jícnu vůči levé síni v podpoře katétrových ablací fibrilace síní.
7. Ověřit stabilitu fúze 3D modelu levé síně vytvořeného pomocí 3D rotační angiografie a live skiaskopie během několikahodinové katétrové abace fibrilace síní

Tyto cíle byly řešeny v dílčích projektech, které jsou uvedeny v následujících kapitolách 2.1. – 2.11., které byly úspěšně publikovány v impaktovaných odborných časopisech.

3.9 Literatura k úvodním kapitolám

1. **Khurshid S, Choi SH, Weng LC, Wang EY, Trinquart L, Benjamin EJ, etal.** Frequency of Cardiac Rhythm Abnormalities in a Half Million Adults. . *Circ Arrhythm Electrophysiol. 2018 Jul;11(7).*

2. **Orejarena LA, Vidaillet H, DeStefano F, Nordstrom DL, Vierkant RA, Smith PN, et al.** Paroxysmal supraventricular tachycardia in the general population. *J Am Coll Cardiol. 1998; 31:150–157.*

3. **Chugh SS, Reinier K, Teodorescu C, Evanado A, Kehr E, Al Samara M, et al.** Epidemiology of sudden cardiac death: clinical and research implications. *Prog Cardiovasc Dis. 2008; 51:213–228.*

4. **Vaughan, Williams EM: A classification of antiarrhythmic actions reassessed after a decade of new drugs, J Clin Pharmacol April 1, 1984 vol. 24 no. 4 129-147.**

5. **Gosselink M, Crijns H, Van Gelder I et al.** Low-Dose Amiodarone for Maintenance of Sinus Rhythm After Cardioversion of Atrial Fibrillation or Flutter. *JAMA. 1992;267(24):3289-3293.*

6. **Kerin NZ, Faitel K, Kerin IA, et al.** Efficacy of low-dose amiodarone in the prevention of paroxysmal atrial fibrillation resistant to type IA antiarrhythmic drugs. *Am J Ther.* 2000 Aug;7(4):245-50.

7. **Investigators., Cardiac Arrhythmia Suppression Trial (CAST).** Preliminary report: effect of encainide and flecainide on mortality in a randomized trial of arrhythmia suppression after myocardial infarction. *N Engl J Med. 1989;321:406-412. .*

8. **Investigators., The Cardiac Arrhythmia Suppression Trial-II.** Effect of the antiarrhythmic agent moricizine on survival after myocardial infarction. The Cardiac Arrhythmia Suppression Trial II Investigators. *N Engl J Med.* 1992 Jul 23;327(4):227-33.

9. **Scherlag BJ, Lau SH, Helfant RH, Berkowitz WD, Stein E, Damato AN.** Catheter technique for recording His bundle activity in man. *Circulation. 1969 Jan;39(1):13-8.*

10. **Durrer D, Schoo L, Schuilenburg RM, Wellens HJ.** The role of premature beats in the initiation and the termination of supraventricular tachycardia in the Wolff-Parkinson-White syndrome. *Circulation. 1967 Nov;36(5):644-62.*

11. **Welens, HJ.** Value and limitations of programmed electrical stimulation of the heart in the study and treatment of tachycardias. *Circulation. 1978 May;57(5):845-53.*

12. **Harrison L, Gallagher JJ, Kasell J, Anderson RH, Mikat E, Hackel DB, Wallace AG.** Cryosurgical ablation of the A-V node-His bundle: a new method for producing A-V block. *Circulation. 1977 Mar;55(3):463-70.*

13. **Cobb FR, Blumenschein SD, Sealy WC, Boineau JP, Wagner GS, Wallace AG.** Successful surgical interruption of the bundle of Kent in a patient with Wolff-Parkinson-White syndrome. *Circulation. 1968 Dec;38(6):1018-29.*

14. **Coumel P, Aigueperse J, Perrault MA, Fantoni A, Slama R, Bouvrain Y.** Detection and attempted surgical exeresis of a left auricular ectopic focus with refractory tachycardia. Favorable outcome. *Ann Cardiol Angeiol (Paris). 1973 May-Jun;22(3):189-99.*

15. **Gonzalez R, Scheinman M, Margaretten W, Rubinstein M.** Closed-chest electrode-catheter technique for His bundle ablation in dogs. *Am J Physiol. 1981 Aug;241(2):H283-7.*

16. **Scheinman MM, Morady F, Hess DS, Gonzalez R.** Catheter-induced ablation of the atrioventricular junction to control refractory supraventricular arrhythmias. *JAMA. 1982 Aug 20;248(7):851-5.*

17. **Weber H, Schmitz L.** Catheter technique for closed-chest ablation of an accessory atrioventricular pathway. *N Engl J Med. 1983 Mar 17;308(11):653-4.*

18. **Morady F, Scheinman MM.** Transvenous catheter ablation of a posteroseptal accessory pathway in a patient with the Wolff-Parkinson-White syndrome. *N Engl J Med. 1984 Mar 15;310(11):705-7.*

19. **Borggrefe M, Budde T, Podczeck A, Breithardt G.** High frequency alternating current ablation of an accessory pathway in humans. *J Am Coll Cardiol. 1987 Sep;10(3):576-82.*

20. **Nath S, DiMarco JP, Haines DE.** Basic aspects of radiofrequency. *J Cardiovasc Electrophysiol 1994; 5:863.*

21. **Committee Members, C. Blomstrom-Lundqvist, M. M. Scheinman, E. M. Aliot, et al.** ACC/AHA/ESC guidelines for the management of patients with supraventricular arrhythmias -- executive summary: a report of the American college of cardiology/American heart association

task force on practice guidelines and the European society of cardiology. *J. Am. Coll. Cardiol.* 2003;42(8):1493-1531.

22. **Dinerman JL, Berger RD, Calkins H.** Temperature monitoring during radiofrequency ablation. *J Cardiovasc Electrophysiol. 1996 Feb;7(2):163-73.*

23. **Ruffy R, Imran MA, Santel DJ, Wharton JM.** Radiofrequency delivery through a cooled catheter tip allows the creation of larger endomyocardial lesions in the ovine heart. *J Cardiovasc Electrophysiol 1995; 6:1089.*

24. **Jaïs P, Shah DC, Haïssaguerre M, Hocini M, Garrigue S, Le Metayer P, Clémenty J.** Prospective randomized comparison of irrigated-tip versus conventional-tip catheters for ablation of common flutter. *Circulation. 2000 Feb 22;101(7):772-6.*

25. **Calkins H, Kuck KH, Cappato R, et al.** 2012 HRS/EHRA/ECAS expert consensus statement on catheter and surgical ablation of atrial fibrillation: recommendations for patient selection, procedural techniques, patient management and follow-up, definitions, endpoints, and research trial design. *J Interv Card Electrophysiol.* 2012 Mar;33(2):171-257.

26. **Michelucci A, Antonucci E, Conti AA, Alessandrello Liotta A,.** Electrophysiologic procedures and activation of the hemostatic system. *Am Heart J 1999;138:128.*

27. **Calkins H, Hindricks G, Cappato R, Kim YH, Saad EB, Aguinaga L, et al.** 2017 HRS/EHRA/ECAS/APHRS/SOLAECE expert consensus statement on catheter and surgical ablation of atrial fibrillation. *Europace. 2018 Jan 1;20(1):e1-e160.*

28. **Katritsis DG, Boriani G, Cosio FG, Hindricks G, Jaïs P, Josephson ME, et al.** European Heart Rhythm Association (EHRA) consensus document on the management of supraventricular arrhythmias, endorsed by Heart Rhythm Society (HRS), Asia-Pacific Heart Rhythm Society (APHRS), and Sociedad Latinoamericana de Estimulación Cardiaca y Elect. *Europace. 2017 Mar 1;19(3):465-511.*

29. **Cronin EM, Bogun FM, Maury P, Peichl P, Chen M, Namboodiri N, et al.** 2019 HRS/EHRA/APHRS/LAHRS expert consensus statement on catheter ablation of ventricular arrhythmias. *Europace. 2019 May 10. pii: euz132. doi: 10.1093/europace/euz132. [Epub ahead of print].*

30. **Cappato R, Calkins H,Chen SA, et al.** Updated Worldwide Survey on the Methods, Efficacy, and Safety of Catheter Ablation for Human Atrial Fibrillation. *Circ Arrhythm Electrophysiol.* 2010 Feb;3(1):32-8.

31. **Verma A, Natale A.** Why atrial fibrillation ablation should be considered. *Circulation 2005;112:1214 –1222.*

32. **Packer DL, Mark DB, Robb RA, Monahan KH, Bahnson TD, Poole JE, et al.** Effect of Catheter Ablation vs Antiarrhythmic Drug Therapy on Mortality, Stroke, Bleeding, and Cardiac Arrest Among Patients With Atrial Fibrillation: The CABANA Randomized Clinical Trial. *JAMA. 2019 Mar 15. doi: 10.1001/jama.2019.0693. [Epub ahead of print].*

33. **Pappone C, Rosanio S, Augello G, Gallus G.** Mortality, Morbidity, and Quality of Life After Circumferential Pulmonary Vein Ablation for Atrial Fibrillation Outcomes From a Controlled Nonrandomized Long-Term Study. . *JACC Vol. 42, No. 2, 2003 July 16, 2003:185–97.*

34. **Mark DB, Anstrom KJ, Sheng S, Piccini JP, Baloch KN, Monahan KH, et al.** Effect of Catheter Ablation vs Medical Therapy on Quality of Life Among Patients With Atrial Fibrillation: The CABANA Randomized Clinical Trial. *JAMA. 2019 Mar 15. doi: 10.1001/jama.2019.0692. [Epub ahead of print].*

35. **Gepstein L, Hayam G, Ben-Haim SA.** A novel method for nonfluoroscopic catheter-based electroanatomical mapping of the heart. In vitro and in vivo accuracy results. *Circulation.* 97 Mar 18;95(6):1611-22.

36. **Kato R, Lickfett L, Meininger G, et al.** Pulmonary vein anatomy in patients undergoing catheter ablation of atrial fibrillation: lessons learned by use of magnetic resonance imaging. *Circulation.* 2003 Apr 22;107(15):2004-10.

37. **Jongbloed MR, Bax JJ, Lamb HJ, Dirksen MS, Zeppenfeld K, Van Der Wall EE, De Roos A, Schalij MJ.** Multislice computed tomography versus intracardiac echocardiography to evaluate the pulmonary veins before radiofrequency catheter ablation of atrial fibrillation: A head-to-head comparison. *J Am Coll Cardiol 2005;343-350.*

38. **Cormack, AM.** Reconstruction of densities from their projections, with applications in radiological physics. *Phys Med Biol 1973;18:195-207.*

39. **Hounsfield, GN.** Computerized transverse axial scanning (tomography). 1. Description of system. *Br J Radiol 1973;46:1016-22.*

40. **Flohr TG, Schoepf UJ, Keuttner et al.** Advances in cardiac imaging with 16-section CT systems. *Acad Radiol 2003;10:386-401.*

41. **Ohnesorge B, Flohr T, Becker C et al.** Cardiac imaging by means of electrocardiographically gated multisection spiral CT: initial experience. *Radiology 2000;217:564-71.*

42. **Leschka S, Alkhadi H, Plass A et al.** Accuracy of MSCT coronary angiography with 64-slice technology: first experience. *Eur Heart J 2005;26: 1482-7.*

43. **Taylor & Francis, 2005, Yamamuro M, Tadamura E, Kubo S, et al.** Cardiac functional analysis with Multidetector row CT and segmental reconstruction algorithm: comparison with echocardiography, SPECT, and MR imaging. *imaging. Radiology 2005;234:381–390.*

44. **Feuchtner GM, Dichtl W, Friedrich GJ, et al.** Multislice computed tomography for detection of patients with aortic valve stenosis and quantification of severity. *J Am Coll Cardiol 2006;47:1410–1417.*

45. **Ou P, Celermajer DS, Calcagni G, et al.** Three-dimensional CT scanning: a new diagnostic modality in congenital heart disease. *Heart 2007;93:908–913.*

46. **Kim EY, Kim HH, Yoon Y.** Y. Imaging of pericardial diseases. *Clin Radiol 2007;62:626–631.*

47. **van Huls van Taxis CF, Wijnmaalen AP, Piers SR, van der Geest RJ, Schalij MJ, Zeppenfeld K.** Real-time integration of MDCT-derived coronary anatomy and epicardial fat: impact on epicardial electroanatomic mapping and ablation for ventricular arrhythmias. *JACC Cardiovasc Imaging. 2013 Jan;6(1):42-52.*

48. **Tian J, Jeudy J, Smith MF, Jimenez A, Yin X, Bruce PA, Lei P, Turgeman A, Abbo A, Shekhar R, Saba M, Shorofsky S, Dickfeld T.** Three-dimensional contrast-enhanced multidetector CT for anatomic, dynamic, and perfusion characterization of abnormal myocardium to guide ventricular tachycardia ablations. *Circ Arrhythm Electrophysiol. 2010 Oct;3(5):496-504.*

49. **Shiozaki AA, Senra T, Arteaga E, Martinelli Filho M, Pita CG, Ávila LF, Parga Filho JR, Mady C, Kalil-Filho R, Bluemke DA, Rochitte CE.** Myocardial fibrosis detected by cardiac CT predicts ventricular fibrillation/ventricular tachycardia events in patients with hypertrophic cardiomyopathy. *J Cardiovasc Comput Tomogr. 2013 May-Jun;7(3):173-81.*

50. **Kim RJ, Fieno DS, Parrish TB, Harris K, Chen EL, Simonetti O, Bundy J, Finn JP, Klocke FJ, Judd RM.** Relationship of MRI delayed contrast enhancement to irreversible injury, infarct age, and contractile function. *Circulation. 1999 Nov 9;100(19):1992-2002.*

51. **Ashikaga H, Sasano T, Dong J, Zviman MM, Evers R, Hopenfeld B, Castro V, Helm RH, Dickfeld T, Nazarian S, Donahue JK, Berger RD, Calkins H, Abraham MR, Marbán E, Lardo AC, McVeigh ER, Halperin HR.** Magnetic resonance-based anatomical analysis of scar-related ventricular tachycardia: implications for catheter ablation. *Circ Res. 2007 Oct 26;101(9):939-47.*

52. **Mesubi O, Ahmad G, Jeudy J, Jimenez A, Kuk R, Saliaris A, See V, Shorofsky S, Dickfeld T.** Impact of ICD artifact burden on late gadolinium enhancement cardiac MR imaging in patients undergoing ventricular tachycardia ablation. *Pacing Clin Electrophysiol. 2014 Oct;37(10):1274-83.*

53. **Starek Z, Lehar F, Jez J, Scurek M, Wolf J, Kulik T, Zbankova A.** Esophageal positions relative to the left atrium; data from 293 patients before catheter ablation of atrial fibrillation. *Indian Heart J. 2018 Jan - Feb;70(1):37-44.*

54. **Lemola K, Sneider M, Desjardins B, Case I, Han J, Good E, Tamirisa K, Tsemo A, Chugh A, Bogun F, Pelosi F Jr, Kazerooni E, Morady F, Oral H.** Computed tomographic analysis of the anatomy of the left atrium and the esophagus: implications for left atrial catheter ablation. *Circulation. 2004 Dec 14;110(24):3655-60.*

55. **Kottkamp H, Piorkowski C, Tanner H, Kobza R, Dorszewski A, Schirdewahn P, Gerds-Li JH, Hindricks G.** Topographic variability of the esophageal left atrial relation influencing ablation lines in patients with atrial fibrillation. *J Cardiovasc Electrophysiol. 2005 Feb;16(2):146-50.*

56. **Cappato R, Calkins H, Chen SA, Davies W, Iesaka Y, Kalman J, Kim YH, Klein G, Natale A, Packer D, Skanes A.** Prevalence and causes of fatal outcome in catheter ablation of atrial fibrillation. *J Am Coll Cardiol. 2009 May 12;53(19):1798-803.*

57. **Kistler PM, Earley MJ, Harris S, Abrams D, Ellis S, Sporton SC, Schilling RJ.** Validation of three-dimensional cardiac image integration: use of integrated CT image into electroanatomic mapping

system to perform catheter ablation of atrial fibrillation. *J Cardiovasc Electrophysiol. 2006 Apr;17(4):341-8.*

58. **Malchano ZJ, Neuzil P, Cury RC, Holmvang G, Weichet J, Schmidt EJ, Ruskin JN, Reddy VY.** Integration of cardiac CT/MR imaging with three-dimensional electroanatomical mapping to guide catheter manipulation in the left atrium: implications for catheter ablation of atrial fibrillation. *J Cardiovasc Electrophysiol. 2006 Nov;17(11):1221-9.*

59. **Martinek M, Nesser HJ, Aichinger J, Boehm G, Purerfellner H.** Impact of integration of multislice computed tomography imaging into three-dimensional electroanatomic mapping on clinical outcomes, safety, and efficacy using radiofrequency ablation for atrial fibrillation. *Pacing Clin Electrophysiol. 2007 Oct;30(10):1215-23.*

60. **Kim RJ, Fieno DS, Parrish TB, Harris K, Chen EL, Simonetti O,.** Relationship of MRI delayed contrast enhancement to irreversible injury, infarct age, and contractile function. *Circulation. 1999; 100:1992–2002.*

61. **Bogun FM, Desjardins B, Good E, Gupta S, Crawford T, Oral H, et al.** Delayed-enhanced magnetic resonance imaging in nonischemic cardiomyopathy: utility for identifying the ventricular arrhythmia substrate. *J Am Coll Cardiol. 2009; 53:1138–1145.*

62. **Luetkens JA, Homsi R, Sprinkart AM, Doerner J, Dabir D, Kuetting DL, et a.** Incremental value of quantitative CMR including parametric mapping for the diagnosis of acute myocarditis. *Eur Heart J Cardiovasc Imaging. 2016; 17:154–161.*

63. **Sueyoshi E, Sakamoto I, Okimoto T, Hayashi K, Tanaka K, Toda G. et al.** Cardiac amyloidosis: typical imaging findings and diffuse myocardial damage demonstrated by delayed contrast-enhanced MRI. *Cardiovasc Intervent Radiol. 2006;29:710–712.*

64. **Andreu D, Berruezo A, Ortiz-Pérez JT, Silva E, Mont L, et al.** . Integration of 3D electroanatomic maps and magnetic resonance scar characterization into the navigation system to guide ventricular tachycardia ablation. *Circ Arrhythm Electrophysiol. 2011; 4:674–683.*

65. **Wijnmaalen AP, van der Geest RJ, van Huls van Taxis CF, Siebelink HM, Kroft LJ, Bax JJ, Reiber JH, Schalij MJ, Zeppenfeld K.** Head-to-head comparison of contrast-enhanced magnetic resonance imaging and electroanatomical voltage mapping to assess post-infarct scar characteristics in patients with ventricular tachycardias: real-time image integration and reversed registration. *Eur Heart J. 2011 Jan;32(1):104-14.*

66. **Komatsu Y, Cochet H, Jadidi A, Sacher F, Shah A, Derval N, et al.** Regional myocardial wall thinning at multidetector computed tomography correlates to arrhythmogenic substrate in postinfarction ventricular tachycardia: assessment of structural and electrical substrate. *Circ Arrhythm Electrophysiol. 2013 Apr;6(2):342-50.*

67. **Esposito A, Palmisano A, Antunes S, Maccabelli G, Colantoni C, Rancoita PMV, Baratto F, Di Serio C, Rizzo G, De Cobelli F, Della Bella P, Del Maschio A.** Cardiac CT With Delayed Enhancement in the Characterization of Ventricular Tachycardia Structural Substrate: Relationship

Between CT-Segmented Scar and Electro-Anatomic Mapping. *JACC Cardiovasc Imaging. 2016 Jul;9(7):822-832.*

68. **Desjardins B, Morady F, Bogun F.** Effect of epicardial fat on electroanatomical mapping and epicardial catheter ablation. *J Am Coll Cardiol. 2010 Oct 12;56(16):1320-7.*

69. **Cochet H, Komatsu Y, Sacher F, Jadidi AS, Scherr D, Riffaud M, Derval N, Shah A, Roten L, Pascale P, Relan J, Sermesant M, Ayache N, Montaudon M, Laurent F, Hocini M, Haïssaguerre M, Jaïs P.** Integration of merged delayed-enhanced magnetic resonance imaging and multidetector computed tomography for the guidance of ventricular tachycardia ablation: a pilot study. *J Cardiovasc Electrophysiol. 2013 Apr;24(4):419-26.*

70. **Tian J, Smith MF, Chinnadurai P, Dilsizian V, Turgeman A, Abbo A, Gajera K, Xu C, Plotnick D, Peters R, Saba M, Shorofsky S, Dickfeld T.** Clinical application of PET/CT fusion imaging for three-dimensional myocardial scar and left ventricular anatomy during ventricular tachycardia ablation. *J Cardiovasc Electrophysiol. 2009 Jun;20(6):567-604.*

71. **Rostamian A, Narayan SM, Thomson L, Fishbein M, Siegel RJ.** The incidence, diagnosis, and management of pulmonary vein stenosis as a complication of atrial fibrillation ablation. *J Interv Card Electrophysiol. 2014 Jun;40(1):63-74.*

72. **Thiagalingam A, Manzke R, D'Avila A, et al.** Intraprocedural volume imaging of the left atrium and pulmonary veins with rotational X-ray angiography: implications for catheter ablation of atrial fibrillation. *J Cardiovasc Electrophysiol.* 2008 Mar;19(3):293-300.

73. **Kriatselis C, Tang M, Nedios S, et al.** Intraprocedural reconstruction of the left atrium and pulmonary veins as a single navigation tool for ablation of atrial fibrillation: a feasibility, efficacy, and safety study. *Heart Rhythm.* 2009 Jun;6(6):733-41.

74. **Lehar, F, Starek, Z, Jez, J, Novak M, Wolf J, Kruzliak P, Kulik T, Zbankova A, Jancar R.** Rotational atriography of left atrium - A new imaging technique used to support left atrial radiofrequency ablation: A comparison of anatomical data of left atrium obtained from 3D rotational atriography and computed tomography. *2013, Intervencni a Akutni Kardiologie, 12(4), pp. 184-189* .

75. **Li JH, Haim M, Movassaghi B, et al.** Segmentation and registration of three-dimensional rotational angiogram on live fluoroscopy to guide atrial fibrillation ablation: a new online imaging tool. *Heart Rhythm.* 2009 Feb;6(2):231-7.

76. **Starek Z, Lehar F, Jez J, Wolf J, Kulik T, Kulikova A.** Comparison of radiation exposure, contrast agent consumption and cost effectiveness between computer tomography and 3D rotational angiography of the left atrium to guide catheter ablation in patients with atrial fibrillation. *2017, Biomedical Papers, 161, pp. S29-S34* .

77. **Kriatselis C, Tang M, Roser M, Fleck E, Gerds-Li H.** A new approach for contrast-enhanced X-ray imaging of the left atrium and pulmonary veins for atrial fibrillation ablation: rotational angiography during adenosine-induced asystole. *Europace. 2009 Jan;11(1):35-41.*

78. **Tang M, Kriatselis C, Ye G, Nedios S, Roser M, Solowjowa N, Fleck E, Gerds-Li JH.** Reconstructing and registering three-dimensional rotational angiogram of left atrium during ablation of atrial fibrillation. *Pacing Clin Electrophysiol. 2009 Nov;32(11):1407-16.*

79. **Starek Z, Lehar F, Jez J, Wolf J, Kulik T, Zbankova A, Novak M.** Periprocedural 3D imaging of the left atrium and esophagus: comparison of different protocols of 3D rotational angiography of the left atrium and esophagus in group of 547 consecutive patients undergoing catheter ablation of the complex atrial arrhythmias. *Int J Cardiovasc Imaging. 2016 Jul;32(7):1011-9.*

80. **Starek, Z., Lehar, F., Jez, J., Wolf J, Kulik, T., Kulikova, A.** Detailed analysis of the relationship between the left atrium and esophagus in patients prior to catheter ablation of atrial fibrillation: An analysis using 3D computed tomography. *2017, Biomedical Papers, 161, pp. S42-S49 .*

81. **Knecht S, Wright M, Akrivakis S, Nault I, Matsuo S, Chaudhry GM, Haffajee C, Sacher F, Lellouche N, Miyazaki S, Forclaz A, Jadidi AS, Hocini M, Ritter P, Clementy J, Haïssaguerre M, Orlov M, Jaïs P.** Prospective randomized comparison between the conventional electroanatomical system and three-dimensional rotational angiography during catheter ablation for atrial fibrillation. *Heart Rhythm. 2010 Apr;7(4):459-65.*

82. **Orlov MV, Ansari MM, Akrivakis ST, Jadidi A, Nijhof N, Natan SR, Wylie JV, Hicks A, Armstrong J, Jais P.** First experience with rotational angiography of the right ventricle to guide ventricular tachycardia ablation. *Heart Rhythm. 2011 Feb;8(2):207-11. .*

83. **Starek Z, Wolf J, Lehar F, Jez J, Kulik T, Kulikova A.** Feasibility and safety of right and left ventricular three-dimensional rotational angiography for guiding catheter ablation of ventricular arrhythmias. *Biomedical Papers, 2017, S35-S41.*

84. **Wolf J, Starek Z, Jez J, Lehar F, Lukasova M, Kulik T, Novak M.** Rotational angiography of left ventricle to guide ventricular tachycardia ablation. *Int J Cardiovasc Imaging. 2015 Jun;31(5):899-904.*

85. **Starek, Z., Wolf, J., Lehar, F., Jez J, Kulik, T., Kulikova, A.** Feasibility and safety of right and left ventricular three-dimensional rotational angiography for guiding catheter ablation of ventricular arrhythmias. *2017: Biomedical Papers, 161, pp. S35-S41 .*

86. **Wang SL, Ooi CG, Siu CW, Yiu MW, Pang C, Lau CP, Tse HF.** Endocardial visualization of esophageal-left atrial anatomic relationship by three-dimensional multidetector computed tomography "navigator imaging". *Pacing Clin Electrophysiol. 2006 May;29(5):502-8.*

87. **Haïssaguerre M, Jaïs P, Shah DC, Takahashi A, Hocini M, Quiniou G, Garrigue S, Le Mouroux A, Le Métayer P, Clémenty J.** Spontaneous initiation of atrial fibrillation by ectopic beats originating in the pulmonary veins. *N Engl J Med. 1998 Sep 3;339(10):659-66.*

88. **Haïssaguerre M, Jaïs P, Shah DC, Gencel L, Pradeau V, Garrigues S, Chouairi S, Hocini M, Le Métayer P, Roudaut R, Clémenty J.** Right and left atrial radiofrequency catheter therapy of paroxysmal atrial fibrillation. *J Cardiovasc Electrophysiol. 1996 Dec;7(12):1132-44.*

89. **Ghia KK, Chugh A, Good E, Pelosi F, Jongnarangsin K, Bogun F, Morady F, Oral H.** A nationwide survey on the prevalence of atrioesophageal fistula after left atrial radiofrequency catheter ablation. *J Interv Card Electrophysiol. 2009 Jan;24(1):33-6. .*

90. **Ejima K, Shoda M, Yagishita D, Futagawa K, Yashiro B, Sato T, Manaka T, Nakajima T, Ohmori H, Hagiwara N.** Image integration of three-dimensional cone-beam computed tomography angiogram into electroanatomical mapping system to guide catheter ablation of atrial fibrillation. *Europace. 2010 Jan;12(1):45-51.*

91. **Kobza R, Auf der Maur C, Kurtz C, Hoffmann A, Allgayer B, Erne P.** Esophagus imaging for radiofrequency ablation of atrial fibrillation using a dual-source computed tomography system: preliminary observations. *J Interv Card Electrophysiol. 2007 Sep;19(3):167-70.*

92. **Piorkowski C, Hindricks G, Schreiber D, Tanner H, Weise W, Koch A, Gerds-Li JH, Kottkamp H.** Electroanatomic reconstruction of the left atrium, pulmonary veins, and esophagus compared with the "true anatomy" on multislice computed tomography in patients undergoing catheter ablation of atrial fibrillation. *Heart Rhythm. 2006 Mar;3(3):317-27.*

93. **Kennedy R, Good E, Oral H, Huether E, Bogun F, Pelosi F, Morady F, Chugh A.** Temporal stability of the location of the esophagus in patients undergoing a repeat left atrial ablation procedure for atrial fibrillation or flutter. *J Cardiovasc Electrophysiol. 2008 Apr;19(4):351-5.*

94. **Daoud EG, Hummel JD, Houmsse M, Hart DT, Weiss R, Liu Z, Augostini R, Kalbfleisch S, Smith MC, Mehta R, Gangasani A, Raman SV.** Comparison of computed tomography imaging with intraprocedural contrast esophagram: implications for catheter ablation of atrial fibrillation. *Heart Rhythm. 2008 Jul;5(7):975-80.*

95. **Nölker G, Gutleben KJ, Marschang H, Ritscher G, Asbach S, Marrouche N, Brachmann J, Sinha AM.** Three-dimensional left atrial and esophagus reconstruction using cardiac C-arm computed tomography with image integration into fluoroscopic views for ablation of atrial fibrillation: accuracy of a novel modality in comparison with multislice computed tomo. *Heart Rhythm. 2008 Dec;5(12):1651-7.*

96. **Starek Z, Lehar F, Jez J, Zbankova A, Kulík T, Wolf J, Novak M.** Long-term mobility of the esophagus in patients undergoing catheter ablation of atrial fibrillation: data from computer tomography and 3D rotational angiography of the left atrium. *J Interv Card Electrophysiol. 2016 Aug;46(2):81-7.*

97. **Orlov MV, Hoffmeister P, Chaudhry GM, et al.** Three-dimensional rotational angiography of the left atrium and esophagus--A virtual computed tomography scan in the electrophysiology lab? *Heart Rhythm.* 2007 Jan;4(1):37-43.

98. **Sherzer AI, Feigenblum DY, Kulkarni S, Pina JW, Casey JL, Salka KA, Simons GR.** Continuous nonfluoroscopic localization of the esophagus during radiofrequency catheter ablation of atrial fibrillation. *J Cardiovasc Electrophysiol. 2007 Feb;18(2):157-60.*

99. **Good E, Oral H, Lemola K, Han J, Tamirisa K, Igic P, Elmouchi D, Tschopp D, Reich S, Chugh A, Bogun F, Pelosi F Jr, Morady F.** Movement of the esophagus during left atrial catheter ablation for atrial fibrillation. *J Am Coll Cardiol. 2005 Dec 6;46(11):2107-10.*

100. **Starek Z, Lehar F, Jez J, Scurek M, Wolf J, Kulik T, Zbankova A, Novak M.** Three-dimensional rotational angiography of the left atrium and the oesophagus: the short-term mobility of the oesophagus and the stability of the fused three-dimensional model of the left atrium and the oesophagus during catheter ablation for atrial fibr. *Europace. 2017 Aug 1;19(8):1310-1316.*

101. **Stárek Z, Lehar F, Jež J, Wolf J, Novák M.** 3D X-ray imaging methods in support catheter ablations of cardiac arrhythmias. *Int J Cardiovasc Imaging.* 2014 Oct;30(7):1207-23.

102. **Lehar F, Starek Z, Jez J, Novak M, Wolf J, Stepanova R, Kruzliak P, Kulik T, Zbankova A, Jancar R, Vitovec J.** Comparison of clinical outcomes and safety of catheter ablation for atrial fibrillation supported by data from CT scan or three-dimensional rotational angiogram of left atrium and pulmonary veins. *Biomed Pap Med Fac Univ Palacky Olomouc Czech Repub.* 2015 Dec;159(4):622-8.

103. **Orlov MV, Jais P, O'Neill M, Akrivakis ST, Wright M, Jadidi AS, et al.** First experience with ElectroNav: combining anatomy and electrograms for AF ablation. *Heart Rhythm. 2010;7(Suppl):328–329.*

4 VÝSLEDKY – PUBLIKOVANÉ VĚDECKÉ PRÁCE

4.1 Esophageal positions relative to the left atrium; data from 293 patients before catheter ablation of atrial fibrillation.

4.2 Detailed analysis of the relationship between the left atrium and esophagus in patients prior to catheter ablation of atrial fibrillation: an analysis using 3D computed tomography

4.3 Periprocedural 3D imaging of the left atrium and esophagus: comparison of different protocols of 3D rotational angiography of the left atrium and esophagus in group of 547 consecutive patients undergoing catheter ablation of the complex atrial arrhythmias.

4.4 Rotational atriography of left atrium - A new imaging technique used to support left atrial radiofrequency ablation: A comparison of anatomical data of left atrium obtained from 3D rotational atriography and computed tomography

4.5 Comparison of clinical outcomes and safety of catheter ablation for atrial fibrillation supported by data from CT scan or three-dimensional rotational angiogram of left atrium and pulmonary veins

4.6 Comparison of radiation exposure, contrast agent consumption and cost effectiveness between computer tomography and 3D rotational angiography of the left atrium to guide catheter ablation in patients with atrial fibrillation

4.7 Rotational angiography of left ventricle to guide ventricular tachycardia ablation.

4.8 Feasibility and safety of right and left ventricular three-dimensional rotational angiography for guiding catheter ablation of ventricular arrhythmias

4.9 Long-term mobility of the esophagus in patients undergoing catheter ablation of atrial fibrillation: data from computer tomography and 3D rotational angiography of the left atrium.

4.10 Three-dimensional rotational angiography of the left atrium and the oesophagus: the short-term mobility of the oesophagus and the stability of the fused three-dimensional model of the left atrium and the oesophagus during catheter ablation for atrial fibrillation.

Indian Heart Journal 70 (2018) 37–44

Contents lists available at ScienceDirect

Indian Heart Journal

journal homepage: www.elsevier.com/locate/ihj

Original article

Esophageal positions relative to the left atrium; data from 293 patients before catheter ablation of atrial fibrillation

Zdenek Starek[*,a,b], Frantisek Lehar[a,b], Jiri Jez[a,b], Martin Scurek[a,b], Jiri Wolf[a,b], Tomas Kulik[a,b], Alena Zbankova[a,b]

[a] International Clinical Research Center, 1 st Department of Internal Medicine – Cardioangiology, St. Anne's University Hospital Brno, Pekarska 53, 656 91 Brno, Czech Republic

[b] Masaryk University, Faculty of Medicine, Kamenice 5, 625 00 Brno, Czech Republic

ARTICLE INFO

Article history:
Received 13 November 2016
Accepted 23 June 2017
Available online 29 June 2017

Keywords:
3D rotational angiography of the left atrium and esophagus
Position of esophagus to the left atrium
Image integration
Catheter ablation of atrial fibrillation
Atrioesophageal fistula
Shortterm mobility of the esophagus

ABSTRACT

Aims: Three-dimensional rotational angiography (3DRA) of the left atrium (LA) and the esophagus is a simple and safe method for analyzing the relationship between the esophagus and the LA during catheter ablation of atrial fibrillation. The purpose of this study is to describe the location of the esophagus relative to the LA and mobility of the esophagus during ablation procedure.
Methods: From 3/2011 to 9/2015, 3DRA of the LA and esophagus was performed in 326 patients before catheter ablation of atrial fibrillation. 3DRAwas performed with visualization of the esophagus via peroral administration of a contrast agent. The positions of the esophagus were determined at the beginning of the procedure, for part of patients also at the end of procedure with contrast esophagography.
Results: The most frequent position is behind the center of the LA (91 pts., 31.9%) The least frequent position is behind the right pulmonary veins (27 pts., 9.4%). The average shift of the esophagus position was 3.36 ± 2.15 mm, 3.59 ± 2.37 mm and 3.67 ± 3.23 mm for superior, middle and inferior segment resp.
Conclusions: The position of the esophagus to the LA is highly variable. The most common position of the esophagus relative to the LA is behind the middle and left part of the posterior wall of the LA. The least frequently observed position is behind the right pulmonary veins. No significant position change of esophagus motion from before to after the ablation procedure in the majority (≥95%) of the patients was observed.

1. Introduction

A catheter ablation of complex atrial arrhythmias, especially a catheter ablation for atrial fibrillation, has become the most common ablation.[1] Ablation procedures are performed in the complex anatomy of the left atrium[2] with the support of 3D electroanatomical mapping systems that create virtual 3D non-fluoroscopic maps of the left atrium[3] (CARTO, Biosense Webster, and EnSite Velocity, St. Jude Medical). Support of catheter ablations with a 3D X-ray model of the left atrium, mainly from CT, is currently often.[4] 3D rotational angiography (3DRA) of the left atrium represents a new alternative to CT cardiac imaging. This method is used mainly for left atrium imaging, but imaging of other cardiac and extracardiac structures is possible (cardiac ventricles,[5] esophagus).[6,7] Images created by rotational angiography of the heart are fully comparable with CT Images[6,8–10]. The final models of the left atrium are used to guide the creation of non-fluoroscopic 3D electroanatomical maps, direct fusion/integration with the 3D electroanatomical mapping system[4,9], and/or direct fusion/integration of a 3D model with live fluoroscopy.[4,10]

The esophagus is an important noncardiac structure that can be imaged with 3DRA.[6,7,11,12] During ablation on the posterior wall, which is in close anatomical relation with the esophagus,[13] an atrioesophageal fistula develops in 0.04% of cases.[2] An atrioesophageal fistula is the cause of almost 16% of all deaths related to catheter ablation of atrial fibrillation,[14] and it is fatal in 70 to 80% of cases.[14] A 3D model of the esophagus can be useful in preventing damage to this vulnerable structure during left atrial ablation.

The position of the esophagus from the CT of the heart have been described in a lot of works since 2004.[15–18] Some authors also proved longterm mobility of the esophagus comparing preprocedural CT of the left atrium and esophagus and 3DRA of the left

* Corresponding author.
E-mail address: zdenek.starek@fnusa.cz (Z. Starek).

http://dx.doi.org/10.1016/j.ihj.2017.06.013
0019-4832/

atrium with esophagus imaging or contrast esophagogram during ablation procedure.[6,12,19,20] Two works with small group of patients assessed position of the esophagus from the 3DRA of the left atrium and esophagus[6,12] and data about mobility of the esophagus during ablation procedure are ambiguous.[21,22]

The objective of this study is to describe the location of the esophagus relative to the left atrium and mobility of the esophagus during ablation procedure from large group of patients who underwent 3DRA of the left atrium with esophageal imaging.

2. Methods

2.1. Patient population

This retrospective study enrolled 326 consecutive patients who were referred for catheter ablation of atrial fibrillation and who underwent 3D rotational angiography of the left atrium with esophageal imaging in the period from March 2011 to September 2015. Thirty-three patients participated in prospective study dealing with periprocedural mobility of the esophagus – comparison of the position of the esophagus at the beginning and at the end of the procedure. The institutional review board approved the study protocol for this study, and written informed consent was obtained from these patients. Patients with a history of iodine allergy or with impaired renal function (glomerular filtration rate estimated using Modification of Diet in Renal Disease (MDRD) formula less than 45 ml/s/1.73 m^2) were excluded from the study.

2.2. Rotational angiography imaging

All 3DRA of the left atrium and esophagus were carried out with the Allura Xper FD 10 X-ray system (Philips Medical Systems Inc., Best, Netherlands). The basic principle of 3DRA is application of the contrast agent (Ultravist 370, Bayer Pharma AG, Berlin, Germany) to the atrium to acquire the rotational image. After opacification of the left atrium and pulmonary veins with the applied contrast agent, the C-arm is isocentrically rotated over 240° (from 120° right anterior oblique to 120° left anterior oblique) over 4.1 s with an X-ray acquisition speed of 30 frames per second. The patients are in a supine position during rotational imaging with the natural position of the arms along the body and normal breathing. Isocentering of the left atrium was achieved from the anteroposterior and left lateral X- ray projections with a maximally raised flat panel.

In total, we used three acquisition protocols: two right atrial protocols with different delays and one left atrial protocol.

Right atrial protocol. The contrast agent was injected using a pigtail catheter into the right atrium and after a certain delay (the time required for passage of the contrast agent through the pulmonary circulation into the left atrium), rotation of the C-arm commenced. The delay of the second protocol was individually adjusted by the system operator when the LA was filled with the contrast agent; an optimized second protocol has a fixed delay of 9 s.

Left atrial protocol. A pigtail catheter was introduced transseptally into the left atrium. A stimulation quadrupolar catheter was inserted into the right ventricle with a pacing threshold ≤5 mA/1.0 ms. After reducing the cardiac output with rapid stimulation of the ventricles (frequency of 230/min) with a drop in blood pressure that was verified by the disappearance of the pulse waveform from the saturation sensor at the distal finger phalanx of the right upper extremity (Philips IntelliVue MP-20, Philips, Eindhoven, The Netherlands), application of the contrast agent was initiated; with a delay of 2 s, we commenced the rotation of the C-arm.[8]

Opacification of the esophagus was achieved via oral administration of 20–30 ml of barium sulphate contrast agent (Micropaque, Guerbet, Roissy, France).[6,9] Swallowing of the contrast agent was initiated in both protocols 1 s. before starting the C-arm rotation. The time remaining until the start of rotation is visible on the angiogram. For protocol details, see Table 1.

At the end of the rotational angiography, the data were automatically transported to the workstation EP Navigator (EP Navigator 3.2, Philips Healthcare, Best, Netherlands). The 3DRA model of the left atrium was automatically reconstructed using the standard algorithms of the EP Navigator Workstation. The 3D model of the esophagus was manually segmented at the same workstation. See Fig. 1.

2.3. Current imaging of the position of the esophagus

To verify the position of the esophagus at the end of the procedure, contrast esophagography was performed. The esophagus was opacified using the oral administration of 20–30 ml of barium sulphate contrast agent, and the current localization of the esophagus was recorded on an X-ray screen with fused 3D model of the LA and the esophagus.

2.4. Qualitative image analysis

For a qualitative evaluation of the resulting models we classified two options: an optimal model', defined as a clearly segmented course of the esophagus with identifiable edges in most areas behind the left atrium, and a suboptimal model', where the course of the esophagus could not be reliably visualized. To determine the position of the esophagus to the atrium, we used a modified method according to Kottkamp et al.[13] For an assessment of the esophageal position, Kottkamp et al. used the grid structure on the CT model of the left atrium. We modified this method and divided the posterior wall of the left atrium and the adjacent pulmonary veins into five vertical columns, A–E, from left to right. Columns A and E were laterally behind the ostia of the pulmonary veins, column C was in the middle of the left atrial posterior wall and columns B and D were in intermediate positions. The course and

Table 1
Overview of the protocols.

	Right atrial protocol 1	Right atrial protocol 2	Left atrial protocol
Injected cavity	RA	RA	LA
Displayed cavity	LA	LA	LA
Amount of contrast agent [ml]	60	60	60
Velocity of injection [ml/s]	15	15	15
Delay [s]	Variable from 8937 s to 11.546 s(Ø 10.67 s)	Fixed 9	Fixed 2
Simulation of RV 220–240 [bpm]	no	no	yes
Succes rate with esophagus imaging	81.81% (9/11)	88.89% (112/126)	97.87% (184/189)

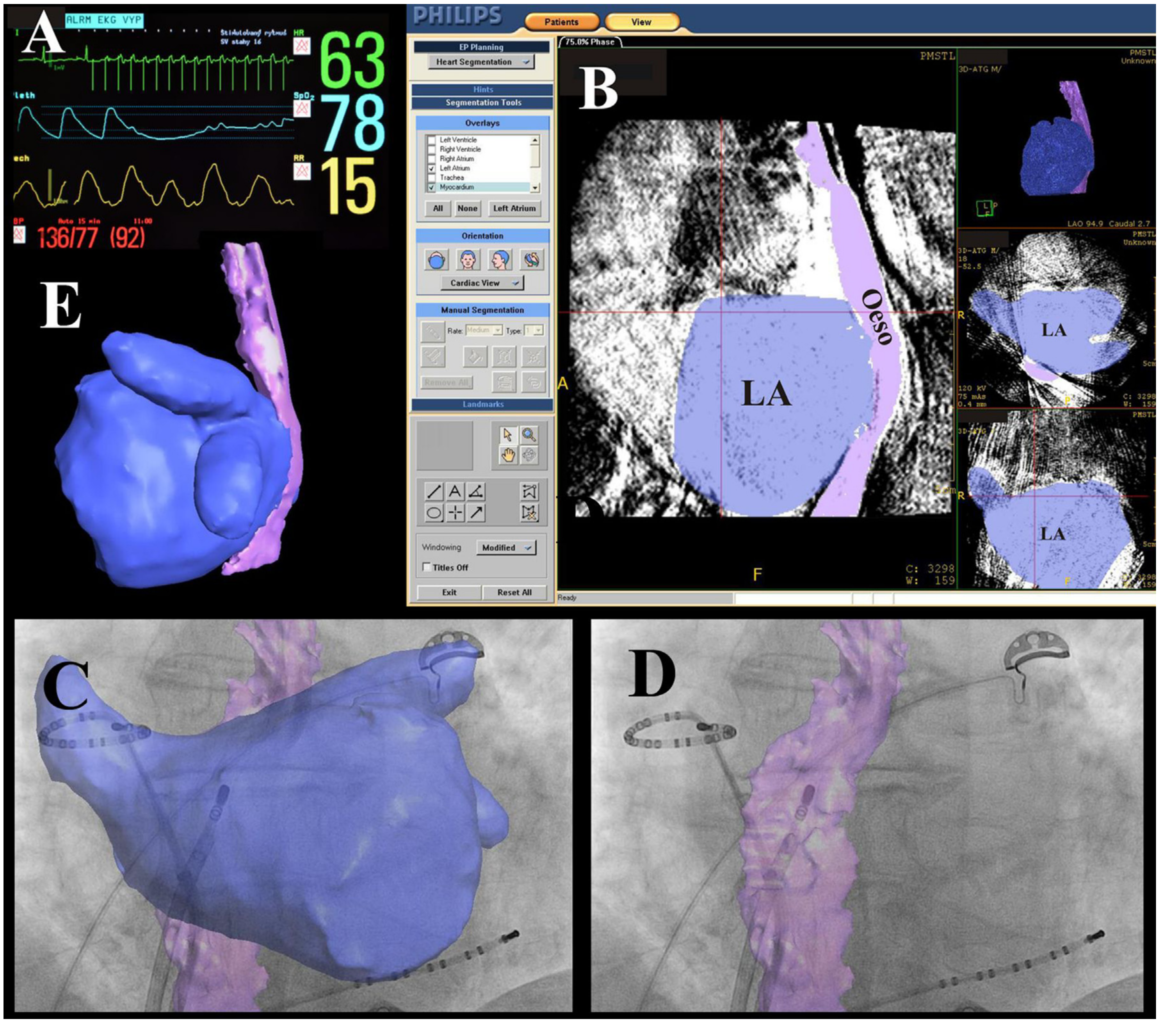

Fig. 1. Acquisition of the 3DRA data and the segmentation of the 3D model of the left atrium and esophagus. A – a reduction in the cardiac output with rapid stimulation of the ventricles (right ventricular pacing at 220/min.) documented by a decrease in saturation and the record from the bedside monitor. B – raw data from the 3D rotational angiography of the left atrium with segmentation of the 3D model. The picture shows a section of raw data in three mutually perpendicular planes and a preview of the resulting 3D model in the left lateral view. The blue color shows the automatic evaluation of the left atrial cavity; the purple color shows the manually segmented esophagus. C and D – examples of an application of the 3D model of the left atrium with visualized esophagus during the isolation of the pulmonary veins (anteroposterior view). The twenty pole circular catheter is introduced into the RSPV, and the tip of the ablation catheter is in sight of the resulting line on the posterior wall of the left atrium. The tip of the ablation catheter is inside the esophagus model. D – for greater clarity, the model of the left atrium is hidden. E – the final model of the left atrium and esophagus in the left lateral view. We can see the left-sided pulmonary veins, base of the auricle and the esophagus (in purple) adjoined to the posterior wall of the left atrium. LA – left atrium, oeso – esophagus, RSVP – right superior pulmonary vein.

location of the esophagus behind the left atrium was evaluated and described by one of the columns. In the case of an oblique course of the esophagus intersecting multiple columns, we determined the position of the esophagus according to the column where the largest part of the esophagus lies. In all patients with successful segmentation, the esophageal positions in relation to the left atrium were evaluated. See Fig. 2.

2.5. Quantitative imaging analysis

For purpose of our study, we set the shift of analyzed structure lesser than 5 mm as negligible. According to our experiences, shift lesser than 5 mm is non significant for the operator during atrial fibrillation ablation. Two experienced investigators measured the positions of the esophagus and LA. Each measurement was repeated three times to reduce the intra-individual variability, and the result was the average of these three measurements. Average of the two results measured by the two investigators was used for statistical analysis. Intraindividual and interindividual variability was calculated.

At the beginning of the procedure position of the 3D model of the esophagus fused with live fluoroscopy was measured. At the end of the procedure position of the contrast esophagogram was measured. The positions of both the 3D model of the esophagus and the contrast esophagogram were measured in the anteroposterior projection in the superior, middle and inferior segments of the esophagus, with the spine serving as a stationary reference structure. The superior segment of the esophagus corresponded to the highest level of the 3D model of the LA, the inferior segment corresponded to the bottom level of the LA 3D model, and the middle segment corresponded to the level between the upper and lower segments. For details see Fig. 3.

Measurements were performed using GIMP (a free program that enables measurements on JPG images, version 2.8.14, http://

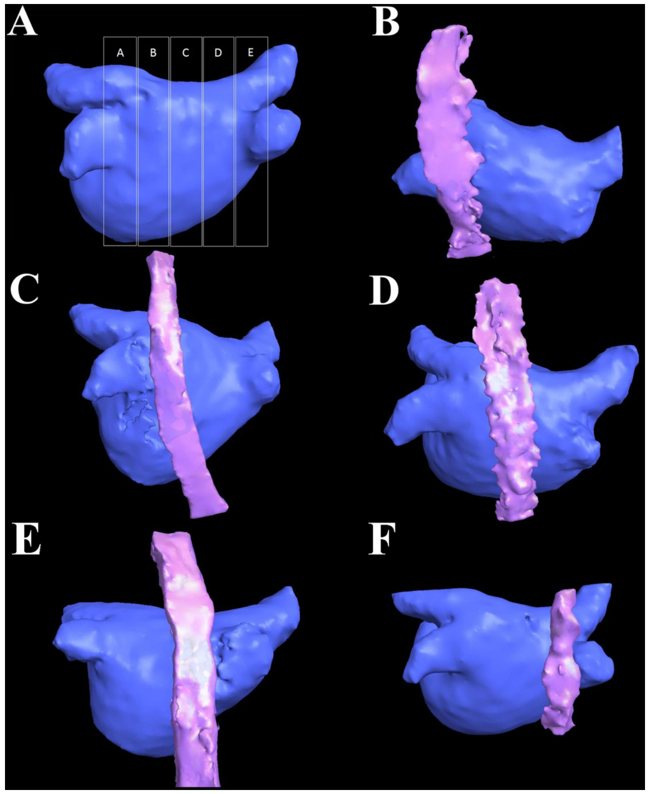

Fig. 2. A – methodology of the assessment of the esophageal position, B to F – examples of different positions of the esophagus in posteroanterior view, B – extremely left lateral position (A), C – left lateral position (B), D – middle position (C), E – right lateral position (D), F – extreme right lateral position (E).

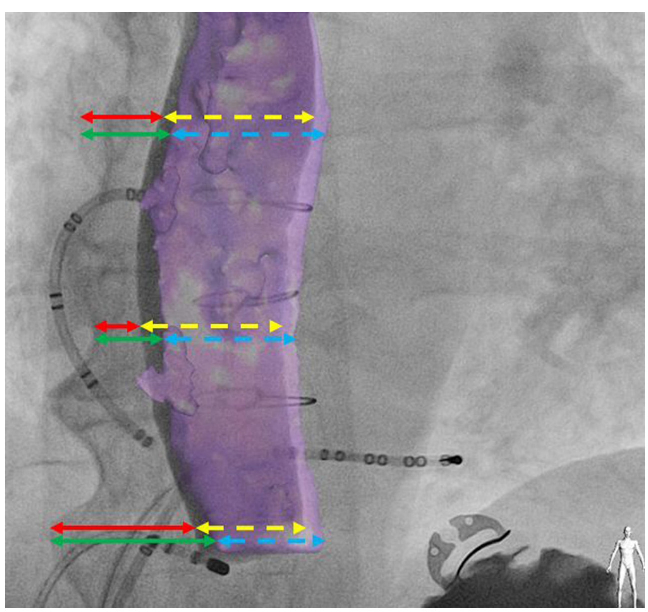

Fig. 3. Methodology of the esophageal shift measurement. Measurement of the position of the esophagogram and 3D model of the esophagus. Green arrows show the measurement of the position of the esophagus at the beginning of procedure (3D model of the esophagus) relative to the nearest vertebra. Red arrows show the measurement of the position of the esophagus at the end of procedure (contrast esophagogram) relative to the nearest vertebra. Blue arrows show the measurement of the width of the esophagus at the beginning of the procedure (3D model of the esophagus), yellow arrows show the measurement of the width of the esophagus at the end of the procedure (esophagogram). Picture shows the small shift of the esophagus by 0.8 mm at the top position, by 2.6 mm at the central position and by 2.1 mm at the lower position.

www.gimp.org/). We measured the distances from the vertebrae to the lateral wall of the esophagus and the width of the esophagus in all segments, which allowed us to calculate the position of the center of the esophagus in every segment.

We evaluated the position of the esophagus before and after the ablation – the shift of the position of the esophagus at the end of procedure (contrast esofagogram) in the left-right direction toward the input position (3D model of the esophagus acquired at the beginning of the procedure) (Fig. 4).

2.6. Image integration

The resulting 3DRA model of the left atrium was automatically integrated with live fluoroscopy. No registration for a 3D image overlay is necessary if the original X-ray table and the object's position that was imaged during 3DRA are maintained; the overlay takes place automatically within a few seconds. In the case of reregistration after patient movement or in the case of CT models, we use a standard carina-based registration procedure.[10] This technique uses the alignment of a reconstructed overlay and a live fluoroscopic image of the trachea and mainstem of the bronchi.

Ablation procedures were performed in a standard manner, and 3D models of the left atrium were used as support for the creation of 3D electroanatomical maps of the left atrium or for direct fusion with the 3D electroanatomical mapping system. All patients were ablated using an irrigated tip catheter guided by the 3D electroanatomical mapping system EnSite Velocity (St. Jude Medical, St. Paul, MN, USA).

2.7. Statistical analysis

At first, the positions of the esophagus were statistically analyzed by using the Kolmogorov-Smirnov test. The null hypothesis H0 ($\alpha = 0.05$) assumed that the distribution of the esophageal positions were drawn from the normal distribution. Consequently, the position of the esophagus in each group was analyzed by the Mann-Whitney *U* test. The null hypothesis H0 ($\alpha = 0.05$) assumed that there is no statistically significant difference between the esophageal position incidence in individual segments (real distribution of esophageal position in each segment vs. homogeneous distribution of esophageal position throughout all segments). Furthermore, an analysis was carried out in the second case where locations of the esophagus were divided into categories of left or right-sided incidences. The null hypothesis assumed a consistent incidence of the esophageal position in both groups.

The average distances of the esophagus from the spine were measured in three levels. Statistical analysis compares these distances in two time intervals (at the start and at the end of the procedure). The measured data was tested on normality by Kolmogorov k Smirnov test and subsequently they were evaluated by Wilcoxon Matched Pairs test. The null hypothesis H_0 ($\alpha = 0.05$) of this test assumed that there is no statistically significant difference in the mean shift in each level at various time intervals. Furthermore, the general average shift was computed in the three levels (depending on the time). These data were analyzed by *t*-test (against the reference constant). The null hypothesis H_0 ($\alpha = 0.05$) assumed that there is no statistically significant difference between the general average shift and the reference constant in milimetres.

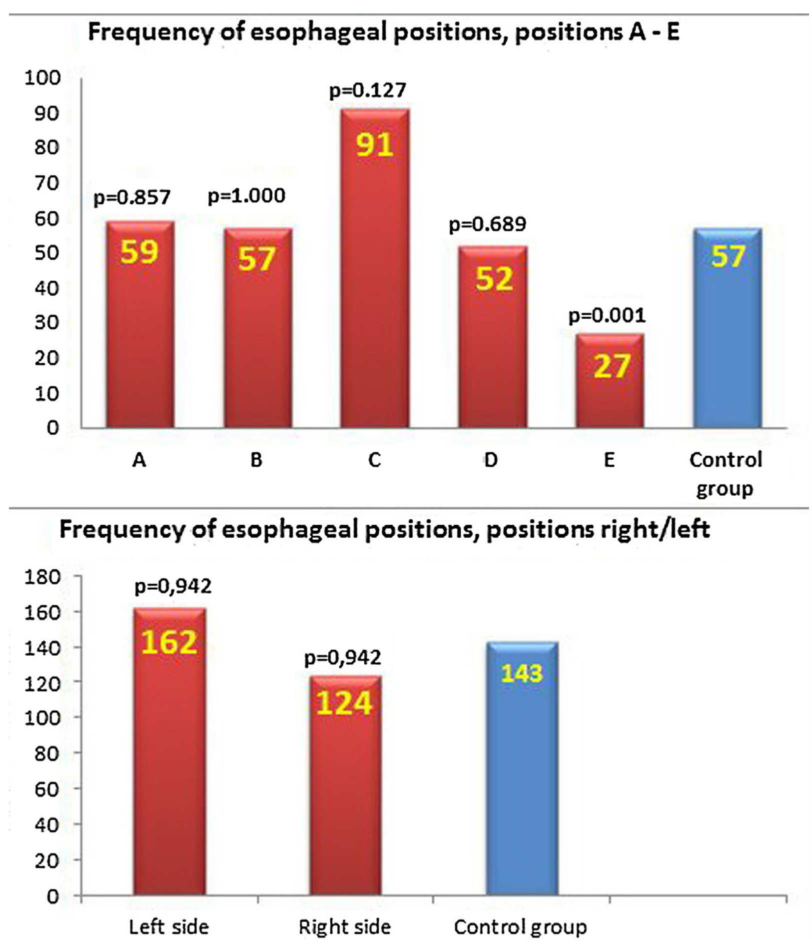

Fig. 4. Graphs of esophageal position frequency.

3. Results

In the period from March 2011 to September 2015, a total of 580 of 3DRA of left atrium in patients prior to catheter ablation of atrial fibrillation were performed. Three hundred twenty-six patients had 3DRA of the left atrium performed together with contrast 3D imaging of the esophagus. Last 33 patients (ablated from March 2015 to September 2015) participated in prospective study analyzing periprocedural mobility of the esophagus. The acquisition of data occurred without major complications. Direct left atrial injection of the contrast agent had no complications. No patients experienced aspiration of the oral contrast agents or other complications associated with the use of contrast agents dosed orally.

3.1. Patient characteristics

Characteristics of the patients including patients from study regarding periprocedural mobility of the esophagus are summarized in Table 2. Most patients were males with a mean age of 60 years and had no structural heart disease, with normal left ventricle function and slightly enlarged LA. The population of patients was highly homogeneous.

3.2. Rotational angiography image acquisition and qualitative image assessment

Only eleven patients underwent the first right atrial protocol (starting protocol with unsatisfactory success). After development of an optimized second right atrial protocol and after realizing a better success rate, we exclusively used this second protocol. From the beginning, we only used one left atrial protocol with a good success rate. Because both protocols have advantages and disadvantages, we used them simultaneously at the discretion of the electrophysiologist. The esophagus was successfully imaged in 87,7% of patients. The failure rate of imaging the esophagus was most often caused by delayed swallowing of the contrast agent or rapid passage through the esophagus.

In 286 patients with a successfully displayed esophagus and LA, we evaluated the position of the esophagus relative to the left atrium. The esophagus was positioned most frequently in the central part of the left atrium (column C, 91 pts., 31.9%), equivalently in the left part of the left atrium (column A, 59 pts., 20.6% and column B, 57 pts., 19.9% resp.) and least often in the right middle and especially in the right lateral part (column D, 52 pts., 18.2%, column E, 27 pts., 9.4% resp.). The significantly least frequent position of the esophagus occurred on the right side behind the right-pulmonary veins (27 pts., 9.4%, $p = 0.001$). The most often observed position of the esophagus that was seen in the middle of the posterior wall of the left atrium did not reach statistical significance (91 pts., 31.9%, $p = 0.127$). If we divide the position of the esophagus to the left atrium only at the position behind the left and right side of the left atrium (like in the study of Cury et al. [14]), then there is a trend towards a more frequent position of the esophagus behind the left vs. right-side of the left atrium (162 pts., 56.6%, $p = 0.942$ vs. 124 pts., 43.4%, $p = 0.942$ resp.). For details see Fig. 3. In our group, we observed the esophagi reaching a maximum of two adjacent segments. For example, see Fig. 2B and 2C, where models of the esophagus reach two adjoining segments.

3.3. Quantitative imaging analysis

Subgroup of 33 patients was subjected to analysis of the periprocedural change in esophagus position. Not in all patients were performed all measurements. Unfortunately, not all dimensions were measurable (unclear outline of the vertebra, esophagus model non- segmented up to the level of the vertebra, overlap of the esophagus model and vertebra). There are 7% of unmeasurable values during measurement (7 unmeasurable values from 99 values measured in the superior, middle and inferior segments of the esophagus). This data was excluded from calculation. Overwiev of esophageal shifts in an individual patients see Table 3.

Interobserver variability was 1.8 ± 1.5 mm. Intraobserver variability was 1.5 ± 1.3 mm.

The average duration of catheter ablation was 112 ± 43 min (time from sheat placement to catheter removal). The total execution time of the 3DRA of the LA and the esophagus including the manual segmentation of the esophagus was 9.92 min. The average radiation dose for all 3D rotational angiography was 11302.4 mGy/cm2, for 33 patients participated in periprocedural mobility substudy was 11204.3 mGy/cm2The average width of the esophagus was 18.8 ± 5.8 mm in the superior position, 19.5 ± 6.1 mm in the medium position and 16.9 ± 4.6 mm at the inferior position.

The average shift of the position of the esophagus during catheter ablation was 3.36 ± 2.15 mm, 3.59 ± 2.37 mm and 3.67 ± 3.23 mm for superior, middle and inferior segment resp. The shift of the esophagus during the procedure was significantly lower than 5 mm for all segments ($p < 0.001$, $p = 0.002$, $p = 0.04$, respectively)

The maximum shift of the esophagus was 11.9 mm, and the minimum shift was 0.1 mm. A shift of the esophagus $\geq$3 mm was present in 44.8% of the patients, and a shift of the esophagus $\geq$8 mm was present in 5% of the patients.

4. Discussion

Our results confirmed the findings of smaller studies based on CT data from a large sample of patients who underwent a different imaging modality. In the study of Kottkamp et al.,[12] the most common position of the esophagus was in the central part of the left atrium, with the next most common position being behind the left pulmonary veins and only a small portion observed on the right side. Additionally, Cury et al., [15] Lemola et al. 16 and several other studies examined in detail the relationship between the left atrium

Table 2
Patient characteristics.

Patient characteristics	3DRA of left atrium with imaging of esophagus	Right atrial protocol	Lef atrial protocol
Number of patients	326	137	189
Age	60.68 ± 9.44	59.7 ± 10.74	60.3 ± 10.78
Male	243 (74.54%)	96 (70.07%)	147 (77.77%)
Ejection fraction of left ventricle	57.01 ± 8.47	57.24 ± 8.38	57.18 ± 8.12
Size of left atrium	43.72 ± 5.72	44.72 ± 5.72	44.12 ± 5.89
Body mass index	28.95 ± 8.53	29.42 ± 5.55	29.02 ± 5.42
Structural heart disease	56 (17.18%)	30 (21.89%)	26 (13.75%)
Hypertension	170 (52.15%)	74 (54.01%)	96 (50.79%)

Table 3
Measurement of esophageal shifts in an individual patients.

Patients/measurement	sup	med	inf
1	2,3	2,7	2,7
2	2,2	2,3	1,2
3	7,3	7,9	7,1
4	1,9	3,9	1,8
5	3,2	3,1	6,2
6	7,7	5,5	3
7	1,4	4,5	2,6
8	3	4,6	8,2
9	1,2	2,7	1,4
10	2,1	4,4	7,7
11	2,5	1	1
12	N/A	1	2,2
13	N/A	0,9	N/A
14	1,3	1,8	0,3
15	0,9	1,6	3,4
16	3,5	2	N/A
17	4,5	1,8	11,6
18	0,4	3,4	2,9
19	6	4,9	1,4
20	3,8	4,6	11,9
21	3,9	4,1	1,8
22	1,8	5,9	4,3
23	2,7	0,2	1,9
24	1	2,9	1
25	2,3	5,7	N/A
26	6,8	1,5	1,6
27	3,4	2,9	1,3
28	5,5	N/A	N/A
29	1,1	2,8	2,1
30	7,7	8,9	8,5
31	1,8	1,1	5,3
32	5,3	4,1	1,3
33	5,9	10,5	1,1

and the esophagus [17–18] and reached similar conclusions. Previous works determined the position of the esophagus using different methods with similar results; the most frequent position of the esophagus is behind the left part of the left atrium.

It is well known that the position of the esophagus to the left atrium is not stable but may change over time. Longterm mobility of the esophagus has been proven in several works comparing periprocedural 3DRA with a preprocedural CT of the heart.[19,20] Interesting result of our work is that the position of the esophagus before and after procedure is a relatively stable within a few hours of the ablation procedure. No significant position change of esophagus motion from before to after the ablation procedure in the majority ($\geq$95%) of the patients was observed. Our findings confirm the results of Sherzer et al.,[21] who reported the stable position of the esophagus in a group of 27 patients undergoing 33 ablations for atrial fibrillation ablated under general anaesthesia. Our results suggest that the position of the esophagus behaves similarly in patients ablated under light sedation. Current study did not confirm results of Daoud et al. or Good et al.,[19,22] which described significant mobility of the esophagus position during these procedures. The cause of this inconsistency is not clear, as both works compared two contrasting esophagograms acquired during catheter ablation for atrial fibrillation conducted under light sedation.

5. Limitations

Comparison of the esophagus position at the beginning and at the end of procedure is limited by the fact that we measured the lumen of the esophagus, not the complete width of the organ (i.e. lumen and wall), during esophagography. According to our data of the long-term mobility of the esophagus,[20] there were no significant differences between the width of the esophagus from 3DRA (esophagography, imaging of the lumen of the esophagus) and CT imaging of the whole esophagus (average widths of 17.13 $\pm$ 4.3 mm and 15.89 $\pm$ 4.03 mm, respectively).[20] In this paper we compared the preprocedural CT of the heart and esophagus (static imaging of the whole esophagus including lumen and wall) and the periprocedural 3DRA of the LA and the esophagus (dynamic imaging of the esophagus lumen during esophagography). This width was in the range of the widths of the esophagus reported in studies dealing with the detailed anatomy of the esophagus and the left atrium using CT data (from 11 to 24 mm).[15,16] Swallowing the contrast agent in 3DRA appears to compensate for the thickness of the esophageal muscle (which is usually $<$5 mm[16]), and the resulting esophagogram approximates the actual esophagus displayed by CT.

In the study, we determined the esophagus position relative to the spine. Hence the esophagus does not change position before and after the ablation procedure with respect to the spine, but not with respect to the left atrium.

Only a two time point measurement of the esophagus was performed which may in turn fail to observe esophagus motion during the ablation.

There is limited number of measurable values. Despite the 7% of unmeasurable values, the results are statistically significant.

Two-dimensional measurements were done in anteroposterior projection and no conclusions about mobility of the esophagus in saggital plane were done.

One of the limitations of the technique is that most of the ablation procedures nowadays are performed under general anaesthesia and oral contrast can not be given to sedated patient.

There exists a concern that swallowing the barium contrast agent could stimulate the motility of the esophagus and increase its mobility. However, this effect has not been demonstrated during the routine investigations of esophageal mobility.[23] Swallowing the barium contrast agent could cause also transient position or volume changes. Also free breathing during imaging of the esophagus can cause artifacts and the esophagus does move with respiration, even though it is only a couple millimeter.

There is a question, if data regarding esophagus mobility are transferable to the general public due to the limited number of esophagus mobility measurements.

6. Conclusion

Imaging of the esophagus in 3D rotational angiography of the left atrium is a simple and safe method that can reliably locate the actual position of the esophagus relative to the left atrium. The most frequently observed position of the esophagus is the middle position behind the middle part of the left atrial posterior wall, and the least frequent position of the esophagus is the right lateral position behind the right pulmonary veins. The most frequently observed position of the esophagus is behind the left part of the left atrium. There was no significant change in the position of the esophagus before and after the procedure during the ablation procedure lasting in average almost two hours with patients in light sedation.

Funding

Supported by the project no. LQ1605 from the National Program of Sustainability II and Masaryk University, Faculty of Medicine, Kamenice 5, 625 00 Brno, Czech republic

Declaration of conflicting interests

The authors declare that they have no conflicts of interest.

References

1. Calkins H, Kuck KH, Cappato R, et al. HRS/EHRA/ECAS expert consensus statement on catheter and surgical ablation of atrial fibrillation: recommendations for patient selection, procedural techniques, patient management and follow-up, definitions, endpoints, and research trial design. *J Interv Card Electrophysiol*. 2012;33:171–257.
2. Cappato R, Calkins H, Chen SA, et al. Updated worldwide survey on the methods, efficacy, and safety of catheter ablation for human atrial fibrillation. *Circ Arrhythm Electrophysiol*. 2010;3:32–38.
3. Gepstein L, Hayam G, Ben-Haim SA. A novel method for nonfluoroscopic catheter-based electroanatomical mapping of the heart. In vitro and in vivo accuracy results. *Circulation*. 1997;95:1611–1622.
4. (a) Stárek Z, Lehar F, Jež J, et al. 3D X-ray imaging methods in support catheter ablations of cardiac arrhythmias. *Int J Cardiovasc Imaging*. 2014;30:1207–12235;
(b) Wolf J, Starek Z, Jez J, et al. Rotational angiography of left ventricle to guide ventricular tachycardia ablation. *Int J Cardiovasc Imaging*. 2015;31:899–904.
6. Orlov MV, Hoffmeister P, Chaudhry GM, et al. Three-dimensional rotational angiography of the left atrium and esophagus—a virtual computed tomography scan in the electrophysiology lab? *Heart Rhythm*. 2007;4:37–43.
7. Starek Z, Lehar F, Jez J, et al. Periprocedural 3D imaging of the left atrium and esophagus: comparison of different protocols of 3D rotational angiography of the left atrium and esophagus in group of 547 consecutive patients undergoing catheter ablation of the complex atrial arrhythmias. *Int J Cardiovasc Imaging*. 2016;26: [Epub ahead of print].
8. Lehar F, Starek Z, Jez J, et al. Comparison of clinical outcomes and safety of catheter ablation for atrial fibrillation supported by data from CT scan or three-dimensional rotational angiogram of left atrium and pulmonary veins. *Biomed Pap Med Fac Univ Palacky Olomouc Czech Repub*. 2015;159:622–628.
9. Thiagalingam A, Manzke R, D'Avila A, et al. Intraprocedural volume imaging of the left atrium and pulmonary veins with rotational X-ray angiography: implications for catheter ablation of atrial fibrillation. *J Cardiovasc Electrophysiol*. 2008;19:293–300.
10. Li JH, Haim M, Movassaghi B, et al. Segmentation and registration of three-dimensional rotational angiogram on live fluoroscopy to guide atrial fibrillation ablation: a new online imaging tool. *Heart Rhythm*. 2009;6:231–237.
11. Knecht S, Wright M, Akrivakis S, et al. Prospective randomized comparison between the conventional electroanatomical system and three-dimensional rotational angiography during catheter ablation for atrial fibrillation. *Heart Rhythm*. 2010;7:459–465.
12. Nölker G, Gutleben KJ, Marschang H, et al. Three-dimensional left atrial and esophagus reconstruction using cardiac C-arm computed tomography with image integration into fluoroscopic views for ablation of atrial fibrillation: accuracy of a novel modality in comparison with multislice computed tomo. *Heart Rhythm*. 2008;5:1651–1657.
13. Kottkamp H, Piorkowski C, Tanner H, et al. Topographic variability of the esophageal left atrial relation influencing ablation lines in patients with atrial fibrillation. *J Cardiovasc Electrophysiol*. 2005;16:146–150.
14. Cappato R, Calkins H, Chen SA, et al. Prevalence and causes of fatal outcome in catheter ablation of atrial fibrillation. *J Am Coll Cardiol*. 2009;53:1798–1803.
15. Cury RC, Abbara S, Schmidt S, et al. Relationship of the esophagus and aorta to the left atrium and pulmonary veins: implications for catheter ablation of atrial fibrillation. *Heart Rhythm*. 2005;2:1317–1323.
16. Lemola K, Sneider M, Desjardins B, et al. Computed tomographic analysis of the anatomy of the left atrium and the esophagus: implications for left atrial catheter ablation. *Circulation*. 2004;110:3655–3660.
17. Jang SW, Kwon BJ, Choi MS, et al. Computed tomographic analysis of the esophagus, left atrium, and pulmonary veins: implications for catheter ablation of atrial fibrillation. *J Interv Card Electrophysiol*. 2011;32:1–6.
18. Maeda S, Iesaka Y, Uno K, et al. Complex anatomy surrounding the left atrial posterior wall: analysis with 3D computed tomography. *Heart Vessels*. 2012;27:58–64.
19. Daoud EG, Hummel JD, Houmsse M, et al. Comparison of computed tomography imaging with intraprocedural contrast esophagram: implications for catheter ablation of atrial fibrillation. *Heart Rhythm*. 2008;5:975–980.
20. Stárek Z, Lehar F, Jež J, et al. Long-term mobility of the esophagus in patients undergoing catheter ablation of atrial fibrillation: data from computer tomography and 3D rotational angiography of the left atrium. *J Interv Card Electrophysiol*. 2016;12: [Epub ahead of print].
21. Sherzer AI, Feigenblum DY, Kulkarni S, et al. Continuous nonfluoroscopic localization of the esophagus during radiofrequency catheter ablation of atrial fibrillation. *J Cardiovasc Electrophysiol*. 2007;18:157–160.
22. Good E, Oral H, Lemola K, et al. Movement of the esophagus during left atrial catheter ablation for atrial fibrillation. *J Am Coll Cardiol*. 2005;46:2107–2710.
23. Summerton SL. Radiographic evaluation of esophageal function. *Gastrointest Endosc Clin N Am*. 2005;15:231–242.

Detailed analysis of the relationship between the left atrium and esophagus in patients prior to catheter ablation of atrial fibrillation: an analysis using 3D computed tomography

Zdenek Starek, Frantisek Lehar, Jiri Jez, Jiri Wolf, Tomas Kulik, Alena Kulikova

Background. Damage to the esophagus during radiofrequency ablation of atrial fibrillation can result in fatal atrio-esophageal fistula. Our aim is to describe the relationship of the left atrium (LA) and esophagus with a focus on contact of the posterior wall (PW) of the LA and the esophagus.
Methods. From 9/2011 to 8/2012, CT of the heart was performed in 56 patients undergoing catheter ablation of atrial fibrillation using CT GE Lightspeed VCT 64 by nongated standard protocol. Positions of the esophagus to the LA, width of the esophagus and contact with the PW of the LA were determined.
Results. The most frequent position of the esophagus was behind the left side of the LA. The average width of the esophagus was 16.0 ± 4.1 mm, and the average distance between the PW and esophagus was 4.8 ± 1.6 mm. On average, 50 ± 4.11 mm of the PW was in close contact with the esophagus. The average length of the fat pad between the esophagus and LA was 9.1 ± 5.5 mm in the upper part of the LA and 15.8 ± 7.3 mm at the bottom. Significantly longer contact occurred behind the right part of the LA.
Conclusions. The most common esophageal position is behind the left side of the LA. The esophagus is located in close contact by approximately 2/3 of the length and 1/4 of the width of the PW of the LA. The esophagus is more adjacent to the upper part of PW of the LA.

Key words: CT of the heart, left atrium and esophagus imaging, relationship of the left atrium and esophagus, catheter ablation of atrial fibrillation, atrioesophageal fistula

International Clinical Research Center, 1st Department of Internal Medicine – Cardioangiology, St. Anne's University Hospital Brno, Pekarska 53, 656 91 Brno, Czech Republic
Corresponding author: Zdenek Starek, e-mail: zdenek.starek@fnusa.cz

INTRODUCTION

Catheter radiofrequency ablation (RFA) of atrial fibrillation is currently the most effective, widely used therapeutic method. In recent years, it even became the most common ablation in the treatment of cardiac arrhythmias[1]. As an invasive, interventional procedure it is connected with a number of risks and potential complications[2]. One very serious, but fortunately rare, complication is atrioesophageal fistula resulting from a close anatomical relation of the posterior wall (PW) of the left atrium (LA) and the esophagus[3]. When this complication occurs within a few days after ablation, communication between the left atrium and esophagus emerges due to thermal damage to the wall of the left atrium and the esophagus with very serious consequences for the patient (a series of ablations can occur in the posterior wall of the left atrium during catheter ablation of atrial fibrillation, and the most common are circular lesions around the ostium of the pulmonary veins). Although atrio-esophageal fistula is rare with an incidence rate of 0.04% (ref.[2]), it is the cause of almost 16% of deaths in connection with catheter ablation of atrial fibrillation[4] and is fatal in 70-80% of cases[4,5]. Atrio-esophageal fistula was first described in connection with the perioperative surgical radiofrequency ablation[6], however, it soon appeared in the first reports of atrioesophageal fistula during percutaneous radiofrequency catheter ablation for atrial fibrillation[7]. Several works describe, in various ways, the relationship of the left atrium and the esophagus on anatomical preparations[3] or from CT data[8-10].

Our aim is to describe, in detail, the relationship between the posterior wall of the left atrium and the esophagus with a focus on objectification of the area of close contact between these structures.

METHODS

Patients

This retrospective study enrolled a group of 56 consecutive patients referred for catheter ablation of atrial fibrillation and examined those patients using a multislice CT of the heart and thorax from September 2011 to August 2012. The study received approval from the ethics committee of our institution.

CT imaging

A CT scan was performed before the procedure using the ECG nongated protocol on a 64-slice unit (GE Lightspeed VCT, General Electric, Fairfield, USA). The CT parameters included: 120 kV, 800 mAs, collimation of 63×0.625 mm, and a spiral pitch factor of 0.984. Image reconstruction was performed on a 512x512 pixel array.

Axial images were reconstructed with a slice thickness of 0,625 mm in 0.5 mm increments. The spatial resolution of the images is 0.574x0.574x0.625 mm. A contrast agent was administered through a peripheral vein; the amount of contrast was 100-150 ml (Ultravist 370, Bayer Pharma AG, Berlin, Germany or Iomeron 400, PNG Gerolymatos AEBE, Kryoneri - Athens, Greece). During the procedure, the patients held their arms up while holding their breath. The procedure was performed a few days before catheterization. The data were burned onto a CD-ROM, and during the procedure, a 3D reconstruction of the left atrium using a workstation EP Navigator (EP Navigator 3.1, Philips Healthcare, Best, The Netherlands) or software of the 3D electroanatomical navigation system (EnSite Velocity, St. Jude Medical, St. Paul, MN, USA) was created from the acquired data.

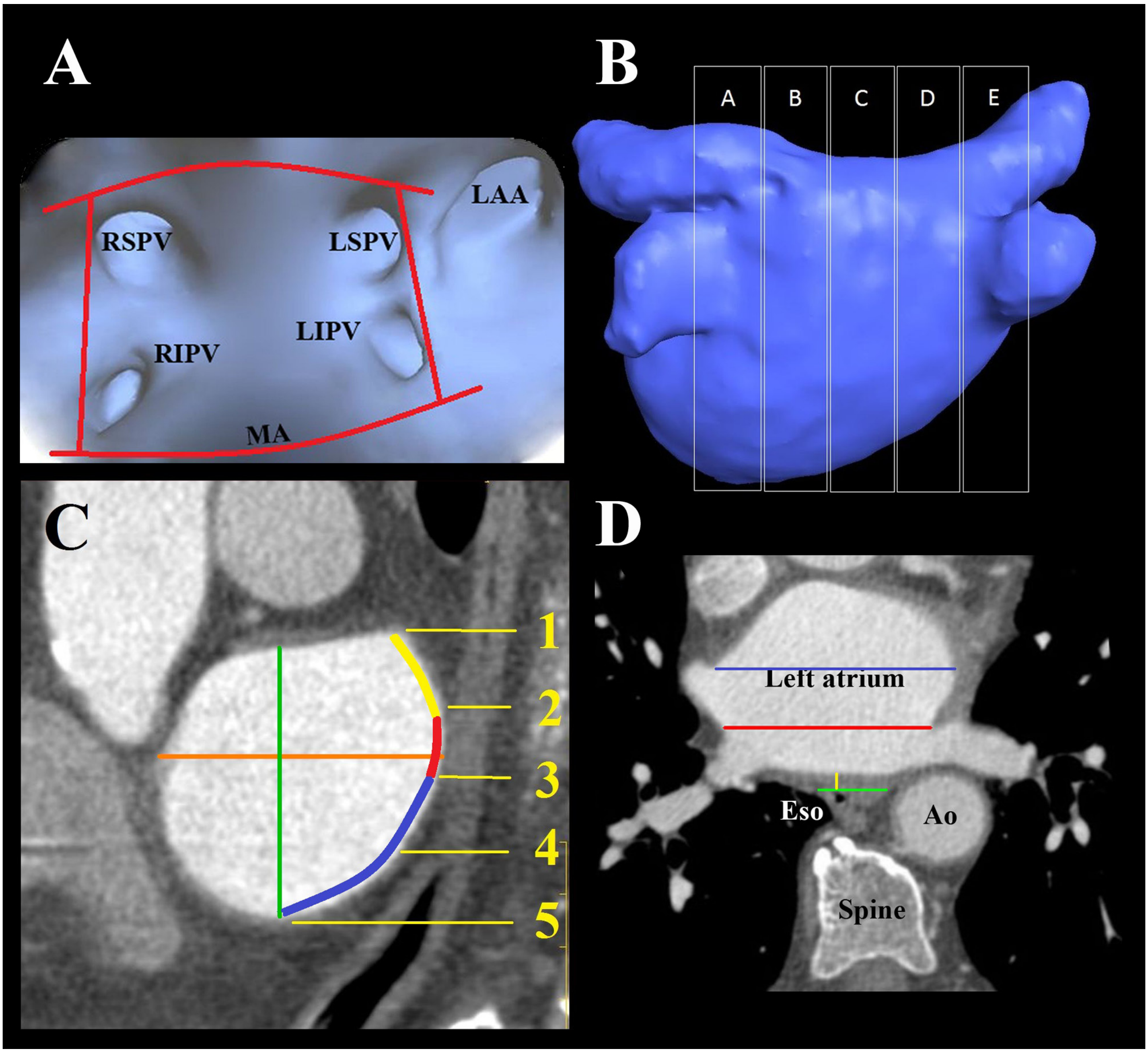

Fig. 1. (A) CT image from endovascular anteroposterior projection. Posterior wall of the LA was defined (red lines) by a superior line formed by the most superior points of the roof of the LA. The medial line tangential to the most medial (right-sided) points of the ostia of the right-sided PVs, a lateral line that was tangential to the most medial (left-sided) points of the ostia of the left-sided PVs, and an inferior line formed by the posterior mitral annulus or the most inferior points of the bottom of the LA, (B) Methodology of assessment of esophageal position, posteroanterior view, (C) Measurement in sagittal plane, the different levels in which the widths of the esophagus and the distance esophagus - LA were measured in the transverse plane, yellow lines 1-5, measurement of the depth of the LA (anteroposterior diameter), orange line, measurement of the height of the LA (superoinferior diameter), green line, measurement of the contact of the esophagus and LA, area of close contact is highlighted in red, superior segment of fat pad in yellow color, inferior segment in blue, (D) Measurement in the transversal plane, width of the LA (transverse diameter) blue line, width of the posterior wall of the LA, red line, width of the esophagus, green line, measurement of the distance of the esophagus and LA, yellow line. LSPV - left superior pulmonary vein, LIPV - left inferior pulmonary vein, RSPV - right superior pulmonary vein, RIPV - right inferior pulmonary vein, LAA - LA appendage, MA - mitral annulus.

Image evaluation

The obtained data were measured and evaluated offline at the workstation EP Navigator V 3.1 by one investigator (ZS). The intraobserver variability was 6 ± 3%.

To define the posterior wall of the left atrium, we used a modified methodology from Lemola et al.[9]. The posterior LA was outlined by (1) a superior line formed by the most superior points of the roof of the LA; (2) the medial line, which was tangential to the most medial (right-sided) points of the ostium of the right-sided PVs; (3) the lateral line, which was tangential to the most medial (left-sided) points of the ostia of the left-sided PVs; and (4) an inferior line formed by the posterior mitral annulus or the most inferior points of the bottom of the LA (see Fig. 1B). In contrast to the work of Lemola et al., our description of the posterior wall included the ostia of the pulmonary veins, as in some patients the esophagus may be located in an extreme position behind the ostium of the left or right sided pulmonary veins. The position of the esophagus against the PW of the LA was evaluated for each patient.

We performed a segmentation of the 3D model of the LA and esophagus, and in the coronal plane (anteroposterior projection), we evaluated the left-right position of the esophagus to the PW of the LA. To determine the position of the esophagus to the atrium, we used a modified method described by Kottkamp et al.[11]. To assess the esophageal position, Kottkamp et al. used a grid structure on the CT model of the left atrium. We modified this method and divided the posterior wall of the left atrium and adjacent pulmonary veins into five vertical columns, A – E from left to right. Columns A and E were laterally behind the ostia of the pulmonary veins, column C was in the middle of the left atrial posterior wall, and columns B and D were in the intermediate position. The course and location of the esophagus behind the left atrium was evaluated and was described by one of the columns. In the case of the oblique course of the esophagus intersecting multiple columns, we determined the position of the esophagus according to the column where the largest part of the esophagus lies. As a second option, we evaluated the simplified version of the description of the occurrence of the esophagus behind the left or right side of the left atrium as previously described by Cury et al.[8].

In the transverse and sagittal planes, we evaluated the width of the esophagus, the size and shape of the left atrium and the contact of the esophagus with the LA posterior wall. A fat pad between the LA and esophagus was identified by an abrupt change in the signal density.

Measurement included:

In the transverse plane

1. The width of the esophagus in five equidistant levels - at the level of the upper and lower borders of the PV of the LA, in the middle, and in the upper and lower quarters of the PV of the LA. Each level of the measurement was numbered 1-5 from top to bottom.

2. The width of the posterior wall of the left atrium - the distance of ostia of the left and right inferior pulmonary veins. This measurement was approximated to a certain extent, but the exact width measurement of the posterior wall was difficult to perform because an ostia of pulmonary veins could not be clearly determined. Our proposed measurement is easy and feasible, and the ostia of pulmonary veins were included into the width of the posterior wall. Thus, width of the PW covers the entire area which can be in contact with the esophagus.

3. The width of the left atrium (transverse diameter, TD) – the widest place in the transverse section in the same plane as the measurement of the width of the posterior wall.

4. Depth of the left atrium (anteroposterior diameter, APD) - the largest distance between the anterior and posterior walls of the left atrium in the sagittal section.

5. The height of the left atrium (superoinferior diameter, SID) - the largest distance between the top and bottom of the left atrium perpendicular to the depth of the left atrium in the sagittal plane.

6. Contact of the esophagus with the LA posterior wall measured in the transverse plane at the same levels as in the measurement of the width of the esophagus. We measured the distance from the lumen of the left atrium to the lumen of the esophagus. If the esophagus had collapsed, with no apparent luminal air density, then we determined the lumen as a half of the anteroposterior size of the esophagus.

In the sagittal plane

7. The length of the posterior wall of the left atrium measured from the transition of the LA roof into the posterior wall to the bottom of the left atrium or mitral annulus at the point of contact of the esophagus with the LA.

8. Length of close contact of the esophagus and posterior wall of LA, which we defined as the area where the esophagus is very close to the posterior wall of the left atrium, and between these structures, it was less than 1 mm of fat pad.

9. Length of fat pad - area of contact between the LA and esophagus in the upper and lower wedge-shaped part (upper and lower segments of the fat pad), where these structures are separated by a layer of muscle and an adipose tissue layer with a thickness greater than 1 mm. The length of the area with fat pad is always measured from the respective edge of the posterior wall.

These data were correlated with the left-right position of the esophagus, age, weight and sex of patients. We aimed to determine whether the LA morphology in the sagittal plane (the ratio of the height and depth, "roundness index") affects the nature of the contact of the LA posterior wall and esophagus. For further details of the measurements, please refer to Fig 1.

Statistical analysis

All data were tested using a normal distribution test at a significance level $\alpha = 0.05$. On the basis of the results of the tests for normal distribution, parametric analysis (a, b, d) or the non-parametric analysis (3c) was performed.

a) Analysis of the length of contact and length of fat pad above and below according to the "roundness index":

a statistical evaluation was performed using parametric correlation analysis (Pearson correlation coefficient).

b) Analysis of the length of contact and length of fat pad at the top and bottom according to the positions: a statistical evaluation was performed using analysis of variance (ANOVA) followed by post-hoc tests (LSD test and Tukey HSD test). All tests were performed at a significance level α = 0.05.

c) The statistical significance of individual positions: a statistical evaluation was performed using a non-parametric sign test at a significance level α = 0.05.

d) The width of the esophagus at various levels: a statistical evaluation was performed using a parametric t-test when the t-test was performed in relation to one reference constant diameter (significance level α = 0.05).

RESULTS

Patient population

From September 2011 to August 2012, 56 consecutive patients who had undergone catheter ablation of atrial fibrillation were examined using multislice CT of the heart. Approximately three-quarters of the patients were males with a mean age of 60 years and a BMI that was slightly over 29. Most patients had no structural heart disease, had normal left ventricle function and had a slightly enlarged left atrium of an average diameter of 45 mm. Half of the patients were ablated for paroxysmal atrial fibrillation. For further details, please see Table 1.

The position of the esophagus relative to the left atrium

The esophagus was positioned most frequently in the left central part of the left atrium (column B, 26 pts., 46.4%) and the left lateral part of the left atrium (column A, 16 pts., 28.6%). In the middle of the left atrial posterior wall was 17.9% of the esophagi (column C, 10 pts.). The esophagus was found least often in the right middle and, specifically, in the right lateral part (column D, 3 pts., 5.4%, column E, 1 pts., 1.8% resp.). The statistically significantly least often position of the esophagus occurred on the right side behind the right-pulmonary veins (*P*=0.001). The most common esophageal position was behind the left side of the posterior wall of the left atrium in column B (*P*=0.001).

If we divide the position of the esophagus by the left atrium only at the position behind the left and right sides of the left atrium, then, similar to the study of Cury et al.[8], the statistically most significant position of the esophagus is behind the left part of the left atrium (47 pts., 58.9% vs. 9 pts., 16%, *P*=0.001). In our group, we observed the esophagi reaching a maximum of two adjacent segments (Fig. 2).

Contact of the left atrium and esophagus

The average transverse diameter was 63.5 mm, the anteroposterior diameter was 48 mm, and the superoinferior diameter was 61 mm. The average width of the posterior wall was 56.1 mm. The average ratio of the anteroposterior diameter and superoinferior diameter, which is known as the "roundness index of the atrium", was 1.3 (0.94 to 2.04, median 1.28).

The average width of the esophagus was 15.97 ± 4.12 mm, and there was no statistically significant difference between the widths of the esophagus at various levels (*P*≥0.130) (see Table 2). The average length of the posterior wall was 75.3 ± 8.9 mm. An average of 50.4 ± 11 mm of the posterior wall was in very close contact with the esophagus (median 51.2 mm, range from 25.7 to 76.6 mm). The average distance of the esophagus from the LA posterior wall was 4.8 ± 1.6 mm. The distance of the

Table 1. Patient characteristics.

Patient characteristics	
Number of patients	56
Age	59.80 ± 9.59
Male	44 (78.57 %)
Ejection fraction of left ventricle	57.12 ± 7.95
Size of left atrium	45.20 ± 6.00
Body mass index	29.15 ± 4.33
Structural heart disease	6 (10.71 %)
Hypertension	27 (48.21 %)
Paroxysmal atrial fibrillation	29 (52.73 %)
Persistent atrial fibrillation	24 (43.64 %)
Long standing persistent atrial fibrillation	1 (1.82 %)
Atypical atrial flutter	1 (1.79 %)

Table 2. Width of the esophagus and distance of the esophagus-LA at each position.

Position of measurement	Average width of eso (mm)	Average distance eso - LA (mm)
1	15.23 ± 3.74	5.87 ± 2.44
2	15.70 ± 4.14	3.97 ± 1.29
3	15.89 ± 4.20	3.63 ± 0.95
4	16.45 ± 4.38	4.39 ± 1.30
5	16.56 ± 4.15	6.34 ± 2.12
Average 1 - 5	15.97 ± 4.12	4.84 ± 1.62
	P≥0.130	

eso - esophagus, LA - left atrium

Table 3. Correlation between the length of close contact and left-right distribution of positions of esophagus.

Position of esophagus	Number of cases (n)	Lenght of tight contact (mm)	Lenght of upper fat pad (mm)	Lenght of lower fat pad (mm)
A	16	50.5 ± 8.9	9.8 ± 5.8	16.8 ± 6.7
B	26	48.6 ±11.4	9.5 ± 5.8	15.8 ± 7.3
C	10	50.4 ± 10.4	8.6 ± 4.4	17.0 ± 7.6
D	3	*68.9 ± 7.1	*2.4 ± 2.1	*12.2 ± 7.8
E	1	40.9	10,1	15.9
		***P*=0.035**	*P*=0.291	*P*=0.314
Left	47	49.2 ± 10.4	9.6 ± 5.5	16.7 ± 7.3
Right	9	56.7 ± 12.5	6.7 ± 5.2	10.8 ± 5.6
		P=0.060	*P*=0.153	***P*=0.027**

esophagus and the LA was shorter in the central and superior part of the posterior wall; the esophagus is closest to the left atrium in plane No. 3 in the middle of the LA posterior wall, where the average distance was 3.63 ± 0.95 mm, while the most distant was in the inferior part of the posterior wall, where the average distance was 6.33 ± 2.11 mm. The measured values were statistically significantly different from the average value of 4.84 mm at each level (P<0.012) (see Table 2).

The fat pad between the esophagus and the left atrium was observed in all patients, and it was discontinuous in 98.3% of patients. In the middle part of the LA PW, the muscle of the esophagus was adjacent directly to the muscle of the left atrium. In only one patient (1.7%), a thin layer of fat pad was observed throughout the whole contact of the esophagus and posterior wall of the left atrium with a thickness from 0.8 to 0.9 mm. For the rest of the patients, the fat pad constituted wedge-shaped segments between the superior and inferior parts of the esophagus and the left atrium (see Fig. 3). The average length of the fat pad on the superior and inferior parts of the LA were 9.1 ± 5.5 mm and 5.8 ± 7.3 mm, respectively. The superior segment of the fat pad was statistically significantly shorter (P=0.001). There was no correlation between close contact length and the length of the segments of the fat pad in the superior and inferior parts (r=0.494, r=0.482, respectively).

Statistical analysis using correlation analysis did not reveal any effect of the shape of the LA in the sagittal plane, or "roundness index", on the contact of the esophagus with the posterior wall of the left atrium (r=0.106). No statistically significant correlation was found between the length of close contact of the esophagus and left atrium, the length of the superior segment of the fat pad and inferior segment of the fat pad and age (r=0.116, r=0.023, r=0.263), BMI (r=0.111, r=0.065, r=0.022), and gender (P=0.976, P=0.152, P=0.865).

Correlation of the length of close contact and length of the superior and inferior fat pads to the position of the esophagus towards the right atrium (the position behind the left atrium A - E and the position on the left or right) revealed statistically significant results. The length of close contact was significantly longer in column D (on average 68.9 ± 7.1 mm, n=3, P=0.035). This difference was also apparent when recalculated to the position of the esophagus on the left or right; however, it did not reach statistical significance (49.2 ± 10.4 mm on the left versus 56.7 ± 12.5 mm on the right, P=0.060).

Longer area of close contact in column D, or behind the right part of the left atrium, was given by shorter length of the superior and inferior segments of the fat pad. However, only shortening of the lower segment of the fat pad reached statistical significance (for details, please see Table 3).

For examples of LA PW contact with the esophagus, please see Fig. 4.

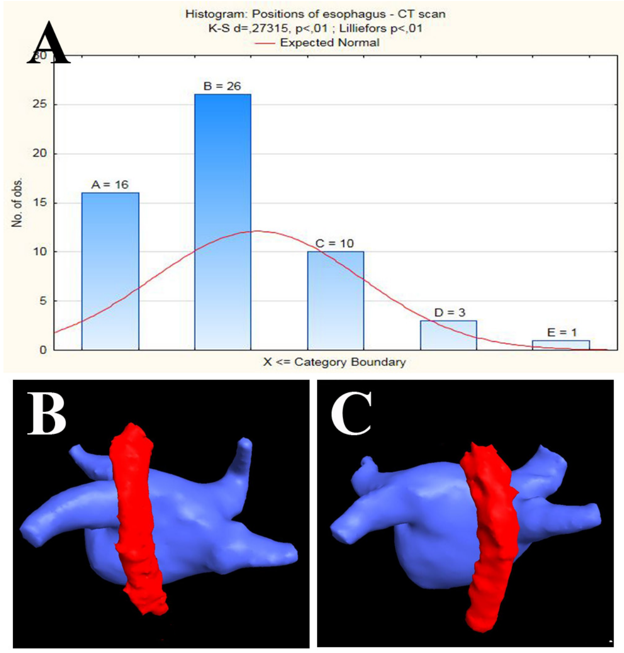

Fig. 2. (A) Graphs of esophageal position frequency, (B, C) Examples of different positions of the esophagus in the postero-anterior view, (B) Extremely left lateral position A, (C) Right lateral position B

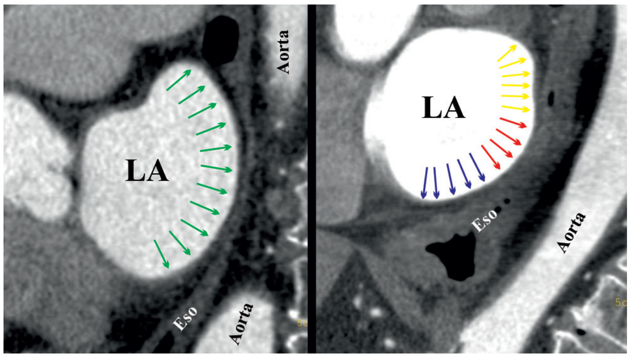

Fig. 3. Nature of fat pad. (A) Continuous fat pad extended throughout the entire length of contact of the left atrium and esophagus, green arrows, (B) Discontinuous fat pad, superior segment of fat pad is highlighted by yellow arrows, the inferior segment of the fat pad is highlighted by blue arrows, the area of direct contact of muscle of the esophagus with musculature of the left atrium is highlighted with red arrows.

DISCUSSION

Main findings

The position of the esophagus was significantly more often behind the left part of the left atrium, usually in position B. The average width of the esophagus was 15.97 mm, which was 28.6% of the width of the posterior wall of the left atrium. The esophagus was in very close contact with the posterior wall of the left atrium in the long section. According to our measurements, we obtained an average of 50.4 mm, which is an average of 66.9% of the length of the posterior wall.

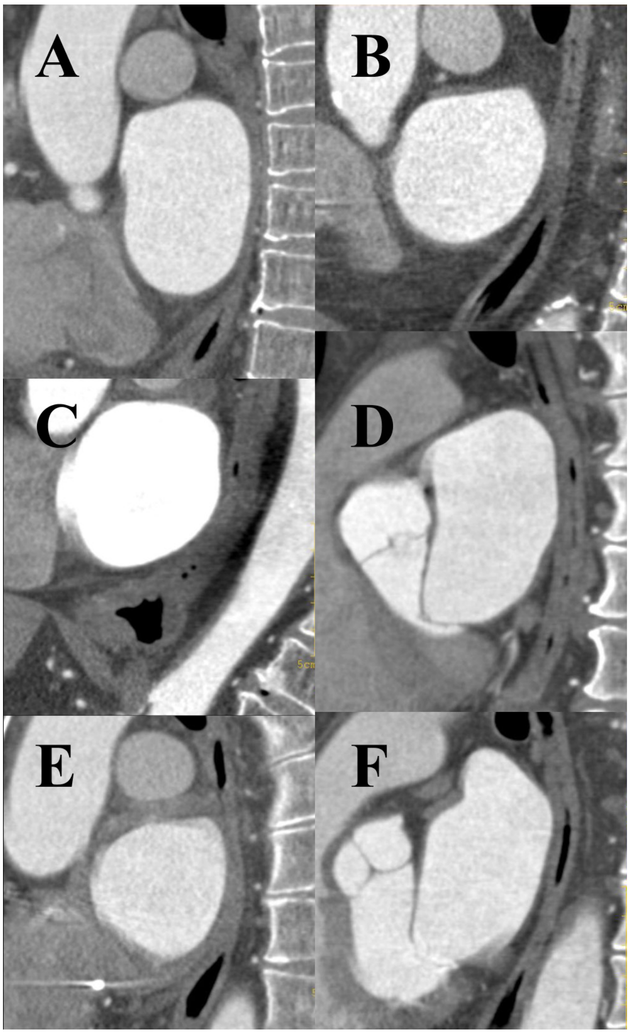

Fig. 4. Examples of different types of contact of the esophagus and left atrium, side view, (A) Maximum contact, the area of close contact goes virtually from the roof of the left atrium up to 3/4 of posterior wall of left atrium, (B) Minimal contact, esophagus and left atrium are in contact in a very short section of the upper third of the posterior wall of the left atrium, (C) Displacement of the area of close contact caudal direction, a short area of close contact is in the lower third of the posterior wall, (D) Shift of the area of close contact in cranial direction, long area of close contact begins completely cranially at the superior edge of the posterior wall and extends up to middle of the posterior wall, (E) Nature of the contact of the esophagus and left atrium in a patient with a "round atrium" with a ratio anteroposterior/superoinferior diameter of 0.94. The area of close contact was significantly shifted in the cranial direction and occupied a greater part of the length of the posterior wall, (F) Nature of the contact esophagus-left atrium in a patient with "flat atrium" with ratio anteroposterior/superoinferior diameter 2.04; the area of close contact was relatively short and was placed at 3/4 of the length of the posterior wall.

The fat pad between the esophagus and the posterior wall of the left atrium was observed in all patients, but in 98.3% of patients, it was discontinuous and the esophagus was adjacent to the muscle of the left atrium in the middle part of the posterior wall of the left atrium. The smallest average distance of the lumen of the esophagus from the LA lumen was only 3.63 mm and was observed in the middle part of the LA PW. The area of close contact between the left atrium and esophagus was shifted upwards to the superior edge of the posterior wall of the left atrium. The area of close contact was significantly longer for the esophagi located behind the right side of the left atrium. We did not find any clinical factors predicting the position of the esophagus and esophageal contact with the left atrium.

Position of the esophagus relative to the left atrium

In accordance with previous works[3,8-10,12,13], the esophagus is significantly more often positioned behind the left part of the left atrium and is typically in position B. Most studies have determined the position of the esophagus relative to the left atrium using a different method: by measuring the distance of the esophagus from spacing between the pulmonary veins in a transverse section[8-10,13]. However, these results are contradictory. For example, Cury et al.[8] observed that the most common esophageal position was behind the left part of the LA. Maeda et al.[13] divided the esophageal positions into A and B, respectively, A1, A2, B1 and B2, in the direction from the ostium of the left-sided pulmonary veins to the ostium of the right-sided pulmonary veins, where 74% of patients had an esophagus in group A1. Only Kottkamp et al.[11], who evaluated the position of the esophagus using a similar method as that described in our work, determined that the most common esophageal position was position C behind the middle part of the left atrium. Moreover, the vast majority of the other positions were in column A and B. The incidence of the esophagus behind the right side of the left atrium was generally minimal, ranging from 6% to 10% (ref.[9,13]).

Contact of the left atrium, esophagus and fat pad

The esophagus in our cohort of patients is in very close contact with the posterior wall of the left atrium and is sectioned long (on average 50.4 mm). In this area, the esophagus is in close contact with the LA PW without the fat pad in 98.3% of patients from our cohort. Our values are within the upper limit of the range of the results of previous studies, in which the average length of close contact was within a broad range (from 26.2 to 58.0 mm, extreme values of 5.4 mm and 97 mm) (ref.[9,12,10]). The new finding of our study is the asymmetry of areas with the fat pad. According to our measurements, the width of the superior segment is substantially shorter than the inferior segment (9.1 ± 5.5 vs. 15.8 mm ± 7.3 mm, P=0.001). These findings contrast with the work of Wang et al., where the length of the superior and inferior fat pads was similar (14.1 ± 7.2 mm and 13.82 ± 6.6 mm, respectively.)

In our cohort of patients, a shift in the area of close contact in the cranial direction to the superior edge of the posterior wall is evident. This shift also corresponds to the average distance of the lumen of the esophagus from the lumen of the left atrium, which are smaller in the superior part of the left atrium (see Table 2). These results are inconsistent with those obtained by Wang et al., who split the posterior wall of the left atrium into four quadrants and found that the esophagus is most often in contact with the inferior quadrants, particularly with the left inferior quadrant (98% of esophagi is in contact with this quadrant). The cause of this discrepancy is still unclear. However, these results are difficult to compare due to the use of different measurement methodologies. Our results are consistent with those of Ho et al.[3], such that anatomical preparations measured the thickness of the posterior LA wall within a range from 2.5 to 5.3 mm (mean, 4.1 ± 0.7 mm), and the distance between the endocardial surface of the left atrium and the esophageal wall is <5 mm in 40% of the 15 cadavers. Lemola et al.[9] indicated that the average shortest distance of the LA lumen and the lumen of the esophagus was 3.5 ± 1.0 mm. The average width of the esophagus is 16 mm, which is within the range of the width of the esophagus in previously published studies (from 11 to 24 mm) (ref.[8-10,12]).

Left-right distribution of close contact and prediction of contact from clinical factors

Another new element is the uneven distribution of the length of close contact, which is dependent on the left-right position of the esophagus to the left atrium. In our patients, we found a significantly longer area of close contact at the esophagi located behind the right side of the left atrium, particularly in column D. In these patients, close contact displacement in the cranial direction is maintained. The average length of the superior segment of the fat pad is only 2.4 mm. In this study, our results differ from those obtained in Wang et al.[12], which describes much more frequent contact of the esophagus with the inferior quadrants of the posterior left atrial wall, particularly with the left inferior quadrant (98% of the esophagi). However, the cause of this discrepancy is not clear. A limitation of our finding is the small number of patients with right-sided localization of the esophagus (column D, n=3, column E, n=1, right-sided localization n=9). If this finding could be confirmed in a larger cohort of patients, then it would be necessary to pay close attention during ablation in the vicinity of the right pulmonary veins along the entire length of the posterior wall of the left atrium.

Unfortunately, we could not define any clinical parameters (age, sex, BMI) predicting the nature of the contact of the esophagus and left atrium. The same conclusions were also obtained by Wang et al.[12], who observed the effect of gender on the width and length of the area of close contact, as well as Lemola et al.[9] who failed to prove any correlation between age, sex, BMI, and the size of the left atrium as well as the presence and thickness of the fat pad.

The esophagus is a mobile structure in both the long-[14,15] and short-term[16,17]. A static image of the esophagus itself has limited value. However, clinical effect of the adipose tissue (fat pad) between the esophagus and left atrium, which have been described in detail in our study and other studies, remains unclear. Moreover, we do not know whether this layer contributes to the protection of the esophagus prior to thermal damage during radiofrequency ablation. Thus, a longer area of physical contact between the esophagus and left atrium in the case of right-sided locations of the esophagus can be given by a small number of patients in this group, and it would require a larger group of patients to definitively confirm this conclusion.

CONCLUSION

From our results, it is apparent that the esophagus is a greatly variable structure in relation to the left atrium, both in regards to the distribution of the positions of the esophagus to the left atrium in the AP projection, as well as the contact of the esophagus with the posterior wall of the left atrium. The location of the esophagus in the posterior mediastinum is variable. Although the esophagus is most often located behind the left side of the left atrium, it may be situated in the entire area of the posterior wall of the left atrium and adjacent pulmonary veins. The area of close contact of the esophagus and posterior wall of the left atrium is relatively large, and it is on average 2/3 of the length and 1/4 of the width of the posterior wall of the left atrium and is shifted toward the left atrial roof. It begins just below the transition of the roof and posterior wall of the left atrium; in the area of posterior mitral annulus at the bottom part of the posterior wall, in most cases, there is a relatively large space filled with a fat pad.

Without imaging the esophagus using a specific imaging method, we were unable to predict where the esophagus was located in a particular patient during the procedure and the proximity of its contact with the posterior wall of the left atrium. The risk of damage to the esophagus during catheter radiofrequency ablation is in the area of the posterior wall of the left atrium and adjacent pulmonary veins and thus we have to take into account this fact and try to reduce that risk using all available methods.

Acknowledgement: This work was supported by the project no. LQ1605 from the National Program of Sustainability II.

Author contributions: All authors had full access to all the data in the study and take responsibility for the integrity of the data and the accuracy of the data analysis; ZS: study concept and design, acquisition of data, data analysis, manuscript drafting; FL, JJ: acquisition of data, critical revision; AK, TK, JW: Data analysis and interpretation, critical revision; TK: statistical analysis.

Conflict of interest statement: The authors state that there are no conflicts of interest regarding the publication of this article.

REFERENCES

1. Calkins H, Kuck KH, Cappato R, Brugada J, Camm AJ, Chen SA, Crijns HJ, Damiano RJ Jr, Davies DW, DiMarco J, Edgerton J, Ellenbogen K, Ezekowitz MD, Haines DE, Haissaguerre M, Hindricks G, Iesaka Y, Jackman W, Jalife J, Jais P, Kalman J, Keane D, Kim YH, Kirchhof P, Klein G, Kottkamp H, Kumagai K, Lindsay BD, Mansour M, Marchlinski FE, McCarthy PM, Mont JL, Morady F, Nademanee K, Nakagawa H, Natale A, Nattel S, Packer DL, Pappone C, Prystowsky E, Raviele A, Reddy V, Ruskin JN, Shemin RJ, Tsao HM, Wilber D. 2012 HRS/EHRA/ECAS expert consensus statement on catheter and surgical ablation of atrial fibrillation: recommendations for patient selection, procedural techniques, patient management and follow-up, definitions, endpoints, and research trial design. J Interv Card Electrophysiol 2012; 33(2):171-257.
2. Cappato R, Calkins H,Chen SA, Davies W, Iesaka Y, Kalman J, Kim YH, Klein G, Natale A, Packer D, Skanes A, Ambrogi F, Biganzoli E. Updated Worldwide Survey on the Methods, Efficacy, and Safety of Catheter Ablation for Human Atrial Fibrillation. Circ Arrhythm Electrophysiol 2010;3(1):32-8.
3. Ho SY, Cabrera JA, Sanchez-Quintana D. Left atrial anatomy revisited. Circ Arrhythm Electrophysiol 2012;5(1):220-8.
4. Cappato R, Calkins H, Chen SA, Davies W, Iesaka Y, Kalman J, Kim YH, Klein G, Natale A, Packer D, Skanes A. Prevalence and causes of fatal outcome in catheter ablation of atrial fibrillation. J Am Coll Cardiol 2009;53(19):1798-803.
5. Stöllberger C, Pulgram T, Finsterer J. Neurological consequences of atrioesophageal fistula after radiofrequency ablation in atrial fibrillation. Arch Neurol 2009;66(7):884-7.
6. Kottkamp H, Hindricks G, Autschbach R, Krauss B, Strasser B, Schirdewahn P, Fabricius A, Schuler G, Mohr FW. Specific linear left atrial lesions in atrial fibrillation: intraoperative radiofrequency ablation using minimally invasive surgical techniques. J Am Coll Cardiol 2002;40(3):475-80.
7. Pappone C, Oral H, Santinelli V, Vicedomini G, Lang CC, Manguso F, Torracca L, Benussi S, Alfieri O, Hong R, Lau W, Hirata K, Shikuma N, Hall B, Morady F. Atrio-esophageal fistula as a complication of percutaneous transcatheter ablation of atrial fibrillation. Circulation 2004;109(22):2724-6.
8. Cury RC, Abbara S, Schmidt S, Malchano ZJ, Neuzil P, Weichet J, Ferencik M, Hoffmann U, Ruskin JN, Brady TJ, Reddy VY. Relationship of the esophagus and aorta to the left atrium and pulmonary veins: Implications for catheter ablation of atrial fibrillation. Heart Rhythm 2005;2:1317-23.
9. Lemola K, Sneider M, Desjardins B, Case I, Han J, Good E, Tamirisa K, Tsemo A, Chugh A, Bogun F, Pelosi F Jr, Kazerooni E, Morady F, Oral H. Computed tomographic analysis of the anatomy of the left atrium and the esophagus: implications for left atrial catheter ablation. Circulation 2004;110(24):3655-60.
10. Jang SW, Kwon BJ, Choi MS, Kim DB, Shin WS, Cho EJ, Kim JH, Oh YS, Lee MY, Rho TH, Kim JH, Lee BY, Kim HL, Jung JI, Song KS. Computed tomographic analysis of the esophagus, left atrium, and pulmonary veins: implications for catheter ablation of atrial fibrillation. J Interv Card Electrophysiol 2011;32(1):1-6.
11. Kottkamp H, Piorkowski C, Tanner H, Kobza R, Dorszewski A, Schirdewahn P, Gerds-Li JH, Hindricks G. Topographic variability of the esophageal left atrial relation influencing ablation lines in patients with atrial fibrillation. J Cardiovasc Electrophysiol 2005;16(2):146-50.
12. Wang SL, Ooi CG, Siu CW, Yiu MW, Pang C, Lau CP, Tse HF. Endocardial visualization of esophageal-left atrial anatomic relationship by three-dimensional multidetector computed tomography "navigator imaging". Pacing Clin Electrophysiol 2006;29(5):502-8.
13. Maeda S, Iesaka Y, Uno K, tomo K, Nagata Y, Suzuki K, Hachiya H, Goya M, Takahashi A, Fujiwara H, Hiraoka M, Isobe M. Complex anatomy surrounding the left atrial posterior wall: analysis with 3D computed tomography. Heart Vessels 2012;27(1):58-64.
14. Daoud EG, Hummel JD, Houmsse M, Hart DT, Weiss R, Liu Z, Augostini R, Kalbfleisch S, Smith MC, Mehta R, Gangasani A, Raman SV. Comparison of computed tomography imaging with intraprocedural contrast esophagram: implications for catheter ablation of atrial fibrillation. Heart Rhythm 2008;5:975-80.
15. Starek Z, Lehar F, Jez J, Scurek M, Wolf J, Kulik T, Zbankova A, Novak M. Three-dimensional rotational angiography of the left atrium and the oesophagus: the short-term mobility of the oesophagus and the stability of the fused three-dimensional model of the left atrium and the oesophagus during catheter ablation for atrial fibr fibrillation. Europace 2017;19(8):1310-6.
16. Good E, Oral H, Lemola K, Han J, Tamirisa K, Igic P, Elmouchi D, Tschopp D, Reich S, Chugh A, Movement of the esophagus during left atrial catheter ablation for atrial fibrillation. J Am Coll Cardiol 2005;46(11):2107-10.
17. Stárek Z, Lehar F, Jež J, Žbánková A, Kulík T, Wolf J, Novák M. Long-term mobility of the esophagus in patients undergoing catheter ablation of atrial fibrillation: data from computer tomography and 3D rotational angiography of the left atrium. J Interv Card Electrophysiol 2016;46(2):81-7.

Int J Cardiovasc Imaging (2016) 32:1011–1019
DOI 10.1007/s10554-016-0888-y

ORIGINAL PAPER

Periprocedural 3D imaging of the left atrium and esophagus: comparison of different protocols of 3D rotational angiography of the left atrium and esophagus in group of 547 consecutive patients undergoing catheter ablation of the complex atrial arrhythmias

Zdenek Starek[1,2] · František Lehar[1,2] · Jiri Jez[1,2] · Jiri Wolf[1,2] · Tomas Kulik[1,2] · Alena Zbankova[1,2] · Miroslav Novak[2]

Received: 22 September 2015 / Accepted: 30 March 2016 / Published online: 26 April 2016

Abstract A new method in creating 3D models of the left atrium (LA) and esophagus before catheter ablation of atrial arrhythmias is 3D rotational angiography (3DRA) of the LA. The purpose of this retrospective study was to test various acquisition protocols of the 3DRA and attempt to define the parameters influencing the success of the protocols. From August 2010 to November 2014, 3DRA of the LA using the Philips Allura FD 10 X-ray system was performed in 547 consecutive patients using right atrial and left atrial protocols. Visualization of the esophagus was performed after oral administration of a contrast agent. Patients were monitored for success (creation of a useful 3D models) and evaluated for a number of parameters affecting the success of 3DRA. The success of the RA protocol was 88.89% with and 91.91% without esophagus imaging. The success of the LA protocol was 97.42% with and 94.54% without esophagus imaging. The only factor reducing the success of the RA protocol was BMI; the LA protocol was not influenced by any factor. Ventricular fibrillation induced in two patients was successfully treated with defibrillation. 3DRA of the LA is a reliable method that supports catheter ablation of complex atrial arrhythmias. The LA protocol with esophagus imaging was significantly more reliable than the RA protocol; the other protocols were comparable. The RA protocol may be negatively affected by high BMI. Simultaneous imaging of the esophagus is safe and feasible, and the LA protocol can be recommended.

Keywords 3D rotational angiography of the left atrium · Acquisition protocols · Complex atrial arrhythmias · Catheter ablation of arrhythmias · Image integration

✉ Zdenek Starek
zdenek.starek@fnusa.cz

František Lehar
frantisek.lehar@gmail.com

Jiri Jez
jiri.jez@fnusa.cz

Jiri Wolf
jiri.wolf@fnusa.cz

Tomas Kulik
tomas.kulik@fnusa.cz

Alena Zbankova
alena.zbankova@fnusa.cz

Miroslav Novak
miroslav.novak@fnusa.cz

1 International Clinical Research Center, 1st Department of Internal Medicine, Cardioangiology, St. Anne's University Hospital Brno, Pekařská 53, 656 91 Brno, Czech Republic

2 Faculty of Medicine, Masaryk University, Kamenice 5, 625 00 Brno, Czech Republic

Introduction

Radiofrequency ablation (RFA) is the method of choice for complex atrial arrhythmias and is most often performed for atrial fibrillation [1]. Complications may arise during the mapping of the left atrium with 3D electroanatomical mapping systems because of the complicated and variable anatomy of the left atrium [2]; however, this risk may be minimized by employing 3D X-ray heart models, which provide objective information on the true anatomy of a patient's heart. The standard method is a contrast-enhanced CT of the left atrium [3].

3DRA represents a new comparable alternative to CT cardiac imaging by creating an image with a standard X-ray machine [4–7]. The advantages of cardiac rotational angiography are primarily the flexibility in creating a model of the left atrium (3DRA can be provided periprocedurally at the time of the ablation procedure). Another structure that can be imaged with CT or 3DRA is the esophagus [4, 5]. Imaging of the esophagus may contribute to the improved safety of procedures because atrioesophageal fistula is a rare but fatal complication of catheter ablation of atrial fibrillation [8].

In a relatively large group of patients, we tested the success (defined as the creation of a useful 3D model of the left atrium) of various protocols and attempted to define the parameters influencing the protocols' success.

Materials and methods

Patient population

This retrospective study enrolled 547 consecutive patients who were referred for catheter ablation of a complex atrial arrhythmia and underwent 3DRA of the left atrium with or without esophagus imaging from August 2010 to November 2014. This study received approval from the ethics committee of our institution.

Rotational angiography imaging

The primary steps of the 3DRA were injecting the contrast agent (Ultravist 370, Bayer Pharma AG, Berlin, Germany) into the atrium and acquiring the rotational image with the X-ray system Allura Xper FD 10 (Philips Medical Systems Inc., Best, The Netherlands). After opacification of the left atrium and pulmonary veins, the C-arm was isocentrically rotated over 240° (120° right anterior oblique to 120° left anterior oblique) for 4.1 s with an X-ray acquisition speed of 30 frames per second. The patients were in a lying position with their arms in a natural position along the body and were breathing normally. Left atrium isocentering was achieved from the anteroposterior and left lateral X-ray view. An injection of the contrast agent was performed with a standard power injector (Mark V, Medrad Inc., Indianola, PA, USA) [7, 9].

Right atrial protocol

A contrast agent was injected into the right atrium, and after a set delay, the rotation of the C-arm began. Protocols 1 and 3 had a fixed delay based on the manufacturer's recommendation, and the delay of protocol 2 was adjusted individually by a system operator based on the filling of the LA with the contrast agent.

Left atrial protocol

A pigtail catheter was placed into the left atrium via an Agilis sheath. After reducing the cardiac output with rapid stimulation of the right ventricle (frequency 230/min), the contrast agent was administered. After a delay of 2 s, we began rotating the C-arm [6].

The esophagus was visualized using an oral administration of 20–30 ml of barium sulfate contrast agent (Micropaque, Guerbet, Roissy, France) during both the left and right protocols [4, 7]. For further details on the protocols, see Table 1.

After the rotational angiography was performed, the data were automatically transported from the Allura X-ray System to the workstation EP Navigator (EP Navigator 3.2, Philips Healthcare, Best, The Netherlands). The 3DRA model of the left atrium was automatically reconstructed using the

Table 1 Protocols

Protocol	Right atrial protocol 1	Right atrial protocol 2	Right atrial protocol 3	Left atrial protocol	p
Injected cavity	RA	RA	RA	LA	
Displayed cavity	LA	LA	LA	LA	
Amount of contrast agent (ml)	100	60	60	60	
Velocity of injection (ml/s)	20	15	15	15	
Delay (s)	Fixed 8–9	Variable from 8.937 to 11.546 s (Ø 10.67 s)	Fixed 9	Fixed 2	
Stimulation of RV 220–240 (bpm)	No	No	No	Yes	
Total success rate	70.97 % (22/31)	77.27 % (17/22)	90.22 % (203/225)*	94.54 % (225/238)*	0.181*
Success rate without esophagus imaging	NA	72.72 % (8/11)	91.91 % (91/99)*	89.16 % (74/83)*	0.472*
Success rate with esophagus imaging	NA	81.81 % (9/11)	88.89 % (112/126)*	97.42 % (151/155)*	0.010*

Asterisks specify which values are statisticaly compared (right protocol 3 vs left protocol)

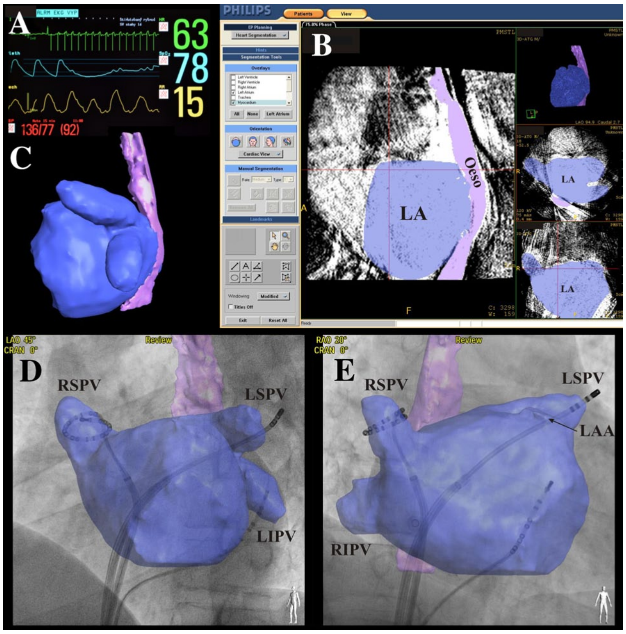

Fig. 1 The acquisition of the data from 3DRA and the segmentation of the 3D model of the left atrium (LA). **a** Reduction in the cardiac output with rapid stimulation documented by a decrease in saturation. **b** Raw data from the 3D rotational angiography of the left atrium with a segmentation of the 3D model. **c** Final model of the LA in the left lateral view. **d, e** 3D model of the LA and esophagus overlay on live fluoroscopy. **d** Left oblique view, **e** right oblique view

standard algorithms of the EP Navigator Workstation. Automatic segmentation was supplemented by manual segmentation when necessary. The 3D model of the esophagus was segmented manually at the same workstation (see Fig. 1).

We measured the total procedure time and the time required to perform a complete 3DRA of the left atrium for all patients. In particular, we measured the time required for manual segmentation of the esophagus and the time required to export data from the EP Navigator into the 3D electroanatomical mapping system.

We determined the average radiation dose (DAP—dose area product, mGycm²) for all 3DRA procedures. The average radiation dose was converted into an effective dose (ED) using a converting factor of 0.18 mSv/Gy/cm [10].

Qualitative image analysis

All patients were monitored for physiological parameters that potentially affected success, such as gender, body mass index (BMI), size of LA, ejection fraction of the left ventricle (EF) or the presence of structural heart disease, and the parameters monitored during the acquisition of data were also obtained, i.e., blood pressure, pulse rate and the current heart rate. These factors were analyzed individually as well as on a multidimensional basis, and their impact on the success of 3DRA was evaluated.

Left atrium models

Two expert physicians independently assessed the rotational angiography image results. For each patient, rotational angiography was assessed in 23 projections (RAO 55° to LAO 55° in steps of 5°). The classification of the datasets was based on a scale of 1–3 using the following criteria: (1) 'not diagnostic', no identification of the LA–PV junction in at least one RAO or one LAO projection; (2) 'useful', identification of the LA–PV junction in at least one RAO or one LAO projection; and (3) 'optimal', identification of the PV–LA junction in at least one RAO and one LAO projection. If there was any discrepancy in the 'grading' of the angiograms between the two reviewers, the images were re-assessed by both and a consensus had to be reached [11]. Failure of the protocol was defined as a non-diagnostic model after automatic and subsequent manual segmentation. In patients with a failed protocol were two alternatives—aborting the procedure or proceeding without 3D Xray imaging (using 3D electroanatomical mapping alone). In our group of patients with a failed protocol we used second possibility and ablated them without the support of a 3D model from 3DRA data guided only by 3D electroanatomical mapping.

Esophagus models

The esophagus models were classified into two groups: a 'usable model', defined as a clearly segmented course of the esophagus with identifiable edges in most areas behind the left atrium, and a 'unusable model', in which the course of the esophagus could not be reliably visualized. Examples of esophagus models are shown in Fig. 2.

Image integration and ablation procedures

The resulting 3DRA model of the left atrium was automatically integrated with the live fluoroscopy [7, 12].

For the procedures guided by 3D electroanatomical mapping systems, we used 3D models of the LA to support the creation of a 3D electroanatomical map in two standard ways: synchronized projection of the 3DRA model and the 3D electroanatomical mapping system and direct fusion of the 3D models with the 3D electroanatomical map [3, 6, 13].

Ablation procedures were performed in a standard manner under light sedation (boluses of fentanyl and diazepam i.v.) using an irrigated tip catheter with the 3D electroanatomical mapping system EnSite Velocity (St. Jude Medical, St. Paul, MN, USA). Circumferential PV isolation confirmed by a 20-pole circumferential mapping catheter was the basis of all procedures of paroxysmal atrial fibrillation. Additional roof and mitral isthmus lines and coronary sinus ablation were performed in cases of persistent atrial fibrillation. Tricuspid isthmus and superior vena cava ablation

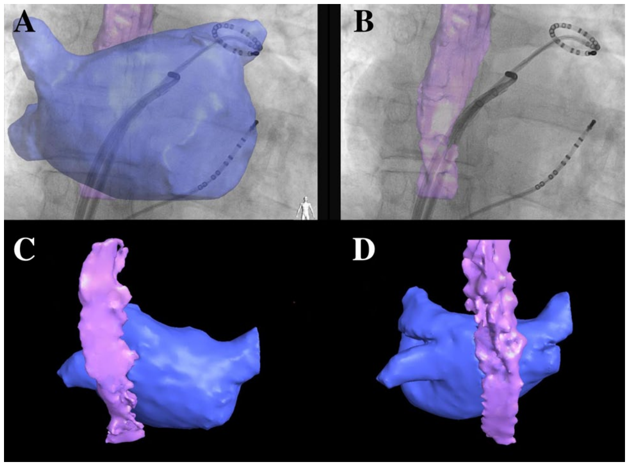

Fig. 2 3DRA of the left atrium with esophagus imaging. **a, b** Example of an application of the 3D model of the left atrium (LA) with visualized esophagus during the isolation of the pulmonary veins, anteroposterior view. **a** A twenty-polar circular catheter is introduced into the left superior pulmonary vein, and the tip of the ablation catheter is in the site of the resulting line on the posterior wall of the LA. **b** Due to the clarity, the left atrium model is hidden. **c, d** Examples of the positions of esophagus. **c** Extremely left position, **d** slightly right position

were performed in some patients. Atypical flutters and focal tachycardias were ablated with a support voltage, LAT electroanatomical maps and conventional diagnostic maneuvers. Esophagus imaging was accounted for in the creation of ablation lines in the posterior wall of the left atrium.

Statistical analysis

All variables were first statistically analyzed using Kolmogorov–Smirnov tests. The null hypothesis H0 ($\alpha = 0.05$) assumed that the variables were normally distributed. Consequently, depending on the parametric or non-parametric character of the data, a T-test for two independent samples or a Mann–Whitney U-test, respectively, was performed.

The entire dataset was then subjected to multivariate analysis, specifically stochastic modeling with a binary endpoint (with a logit linking function). The independent variables entered into this model included those affecting the success rate of 3DRA: blood pressure, heart rate, left ventricular ejection fraction, left atrial size, body mass index (BMI), age of the patient and the presence of structural heart disease and atrial fibrillation during image acquisition. The significance level for this type of statistical processing was set to 0.05, and to evaluate the chosen model of logistic regression, odds ratio (OR) values were used. For the purposes of statistical processing, the clinical population was divided into two groups: right atrial acquisition protocol and left atrial acquisition protocol. These groups were further divided into 3DRA without esophagus imaging and 3DRA with esophagus imaging.

Results

From August 2010 to November 2014, a total of 547 3DRA of the left atrium were performed. Data from 516 patients were statistically evaluated. The right atrial protocol was conducted in 140 patients without esophagus imaging and in 138 patients with esophagus imaging. The left atrial protocol was performed alone in 83 patients and was performed with esophagus imaging in 155 patients.

The acquisition of data occurred without major complications. The average duration of the rapid ventricle stimulation was 7.2 s. Hypotension during the rapid ventricle stimulation was tolerated very well without subjective or objective problems, likely due to the preserved ejection fraction. Two patients developed ventricular fibrillation as a consequence of the rapid ventricular stimulation. One patient had hypertrophic cardiomyopathy, and the second patient had no structural heart disease. Both arrhythmias were successfully treated with defibrillation. Direct left atrial injection of the contrast agent had no complications. No patients experienced aspiration of the oral contrast agents or other complications associated with the use of contrast agents dosed orally.

Left atrium imaging

Patient characteristics

The characteristics of the patients are summarized in Table 2. In accordance with the protocols, the average radiation dose of the right atrial protocol was 10913.07 ± 2147.43 mGycm² and was 11093.32 ± 2153.28 mGycm² for the left atrial protocol (1.96 ± 0.39 and 1.99 ± 0.39 mSv, respectively).

Rotational angiography image acquisition and qualitative image assessment

The time required to create a 3D model of the LA was comparable between the left atrial and right atrial protocol. The creation time of the LA models and the time needed to export the data to the 3D mapping system were also comparable. For details, see Table 3.

The average total time of all of the procedures was 187.4 ± 82.7 min, and the average total time of 3DRA was 8.5 ± 1.3 min. 3DRA constituted 4.5 % of the total catheter ablation time.

The success rate of 3DRA varied by the protocol used. When evaluating the quality of the model, we found that there were essentially two possible outcomes: the model was either optimal, with well-drawn pulmonary veins and junctions, or was a completely unusable, deformed model. The most often used 'definitive' right protocol, right protocol 3, and the left protocol were comparable in terms of

Table 2 Patient characteristics and monitored parameters

Patient characteristics	3DRA of left atrium (LA)	3DRA of LA without imaging of esophagus	3DRA of LA with imaging of esophagus	Statistical significance (p)
Number of patients	516	223	293	
Age	59.82 ± 10.5	59.81 ± 10.48	59.69 ± 10.63	1.000
Men	376 (72.87 %)	158 (70.85 %)	218 (74.40 %)	0.637
Ejection fraction of the left ventricle	57.16 ± 8.02	57.10 ± 8.10	57.07 ± 8.33	1.000
Size of left atrium	44.52 ± 5.85	44.52 ± 5.84	44.56 ± 5.81	1.000
Body mass index	29.42 ± 8.12	29.49 ± 8.27	29.61 ± 8.69	1.000
Structural heart disease	91 (17.64 %)	43 (19.28 %)	48 (16.38 %)	0.579
Hypertension	294 (56.98 %)	139 (62.33 %)	155 (52.90 %)	0.200
Atrial fibrillation	465 (90.12 %)	195 (87.44 %)	270 (92.15 %)	0.251
Paroxysmal Afib	298 (64.09 %)	123 (63.08 %)	175 (64.81 %)	0.770
Persistent Afib	149 (32.04)	60 (30.77 %)	89 (32.96 %)	0.763
Long standing pers Afib	18 (3.87 %)	12 (6.15 %)	6 (2.22 %)	0.151
Atypical left atrial flutter	46 (8.91 %)	26 (11.66 %)	20 (6.83 %)	0.230
Focal left atrial tachycardia	5 (0.97 %)	2 (0.90 %)	3 (1.02 %)	1.000
Heart rate during acquisition	76.91 ± 20.15	76.74 ± 20.17	76.86 ± 20.23	1.000
Systolic blood pressure during acquisition	132.89 ± 16.39	132.98 ± 16.52	133.38 ± 16.30	1.000
Diastolic blood pressure during acquisition	78.60 ± 13.10	78.67 ± 13.27	78.65 ± 12.64	1.000
Sinus rhythm during acquisition	293 (56.78 %)	118 (52.91 %)	175 (59.73 %)	0.320
Atrial fibrillation during acquisition	174 (33.72 %)	79 (35.43 %)	95 (32.43 %)	0.655
Different rhythm during acquisition	49 (9.5 %)	26 (11.66 %)	23 (7.85 %)	0.237

p value is for 3DRA of LA with and without imaging of the esophagus

Table 3 Duration of 3DRA

Duration of individual steps of 3DRA	Total time from the introduction of the pigtail to the end of segmentation in the EP navigator (min)	Time for data to be exported from the EP Navigator to the 3D mapping system (min)	Time for segmentation of the esophagus (min)
Right atrial protocol without esophagus imaging	6.95	4.58	NA
Left atrial protocol without esophagus imaging	8.37 (p = 0.090)	4.34 (p = 0.698)	NA
Right atrial protocol with esophagus imaging	8.03	5.22	1.25
Left atrial protocol with esophagus imaging	10.52 (p = 0.005)	5.03 (p = 0.713)	1.18 (p = 0.149)

their overall success rate and in their success rate without esophagus imaging (90.22 % vs. 94.54 % and 91.91 % vs. 89.16 %, respectively). For details, see Table 1.

Based on the logistic regression analysis, it was clear that BMI was the only factor that had a significant effect on the failure to create an image in 3DRA (OR = 1.13, p = 0.033). The 'cut off' value of ROC curves for BMI was set to 30 [–].

Left atrium and esophagus imaging

Patient characteristics

The patients who received esophagus imaging were virtually identical to those without esophagus imaging (Table 2). The average radiation dose for the right atrial protocol was 11243.33 ± 2115.65 mGycm² and for the left atrial protocol was 11342.99 ± 2229.61 mGycm² (2.02 ± 0.38 and 2.04 ± 0.4 mSv, respectively).

Rotational angiography image acquisition and qualitative image assessment

The time required to perform 3DRA of the left atrium with esophagus imaging was extended by manual segmentation of the esophagus with the same duration in the left and right atrial protocols (1.25 vs. 1.18 min, respectively). The total execution time of the 3DRA of the left atrium and esophagus was significantly longer using the left atrial protocol than the right atrial protocol (8.03 vs. 10.52 min, respectively; p = 0.005), see Table 3.

The first 11 patients underwent the 3DRA using right atrial protocol 2; another 127 patients were analyzed using right atrial protocol 3, and 155 patients were examined using the left atrial protocol. For details, see Table 1.

We performed a statistical analysis to identify independent predictors of failure using individual protocols. There was no statistically significant factor affecting the success of imaging for the left atrial protocol.

For the right atrial protocol, the only evident independent parameter affecting the failure of 3DRA was BMI (OR = 1.13, 1.17; p = 0.039, 0.014, respectively). The chance of failure increased from 1.13 to 1.17 times for each nominal increase in BMI above the 'cut off' value (also with a value of 30 [–]).

The left atrial protocol had a significantly better success rate with esophagus imaging (97.42 %) in comparison to right atrial protocol 3 (88.89 %), p = 0.010.

The occurrence of failed esophagus imaging with successful LA imaging was comparable between the right and left atrial protocols (5.07 % vs. 8.39 %, p = 0.392). In 4.78 % of the cases, we were unsuccessful in visualizing both the esophagus and the atrium. In these patients, we detected a specific type of fault segmentation of the 3D model, with failure of segmentation occurring because the workstation software was confused between the contrast-visualized esophagus and the less contrasted left atrium. This failure occurred significantly more frequently in the right atrial protocol models (8.7 %) than in the left atrial protocol (1.3 %), p = 0.009.

Catheter ablation with the support of 3DRA of the left atrium

All patients with a 3DRA model of the left atrium with or without esophagus imaging were ablated using a direct overlay 3D model and 2D fluoroscopy. A total of 482 patients were ablated under the guidance of 3D velocity maps created using the 3DRA model synchronously displayed in the 3D electroanatomic mapping system, and 28 patients were ablated using the guidance of the 3DRA model of the LA directly fused with the 3D electroanatomic map system.

Esophagus imaging was performed when ablating the posterior wall of the left atrium, using lower ablation energies in the proximity of the esophagus, or when an ablation line was created in another location.

The 1-year success rate of paroxysmal atrial fibrillation ablation was 73 % and was 61 % for persistent atrial fibrillation. All ablation procedures were standard, and the number of periprocedural complications was not above the average [8]. The most frequent complications were minor complications in the groin–femoral region hematomas, femoral pseudoaneurysms and occasionally artero-venous fistulae were present in 2.1 % of the cases overall. Of the serious complications, there were 8 cases in which a pericardial effusion with cardiac tamponade was successfully managed with pericardial puncture without any sequelae; in three cases, a transient ischemic attack with rapid recovery without neurological sequelae was observed. In one case, right-sided stroke symptoms and phatic disorder appeared. There were no fatal complications.

Discussion

In our study, we performed 3DRA of the left atrium with four different protocols. The success rate of right atrial protocol 1 was quite low (less than 71 %), which corresponds with the success rate of the right atrial protocol described in a study by Thiagalingam et al. [6]. We then started using the left atrial protocol, which quickly proved to be sufficiently reliable with a long-term success rate of almost 95 %. Tang et al. reported a success rate of the left atrial protocol of 95.7 % (11), and Kriatselis et al. reported a rate of almost 100 % [14].

However, the right atrial protocol has its advantages. The right protocol enables the creation of a 3D model of the left atrium before transseptal puncture (and can be used to guide transseptal puncture) and provides more time for model segmentation and transfer of the data into a 3D electroanatomical mapping system, which is advantageous in terms of workflow.

Therefore, we tested right protocol 2 with variable timing. Despite our expectations, we did not observe any improvement in success rate, most likely due to insufficiently contrasting the imaging of the left atrium at the beginning of the rotation. Determining when the left atrium has been filled by the contrast agent is difficult even for an experienced X-ray system operator. The protocol that used a fixed delay had a better success rate, most likely because it removed operator error.

The success rate of the optimized right atrial protocol, right protocol 3, which had a fixed delay timing of 9 s., is consistent with published data; Li et al. reported a right atrial protocol success rate of 93.7 % [7], and Orlov et al. observed a rate of 90 % [4].

Thiagalingam et al. [6] analyzed the cause of the low success rate of the right atrial protocol in the 42 patients included in their study; however, they found that the actual heart rhythm or heart rate did not affect the success rate. The results of our analysis of the right atrial protocol confirmed these conclusions; the only factor that reduced the success rate was BMI, with a cut-off value of around 30.

The extended duration of the procedure due to the addition of the periprocedural performance of the 3DRA of the left atrium was clinically insignificant. The creation of the 3DRA model constituted only 4.5 % of the average total time of catheter ablation.

In our department, the time required to perform 3DRA, including the segmentation of the 3D model, was 6.95–10.52 min using a specific protocol and eventual esophagus imaging. These measured times are comparable with the times reported in published studies (which are on average 10–14 min regardless of the type of protocol used [11, 12, 15]). The total time needed to create the 3D model was longer in all of the left atrial protocol patients than those undergoing the right atrial protocol. Regarding the creation of the left atrial and esophagus model, the difference in total time reached statistical significance. The reason for this difference is likely the higher proportion of left atrial protocol cases that required manual segmentation. The higher contrast of the left atrium achieved with the left atrial protocol allowed us to intervene more in the automatic segmentation and to manually segment left atrial, mainly pulmonary vein, anomalies. The transfer of the 3D model into the 3D mapping system in our department took approximately 5 min. This delay occurred primarily because the transfer of data was performed manually using a flash drive. The duration of the manual segmentation of the esophagus was, in our opinion, clinically insignificant and constituted only 0.6% of the average total time of the procedure.

3DRA of the left atrium with esophagus imaging was performed using right and left atrial protocols. The left atrial protocol was reliable and its success rate was high. There was a difference of 8.26% between left atrial protocols with and without esophagus imaging; this difference may be due to the nonrandomized character of retrospective observation, as a higher proportion of the successful procedures with esophagus imaging occurred more recently. The success rates of the left atrial protocol procedures performed up to January 2014 (73 without and 103 with esophagus imaging) were identical (94.52% vs. 94.17%). The total success rate was virtually the same—94.54% for November 2014 vs. 94.32% for January 2014.

Failed esophagus imaging despite successful LA imaging was most often caused by delayed swallowing of the contrast agent or rapid passage through the esophagus. The success rate of right atrial protocol 3 with esophagus imaging was approximately 3% lower than that of the same protocol without esophagus imaging (88.89% vs. 91.91%). A detailed analysis of our results (see Table 4) found that 4.78% of the patients had a specific segmentation error due to confusion caused by the contrast that led to the esophagus being imaged for the left atrium, which was significantly less contrasted. The workstation software tried to reconstruct the esophageal area as the left atrium, which led to imaging failure. Only two patients with the left atrial protocol had this type of incorrect segmentation. In one patient, the cause of the error was the incorrect operation of the device; ventricular stimulation was omitted, and the atrium was poorly filled with the contrast agent. In the second patient, the C-arm had the wrong isocenter, resulting in a large part of the atrium not being captured. All other cases occurred in the right atrial protocol (8.7%), as the lower density of the left atrium during rotational angiography was predisposed to this problem. No published study has paid more attention to this topic. To some extent, this gap in the literature may be because of the small number of patients in each study (11–47 patients) and because these studies lacked a control group of patients with 3DRA of the left atrium without esophagus imaging [4, 5, 7, 9].

Table 4 Success rate of 3DRA with and without esophagus imaging

Success rate of individual protocols with and without esophagus imaging	Successful imaging of LA	Unsuccessful imaging of LA
RA and LA protocol n = 293 pts		
Successful esophagus imaging	253/293 (86.35%)	6/293 (2.05%)
Unsuccessful esophagus imaging	20/293 (6.83%)	14/293 (4.78%)
RA protocol n = 138 pts		
Successful esophagus imaging	115/138 (83.33%)	4/138 (2.9%)
Unsuccessful esophagus imaging	7/138 (5.07%)*	12/138 (8.7%)†
LA protocol n = 155 pts		
Successful esophagus imaging	138/155 (89.03%)	2/155 (1.3%)
Unsuccessful esophagus imaging	13/155 (8.39%)*	2/155 (1.3%)†

Statistical significance: * p = 0.392, † p = 0.009

RA right atrial, *LA* left atrial

Our group of patients with 3DRA of the left atrium and esophagus imaging is likely the largest database of patients receiving oral contrast during cardiac catheterization. Despite the fact that the patients were under light sedation, no complications were noted. No instances of aspiration of oral contrast were observed.

Regarding the radiation burden, 3DRA of the left atrium is a rather low dose technique with an average effective dose of 2.00 ± 0.39 mSv. A CT scan of the left atrium with a standard 64-slice CT using a retrospective gated protocol has an effective dose of almost 14 mSv [16]. According to our unpublished data, an ungated protocol with the same CT has an effective dose of approximately 10 mSv. Nevertheless, with development of new generation CT machines, the effective dose has become comparable with 3DRA [17].

Limitations

This study was not designed to assess the impact of 3DRA use on the procedural outcomes or safety aspects of the procedure. Several smaller studies have demonstrated non-inferior and some superior results when using 3DRA models to guide catheter ablation of left atrial arrhythmias compared to CT models of the left atrium [17] and the 3D electroanatomic mapping systems EnSite NavX and Carto [9, 18].

Unlike CT, 3DRA involves specific risks. Most importantly, rapid ventricular pacing can cause ventricular tachycardia or ventricular fibrillation. However, the resolution of malignant arrhythmias is common in EP labs.

A direct left atrium injection of the contrast agent may be risky in terms of inducing atrial fibrillation. As for our patients in sinus rhythm, no induction of atrial fibrillation appeared after injection of the contrast agent.

Damage to the left atrium appendage during the insertion of a pigtail catheter or during the injection of the contrast agent close to the left atrium appendage can cause a perforation of the left atrium and development of acute tamponade. However, this complication was not observed in our group of patients.

Conclusion

3DRA of the LA is a currently recognized method used to support catheter ablations of left atrial arrhythmias. The left and right atrial acquisition protocols were comparable. However, when choosing between the right atrial protocols, we recommend the optimized protocol number 3, and in patients with a BMI above 30, the left atrial protocol should be considered. Imaging of the esophagus in 3D angiography of the left atrium is a simple and safe method that can reliably locate the position of the esophagus in relation to the left atrium. To image the esophagus, it is appropriate to perform the procedure using the left atrial acquisition protocol. The advantage of 3DRA is that it introduces the possibility of performing a periprocedural procedure directly on the X-ray table with automatic overlay of the 3D model on live fluoroscopy without significant prolongation of the procedure.

Funding This study was funded by a Grant of the European Regional Development Fund—Project FNUSA-ICRC (No. CZ.1.05/1.1.00/02.0123) and Masaryk University, Faculty of Medicine, Kamenice 5, 625 00 Brno, Czech Republic.

Compliance with ethical standards

Conflict of interest The authors have no conflicts of interest to declare.

Ethical approval All procedures performed in the study involving human participants were in accordance with the ethical standards of the institutional and/or national research committee and with the 1964 Helsinki declaration and its later amendments or comparable ethical standards. This retrospective study received approval from the ethics committee of our institution. Informed consent was not necessary because the current study was retrospective in nature and retrospectively processed common clinical data.

References

1. Calkins H, Kuck KH, Cappato R et al (2012) 2012 HRS/EHRA/ECAS expert consensus statement on catheter and surgical ablation of atrial fibrillation: recommendations for patient selection, procedural techniques, patient management and follow-up, definitions, endpoints, and research trial design. J Interv Card Electrophysiol 33:171–257
2. Jongbloed MR, Bax JJ, Lamb HJ, Dirksen MS, Zeppenfeld K, van der Wall EE, de Roos A, Schalij MJ (2005) Multislice computed tomography versus intracardiac echocardiography to evaluate the pulmonary veins before radiofrequency catheter ablation of atrial fibrillation: a head-to-head comparison. J Am Coll Cardiol 45:343–350
3. Malchano ZJ, Neuzil P, Cury RC, Holmvang G, Weichet J, Schmidt EJ, Ruskin JN, Reddy VY (2006) Integration of cardiac CT/MR imaging with three-dimensional electroanatomical mapping to guide catheter manipulation in the left atrium: implications for catheter ablation of atrial fibrillation. J Cardiovasc Electrophysiol 17:1221–1229
4. Orlov MV, Hoffmeister P, Chaudhry GM, Almasry I, Gijsbers GH, Swack T, Haffajee CI (2007) Three-dimensional rotational angiography of the left atrium and esophagus—a virtual computed tomography scan in the electrophysiology lab? Heart Rhythm 4:37–43
5. Nölker G, Gutleben KJ, Marschang H, Ritscher G, Asbach S, Marrouche N, Brachmann J, Sinha AM (2008) Three-dimensional left atrial and esophagus reconstruction using cardiac C-arm computed tomography with image integration into fluoroscopic views for ablation of atrial fibrillation: accuracy of a novel modality in comparison with multislice computed tomo. Heart Rhythm 5:1651–1657
6. Thiagalingam A, Manzke R, D'Avila A, Ho I, Locke AH, Ruskin JN, Chan RC, Reddy VY (2008) Intraprocedural volume imaging of the left atrium and pulmonary veins with rotational X-ray angiography: implications for catheter ablation of atrial fibrillation. J Cardiovasc Electrophysiol 19:293–300
7. Li JH, Haim M, Movassaghi B, Mendel JB, Chaudhry GM, Haffajee CI, Orlov MV (2009) Segmentation and registration of three-dimensional rotational angiogram on live fluoroscopy to guide atrial fibrillation ablation: a new online imaging tool. Heart Rhythm 6:231–237
8. Cappato R, Calkins H, Chen SA, Davies W, Iesaka Y, Kalman J, Kim YH, Klein G, Natale A, Packer D, Skanes A, Ambrogi F, Biganzoli E (2010) Updated worldwide survey on the methods, efficacy, and safety of catheter ablation for human atrial fibrillation. Circ Arrhythm Electrophysiol 3:32–38
9. Carpen M, Matkins J, Syros G, Gorev MV, Alikhani Z, Wylie JV, Natan SR, Griben A, Hicks A, Armstrong J, Orlov MV (2013) First experience of 3D rotational angiography fusion with NavX electroanatomical mapping to guide catheter ablation of atrial fibrillation. Heart Rhythm 10:422–427
10. Einstein AJ, Moser KW, Thompson RC, Cerqueira MD, Henzlova MJ (2007) Radiation dose to patients from cardiac diagnostic imaging. Circulation 116:1290–1305
11. Tang M, Kriatselis C, Ye G, Nedios S, Roser M, Solowjowa N, Fleck E, Gerds-Li JH (2009) Reconstructing and registering three-dimensional rotational angiogram of left atrium during ablation of atrial fibrillation. Pacing Clin Electrophysiol 32:1407–1416

12. Kriatselis C, Tang M, Nedios S, Roser M, Gerds-Li H, Fleck E (2009) Intraprocedural reconstruction of the left atrium and pulmonary veins as a single navigation tool for ablation of atrial fibrillation: a feasibility, efficacy, and safety study. Heart Rhythm 6:733–741
13. Dong J, Calkins H, Solomon SB, Lai S, Dalal D, Lardo AC, Brem E, Preiss A, Berger RD, Halperin H, Dickfeld T (2006) Integrated electroanatomic mapping with three-dimensional computed tomographic images for real-time guided ablations. Circulation 113:186–194
14. Kriatselis C, Tang M, Roser M, Fleck E, Gerds-Li H (2009) A new approach for contrast-enhanced X-ray imaging of the left atrium and pulmonary veins for atrial fibrillation ablation: rotational angiography during adenosine-induced asystole. Europace 11:35–41
15. Kriatselis C, Nedios S, Akrivakis S, Tang M, Roser M, Gerds-Li JH, Fleck E, Orlov M (2011) Intraprocedural imaging of left atrium and pulmonary veins: a comparison study between rotational angiography and cardiac computed tomography. Pacing Clin Electrophysiol 34:315–322
16. Thorning C, Hamady M, Liaw JV, Juli C, Lim PB, Dhawan R, Peters NS, Davies DW, Kanagaratnam P, O'Neill MD, Wright AR (2011) CT evaluation of pulmonary venous anatomy variation in patients undergoing catheter ablation for atrial fibrillation. Clin Imaging 35:1–9
17. Yang L, Xu L, Yan Z, Yu W, Fan Z, Lv B, Zhang Z (2012) Low dose 320-row CT for left atrium and pulmonary veins imaging–the feasibility study. Eur J Radiol 81:1549–1554
17. Lehar F, Starek Z, Jez J, Novak M, Wolf J, Stepanova R, Kruzliak P, Kulik T, Zbankova A, Jancar R, Vitovec J (2015) Comparison of clinical outcomes and safety of catheter ablation for atrial fibrillation supported by data from CT scan or three-dimensional rotational angiogram of left atrium and pulmonary veins. Biomed Pap Med Fac Univ Palacky Olomouc Czech Repub 159:622–628
18. Knecht S, Wright M, Akrivakis S, Nault I, Matsuo S, Chaudhry GM, Haffajee C, Sacher F, Lellouche N, Miyazaki S, Forclaz A, Jadidi AS, Hocini M, Ritter P, Clementy J, Haïssaguerre M, Orlov M, Jaïs P (2010) Prospective randomized comparison between the conventional electroanatomical system and three-dimensional rotational angiography during catheter ablation for atrial fibrillation. Heart Rhythm 7:459–465

Rotační atriografie levé síně – nová zobrazovací metoda sloužící k podpoře radiofrekvenční ablace v levé síni: srovnání anatomických dat levé síně získaných z trojrozměrné rotační atriografie a počítačové tomografie

František Lehar, Zdeněk Stárek, Jiří Jež, Miroslav Novák, Jiří Wolf, Peter Kružliak, Tomáš Kulík, Alena Žbánková, Radek Jančár

I. interní kardioangiologická klinika Fakultní nemocnice u sv. Anny v Brně, Mezinárodní centrum klinického výzkumu, Brno

Úvod: Katetrová léčba fibrilace síní je běžně používanou léčebnou metodou. Vzhledem k anatomické složitosti levé síně se používají k podpoře výkonu trojrozměrné modely této srdeční dutiny získané z počítačové tomografie (CT). Rotační atriografie je nová zobrazovací metoda sloužící k získání stejných dat, která nám poskytuje CT vyšetření.

Metody: Cílem naší práce bylo u 65 pacientů podstupujících ablační výkon pro fibrilaci síní srovnat anatomické parametry levé síně získané metodou 3D rotační atriografie s daty získanými z CT. Dále jsme se zaměřili na porovnání radiační zátěže.

Výsledky: Výsledky měření rozměru ústí žil ukázaly dobrou korelaci mezi oběma sledovanými metodami. Při porovnání rozměrů nebyl prokázán statistický rozdíl mezi daty z CT srdce a z 3D rotační atriografie, kromě rozměru levé dolní plicní žíly měřeného v předozadní projekci. Byla prokázána statisticky významná redukce radiační zátěže při použití 3D rotační atriografie oproti CT vyšetření (10,2 ± 2,318 vs. 2,3 ± 0,6 mSV mGy-1cm-1, p < 0,001).

Závěr: Metoda 3D rotační atriografie levé síně nám poskytuje stejné anatomické informace jako CT srdce. Při použití této nové metody dochází ke statisticky významné redukci radiační zátěže pro pacienta.

Klíčová slova: fibrilace síní, radiofrekvenční ablace, levá síň, 3D rotační atriografie, počítačová tomografie.

Rotational atriography of left atrium – a new imaging technique used to support left atrial radiofrequency ablation: a comparison of anatomical data of left atrium obtained from 3D rotational atriography and computed tomography

Introduction: Catheter ablation therapy for atrial fibrillation is a commonly used therapeutic method. Given the anatomical complexity of the left atrium, three-dimensional models of this chamber of the heart obtained by computed tomography (CT) are employed. Rotational atriography is a new imaging technique used to obtain the same data as those obtained by CT scans.

Methods: Our aim was to compare anatomical parameters of the left atrium obtained by the method of 3D rotational atriography with the data obtained by CT scans in 65 patients undergoing ablation therapy for atrial fibrillation. In addition, we aimed at comparing the radiation burden.

Results: The results of measurements of the dimensions of venous orifices showed a good correlation between the two methods observed; when comparing the dimensions, no statistical difference was found between the use of data from the CT of the heart and from 3D rotational atriography, except for the dimension of the left inferior pulmonary vein measured in the anteroposterior projection. A statistically significant reduction in the radiation burden was shown with the use of 3D rotational atriography versus CT examination (10.2 ± 2.318 vs. 2.3 ± 0.6 mSV mGy-1cm-1, p < 0.001).

Conclusion: The method of 3D rotational atriography of the left atrium provides the same anatomical information as does CT of the heart. With the use of this new method, there is a statistically significant reduction in the radiation burden for the patient.

Key words: atrial fibrillation, radiofrequency ablation, left atrium, 3D rotational atriography, computed tomography.

Interv Akut Kardiol 2013; 12(4): 184–189

Úvod

Katetrová léčba fibrilace síní je v současné době běžně používanou léčebnou metodou (1). Cílem tohoto intervenčního zákroku, prováděného v levé síni, je zabránit recidivám arytmie. Rozhodujícím faktorem jak z hlediska úspěšnosti výkonu, tak i rizika komplikací je co nejlepší orientace v levé síni (2). Provádění těchto výkonů pouze za kontroly klasické skiaskopie a skiagrafie je velmi obtížné, a proto byla vyvinuta řada metod usnadňující orientaci v levé síni (3). Standardní metodou užívanou při těchto vyšetřeních se staly 3-dimenzionální elektroanatomické mapovací systémy. V současnosti se používají různé verze systému CARTO (Biosense Webster, Diamond Bar, CA, USA) a systému EnSite Velocity (St. Jude Medical, St. Paul, MN, USA) (4). Tyto systémy dovedou na podkladě různých fyzikálních principů vytvářet trojrozměrné non-fluoroskopické mapy srdečních dutin. Vzhledem k anatomické složitosti a rozmanitosti levé síně a plicních žil se jako podklad při vytváření těchto map používá trojrozměrný (3D) model levé síně získaný z dat z počítačové tomografie (CT), nebo méně často z vyšetření srdce pomocí magnetické rezonance (MR) (5, 6, 7). Nevýhodou tohoto postupu je nutnost provedení CT nebo MR vyšetření ještě před samotným zákrokem a přítomnost mnoha faktorů, které mohou ovlivnit samotný model levé síně (rozdílná pozice pacienta při CT vyšetření a při elektrofyziologickém vyšetření, žilní náplň, srdeční rytmus, srdeční frekvence).

Nově se k vytváření anatomického modelu levé síně začala používat metoda 3D rotační atriografie, kterou lze provést přímo na elektrofyziologickém sále pomocí angiolinky (8, 9). Jednoznačnou výhodou této metody je možnost fúze takto získaného obrazu do „live“ skiaskopického obrazu, a tím i mnohem lepší orientace při samotném výkonu.

Cílem naší práce bylo srovnat u stejného pacienta anatomické parametry levé síně získané metodou 3D rotační atriografie s daty získanými z CT srdce. Dále jsme se zaměřili na porovnání radiační zátěž při použití obou metod. Také jsme se zabývali porovnáním finanční nákladnosti obou metod v podmínkách České republiky.

Metody

V období 9/2011–8/2012 jsme do sledování prospektivně zařadili 65 pacientů, kteří na I. interní kardioangiologické klinice FN u sv. Anny v Brně podstoupili radiofrekvenční ablaci v levé síni pro fibrilaci síní. Tato studie byla schválena Etickou komisí FN u sv. Anny v Brně a pacienti podepsali před vstupem do studie informovaný souhlas. Do studie nebyli zařazeni pacienti s alergií na jodovou kontrastní látku a pacienti s renální insuficiencí charakterizovanou jako pokles glomerulární filtrace méně než 45ml/s/1,73m[2].

Předoperační průběh

Všichni zařazení pacienti byli vyšetřeni v arytmologické ambulanci a byli indikováni k ablačnímu řešení pro paroxyzmální či perzistující fibrilaci síní rezistentní na farmakologickou léčbu. Všichni pacienti před vyšetřením podstoupili transtorakální echokardiografii a laboratorní odběry ke zjištění renálních parametrů, potřebných k výpočtu glomerulární filtrace. Zavedení antikoagulační léčby se řídilo dle CHA2DS2-VASc score (12). Případná antikoagulační terapie byla vysazena pět dní před plánovaným zákrokem, po poklesu hodnot INR k neúčinným hodnotám byl dle hmotnosti aplikován subkutánně nízkomolekulární heparin, pouze v den přijetí k zákroku již aplikován nebyl. Všichni pacienti podstoupili CT vyšetření srdce maximálně 7 dnů před přijetím k hospitalizaci k plánovanému výkonu. Před samotným ablačním výkonem byla u všech pacientů provedena jícnová echokardiografie s vyloučením intrakardiálního trombu.

CT vyšetření

CT vyšetření bylo provedeno na 64-slice přístroji (GE Lightspeed VCT, General Electric, Fairfield, USA). Parametry CT obsahovaly: 120 KV, 800 mAs, kolimace 63 × 0,625 mm, spiral pitch faktor 0,98. Rekonstrukce obrazu byla provedena na 512 × 512 pixelové matici. Kontrastní látka byla aplikována cestou periferní žíly, množství použitého kontrastu bylo 100–150 ml (Ultravist 370, Bayer Pharma AG, Berlín, Německo nebo Iomeron 400, PNG Gerolymatos A.E.B.E., Kryoneri – Athens, Řecko). Během vyšetření měli pacienti zadržený dech a leželi se vzpaženýma rukama. Následně byla data vypálena na CD ROM a při samotném zákroku proběhla ze získaných dat 3D rekonstrukce levé síně pomocí softwaru 3D elektroanatomického navigačního systému (EnSite Velocity, St. Jude Medical, St. Paul, MN, USA).

3D rotační atriografie levé síně

Rotační atriografie levé síně byla provedena u všech pacientů na angiografickém přístroji s 10palcovým flat detektorem (Philips – Allura Xper FD 10, Philips Healthcare, Best, The Netherlands). Po nástřiku kontrastní látky do levé síně následovalo během 4,1 sekundy otočení C ramene rtg přístroje z polohy 120° vpravo (RAO) do polohy 120° vlevo (LAO). Rychlost snímání jednotlivých řezů byla 30 snímků za minutu, z nichž se následně vytvořil výsledný obraz pomocí speciálního softwaru pracovní stanice s automatickou segmentací 3D obrazu (EP Navigator 3.0, Philips Healthcare, Best, The Netherlands). Použito bylo 60 ml kontrastní látky (Ultravist 370 I/ml, Bayer Pharma AG, Berlin, Germany), kontrast byl podán rychlostí 15 ml/s pomocí injekční pumpy (Mark-V ProVis, Medrad, Inc., Indianola, PA, USA).

Před přímou aplikací kontrastní látky do levé síně byl zaveden kvadrupolární katétr (Irvine Biomedicals, Irvine, CA, USA) do hrotu pravé komory. Při rychlé komorové stimulaci s frekvencí 220/min s významným poklesem krevního tlaku (ověřeno vymizením pulzové křivky saturačního čidla – Phillips IntelliVue MP-20, Philips, Eindhoven, The Netherlands) byla provedena injekce kontrastní látky do levé síně, poté s 2sekundovým zpožděním proběhla rotace C ramene (10, 11, 13).

Obrázek 1. Příklad měření ústí levostranných plicních žil v bočné projekci, u každé žíly jsou vždy uvedeny dva rozměry v textu označované „bočná 1“ a „bočná 2“. Na levé straně obrázku jsou data z trojrozměrné rotační atriografie a vlevo data z CT vyšetření u stejného pacienta

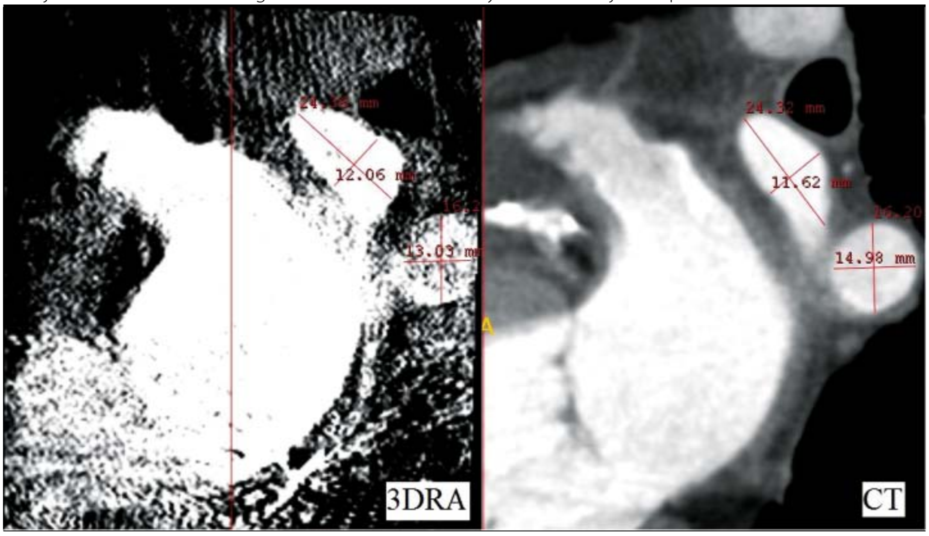

Obrázek 2. Příklad měření odstupu pravé horní plicní žíly v předozadní projekci. Na levé straně obrázku jsou data z trojrozměrné rotační atriografie a vlevo data z CT vyšetření u stejného pacienta

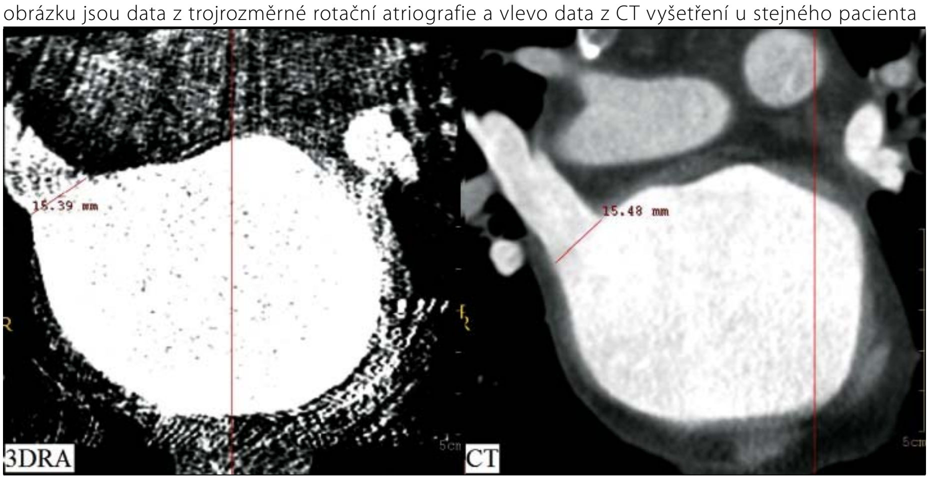

Vlastní ablační výkon

Všechny výkony byly provedeny za standardních podmínek v analgosedaci na angiografickém přístroji vybaveném Philips Alura FD 10 (Philips Healthcare, Best, The Netherlands). V lokální anestezii obou třísel byly zavedeny sheaty a následně katétry. Dekapolární katétr byl zaveden do koronárního sinu. Následně byla provedena nekomplikovaná transseptální punkce. Po úspěšné transseptální punkci byl zaveden do levé síně 8,5F řiditelný sheath Agilis (St. Jude Medical, St. Paul, MN, USA) a po druhé transseptální punkci byl zaveden 8F sheath SL1 (St. Jude Medical, St. Paul, MN, USA). Po provedení punkce byl podán bolus heparinu s následným kontinuálním podáváním dle hodnot ACT. Následně cestou řiditelného sheatu Agilis byl do levé síně zaveden ablační katétr s chlazeným hrotem (Celsius Thermo-cool, Biosense Webster, Diamond Bar, CA, USA), cestou transseptálního sheatu SL1 byl zaveden duodekapolární lasso katétr (Reflexion Spiral Variable Radius Catheter, St. Jude Medical, St. Paul, MN, USA). Poté dle 3D modelu levé síně získaného z rotační atriografie byla vytvořena elektroanatomická mapa levé síně se zobrazením levostranných plicních žil, a to pomocí systému EnSite NavX (St. Jude Medical, St. Paul, MN, USA). Poté byla pomocí radiofrekvenční energie provedena izolace plicních žil pomocí cirkulárních linií kolem plicních žil, definovaná jako vstupní či výstupní blok. V případě perzistující fibrilace síní byly provedeny lineární ablační linie na stropě levé síně, na mitrálním isthmu a v distálním koronárním sinu. Pacienti byli propuštěni do ambulantní péče druhý den po výkonu.

Analýza anatomických dat

Anatomická data levé síně získaná jak z CT vyšetření, tak z 3D rotační atriografie byla hodnocena dvěma nezávislými výzkumníky pomocí stejného softwaru pracovní stanice EP Navigator (EP Navigator 3.0, Philips Healthcare, Best, The Netherlands). Byly hodnoceny rozměry odstupu plicních žil z levé síně, zaznamenal se ostiální rozměr levé žíly v bočné projekci (obrázek 1) a také vertikální rozměr v předozadní projekci (obrázek 2). Při měření rozměru v bočné projekci byly zaznamenány 2 hodnoty (bočná 1 a bočná 2). V případě rozměru „bočná 1“ se jedná o největší průměr žíly, následně bylo v kolmé rovině na toto měření provedeno druhé měření a největší průměr žíly v této rovině byl zaznamenán a označen jako „bočná 2“ (obrázek 1). Rozměr v odstupu žíly byl definován jako rozměr žíly v kolmé rovině na dlouhou osu žíly v místě přechodu plicní žíly na levou síň. Nejdříve byla vyhodnocena data z CT vyšetření jedním výzkumníkem a následně druhým výzkumníkem data z 3D rotační atriografie, tak aby nedošlo k jakémukoliv ovlivnění měření.

Analýza radiační zátěže

U každého pacienta jsme porovnávali radiační zátěž při CT vyšetření a 3D rotační atriografii přepočtenou na efektivní dávku (ED). Pro CT vyšetření, u kterého byla dávka uvedena v jednotkách „dose lenght product“ (mGy cm^{1}), byl použit konvertující faktor 0,017 mSV $mGy^{-1}cm^{-1}$. (14). Pro 3D rotační atriografii, kdy byla dávka měřena v jednotkách „dose area product“ (mGy cm^2), byl použit konvertující faktor 0,18 mSV $mGy^{-1}cm^{-1}$ (15).

Analýza ekonomické nákladnosti

Analýza finanční nákladnosti byla provedena ekonomickým oddělením Fakultní nemocnice u sv. Anny v Brně a může reprezentovat podmínky, které platí ve většině nemocnic v České republice. Do analýzy byly započítány všechny položky, jako je mzda jednotlivých pracovníků (lékařů, biomedicínských inženýrů, laborantů a sester), spotřební materiál, správní režie i odpisy jednotlivých přístrojů tak, aby mohla být vypočtena cena jak CT vyšetření, tak i rotační atriografie.

Statistické zpracování

Základní charakteristiky pacientů a rozměry žil získané pomocí dvou rozdílných metod byly popsány metodami deskriptivní analýzy. Výsledky jsou v případě spojitých parametrů prezentovány pomocí průměru se směrodatnou odchylkou (SD), u kategoriálních parametrů pomocí absolutního a relativního počtu.

Tabulka 1. Radiační zátěž je uvedena jako efektivní dávka radiační zátěže (mSV $mGy^{-1}cm^{-1}$). Dále jsou v tabulce uvedeny rozměry jednotlivých žil (mm). Porovnání rozměru plicních žil je uvedeno v jednotlivých projekcích (AP = předozadní projekce, bočná 1 a bočná 2 jsou nejmenší a největší rozměr žíly při odstupu z levé síně patrné z bočné projekce)

	CT (N=65)			DRA (N=65)			
Parametr	**Průměr (SD)**	**Median (95 % CI)**	**Min-Max**	**Průměr (SD)**	**Median (95 % CI)**	**Min-Max**	**p-value***
AP LIPV	18,082 (2,6010)	17,920 (17,110–18,690)	12,84–24,73	16,841 (2,5333)	16,580 (15,740–17,380)	10,84–24,97	**0,010**
AP LSPV	18,734 (3,4496)	18,085 (17,560–18,950)	13,54–32,41	18,626 (3,7874)	18,160 (17,560–19,010)	11,47–33,41	0,895
AP RIPV	18,525 (3,3787)	18,330 (17,210–19,550)	11,68–31,84	17,963 (3,8291)	17,480 (16,330–18,650)	11,24–33,65	0,238
AP RSPV	18,867 (2,8143)	18,960 (18,090–19,510)	12,50–25,70	19,192 (2,9872)	19,090 (17,980–20,080)	13,02–26,51	0,536
Bočná LIPV 1	19,586 (2,9078)	19,510 (18,510–20,640)	11,79–26,43	19,664 (3,1320)	19,385 (18,110–21,050)	12,09–26,24	0,889
Bočná LIPV 2	13,225 (2,8934)	12,870 (12,190–14,080)	6,64–20,30	13,280 (2,5388)	13,045 (12,480–13,900)	7,74–21,10	0,913
Bočná LSPV 1	21,612 (3,8254)	20,880 (20,260–21,840)	16,30–36,77	21,325 (3,6324)	21,065 (19,920–21,870)	15,20–34,69	0,709
Bočná LSPV 2	14,351 (2,9571)	13,805 (13,270–14,810)	9,70–26,40	15,067 (2,8125)	14,610 (13,740–15,480)	10,07–27,27	0,088
Bočná RIPV 1	20,576 (3,8625)	20,480 (19,120–21,340)	13,57–31,66	20,861 (3,7945)	20,330 (19,010–21,750)	13,22–32,08	0,722
Bočná RIPV 2	15,803 (3,4358)	15,620 (14,910–16,700)	7,92–29,89	15,403 (3,1276)	15,170 (13,990–16,210)	10,05–23,62	0,476
Bočná RSPV 1	24,599 (4,5194)	24,700 (23,160–26,280)	16,13–36,77	24,390 (4,5045)	23,700 (22,120–25,610)	14,59–37,68	0,798
Bočná RSPV 2	16,988 (3,5593)	16,650 (15,560–18,470)	8,86–26,30	17,607 (3,1347)	17,530 (16,150–18,560)	10,95–26,52	0,309
Pacienti s BMI > 30							
AP LIPV	17,837 (2,9652)	16,925 (16,720–18,850)	12,84–24,73	16,770 (2,9327)	15,940 (15,480–17,220)	10,84–24,97	0,160
Pacienti s BMI < 30							
AP LIPV	18,303 (2,1939)	18,190 (17,470–19,230)	13,11–24,67	16,756 (2,0400)	16,600 (15,680–17,490)	12,91–20,92	**0,012**

LIPV – levá dolní plicní žíla; LSPV – levá horní plicní žíla; RIPV – pravá dolní plicní žíla; RSPV – pravá horní plicní žíla

Tabulka 2. Náklady jsou uvedeny v Kč a odpovídají ceně jednoho vyšetření ve FN u sv. Anny v Brně

	3-DRA	CT vyšetření
Mzda zdravotnického perzonálu	336	296
Odpis + servis přístrojů	600	1 171
Spotřební materiál	2 460	2 988
Náklady celkem	3 396	4 456

DRA – trojrozměrná rotační atriografie

Sledované parametry byly porovnány mezi skupinami pacientů rozdělenými dle použité metody. Kategoriální parametry byly porovnány pomocí χ2-kvadrát testu, případně Fisherova testu. Pro porovnání spojitých parametrů mezi skupinami byl použit dvouvýběrový t-test, pokud nebyla normalita dat výrazně porušena, případně neparametrický Mann-Whitney test. Všechny analýzy byly provedeny na 5% hladině významnosti (tj. p-hodnoty < 0,05 jsou považovány za statisticky významné).

Výsledky

Celkem bylo do sledování zařazeno 65 pacientů podstupujících komplexní ablační výkon v levé síni pro fibrilaci síní. Převážná část pacientů byli muži (78 %), průměrný věk pacientů byl 57,7 ± 9,6 let a byl shledán sklon k nadváze (BMI 29,3 ± 4). U většiny pacientů byl přítomen nález dobré systolické funkce LK (EF LK 56 ± 8,2 %) s nálezem dilatované levé síně (diametr levé síně v parasternální projekci: 45 ± 6 mm).

Provedení CT vyšetření a následná segmentace proběhla úspěšně u 100 % pacientů. Úspěšnost provedení rotační atriografie levé síně byla 98,5 %, v jednom případě se zobrazení levé síně nepodařilo z důvodů velkého rozměru levé síně se špatným vycentrováním obrazu a následným nezobrazení odstupu plicních žil. Při komorové stimulaci 220/min před provedením rotace C ramene rtg přístroje nebyly zaznamenány žádné komplikace.

Výsledky měření rozměru ústí žil ukázaly dobrou korelaci mezi oběma sledovanými metodami, při porovnání rozměrů nebyl prokázaný statistický rozdíl mezi použitím dat z CT srdce a z 3D rotační atriografie, kromě rozměru levé dolní plicní žíly měřeného v předozadní projekci (tabulka 1, graf 1–4). Tento statisticky významný rozdíl byl shledán pouze u pacientů s BMI > 30.

Při porovnání efektivní dávky radiační zátěže pro jednotlivé pacienty byla prokázána statisticky významná redukce radiační zátěže při použití 3D rotační atriografie než při CT vyšetření srdce (10,2 ± 2,318 vs. 2,3 ± 0,6 mSV mGy-1cm-1, p < 0,001) (graf 5)

Z ekonomické analýzy nákladnosti vyplývá, že po započítání všech nákladů potřebných k provedení jednotlivých výkonů, včetně odpisů přístrojů, se jeví výhodnější 3D rotační atriografie, kdy celková cena jednoho výkonu činí 3 396 Kč, na rozdíl od CT vyšetření, kde vypočítaná cena byla 4 455 Kč (tabulka 2).

Diskuze

První zkušenosti s rotační atriografií levé síně byly publikovány již v roce 2006 v práci Manzke, et al., kde autoři popsali první zkušenosti s provedením této metody při animálních a humánních studiích (16). Následovaly práce, které se zaměřily na úspěšnost rotační atriografie levé síně k vytvoření použitelného 3D modelu levé síně, hodnotící viditelnost odstupu jednotlivých žil (10). Jednotlivé práce se zaměřily i na popis a srovnání jednotlivých metodologických postupů s nástřikem kontrastní látky do pravé síně, plicnice či levé síně (11, 17). Postupně se ukázalo, že tato nová metoda je bezpečná, s minimálním množstvím komplikací a má vysokou míru úspěšného provedení. Další práce, ve kterých byly využity již nové verze systémů, ukázaly dobrou korelaci mezi daty získanými z CT srdce a z 3D rotační atriografie (9).

Graf 1–4. Altmanův-Blandův graf, který zobrazuje rozdíly jednotlivých rozměrů plicních žil měřených buď z trojrozměrné rotační atriografie nebo z CT vyšetření, tyto rozdíly jsou uvedeny na ose y. Absolutní hodnoty rozměrů jednotlivých žil jsou uvedeny na ose x. Barevně jsou odlišeny jednotlivé projekce, ze kterých bylo prováděno měření. Postupně jsou uvedeny grafy pro jednotlivé žíly

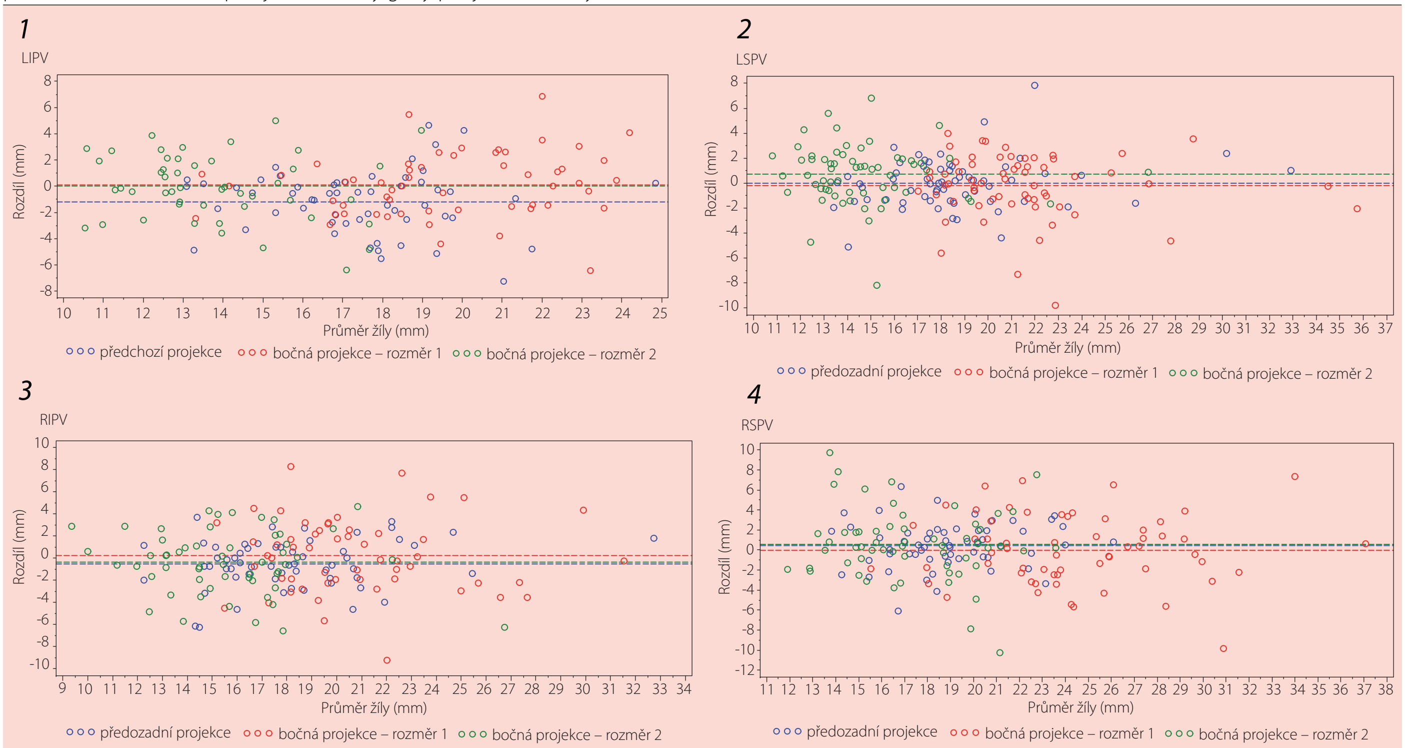

Graf 1. LIPV – levá dolní plicní žíla; Graf 2. LSPV – levá horní plicní žíla; Graf 3. RIPV – pravá dolní plicní žíla; Graf 4. RSPV – pravá horní plicní žíla

Graf 5. Rozdíl efektivní dávky radiační zátěže při použití trojrozměrné rotační atriografie nebo CT vyšetření, hodnoty jsou uvedeny v jednotkách mSV $mGy^{-1}cm^{-1}$

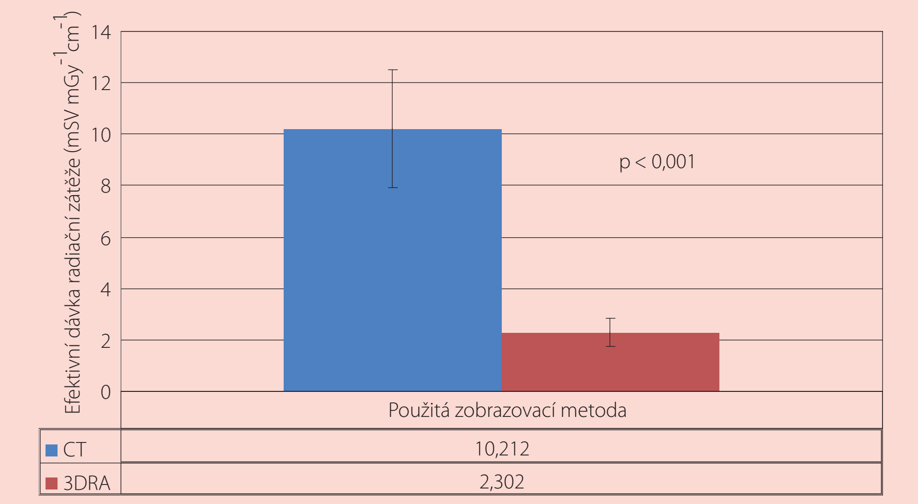

Naše výsledky potvrzují velmi dobrou korelaci mezi rozměry jednotlivých žil získanými z CT vyšetření a z 3D rotační atriografie levé síně. Kromě jednoho měření nebyl zjištěn žádný statisticky významný rozdíl. Pouze při měření rozměru levé dolní plicní žíly v předozadní projekci byl nalezen statisticky významný rozdíl. Při analýze pacientů rozdělených dle BMI byl ale tento rozdíl pozorován pouze u pacientů obézních, s BMI větším jak 30. Tyto výsledky naznačují určité možné limitace této metody u obézních pacientů, přestože samotná obezita nebyla limitací 3D rotační atriografie při tvorbě použitelného modelu levé síně. Příčinou neúspěšné 3D rotační atriografie byl velký rozměr levé síně spolu se špatným vycentrováním obrazu a následným nezobrazením plicních žil. Na druhou stranu v našem souboru pacientů a i ve většině výše uvedených studií byl použit nástřik kontrastní látky přímo do levé síně, kdy tento postup má vyšší úspěšnost provedení oproti nástřiku kontrastní látky do pravostranných oddílů (9). Jeho nevýhodou je naopak absence 3D modelu levé síně, který je fúzovaný do skiaskopického obrazu při transseptální punkci, kdy tento model může pomoci s orientací při této rizikovější části samotného ablačního výkonu. Pro běžnou praxi bude potřeba provést studie se zaměřením na klinické výsledky při použití této metody jako podpory ablační léčby fibrilace síní.

Naše výsledky ukazují jednoznačný profit pacientů z této nové metody díky statisticky významné redukci radiační zátěže oproti CT vyšetření. Tento závěr byl pozorován ve většině prací porovnávajících tyto dvě metody. Na druhou stranu stejná data jako z CT srdce lze získat i pomocí MR srdce při absenci jakékoliv radiační zátěže. Tato metoda ale není v běžné klinické praxi často používána vzhledem k mnoha faktorům, jako je finanční nákladnost, dostupnost a technické limitace u pacientů s poruchami rytmu. V některých centrech mohou operatéři s dostatečnými zkušenostmi provést ablaci v levé síni pouze za pomoci elektroanatomického mapování, i v tomto případě samozřejmě ztrácí metoda 3D rotační atriografie výhodu stran redukce radiační zátěže. Jako další výhoda 3D rotační atriografie oproti CT je menší spotřeba kontrastní látky nutné k provedení vyšetření (8). Určitou limitací samotného srovnání efektivní radiační dávky obou vyšetření může být přepočet na jednotky efektivní dávky za pomoci konvertujících faktorů. Konvertující faktory použité v naší studii se shodují s těmi, které byly použity v jiných studiích, zabývajících se podobným tématem. Konvertující faktor, používaný při CT vyšetřeních k přepočtu z jednotek „dose lenght product" na jednotky efektivní radiační dávky, je ověřen mnohými studiemi. Méně studií se zabývá přepočtem z jednotek „dose area product" v případě 3D rotační atriografie. Tyto konvertující faktory jsou bohužel pouze určitým kompromisem, používaným při těchto převodechk. Hodnota konvertujícího faktoru totiž není ovlivněna pouze samotným přístrojem a jeho parametry, ale i rozdíly mezi jednotlivými pacienty, jako jsou jejich konstituce nebo pohlaví. Proto se hodnota konvertujícího faktoru může lišit mezi jednotlivými vyšetřeními.

Další z faktorů, které mohou ovlivnit používání této metody v běžné klinické praxi je finanční nákladnost. Touto problematikou se ve své práci zabýval Kriatselis, et al., přičemž zjistil, že v ekonomických podmínkách Deutsches Herzzentrum Berlin vychází jedno vyšetření pomocí CT v průměru o 45 € dráž (9). To odpovídá i výsledkům, které se týkají zdravotnictví v České republice, kdy po započítání všech nákladů je CT vyšetření dražší o více jak 1 000 Kč. Tyto údaje se ale díky mnoha faktorům mohou v čase měnit.

Závěr

Metoda 3D rotační atriografie levé síně nám poskytuje stejné anatomické informace jako CT srdce. Tyto data jsme navíc schopni získat přímo na elektrofyziologickém sále při ablačním výkonu levé síně. Při použití této nové metody dochází ke statisticky významné redukci radiační zátěže pro pacienta a finanční náklady na jedno vyšetření jsou nižší oproti CT vyšetření.

Práce byla vypracována s podporou Evropského fondu pro regionální rozvoj – Projekt FNUSA-ICRC No. CZ.1.05/1.1.00/02.0123.

Literatura

1. Anderson JL, Halperin JL, Albert NM, Bozkurt B, Brindis RG, Curtis LH, et al. Management of Patients With Atrial Fibrillation (Compilation of 2006 ACCF/AHA/ESC and 2011 ACCF/AHA/HRS Recommendations) A Report of the American College of Cardiology/American Heart Association Task Force on Practice Guidelines. Circulation. 2013; 127(18): 1916–1926.

2. Schwartzman D, Lacomis J, Wigginton WG. Characterization of left atrium and distal pulmonary vein morphology using multidimensional computed tomography. J Am Coll Cardiol. 2003; 41(8): 1349–1357.

3. Dong J, Calkins H, Solomon SB, Lai S, Dalal D, Lardo A, et al. Integrated Electroanatomic Mapping With Three-Dimensional Computed Tomographic Images for Real-Time Guided Ablations. Circulation. 2006; 113(2): 186–194.

4. Earley MJ, Showkathali R, Alzetani M, Kistler PM, Gupta D, Abrams DJ, et al. Radiofrequency ablation of arrhythmias guided by non-fluoroscopic catheter location: a prospective randomized trial. Eur Heart J. 2006; 27(10): 1223–1229.

5. Dong J, Dickfeld T, Dalal D, Cheema A, Vasamreddy CR, Henrikson CA, et al. Initial experience in the use of integrated electroanatomic mapping with three-dimensional MR/CT images to guide catheter ablation of atrial fibrillation. J Cardiovasc Electrophysiol. 2006; 17(5): 459–466.

6. Martinek M, Nesser HJ, Aichinger J, Boehm G, Purerfellner H. Impact of integration of multislice computed tomography imaging into three-dimensional electroanatomic mapping on clinical outcomes, safety, and efficacy using radiofrequency ablation for atrial fibrillation. Pacing Clin Electrophysiol. 2007; 30(10): 1215–1223.

7. Malchano ZJ, Neuzil P, Cury RC, Holmvang G, Weichet J, Schmidt EJ, et al. Integration of cardiac CT/MR imaging with three-dimensional electroanatomical mapping to guide catheter manipulation in the left atrium: implications for catheter ablation of atrial fibrillation. J Cardiovasc Electrophysiol. 2006; 17(11): 1221–1129.

8. Tang M, Kriatselis C, Ye G, Nedios S, Roser M, Solowjowa N, et al. Reconstructing and registering three-dimensional rotational angiogram of left atrium during ablation of atrial fibrillation. Pacing Clin Electrophysiol. 2009; 32(11): 1407–1416.

9. Kriatselis C, Nedios S, Akrivakis S, Tang M, Roser M, Gerds-Li JH, et al. Intraprocedural imaging of left atrium and pulmonary veins: a comparison study between rotational angiography and cardiac computed tomography. Pacing Clin Electrophysiol. 2011; 34(3): 315–322.

10. Thiagalingam A, Manzke R, D'avila A, Ho I, Locke AH, Ruskin JN, et al. Intraprocedural Volume Imaging of the Left Atrium and Pulmonary Veins with Rotational X-Ray Angiography: Implications for Catheter Ablation of Atrial Fibrillation. J Cardiovasc Electrophysiol. 2008; 19(3): 293–300.

11. Orlov MV. How to perform and interpret rotational angiography in the electrophysiology laboratory. Heart Rhythm. 2009; 6(12): 1830–1836.
12. Gage BF, Waterman AD, Shannon W, Boechler M, Rich MW, Radford MJ. Validation of clinical classification schemes for predicting stroke: Results from the national registry of atrial fibrillation. JAMA. 2001; 285(22): 2864–2870.
13. Ector J, Buck SD, Nuyens D, Rossenbacker T, Huybrechts W, Gopal R, et al. Adenosine-induced ventricular asystole or rapid ventricular pacing to enhance three-dimensional rotational imaging during cardiac ablation procedures. Europace. 2009; 11(6): 751–762.
14. Einstein AJ, Moser KW, Thompson RC, Cerqueira MD, Henzlova MJ. Radiation dose to patients from cardiac diagnostic imaging. Circulation. 2007; 116(11): 1290–1305.
15. Schultz FW, Zoetelief J. Dose conversion coefficients for interventional procedures. Radiat Prot Dosimetry. 2005; 117(1–3): 225–230.
16. Manzke R, Reddy VY, Dalal S, Hanekamp A, Rasche V, Chan RC. Intra-operative volume imaging of the left atrium and pulmonary veins with rotational X-ray angiography. Med Image Comput Comput-Assist Interv MICCAI Int Conf Med Image Comput Comput-Assist Interv. 2006; 9(Pt 1): 604–611.
17. Li JH, Haim M, Movassaghi B, Mendel JB, Chaudhry GM, Haffajee CI, et al. Segmentation and registration of three-dimensional rotational angiogram on live fluoroscopy to guide atrial fibrillation ablation: a new online imaging tool. Heart Rhythm Off J Heart Rhythm Soc. 2009; 6(2): 231–237.

Článek přijat redakcí: 14. 10. 2013
Článek přijat k publikaci: 18. 11. 2013
Článek přijat po přepracování: 13. 11. 2013

MUDr. František Lehar
Fakultní nemocnice u sv. Anny v Brně, ICRC
I. Interní kardioangiologická klinika –
elektrofyziologické oddělení
Pekařská 53, 656 91 Brno
frantisek.lehar@fnusa.cz

Comparison of clinical outcomes and safety of catheter ablation for atrial fibrillation supported by data from CT scan or three-dimensional rotational angiogram of left atrium and pulmonary veins

Frantisek Lehar, Zdenek Starek, Jiri Jez, Miroslav Novak, Jiri Wolf, Radka Stepanova, Peter Kruzliak, Tomas Kulik, Alena Zbankova, Radek Jancar, Jiri Vitovec

Background. Catheter ablation in the left atrium has become a common therapeutic strategy in the management of atrial fibrillation (AF). The high degree of success and safety profile of this procedure is dependent on precise knowledge of the true anatomy in the chamber. This information is imported mostly from cardiac computed tomography. A novel method for imaging the left atrial anatomy is three-dimensional rotational angiography (3DRA).
Methods. The aim of our study was to the compare clinical outcome and safety of catheter ablation for atrial fibrillation guided by 3DRA vs. conventional CT scan. One hundred and twenty-five patients referred for AF catheter ablation at St. Anne's University Hospital Brno were included in the retrospective analysis of clinical outcome within the first year after the procedure.
Results. There was a close correlation in overall procedural parameters between the groups. The frequency of recurrent episodes of AF (24% in CT-guided group vs. 27% in 3DRA-guided group, P=0.721) as well as the onset of atypical atrial flutter after the procedure (10% vs. 8%, respectively, P=0.731) were similar in both groups. No difference in the number of patients necessitating repeat ablation (5% vs. 5%, P=0.984) was found. Procedural complications of ablations guided by 3DRA were comparable with those guided by CT (2% vs. 3%, respectively, P=0.568).
Conclusion. 3DRA has proven to be a safe and simple method for imaging the left atrium and guiding catheter ablation for AF. This approach is anticipated to become a new standard in 3D reconstruction of the left atrium.

Keywords: atrial fibrillation, catheter ablation, electrophysiology, three dimensional rotational atriography, computed tomography, imaging, left atrium

Received: October 14, 2013; Accepted: July 3, 2014; Available online July 17, 2014
http://dx.doi.org/10.5507/bp.2014.040

International Clinical Research Center, Department of Cardiovascular Disease, St. Anne's University Hospital in Brno and Faculty of Medicine, Masaryk University Brno, Czech Republic
Corresponding author: Frantisek Lehar, e-mail: frantisek.lehar@fnusa.cz

INTRODUCTION

Catheter ablation for atrial fibrillation is a technically challenging but highly effective left atrial procedure[1]. Given the variability of the left atrium and pulmonary vein ostia, precise knowledge of true anatomy is the key to a successful and safe intervention[2]. Therefore, preprocedural computer tomography (CT) or magnetic resonance (MR) is frequently used as anatomical guidance for catheter ablation[3–5]. A novel method allowing reconstruction of the left atrium is three-dimensional rotational angiogram (3DRA), which is carried out intra-procedurally right in the EP lab[6,7]. The acquired 3D volume is then used as a template for non-fluoroscopic 3D electroanatomic mapping in the systems Carto (Biosense Webster, Diamond Bar, CA, USA) or Velocity (St. Jude Medical, St. Paul, MN, USA) (ref.[8,9]). Three-dimensional rotational angiogram also enables merging the resulting 3D image with live fluoroscopy, which is a great help for orientation in the left atrium during the map acquisition (Fig. 1). Moreover, the anatomical data obtained from 3D rotational angiogram of left atrium has proven to be comparable with the information from conventional CT scan and radiation exposure is lower by using 3DRA (ref.[10,11]). Another advantage is the possibility of integrating the 3D image from the rotational angiography into the electroanatomical mapping system, which facilitates the execution of AF ablation and reduces the total procedural time and radiation exposure while providing similar clinical outcomes[12]. Previous studies have proven that the fusion of CT or MR image of the left atrium with the electroanatomical map in the Carto-Merge system is beneficial for the clinical outcome of the AF ablation and reduction in fluoroscopic guidance[4,13,14]. The range of 3D rotational angiography application is even wider. There are reports of registration of 3D volume obtained from 3DRA with intracardiac echocardiography (ICE) allowing for electroanatomical mapping of the left atrium. This was the first ever image integration of two left atrial reconstructions by means of two different intraprocedural methods of noninvasive cardiac imaging – 3D rotational angiography and ICE-based image registration in electroanatomical mapping system[15].

Three-dimensional rotational angiogram is performed

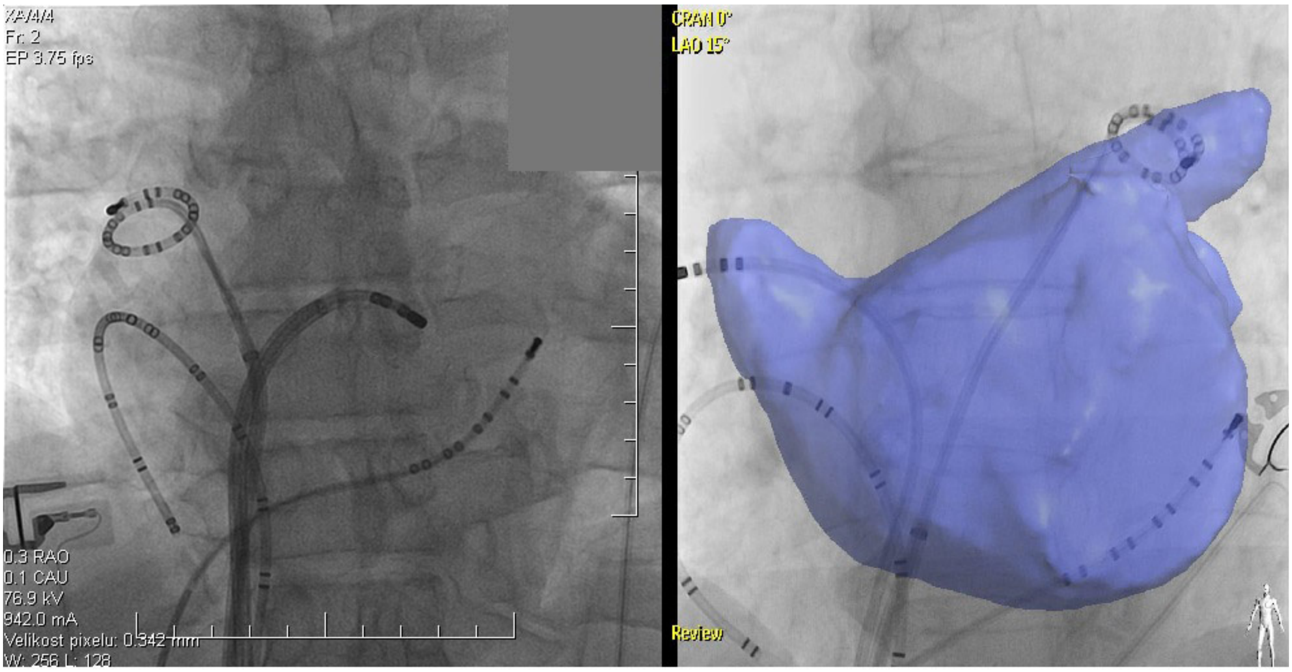

Fig. 1. On the left, there is a skiascopic view of catheter ablation of atrial fibrillation without using three-dimensional rotational angiography. On the right, there is a fused image of the skiascopic view and the 3D image of the left atrium obtained from three dimensional angiography. This fused image is great guidance for catheter ablation of atrial fibrillation.

using cardiac X-ray system with custom software for 3D image post-processing. Following the initial intracardial contrast injection, a fixed C-arm rotates around the patient and acquires a series of x-ray images immediately reconstructed by a software algorithm into the 3D volume representing the left atrium and pulmonary vein ostia. The contrast medium can be injected either directly into the left atrium with subsequent rapid ventricular pacing or intravenous administration of adenosine to induce short-term asystoly and allow for homogenous contrast opacification, or indirectly in the right atrium with a delay of 9 s preceding the initiation of rotational run to permit the transit of contrast medium through the lungs into the left atrium[16,17]. Advanced angiography systems equipped with 3DRA (e.g. EP Navigator – Philips, DynaCT Cardiac – Siemens, Innova – GE Healthcare) are currently available to enhance and support electrophysiological intervention.

From 2010 to June 2013, our center performed more than 408 left atrial and 33 right or left ventricular angiograms. To the best of our knowledge, there are no data available on the clinical outcome of catheter ablation for atrial fibrillation guided by 3D rotational angiogram of left atrium. The aim of our study was to compare clinical outcome and safety of the catheter ablation for atrial fibrillation guided by 3D rotational angiography vs. conventional CT scan.

METHODS

One hundred and twenty-five patients referred for AF catheter ablation at St. Anne's University Hospital in Brno were included in the retrospective analysis of clinical outcome within the first year after the procedure. Data from January 2011 to August 2011 reported only CT-guided ablations while the majority of the procedures between September 2011 and August 2012 have already used the 3D rotational angiography with left atrial injection and those were involved in the study. Had there been a history of iodine allergy or renal insufficiency indicated by a decline in glomerular filtration rate of less than 45 mL/min, no 3DRA or CT were performed.

Patient preparation

All patients underwent a full clinical assessment in an outpatient service for cardiac arrhythmia and were submitted to catheter ablation for drug refractory paroxysmal or persistent atrial fibrillation. Transthoracic echocardiography was performed preoperatively in all of them. If considered necessary, anticoagulant therapy followed CHA2DS2-VASc score guidelines and was discontinued five days prior to the scheduled procedure[18]. Patients were supplemented with subcutaneous low molecular heparin adjusted according to their weight until the day of the procedure to compensate for ineffective levels of INR. Those treated from January 2011 to August 2011 underwent preprocedural cardiac CT. Before the procedure, transesophageal echocardiography was performed to exclude the presence of intracardiac thrombus.

Computed tomography

Patients underwent a CT scan within seven to 14 days preceding the procedure using 64 Slice CT Scanner (GE Lightspeed VCT, General Electric, Fairfield, USA) with configuration 120 KV, 800 mAs, a collimation width of 63 x 0.625 mm, and a spiral pitch factor of 0.98. The images were then reconstructed in a resolution of 512 x 512 pixels. Contrast medium injection (100-150 mL of Ultravist 370, Bayer Pharma AG, Berlin, Germany or Iomeron 400, PNG Gerolymatos A.E.B.E., Kryoneri – Athens, Greece) was administered via the peripheral vein. During the acquisition, patients remained lying down with both arms raised and breath-holding. The obtained x-ray images were then transferred to a data CD. At the time of the procedure, 3D representation of the left atrium was reconstructed in the 3D electroanatomical mapping system (EnSite Velocity, St. Jude Medical, St. Paul, MN, USA) based on the anatomic shell imported from CT.

Three-dimensional rotation angiography

Rotational angiography was performed using a C-arm angiography system Philips Allura Xper FD 10 with a 10-inch flat detector (Philips Healthcare, Best, The Netherlands). After injecting the contrast medium into the left atrium, C-arm was rotated from 120° right anterior oblique (RAO) to 120° left anterior oblique position (LAO) over 4.1 s. Images acquired at a rate of 30 frames per minute were then transferred to a working station and reconstructed into a 3D volume using the specialized software for automated segmentation (EP Navigator 3.0, Philips Healthcare, Best, The Netherlands). For a contrast injection, a pigtail catheter (Cordis, Miami, FL, USA) advanced to the left atrium was used and a bolus of 60 mL contrast medium (Ultravist 370 I/mL, Bayer Pharma AG, Berlin, Germany) was administered at a speed of 15 mL/s via power injector (Mark-V ProVis, Medrad, Inc., Indianola, PA, USA). Patients were lying down with the hands along the body and were asked for shallow breathing. Prior to contrast application, a quadrupolar steerable catheter (Irvine Biomedicals, Irvine, CA, USA) was positioned into the right atrial apex and rapid ventricular pacing of 220 beats per min was performed with a substantial decrease in blood pressure detected by the absence of oxygen saturation curve on the pulse oximetry monitor screen (Philips IntelliVue MP-20, Philips, Eindhoven, The Netherlands) (ref.[19]). Finally, the contrast medium was injected and C-arm rotation initiated with a 2 s delay. Along with the left atrial rotational angiography, all patients underwent a 3D rotational esophagography to visualize the position of the esophagus and its relation to other cardiac structures[20]. Opacification was achieved by swallowing 30-50 mL of barium sulfate esophageal cream (Micropaque – Guerbet, Roissy, France) five seconds before the initiation of rotational run.

Catheter ablation

All patients underwent the ablation procedure under a standard protocol using Philips Allura Xper FD10 system (Philips Healthcare, Best, The Netherlands). Sheaths and electrophysiological catheters were inserted via both femoral veins under local anaesthesia. The 8F sheath was introduced through the left femoral vein and used for advancement of a decapolar catheter into the coronary sinus. Double transseptal puncture was performed via right femoral venous access with the guidance of fluoroscopy, local injection of an iodinated contrast medium with an invasive blood pressure monitoring system on a needle tip, and intracardial ultrasound. Then, both an 8.5F Agilis steerable introducer and an 8F SL1 sheath (St. Jude Medical, St. Paul, MN, USA) were positioned into the left atrium and a bolus of intravenous heparin with continuous infusion adjusted according to the ACT (target levels of 350 to 300 s) was administered. An irrigated-tip ablation catheter (Celsius™ Thermo-cool, Biosense Webster, Diamond Bar, CA, USA) was inserted over the Agilis steerable sheath and placed into the left atrium as well as a duodecapolar spiral catheter (ReflexionSpiral Variable Radius Catheter™, St. Jude Medical, St. Paul, MN, USA) advanced over the SL1 transseptal sheath. An electroanatomical map of the left atrium and left pulmonary veins was made based on a 3D anatomic shell from either CT or 3DRA in the EnSite NavX system

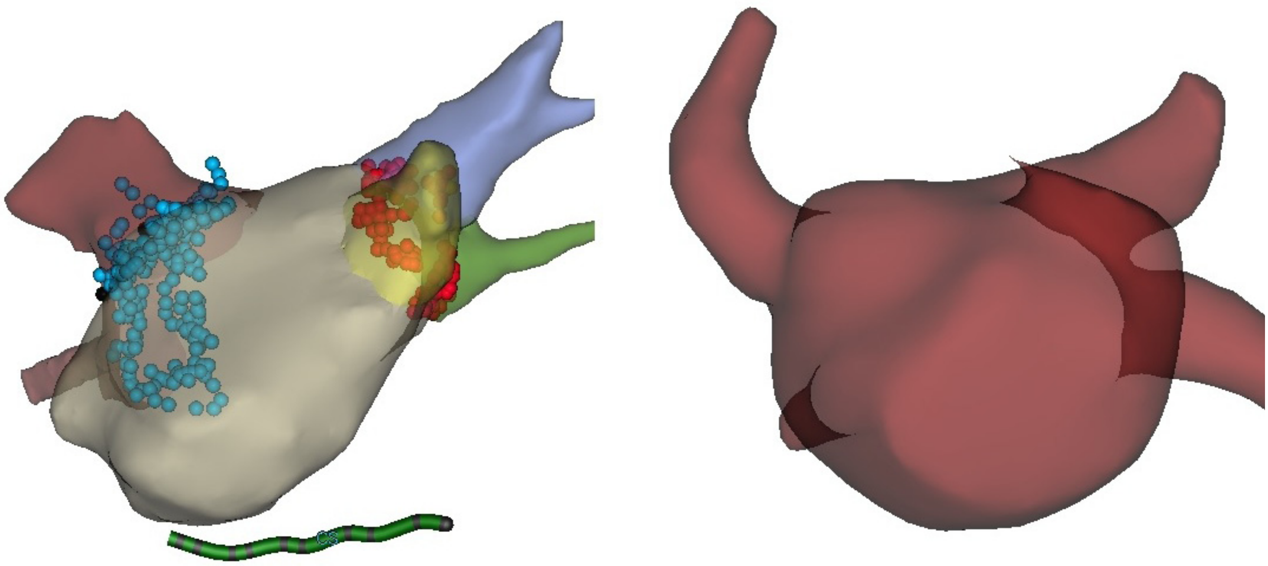

Fig. 2. On the right, there is a 3D image of the left atrium obtained from CT scan. On the left, there is shown an electroanatomical map of the left atrium based on the image obtained from CT (the red and blue points mark location of RF ablations).

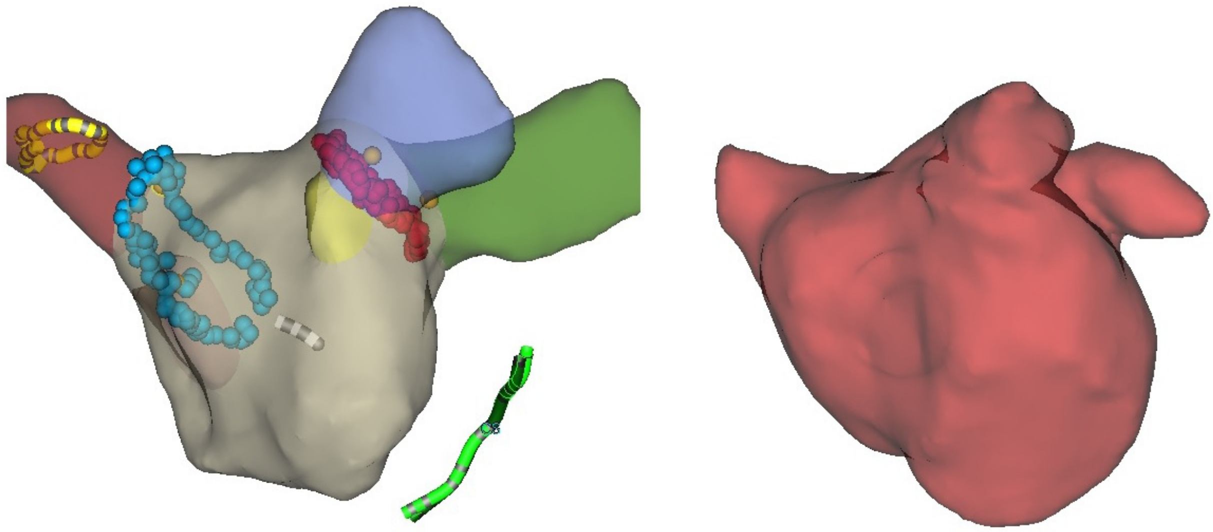

Fig. 3. On the right, there is a 3D image of the left atrium obtained from three-dimensional rotational angiography. On the left, there is shown an electroanatomical map of the left atrium based on the image obtained from CT (the red and blue points mark location of RF ablations).

(St. Jude Medical, St. Paul, MN, USA) (Fig. 2 and 3). Radio-frequency energy was delivered creating circular ablation lesions to isolate pulmonary vein ostia. The successful isolation was defined by achieving the entrance and/or exit block. In patients with persistent atrial fibrillation, adjacent lines of ablation at the left atrial roof, mitral isthmus and distal coronary sinus were performed. During the procedure, patients remained under mild sedation with midazolam and fentanyl. Femoral sheaths were removed within three hours post procedure upon a decrease of intravenously administered heparin and groin compressions were applied. Patients were discharged the day after the ablation.

Follow up

Patients were followed during regular visits at one, six and 12 month(s) after the index procedure in the outpatient service for cardiac arrhythmias. Evaluation of prior 24-h holter monitoring, 12-lead ECG recordings, and arrhythmia episodes were documented. If considered necessary, patients were provided with an episodic ECG portable heart scan (Omron Healthcare Co. Ltd., Kyoto, Japan) for a period of 14 days and the results were analyzed in an extra visit. All data were entered into the hospital information system, which served as source documentation for our analysis.

Radiation dose assessment

A total radiation dose was calculated for both the ablation procedure and the left atrial imaging (3DRA or CT). Regarding the different use of units, we compared the effective radiation dose (mSv). The amount of radiation during cardiac CT scan was expressed as „dose length product" (mGy cm^1) and was adjusted using a conversion coefficient 0,017 mSV $mGy^{-1}cm^{-1}$ (ref.[21]). Radiation exposure for 3D rotational angiography was measured as „dose area product" (mGy cm^2) and the effective dose was calculated using a conversion coefficient 0,18 $mSVmGy^{-1}cm^{-2}$ (ref.[22]).

Statistical analysis

Patient characteristics and the clinical outcome of both groups were described using descriptive statistics. Continuous variables are expressed as a mean ± standard deviation (SD) and categorical variables as absolute values and percentages. All parameters were compared according to the imaging method used. Categorical data were analyzed using chi-squared test or Fisher's exact test. Continuous data were evaluated using unpaired Student's t-test or nonparametric Mann-Whitney when dealing with non-normal distribution. Results were deemed statistically significant for a P value > 0.5 since all analyses were performed at the 5% significance level.

RESULTS

The study sample involved 125 patients with paroxysmal or persistent atrial fibrillation who received therapeutic catheter ablation at the Arrhythmology Department of St. Anne's University Hospital in Brno between January 2011 and August 2012. The ablation procedure was guided either by preoperational CT scan (62 patients) or periprocedural 3D rotational angiography (63 patients). There was no difference in age, gender, BMI, left atrium diameter, left ventricular ejection fraction, concomitant diseases or proportion of paroxysmal to persistent AF between both groups. The overall characteristics are presented in Table 1.

For rotational angiography, only direct (left atrial) contrast injection approach was applied with a success rate of 98.5%. The 3D reconstruction was unsuccessful in one patient due to large LA diameter and poor isocentering associated with incomplete resulting image (pulmo-

Table 1. Patients' characteristics.

	CT (N=62)	DRA (N=63)	
Parameter	N (%)	N (%)	*P**
Gender (male)	44 (71%)	48 (76%)	0.508
Hypertension	43 (69%)	42 (67%)	0.747
Diabetes mellitus	14 (23%)	9 (14%)	0.231
Hyperlipoproteinemia	32 (52%)	29 (46%)	0.533
Ischemic heart disease	11 (18%)	6 (10%)	0.180
Stroke	4 (6%)	2 (3%)	0.392
Type of atrial fibrillation:			0.480
Paroxysmal	44 (71%)	41 (65%)	
Persistent	18 (29%)	22 (35%)	
	Mean (SD)	Mean (SD)	
Age (years)	60.3 (10.28)	58.3 (9.61)	0.215
Left atrial diameter (mm)	43.2 (6.51)	45.5 (6.27)	0.082
Left ventricular ejection fraction (%)	56.5 (9.55)	57.2 (7.02)	0.888
BMI	29.5 (5.1)	29.3 (4.0)	0.728

nary vein ostia were not depicted). Conversely, the CT scan yielded 100% success profile.

There was a close correlation in overall procedural parameters between both groups. No difference was observed in procedural time (231 ± 38 vs. 249 ± 57 min, *P*=0.094), fluoroscopic time (24.6 ± 8 vs. 24±7.5 min, *P*=0.702) or number of RF applications (78.21 vs. 84±23, *P*=0.174). However, ablation time (2732 ± 748 vs. 3105 ± 850, *P*=0.014) and radiation exposure (17.66 ± 2.32 vs. 5.99 ± 2.68 mGycm^2, *P*<0.01) were significantly lower for 3DRA-guided procedures (Table 2). The mean follow-up period was 13.8 ± 3.5 months. The frequency of recurrent episodes of AF (24% in CT-guided group vs. 27% in 3DRA-guided group, *P*=0.721) as well as the onset of atypical atrial flutter after the index procedure (10% vs. 8%, respectively, *P*=0.731) were similar in both groups (Table 3). No difference in the number of patients necessitating repeat ablation (5% vs. 5%, *P*=0.984) was observed. During the follow-up period, both groups showed a corresponding proportion of prescribed antiarrhythmic drugs (55% vs. 49%, *P*=0.529) and present anticoagulation therapy (42% vs. 46%, *P*=0.777). Procedural complications of ablations guided by 3DRA were comparable with those guided by CT (2% vs. 3%, respectively, *P*=0.568). Only hemodynamically insignificant pericardial effusions not requiring any intervention were reported. No other complications were encountered.

Table 2. Procedure results.

	CT (N=62)	3DRA (N=63)	
Parameters of procedure	Mean (SD)	Mean (SD)	*P**
Procedural time (minutes)	231.6 (38.64)	249.5 (57.68)	0.094
Fluoroscopic time (minutes)	24.6 (7.99)	24.0 (7.46)	0.702
Number of RF applications	78.6 (21.23)	84.2 (22.77)	0.174
Ablation time (seconds)	2732.2 (748.29)	3105.2 (850.13)	0.014
Radiation exposure (mSv)	17.66 (2.32)	5.99 (2.68)	<0.01

Table 3. Clinical results.

	CT (N=62)	3DRA (N=63)	
One-year follow-up	N (%)	N (%)	*P**
Recurrent of atrial fibrillation	15 (24%)	17 (27%)	0.721
Onset of atypical atrial flutter	6 (10%)	5 (8%)	0.731
Antiarrhythmic drugs	34 (55%)	31 (49%)	0.529
Anticoagulation therapy	26 (42%)	28 (44%)	0.777
Repeat ablation	3 (5%)	3 (5%)	0.984
Procedural complications (hemodynamically insignificant pericardial effusions)	1 (2%)	3 (5%)	0.568

DISCUSSION

Prior studies have already shown that 3DRA reconstruction of left atrium is a feasible, simple and safe method with a high rate of success. The main benefit of the approach is online image acquisition during the electrophysiological procedure at the cath lab and the ability to overlay resulting 3D shell onto the live fluoroscopic screen.

The 3DRA data has proven equal to a cardiac CT scan with no difference in terms of left atrial parameters, such as PV ostia or LA volume measurements. Additionally, patients are subjected to a lower dose of radiation and contrast medium compared to CT. More recently, studies investigating the utility of 3DRA for imaging the right or left ventricle as guidance for catheter ablation of ventricular arrhythmias have been published[23].

To the best of our knowledge, there are only limited research data available assessing clinical outcome of AF ablation guided by 3DRA vs. CT. A study conducted by Knecht et al. is one of the few examples addressing the topic[24]. In a randomized trial, they compared clinical outcome of catheter ablation for atrial fibrillation supported by conventional electroanatomical mapping using the CARTO system with procedures guided by 3D rotational angiography. Between 2007 and 2008, they assigned 91 patients with paroxysmal (63%) and persistent (37%) atrial fibrillation referred for ablation in Boston and Bordeaux. Those patients were randomized to either CARTO-guided (47 patients) or 3DRA-guided (44 patients) ablation. The data showed close correlation in procedural time (232 ± 65 vs. 218 ± 67 min, *P*=0.335), fluoroscopy time (75 ±

28 vs. 67 ± 26 min, *P*=0.151), or radiation dose (71810 ± 42954 vs. 68009 ± 38345 mGycm^2, *P*=0.719) between the groups. Patients were followed for a mean period of 10 ± 4 months and no difference in AF recurrence (20% vs. 15%, *P*=0.555) or any episodes of recurrent arrhythmia (34% vs. 38%, *P*=0.668) were observed.

Our results are in concordance with these findings. Only procedural and ablation time were non-significantly longer in the 3DRA-guided group and could be explained by extra time needed for the performance of LA rotational angiography which has been a more aggressive approach in the management of atrial fibrillation at our center during the last two years associated with longer duration of RF delivery. We also found a statistically significant reduction in radiation exposure in those procedures supported by 3DRA compared to CT. Based on our experience, a merger of 3DRA with live fluoroscopy enables us to apply a lower x-ray dose in order to produce the same image sequence which can potentially decrease the radiation exposure in procedures while reaching the same fluoroscopic time. The frequency of AF recurrence was 24% in 3DRA-guided and 27% in the CT-guided group (*P*=0.721) and recurrent arrhythmia in general was 34% vs. 35%, *P*=0.902. The proportion of arrhythmia-free patients in our sample was slightly lower than Knecht et al., but the mean follow-up period was on average four months longer (13.8 ± 3.5 to 10 ± 4 months), possibly leading to a higher occurrence of arrhythmia episodes. The high safety profile of 3D rotational angiography was achieved in both study samples (ours vs. Knecht) with no difference in procedural risks compared to conventional procedures.

Another study investigating clinical outcomes of procedures employing 3D rotational angiography was performed by Carpen et al.[12]. This retrospective analysis confirmed that fusion of 3DRA with the electroanatomical mapping system results in reduction of total procedural time and radiation exposure with similar clinical outcome during the follow-up (10±3 months vs. 11.9±5.3 months) compared to procedures without the fusion. Despite the small sample size (36 patients), this conclusion supports the application of 3DRA to guide ablations for atrial fibrillation.

These findings imply a clinical benefit of 3D rotational angiography employed in routine practice. Knecht et al. used 3DRA as a stand-alone imaging method while we dispute 3DRA as an adequate substitute for the conventional electroanatomical mapping since specific functionalities, such as voltage and activation mapping, are not supported and can be useful in patients converting from AF into another atrial arrhythmia (e. g. atypical atrial flutter) during the procedure. Interventions guided only by 3DRA could also be challenging for less experienced physicians.

However, retrospective analysis and a shorter follow-up period are the main limitations of our study. Another limitation is consecutive inclusion of patients and potential bias of results with the growing experience of operators performing the AF ablation. In contrast, our ablation technique was constant during this period. The sample size in our study was larger than both the retrospective and prospective trials reporting on clinical outcomes of AF ablation using 3DRA (ref.[12,24]). Further confirmation of the retrospective data with a prospective, randomized study is required, but is not ethically justified due to the superiority of 3DRA in reducing radiation exposure documented in a number of studies[6,7,10]. On the other hand, a new state-of-the-art cardiac CT often subjects patients to a lower dose of radiation with values close to the 3D rotational angiography[25].

Based on the literature, no prior study has compared the clinical outcomes of ablation procedures using 3D rotational angiography as a substitute to cardiac CT. Both Tang et al. and Kriatselis et al. reported a reduction in the dose of radiation and contrast medium for patients undergoing 3DRA in comparison to CT. Our clinical results demonstrate the utility of 3D rotation angiography as an adequate alternative to a commonly performed CT scan[6,7].

CONCLUSION

Three-dimensional rotational angiography has proven to be a safe and simple method for imaging the left atrium and guiding catheter ablation for atrial fibrillation. Our clinical experience suggests that 3DRA is comparable to a conventional CT scan. Given the low radiation exposure and use of contrast medium in comparison to CT, this approach could be a useful alternative technique in 3D reconstruction of the left atrium as a support for AF ablation.

ABBREVIATIONS

3D, three dimensional; 3DRA, three-dimensional rotational angiogram; AF, atrial fibrillation; CT, computed tomography; MRI, magnetic resonance imaging.

Acknowledgement: Supported by European Regional Development Fund, Project FNUSA-ICRC (No. CZ 1.05/1.1.00/02.0123)
Author contributions: FL, ZS: study design; FL, JJ, JW, TK, AZ, RJ: data collection; FL, ZS, MN: data interpretation; FL, RS, TK: statistical analysis; FL: manuscript writing; FL, JW: figures; ZS, MN, PK, JV: final approval.
Conflict of interest statement: The authors state that there are no conflicts of interest regarding the publication of this article.

REFERENCES

1. Anderson JL., Halperin JL, Albert NM, Bozkurt B, Brindis RG, Curtis LH, DeMets D. Management of Patients With Atrial Fibrillation (Compilation of 2006 ACCF/AHA/ESC and 2011 ACCF/AHA/HRS Recommendations) A Report of the American College of Cardiology/American Heart Association Task Force on Practice Guidelines. Circulation 2013;127(18):1916-26.
2. Schwartzman D, Lacomis J, Wigginton WG. Characterization of left atrium and distal pulmonary vein morphology using multidimensional computed tomography. J Am Coll Cardiol 2003;41(8):1349-57.
3. Dong J, Dickfeld T, Dalal D, Cheema A, Vasamreddy CR, Henrikson CA, Marine JE. Initial experience in the use of integrated electro-

anatomic mapping with three-dimensional MR/CT images to guide catheter ablation of atrial fibrillation. J Cardiovasc Electrophysiol 2006;17(5):459-66.

4. Martinek M, Nesser H-J, Aichinger J, Boehm G, Purerfellner H. Impact of integration of multislice computed tomography imaging into three-dimensional electroanatomic mapping on clinical outcomes, safety, and efficacy using radiofrequency ablation for atrial fibrillation. Pacing Clin Electrophysiol PACE 2007;30(10):1215-23.
5. Malchano ZJ, Neuzil P, Cury RC, Holmvang G, Weichet J, Schmidt EJ, Ruskin JN, Reddy VY. Integration of cardiac CT/MR imaging with three-dimensional electroanatomical mapping to guide catheter manipulation in the left atrium: implications for catheter ablation of atrial fibrillation. J Cardiovasc Electrophysiol 2006;17(11):1221-9.
6. Tang M, Kriatselis C, Ye G, Nedios S, Roser M, Solowjowa N, Fleck E, Gerds-Li J-H. Reconstructing and registering three-dimensional rotational angiogram of left atrium during ablation of atrial fibrillation. Pacing Clin Electrophysiol PACE 2009;32(11):1407-16.
7. Kriatselis C, Nedios S, Akrivakis S, Tang M, Roser M, Gerds-Li J-H, Fleck E, Orlov MV. Intraprocedural imaging of left atrium and pulmonary veins: a comparison study between rotational angiography and cardiac computed tomography. Pacing Clin Electrophysiol PACE 2011;34(3):315-22.
8. Dong J, Calkins H, Solomon SB, Lai S, Dalal D, Lardo A, Brem E. Integrated Electroanatomic Mapping With Three-Dimensional Computed Tomographic Images for Real-Time Guided Ablations. Circulation 2006;113(2):186-94.
9. Earley MaJ, Showkathali R, Alzetani M, Kistler PM, Gupta D, Abrams DJ, Horrocks JA, Harris SJ, Sporton SC, Schilling RJ. Radiofrequency ablation of arrhythmias guided by non-fluoroscopic catheter location: a prospective randomized trial. Eur Heart J 2006;27(10):1223-9.
10. Lehar F, Starek Z, Jez J, Novak M, Wolf J, Kruzliak P, Kulik T, Zbankova A. Rotational atriography of left atrium – a new imaging technique used to support left atrial radiofrequency ablation: a comparison of anatomical data of left atrium. Interv Akut Kardiol 2013;12(4):184-9.
11. Li JH, Haim M, Movassaghi B, Mendel JB, Chaudhry GM, Haffajee CI, Orlov MV. Segmentation and registration of three-dimensional rotational angiogram on live fluoroscopy to guide atrial fibrillation ablation: a new online imaging tool. Heart Rhythm Off J Heart Rhythm Soc 2009;6(2):231-7.
12. Carpen M, Matkins J, Syros G, Gorev MV, Alikhani Z, Wylie JV, Natan SR. First experience of 3D rotational angiography fusion with NavX electroanatomical mapping to guide catheter ablation of atrial fibrillation. Heart Rhythm Off J Heart Rhythm Soc 2013;10(3):422-7.
13. Bertaglia E, Bella PD, Tondo C, Proclemer A, Bottoni N, Ponti RD, Landolina M. Image integration increases efficacy of paroxysmal atrial fibrillation catheter ablation: results from the CartoMerge Italian Registry. Eur Eur Pacing Arrhythm Card Electrophysiol J Work Groups Card Pacing Arrhythm Card Cell Electrophysiol Eur Soc Cardiol 2009;11(8):1004-10.
14. Caponi D, Corleto A, Scaglione M, Blandino A, Biasco L, Cristoforetti Y, Cerrato N, Toso E, Morello M, Gaita F. Ablation of atrial fibrillation: does the addition of three-dimensional magnetic resonance imaging of the left atrium to electroanatomic mapping improve the clinical outcome?: a randomized comparison of Carto-Merge vs. Carto-XP three-dimensional mapping ablation in patients with paroxysmal and persistent atrial fibrillation. Eur Eur Pacing Arrhythm Card Electrophysiol J Work Groups Card Pacing Arrhythm Card Cell Electrophysiol Eur Soc Cardiol 2010;12(8):1098-104.
15. Nölker G, Gutleben KJ, Asbach A, Vogt J, Heintze J, Brachmann J, Horstkotte D, Sinha AM. Intracardiac echocardiography for registration of rotational angiography-based left atrial reconstructions: a novel approach integrating two intraprocedural three-dimensional imaging techniques in atrial fibrillation ablation. Eur Eur Pacing Arrhythm Card Electrophysiol J Work Groups Card Pacing Arrhythm Card Cell Electrophysiol Eur Soc Cardiol 2011;13(4):492-8.
16. Thiagalingam A, Manzke R, D'avila A, Ho I, Locke AH, Ruskin JN, Chan RC, Reddy VY. Intraprocedural Volume Imaging of the Left Atrium and Pulmonary Veins with Rotational X-Ray Angiography: Implications for Catheter Ablation of Atrial Fibrillation. J Cardiovasc Electrophysiol 2008;19(3):293-300.
17. Orlov MV. How to perform and interpret rotational angiography in the electrophysiology laboratory. Heart Rhythm 2009;6(12):1830-6.
18. Gage BF, Waterman AD, Shannon W, Boechler M, Rich MW, Radford MJ. Validation of clinical classification schemes for predicting stroke: Results from the national registry of atrial fibrillation. JAMA 2001;285(22):2864-70.
19. Ector J, Buck SD, Nuyens D, Rossenbacker T, Huybrechts W, Gopal R, Maes F, Heidbüchel H. Adenosine-induced ventricular asystole or rapid ventricular pacing to enhance three-dimensional rotational imaging during cardiac ablation procedures. Europace 2009;11(6):751-62.
20. Orlov MV, Hoffmeister P, Chaudhry GM, Almasry I, Gijsbers HM, Swack T, Haffajee CI. Three-dimensional rotational angiography of the left atrium and esophagus—A virtual computed tomography scan in the electrophysiology lab? Heart Rhythm 2007;4(1):37-43.
21. Einstein AJ, Moser KW, Thompson RC, Cerqueira MD, Henzlova MJ. Radiation dose to patients from cardiac diagnostic imaging. Circulation 2007;116(11):1290-1305.
22. Schultz FW, Zoetelief J. Dose conversion coefficients for interventional procedures. Radiat Prot Dosimetry 2005;117(1-3):225-30.
23. Orlov MV, Ansari MM, Akrivakis ST, Jadidi A, Nijhof N, Natan SR, Wylie JV, Hicks A, Armstrong J, Jais P. First experience with rotational angiography of the right ventricle to guide ventricular tachycardia ablation. Heart Rhythm 2011;8(2):207-11.
24. Knecht S, Wright M, Akrivakis S, Nault I, Matsuo S, Chaudhry GM, Haffajee C. Prospective randomized comparison between the conventional electroanatomical system and three-dimensional rotational angiography during catheter ablation for atrial fibrillation. Heart Rhythm 2010;7(4):459-65.
25. Yang L, Xu L, Yan Z, Yu W, Fan Z, Lv Z, Zhang Z. Low dose 320-row CT for left atrium and pulmonary veins imaging-the feasibility study. Eur J Radiol 2012;81(7):1549-54.

Comparison of radiation exposure, contrast agent consumption and cost effectiveness between computer tomography and 3D rotational angiography of the left atrium to guide catheter ablation in patients with atrial fibrillation

Zdenek Starek, Frantisek Lehar, Jiri Jez, Jiri Wolf, Tomas Kulik, Alena Kulikova

Background. Catheter ablation of complex atrial arrhythmias guided by 3D models of a left atrium (LA) derived from CT/MRI or 3D rotational angiography of the heart (3DRA) is currently a common practice. Our aim is to compare radiation dose, consumption of a contrast agent and cost of these methods.

Methods. From 10/2012 to 10/2015, either 3DRA (157 patients using the X-ray system Philips Allura FD 10) or computer tomography (CT) (157 patients using 64-slice CT GE Lightspeed VCT) of the LA was performed in patients undergoing complex atrial arrhythmias ablation. All procedures were monitored for average effective radiation dose, dose of the contrast agent and analysis of a financial expenditures.

Results. The average effective radiation dose for 3DRA was 2.11±0.392 mSv compared to 10.52±2.093 mSv for CT. The contrast agent consumption was 22.2 mg and 48.2 mg of iodine for 3DRA and CT, respectively. Total price per procedure is 123€ for 3DRA and 161€ for CT.

Conclusion. Consumption of the contrast agent and radiation burden for LA 3DRA is significantly lower in comparison to most currently used CT scan methods. Cost of both methods is comparable, however, 3DRA is slightly less expensive than CT.

Key words: radiation risk, 3D cardiac rotational angiography of the left atrium, computer tomography, complex atrial arrhythmias, catheter ablation of arrhythmias

International Clinical Research Center, 1st Department of Internal Medicine – Cardioangiology, St. Anne's University Hospital Brno, Pekarska 53, 656 91 Brno, Czech Republic
Corresponding author: Zdenek Starek, e-mail: zdenek.starek@fnusa.cz

INTRODUCTION

Atrial fibrillation (AF) is the most common supraventricular arrhythmia and, in recent years, catheter ablation of AF has become the most frequently performed electrophysiology (EP) procedure[1]. Currently, complex ablations are performed under the guidance of 3D electroanatomical mapping (EAM) systems creating 3D non-fluoroscopic maps of the left atrium (LA) (ref.[2]). In everyday clinical practice, there are two basic systems used for invasive EP (CARTO, Biosense Webster, and EnSite Velocity, St. Jude Medical).

A standard method used for pre-ablation LA imaging is based on contrast-enhanced computer tomography (CT) (ref.[3]). Nevertheless, 3D X-ray model-guided LA mapping provides objective information about real anatomy being an valuable clinical tool[4].

3D Rotational Angiography (3DRA) represents a new alternative to cardiac CT. 3DRA is safe, feasible[5] and fully comparable with CT image quality[6-8]. It was developed as a tool for left atrium imaging, however, it can be used for visualization of several other cardiac and adjacent extracardiac structures such as left and right ventricle[9,10]. Noteworthly, esophagus imaging with CT is safe and feasible[11], but clinical usability is questionable due long-term mobility of the esophagus[12]. On the contrary, 3DRA could be useful in the imaging modality during left atrial arrhythmias radiofrequency ablation (RFA) because of short-term mobility of the esophagus[13]. Moreover, the advantage of this technique is associated with a favourable logistics, time-effectivenes (peri-procedural LA model generation), reduction of radiation dose and amount of the contrast agent. Importantly, final 3DRA- and CT-supported RFA result is identical in terms of non-fluoroscopic 3D electroanatomic maps creation, direct fusion/integration with 3D EAM system[4,7], and/or direct fusion/integration of a 3D model with live fluoroscopy[14].

However, both imaging methods have a clinically relevant impact on a patient rearding radiation and contrast agent. Moreover, economic aspect should be also taken under consideration. The objective of this study is to compare radiation dose, consumption of contrast agent and costs of these methods in patients undergoing pre-RFA left atrium 3DRA and CT imaging.

MATERIALS AND METHODS

Patient population

We performed a retrospective study enroling 314 patients referred for catheter ablation of complex atrial arrhythmias between October 2012 and October 2015. All patients underwent either CT or 3DRA imaging of the left atrium. Patients with a history of iodine allergy or with

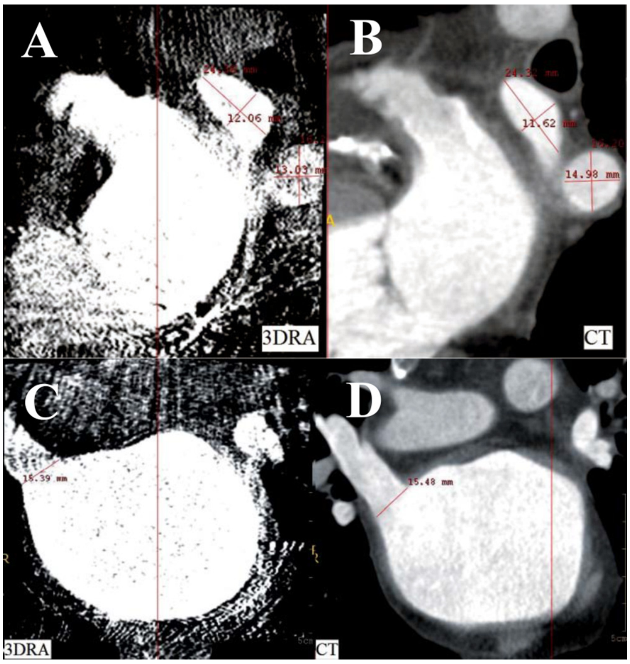

Fig. 1. Comparison of the 3DRA of the left atrium (A,C) and CT of the left atrium (B,D) from one patient.
A,B – lateral view, C,D - anteroposterior view

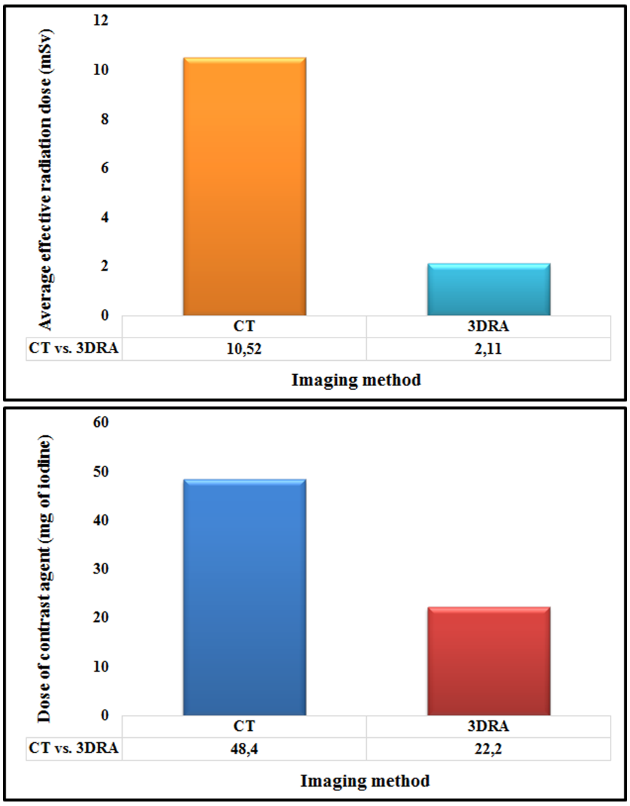

Fig. 2. Comparison of the average effective radiation dose and average dose of contrast agent between 3DRA and CT of the left atrium.

impaired renal function (MDRD / Modification of Diet in Renal Disease/ of less than 45ml/min/1.73m^2) were excluded from the study.

Rotational Angiography Imaging

3RDA imaging was carried out using the X-ray system Allura Xper FD 10 (Philips Medical Systems Inc., Best, The Netherlands). A basic principle of the 3DRA is based on contrast agent injection (Ultravist 370, Bayer Pharma AG, Berlin, Germany) to the atrium and acquisition of rotational image. After opacification of the LA and pulmonary veins, the C-arm was isocentrically rotated over 240° (120° right anterior oblique to 120° left anterior oblique) over 4.1 s with an X-ray acquisition speed of 30 frames per second. The patients were in a lying position during rotational imaging with natural position of the arms along the body and normal breathing.

Pigtail catheter was introduced to the LA over the transseptal sheath Agilis NxT 8,5F. Left atrium isocentering was achieved from antero-posterior and left-lateral X-ray projections.

In aim to achieve optimal imaging parameters, right ventricular temporary pacing (230 beat per min) was introduced with subsequent reduction of cardiac output and drop in blood pressure followed by disappearance of a pulse waveform at the distal finger phalanx of the right upper extremity (Saturation sensor, Philips IntelliVue MP-20, Philips, Eindhoven, The Netherlands.) Afterwards, contrast agent was injected (amount 60 mL, velocity of injection 15 mL/s) and, with a delay of 2 seconds, we commenced the rotation of C-arm[7]. Application of contrast agent was carried out with standard power injector (Mark V, Medrad Inc., Indianola, PA, USA) (ref.[8]). Figure 1 presents an example LA 3DRA and CT imaging.

At the end of the rotational angiography prodecure, data was automatically transferred from the Allura X-ray System to the EP Navigator Workstation (EP Navigator 3.0, Philips Healthcare, Best, The Netherlands). The 3DRA model of LA and pulmonary veins anatomy was automatically reconstructed using the standard algorithms of the EP Navigator Workstation.

CT imaging

A CT scan was performed few days before ablation using non-ECG-gated protocol on a 64-slice CT (GE Lightspeed VCT, General Electric, Fairfield, USA). CT parameters included: 120kV, 800mAs, collimation of 63x0.625 mm, and spiral pitch factor of 0.98. Image reconstruction was performed on a 512x512 pixel array. Contrast agent was administered through a peripheral vein (Ultravist 370, Bayer Pharma AG, Berlin, Germany). During imaging, patients had to have their arms up whilst holding the breath. Afterwards, data was copied into CD and reconstructed during LA RFA procedure using EP Navigator Workstation (EP Navigator 3.0, Philips Healthcare, Best, Netherlands).

Radiation exposure, dose of contrast agent, cost effectiveness

For all 3DRA procedures we determined the average radiation dose presented as a dose area product (DAP, mGycm^2) and consumption of the contrast agent. For CT procedures average radiation dose was determined as a dose length product (DLP, mGycm). The average

Table 1. Baseline characteristics of study group.

	3DRA of the left atrium n=157	CT of the left atrium n=157	*P*
Age, mean±SD	59.42±9.72	59.87±10.45	1.000
Males, n (%)	117 (74.77%)	113 (71.52%)	0.626
LVEF, mean±SD (%)	57.26±7.04	57.11±8.18	1.000
Left atrium dimaeter, mean±SD (mm)	44.23±5.25	44.82±5.73	1.000
BMI, mean±SD (kg/m^2)	29.82±9.14	29.49±8.29	1.000
Structural heart disease, n (%)	29 (18.47%)	31 (19.75%)	0.679
Hypertension, n (%)	94 (59.87%)	99 (63.06%)	0.224
Atrial fibrillation, n (%)	143 (91.08%)	139 (88.53%)	0.254
Paroxysmal atrial fibrillation, n (%)	98 (68.53%)	98 (70.50%)	0.770
Persistent atrial fibrillation, n (%)	45 (31.47%)	41 (29.50%)	0.784
Atypical left atrial flutter, n (%)	12 (7.64%)	13 (8.28%)	0.240
Focal left atrial tachycardia, n (%)	2 (1.27%)	3 (1.91%)	1.000

BMI – body mass index, LVEF – Left ventricle ejection fraction

Table 2. Cost summary of LA 3DRA and CT imaging.

Financial costs/	X-ray system Allura Xper FD 10 + injector + workstation EP Navigator	CT GE Lightspeed VCT + injector + workstation HP WORKSTATION X28200
Purchase price	881 327	1 252 538
Maintenance and service/year	0	93 364
Total depreciation/15 min	22	42
Consumables	89	108
Salaries	12	11
Total cost	123	161

radiation dose was converted to an effective dose (ED) using appropriate converting factor. For 3D rotational angiography where the dose was measured in DAP units a converting factor of 0.18 mSv Gy^{-1}cm^{-1} was used[15]. For CT, where the dose was given in units of DLP, a converting factor of 0.017mSv mGy^{-1}cm^{-1} was applied[16].

In the same group of patients we compared the quantity of the contrast agent. Taking under consideration that CT scans were performed at different sites using various types and concentrations of contrast agent, the doses of the contrast agent were standardized and converted to mg of iodine.

Analysis of the financial expenses was conducted by the Economic Department at the University Hospital of St. Anne, Brno illustrating conditions that applied to most hospitals in Czech Republic in 2015. Technical fees and wages of individual workers (physicians, biomedical engineers, technicians and nurses) were included into the analysis. Technical fee covered consumables (contrast agent and other small supplies) and depreciation of individual devices. Depreciation of equipment constituted the main part of the cost of the performance was calculated from the cost of equipment and prices for service. For angiography, the Allura FD 10 service is included in the price of the device. Oppositely, for CT scan equipment the price of a service is 93364€/year. Lifetime of both devices is calculated at 5 years and depreciation is calculated for a 8-h working week. Turnaround time for both technologies was set at 15 min. The prices are converted to Euros using the exchange rate as of November 2014 (27.58 CZK/€).

Image integration, ablation procedures

The LA 3DRA model was automatically integrated with the live fluoroscopy[14]. We used 3D models of the LA as a guidance for 3D electroanatomical map generation in form of (1) synchronised projection of 3DRA model and 3D EAM system or (2) direct fusion of 3D models with 3D electroanatomical map[4,7].

Ablation procedures were performed in a standard manner using irrigated tip catheter guided by 3D EAM system, EnSite Velocity (St. Jude Medical, St. Paul, MN, USA).

Statistical analysis

Statistical analysis of clinical data set was performed using STATISTICA software StatSoft, Inc. (2013), version 12, www.statsoft.com. The statistical analysis was performed by the Kolmogorov-Smirnov test of normality and by the unpaired two sample Student's t-test. The significance level value for both types of statistical analysis was set to value 0.05.

RESULTS

In the period from March 2013 to October 2015 a total of 157 patients were examined with multislice cardiac CT with segmentation of LA 3D model.

In the period from October 2012 to October 2015 a total of 157 LA 3D rotational angiographies were performed in patients with complex atrial arrhythmias, in most cases atrial fibrillation.

Characteristics of patients are summarised in Table 1. Study population consisted of 230 (73.2%) males, and the mean age was 60 (±9) years. In both groups there was a similar number of patients with structural heart disease. Moreover, individuals were characterized by slightly enlarged left atrium and normal left ventricle ejection fraction. There was no significant statistical differences between 3DRA and CT group.

Radiation exposure, dose of contrast agent, cost effectiveness

The average radiation dose for LA 3DRA was DAP=11746±2178 mGycm^2.

The average radiation dose forLA CT was DLP=619 ±123 mGycm.

Average consumption of contrast agent for LA 3DRA and CT of was 60 mL and 124.5 mL, respectively.

When comparing the average ED of radiation burden we showed a statistically significant reduction of radiation for 3DRA compared to the CT scan (2.11±0.392 mSv vs. 10.52±2.093 mSv, respectively, P<0.001). Data are shown in Fig. 2.

The average dose of the contrast agent used in LA 3DRA and CT imaging was 22.2 mg and 48.4 mg of iodine, respectively. Dose of the contrast agent in 3DRA was significantly lower (Fig. 2)

Total price per procedure is 123€ for 3DRA and 161€ for CT. For details see Table 2.

Catheter ablation guided by 3DRA and CT of the left atrium

All patients with the 3DRA model of LA were ablated with the support of direct overlay 3D model and 2D fluoroscopy. 7 patients with CT and 9 patients were ablated under the guidance of 3D model directly fused with 3D EMA map. Rest of patients were ablated with the support of 3D EnSite Velocity system with LA 3D model superimposed on the 3D EAM map.

DISCUSSION

The modern 3D X-ray imaging methods make the catheter ablations of complex atrial arrhythmias easier and safer. Nevertheless, both methods are expensive and have considerable medical consequences due to radiation and contrast agent application.

In our study, we demonstrated a significantly lower radiation burden and consumption of contrast agent in 3DRA compared to CT imaging method. In published studies, the ED for 3DRA was an average of 2.3±0.3 mSv compared to 19.5±3.1 mSv for CT models[8,17,18]. An explanation for the significantly higher dose for CT models of the left atrium from the cited works vs. CT scanning in our patients is based on the imaging protocol. In the cited studies, retrospective ECG-gated CT was used, whereas in our cohort we applied ECG-non-gated protocol leading to less radiation exposure. Thorning et al.[19] measured an average ED of 13.45 mSv for retrospective ECG-gated protocol evaluating pulmonary vein anomalies with CT, while for ECG-non-gated protocol only 6.1 mSv. In the study by Ector et al.[20], the difference in average ED was significant higher when using the retrospective ECG-gated vs. non-gated preprocedural cardiac CT (3.17±5.2 mSv vs. 4.4±3 mSv, respectively, P<0.001)

Significantly lower consumption of the contrast agent for 3DRA in our study correlates with published results. In the smaller studies comparing 3DRA and CT models of the left atrium, the average quantity of contrast agent used in 3DRA was almost half the amount of contrast agent used in CT (73 mL vs. 120 mL) (ref.[8,7,17,18,21]).

A lower radiation dose and lower consumption of the contrast agent in 3DRA compared to the CT is relative. Noteworthy, due to intensive development of the most advanced CT imaging, modern CT devices have significantly lower radiation burden and consumption of the contrast agent. In recent years, several studies have been published showing decreased radiation dose and consumption of contrast agent, below the average characteristics of 3DRA. In 2010 Blanke et al.[22] published results of LA CT imaging using prospective ECG-triggered sequential dual-source CT scan (Somatom Definition, Siemens) carried out before catheter ablation. The mean ED was 1.1±0.3 mSv and 3.0±0.5 mSv (body mass index [BMI]-dependent tube voltage set on 100 or 120kV).

Yang et al.[23] described the first use of low dose 320-row CT Aquilion ONE, Toshiba for LA and pulmonary veins imaging. The ED was 1.90±0.19 mSv and 3.83±0.31 mSv, respectively (BMI-dependant tube voltage of 100kV or 120kV). In addition to a significantly reduced ED less than half the amount of a contrast agent was used compared to older CT devices (40 and 50 mL according to BMI).

In Czech Republic the economic cost for 3DRA is lower than for CT (Table 2). The difference of the total cost is 39 €, which is 24% of the price of the CT scan. Kristaselis et al.[21] in 2011 published a comparison of costs for both methods in Federal Republic of Germany. The authors calculated the price of one scan for 3DRA 91-95 € and 126-151 € for CT. In this case, the difference in cost is slightly greater and it constitutes 28-37% of the price of the CT imaging. This is mainly due to the mismatch in costs. In the study of Kritselise et al., angiography costs were very low, while CT expenditures doubled in comparison with our devices. The total costs are difficult to compare; the overall technical fee in our department is 111 € for 3DRA and 151 € for CT, thus, slightly higher than those presented by Kriatselis et al. This is due to the fact that the depreciations in the mentioned study are calculated for 6 years and based on a 10-hour working week, which make the costs lower. If we calculated the cost of both centres according to the same formula, the result would be comparable. The question to consider is what would be the cost of these analysis in Germany if they counted the price of labour of the staff. In our calculations the price of labour is negligible (24 € for

3DRA and 47 € for CT). It is a specific characteristic of Central European post-communist countries, where the cost of labour in healthcare services is underestimated. It is quite possible that after accounting for the cost of labour in Germany, the total cost would be completely different. Comparison of costs of individual methods between Czech and Germany is very difficult and can be misleading. However, we can conclude that in our settings and settings of Western Europe, the technical fee for 3DRA is comparatively lower than for CT. Moreover, in Czech Republic settings, the same applies to the total cost, including the cost of labour.

CONCLUSION

Consumption of the contrast agent and radiation burden for 3DRA of the LA is significantly lower than most currently used CT scan methods.

The advantage of a lower X-ray dose and contrast agent when comparing 3DRA and cardiac CT is relative and with new generation of CT devices both methods might be comparable.

Cost of both imaging methods is comparable, however, 3DRA is slightly less expensive then CT.

Comparing financial expenditures between countries is very difficult due to differencies in calculation methodology.

Acknowledgement: This work was supported by the project no. LQ1605 from the National Program of Sustainability II.

Author contributions: All authors had full access to all the data in the study and take responsibility for the integrity of the data and the accuracy of the data analysis; ZS: study concept and design, acquisition of data, manuscript drafting; FL, JJ: acquisition of data, critical revision, JW, TK, AK: Data analysis and interpretation, critical revision; TK: statistical analysis.

Conflict of interest statement: The authors state that there are no conflicts of interest regarding the publication of this article.

REFERENCES

1. Calkins H, Kuck KH, Cappato R, Brugada J, Camm AJ, Chen SA, Chen SA, Crijns HJ, Damiano RJ Jr, Davies DW, DiMarco J, Edgerton J, Ellenbogen K, Ezekowitz MD, Haines DE, Haissaguerre M, Hindricks G, Iesaka Y, Jackman W, Jalife J, Jais P, Kalman J, Keane D, Kim YH, Kirchhof P, Klein G, Kottkamp H, Kumagai K, Lindsay BD, Mansour M, Marchlinski FE, McCarthy PM, Mont JL, Morady F, Nademanee K, Nakagawa H, Natale A, Nattel S, Packer DL, Pappone C, Prystowsky E, Raviele A, Reddy V, Ruskin JN, Shemin RJ, Tsao HM, Wilber D. 2012 HRS/EHRA/ECAS expert consensus statement on catheter and surgical ablation of atrial fibrillation: recommendations for patient selection, procedural techniques, patient management and follow-up, definitions, endpoints, and research trial design. J Interv Card Electrophysiol 2012;33(2):171-257.
2. Gepstein L, Hayam G, Ben-Haim SA. A novel method for nonfluoroscopic catheter-based electroanatomical mapping of the heart. In vitro and in vivo accuracy results. Circulation 1997;95(6):1611-22.
3. Stárek Z, Lehar F, Jež J, Wolf J, Novák M. 3D X-ray imaging methods in support catheter ablations of cardiac arrhythmias. Int J Cardiovasc Imaging 2014;30(7):1207-23.
4. Malchano ZJ, Neuzil P, Cury RC, Holmvang G, Weichet J, Schmidt EJ, Ruskin JN, Reddy VY. Integration of cardiac CT/MR imaging with three-dimensional electroanatomical mapping to guide catheter manipulation in the left atrium: implications for catheter ablation of atrial fibrillation. J Cardiovasc Electrophysiol 2006;17(11):1221-9.
5. Starek Z, Lehar F, Jez J, Wolf J, Kulik T, Zbankova A, Novak M. Periprocedural 3D imaging of the left atrium and esophagus: comparison of different protocols of 3D rotational angiography of the left atrium and esophagus in group of 547 consecutive patients undergoing catheter ablation of the complex atrial arrhythmias. Int J Cardiovasc Imaging 2016;32(7):1011-9.
6. Lehar F, Starek Z, Jez J, Novak M, Wolf J, Stepanova R, Kruzliak P, Kulik T, Zbankova A, Jancar R, Vitovec J. Comparison of clinical outcomes and safety of catheter ablation for atrial fibrillation supported by data from CT scan or three-dimensional rotational angiogram of left atrium and pulmonary veins. Biomed Pap Med Fac Univ Palacky Olomouc Czech Repub 2015;159(4):622-8.
7. Thiagalingam A, Manzke R, D'Avila A, Ho I, Locke AH, Ruskin JN, Chan RC, Reddy VY. Intraprocedural volume imaging of the left atrium and pulmonary veins with rotational X-ray angiography: implications for catheter ablation of atrial fibrillation. J Cardiovasc Electrophysiol 2008;19(3):293-300.
8. Li JH, Haim M, Movassaghi B, Mendel JB, Chaudhry GM, Haffajee CI, Orlov MV. Segmentation and registration of three-dimensional rotational angiogram on live fluoroscopy to guide atrial fibrillation ablation: a new online imaging tool. Heart Rhythm 2009;6(2):231-7.
9. Orlov MV, Ansari MM, Akrivakis ST, Jadidi A, Nijhof N, Natan SR, Wylie JV, Hicks A, Armstrong J, Jais P. First experience with rotational angiography of the right ventricle to guide ventricular tachycardia ablation. Heart Rhythm 2011;8(2):207-11.
10. Wolf J, Starek Z, Jez J, Lehar F, Lukasova M, Kulik T, Novak M. Rotational angiography of left ventricle to guide ventricular tachycardia ablation. Int J Cardiovasc Imaging 2015;31(5):899-904.
11. Orlov MV, Hoffmeister P, Chaudhry GM, Almasry I, Gijsbers GH, Swack T, Haffajee CI. Three-dimensional rotational angiography of the left atrium and esophagus--A virtual computed tomography scan in the electrophysiology lab? Heart Rhythm 2007;4(1):37-43.
12. Stárek Z, Lehar F, Jež J, Žbánková A, Kulík T, Wolf J, Novák M. Long-term mobility of the esophagus in patients undergoing catheter ablation of atrial fibrillation: data from computer tomography and 3D rotational angiography of the left atrium. J Interv Card Electrophysiol 2016;46(2):81-7.
13. Starek Z, Lehar F, Jez J, Scurek M, Wolf J, Kulik T, Zbankova A, Novak M. Three-dimensional rotational angiography of the left atrium and the oesophagus: the short-term mobility of the oesophagus and the stability of the fused three-dimensional model of the left atrium and the oesophagus during catheter ablation for atrial fibr. Europace 2017;19(8):1310-6.
14. Kriatselis C, Tang M, Nedios S, Roser M, Gerds-Li H, Fleck E. Intraprocedural reconstruction of the left atrium and pulmonary veins as a single navigation tool for ablation of atrial fibrillation: a feasibility, efficacy, and safety study. Heart Rhythm 2009;(6):733-41.
15. Schultz FW, Zoetelief J. Dose conversion coefficients for interventional procedures. Radiat Prot Dosimetry 2005;117(1-3):225-30.
16. Einstein AJ, Moser KW, Thompson RC, Cerqueira MD, Henzlova MJ. Radiation dose to patients from cardiac diagnostic imaging. Circulation 2007;116(11):1290-305.
17. Tang M, Kriatselis C, Ye G, Nedios S, Roser M, Solowjowa N, Fleck E, Gerds-Li JH. Reconstructing and registering three-dimensional rotational angiogram of left atrium during ablation of atrial fibrillation. Pacing Clin Electrophysiol 2009;32(11):1407-16.
18. Kriatselis C, Tang M, Roser M, Fleck E, Gerds-Li H. A new approach for contrast-enhanced X-ray imaging of the left atrium and pulmonary veins for atrial fibrillation ablation: rotational angiography during adenosine-induced asystole. Europace 2009;11(1):35-41.
19. Thorning C, Hamady M, Liaw JV, Juli C, Lim PB, Dhawan R, Peters NS, Davies DW, Kanagaratnam P, O'Neill MD, Wright AR. CT evaluation of pulmonary venous anatomy variation in patients undergoing catheter ablation for atrial fibrillation. Clin Imaging 2011;35(1):1-9.
20. Ector J, De Buck S, Huybrechts W, Nuyens D, Dymarkowski S, Bogaert J, Maes F, Heidbüchel H. Biplane three-dimensional augmented fluo-

roscopy as single navigation tool for ablation of atrial fibrillation: Accuracy and clinical value. Heart Rhythm 2008;5(7):957-64.
21. Kriatselis C, Nedios S, Akrivakis S, Tang M, Roser M, Gerds-Li JH, Fleck E, Orlov M. Intraprocedural imaging of left atrium and pulmonary veins: a comparison study between rotational angiography and cardiac computed tomography. Pacing Clin Electrophysiol 2011;34(3):315-22.
22. Blanke P, Baumann T, Langer M, Pache G. Imaging of pulmonary vein anatomy using low-dose prospective ECG-triggered dual-source computed tomography. Eur Radiol 2010;20(8):1851-5.
23. Yang L, Xu L, Yan Z, Yu W, Fan Z, Lv B, Zhang Z. Low dose 320-row CT for left atrium and pulmonary veins imaging--the feasibility study. Eur J Radiol 2012;81(7):1549-54.
24. Fahlenkamp UL, Schurig J, Vogtmann T, A. Lembcke, C.Schwenke, A. Huppertz, et al. Low-Dose Computed Tomography Angiography for Preablational Imaging of the Left Atrium: Intraindividual Comparison to Magnetic Resonance Angiography ECR 2014 / C-1024. EPOS™, Electronic Presentation Online System. [Online] March 6, 2014. [Cited: June 6, 2014.] http://dx.doi.org/10.1594/ecr2014/C-1024.

Int J Cardiovasc Imaging
DOI 10.1007/s10554-015-0636-8

ORIGINAL PAPER

Rotational angiography of left ventricle to guide ventricular tachycardia ablation

Jiri Wolf[1] · Zdenek Starek[1] · Jiri Jez[1] · Frantisek Lehar[1] · Marketa Lukasova[1] · Tomas Kulik[1] · Miroslav Novak[1]

Received: 26 May 2014 / Accepted: 4 March 2015

Abstract Three-dimensional rotational angiography (3DRA) is a novel imaging method introduced to guide complex catheter ablations of the left atrium. Our aim was to investigate the feasibility of the method in visualization of left ventricular anatomy and to develop a corresponding protocol for guidance of ventricular tachycardia ablation. We performed 3D rotational angiography in 13 patients using a direct left atrial protocol for data acquisition and the 3D reconstruction of the left ventricle was achieved in all patients. Clinical data comparison has proved lower use of radiation and contrast medium during 3DRA-guided ablations as compared to CT-guided procedures.

Keywords Catheter ablation · Rotational angiography · Left ventricle · Computed tomography · Computer assisted image processing · Three-dimensional imaging

Abbreviations

LVOT	Left ventricular outflow tract
RVOT	Right ventricular outflow tract
3DRA	Three-dimensional rotational angiography
CT	Computed tomography
VT	Ventricular tachycardia
LAO	Left anterior oblique X-ray projection
RAO	Right anterior oblique X-ray projection
AP	Antero-posterior X-ray projection

Jiri Wolf and Zdenek Starek contributed equally to this paper.

✉ Jiri Wolf
jiri.wolf@fnusa.cz

[1] International Clinical Research Center, 1st Department of Internal Medicine, Cardioangiology, St. Anne's University Hospital Brno, Pekarska 53, 656 91 Brno, Czech Republic

Introduction

In the early twenty first century, catheter ablation of cardiac arrhythmias became a first-line treatment for a majority of heart rhythm disorders [1]. Invasive therapy by means of radio-frequency catheter ablation has prevailed predominantly in the management of supraventricular arrhythmias [1]. In the last decade, catheter ablation for complex atrial arrhythmias has rapidly evolved, especially for atrial fibrillation [2]. Given the complexity of ventricular arrhythmias and the unstable outcome of the ablation procedure with regards to preventing sudden cardiac death in some types of VTs, the employment of ablation techniques as a management strategy for ventricular arrhythmias has been impeded [3]. The main indication has been shown in patients with idiopathic ventricular tachycardia originating from the right and left ventricle. Recently, a rapid growth in number of patients treated with structural heart disease has been observed [4].

During the complex electrophysiological interventions, pre-procedural computer tomography (CT) is frequently used as an anatomical guidance for three-dimensional (3D) electroanatomical mapping of the chamber of interest. A novel imaging tool representing an alternative to CT is 3D rotational angiography. The method has been initially developed and applied to create 3D models of the left atrium to support catheter ablation of complex atrial arrhythmias. The main benefit of 3D rotational angiography is that it can be performed intra-procedurally, directly in the EP lab which subjects the patient to a lower dose of radiation and contrast agent. Imaging of other cardiac structures has been constrained by a number of limitations, most importantly the inability of automated segmentation of acquired data. Dr. Orlov was the first to attempt to obtain representation of other structures of the heart (namely the right ventricle) at Caritas St. Elizabeth's Medical Center of Boston in 2010 [5]. At our center, we investigated the feasibility of the method to guide VT ablation originating in RVOT in 17 patients and developed a protocol for left ventricular outflow tract (LVOT) imaging, which has been successfully applied to support VT ablation from LVOT.

Methods

From December 2011 to February 2013, 13 patients underwent 3D rotational angiography of the left ventricle while receiving catheter ablation for idiopathic ventricular tachycardia arising from LVOT or LV. Of those, five patients had prior cardiac CT performed. The study participants, seven women and six men, demonstrated a mean age of 61.6 ± 11.4 years and an average BMI of 30.7 ± 4.5 (Table 1). 3DRA was performed using X-Ray Philips Allura Xper FD10 (Philips Healthcare, Best, The Netherlands). In all patients, identical protocol of data acquisition was employed with LVOT defined as the isocenter of rotational run. For contrast injection, a 6F pigtail catheter was introduced to the left ventricular apex and the ablation catheter was positioned to the right ventricle. Left ventricle isocentering was achieved by two X-ray projections with maximal raised flat panel. Coronary sinus catheter, the pig-tail catheter in LV apex and ablation catheter in right ventricle outflow tract were visible in anteroposterior projection. Afterwards, we adjusted the height of the table to see the pig-tail catheter in LV apex in the lower fifth of the image. In order to optimize image acquisition [6], cardiac output was substantially reduced by rapid ventricular pacing at a rate of 230 bmp using an ablation catheter and contrast medium was directly injected. A total of 85 ml of Ultravist 370 (Bayer Pharma AG, Berlin, Germany) was administered at 20 ml/s. A delay between contrast injection and initiation of rotation was 1 s. C-arm rotated around the patient over an angle of 240° for 4.1 s, with X-ray acquisition speed at 30 frames per second resulting in 120 two-dimensional images. Patients remained conscious, at rest, with hands along the body and calmly breathing. The obtained raw data was automatically transferred to the EP Navigator workstation (Philips Healthcare) and manually segmented. The 3D representation of the left ventricle was evaluated by two independent physicians and classified into three categories:

Excellent—the entire structure (whole contour of ventricle, outflow tract and apex recognized) is visualized and details (e.g. aortic bulbus, ascending aorta, coronary arteries) are interpretable.
Useful—details are interpretable but apex is missing.
Inadequate—3D reconstruction is not feasible or the details are not interpretable.

The model was then overlaid on live fluoroscopy (EP Navigator system) and in two patients, the composite image was also integrated to 3D electroanatomical mapping system EnSite Velocity (St. Jude Medical, St. Paul, MN, USA).

All patients underwent a routine strategy of conventional activation mapping and pace mapping using different supportive tools, such as electrophysiological diagnostic system BARD LabSystem Pro (C. R. Bard, Lowell, MA, USA), cardiac mapping system EnSite Velocity and anatomic guidance of EP Navigator system. In two patients, EP Navigator with Point Tagging was used for mapping the heart chamber. Likewise with electroanatomical mapping systems, this tagging tool allows lesion points to be tracked in the overlay of 3D volume reconstruction on a live fluoroscopy screen. We were able to identify/detect sites with optimal pace mapping, points of ablation and integrity of lesion sets (Fig. 1). In another two patients, the fusion of resulting 3D image and electroanatomical map using EnSite Velocity was accomplished with aortic bulbus and coronary ostia being the fiducial points. The merged image was similarly used to visualize optimal pace mapping, lesion points and sites of successful ablation. The composite image of the left ventricle was in five patients compared to CT scans. The maximum diameter of outflow tract and aortic bulbus was assessed in both methods (Fig. 2) and total radiation dose and use of contrast medium was compared.

Table 1 Patient characteristics (n = 13)

Characteristic	Value
Age (years)	61.6 ± 11.4
Male (no.)	6
Female (no.)	7
BMI	30.7 ± 4.5
Ejection fraction (%)	53.1 ± 12.6
Diabetes (no.)	3
Hypertension (no.)	5
Hyperlipidemia (no.)	2
Antiarrhythmic therapy (no.)	11
β-blocker (no.)	9
Verapamil (no.)	2

Statistical analysis

The study was designed as a retrospective analysis of our first experience with 3DRA in imaging left ventricular structures. The data were analyzed using descriptive statistics. Results are presented as median and interquartile range (IQR). The difference between the groups (CT vs.

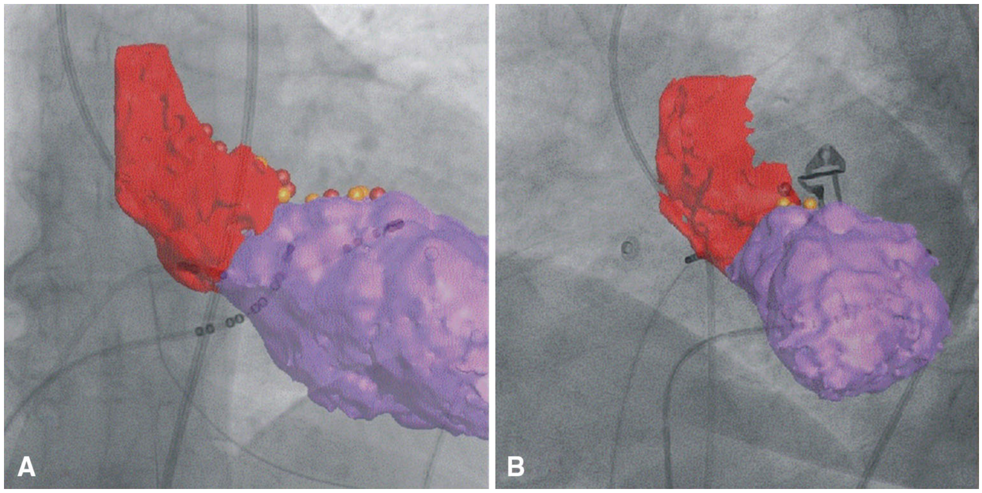

Fig. 1 3D rotational angiogram of the left ventricle in EP Navigator system with Point Tagging function in AP view (**a**) and LAO 45° view (**b**). Left ventricle (*violet color*), aortic bulbus and a part of the ascending aorta (*red color*) are shown. In the lateral part of the LVOT and aortic bulbus, 3D points tracked during the procedure are depicted, such as sites of pacemapping (*red dots*) and RF application (*orange dots*). Also shown are a decapolar catheter placed into the coronary sinus and an ablation catheter advanced through the aorta into the LVOT

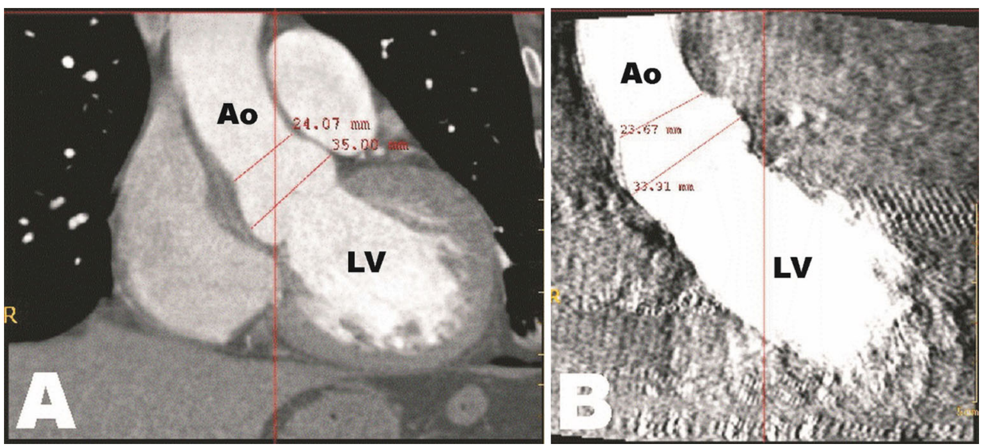

Fig. 2 Example of CT versus 3DRA raw data measurements. **a** CT image representing the left ventricular volume (LV), aortic bulbus with a part of the ascending aorta (Ao). **b** 3D rotational angiogram of the left ventricular volume (LV) and aortic bulbus with a part of the ascending aorta (Ao). Both images demonstrate aortic bulbus and ascending aorta measurements

3DRA) was evaluated by Spearman's rank correlation coefficient with reported confidence intervals and both methods were compared using the Wilcoxon–Mann–Whitney two-sample rank-sum test.

Results

The resulting 3D volume reconstruction was graded as excellent in four patients, as useful in nine patients and none were described as inadequate with respect to an ability to guide catheter ablation of ventricular tachycardia. Non-excellent imaging was most likely associated with a learning curve of the personnel as this was a newly implemented method, for example poor isocentering or suboptimal manual segmentation was encountered. During data acquisition, atrial fibrillation was present in six patients; the remainder was in sinus rhythm. Any qualitative differences between the patients in sinus rhythm and patients in atrial fibrillation were not observed in the final model. The manual segmentation of the 3D left ventricular model required the median time of 6.0 min. The median radiation dose of the rotational run was 10,718.5 mGycm^2. Acquisition of electroanatomical map and fusion with reconstructed 3D image was achieved in 21.5 min (Table 2). Continual reassessment of anatomical accuracy has been done through the whole procedure and no discrepancy was reported.

Corresponding datasets of 3DRA and CT images of five patients were compared and analyzed as well as the measurements of aortic bulbus diameter. Using the Wilcoxon–Mann–Whitney two-sample rank-sum test, we failed to reject null hypothesis that there is no difference between the groups at the 0.05 significance level (Table 3).

The effective radiation dose during data acquisition using CT was 11.47 mSv, respective effective dose for 3D rotational angiography was 2.93 mSv. Median dose of contrast medium was 55,500 mg iodine for CT imaging and 31,450 mg iodine for 3DRA (Table 2). The difference between performing CT and 3D rotational angiography in exposure dose and use of contrast was statistically significant.

No procedural complications associated with the use of 3D rotational angiography were observed.

Discussion

For many heart rhythm disorders, catheter ablation has developed to become the treatment of first choice. The standard imaging method of electrophysiology procedures is X-ray fluoroscopy, however, complex interventions demand more advanced guidance tools such as 3D electroanatomical mapping. Additionally, pre-procedural CT or MRI scans are used to supplement creation of a 3D electroanatomical map [7, 8]. A novel alternative to cardiac CT is 3D rotational angiography. The method was introduced for the acquisition of a 3D image of the left atrium to guide catheter ablation of atrial fibrillation and/or ablation of complex left atrial tachycardias [9]. Multiple papers have investigated different approaches of application and refinement of this method in visualization of the left atrium. Nevertheless, reconstruction of 3D images of other cardiac and non-cardiac structures has also proven feasible as first and only described by prof. Orlov in an article on 3D rotational angiography of right ventricle [5]. On the basis of this knowledge, we attempted 3D reconstruction of both the right and left ventricle. We employed direct contrast injection with a fixed delay as mentioned above. In contrast to our procedure, prof. Orlov employed dynamic protocol of indirect injection of right ventricle with pig-tail catheter positioned between the inferior vena cava and the right atrium, 60–100 ml of contrast medium, a delay of rotational run against injection of 3–4 s or triggering and patients maintaining breath-hold during the acquisition. Our protocol has proven robust and highly effective, and unedited data can be interpreted more easily even by less experienced physicians.

Table 2 Procedural characteristics

Characteristic	Median	IQR
Procedure time (min)	165.0	99.0
Total fluoroscopy time (min)	16.0	11.0
Total fluoroscopy exposure DAP ($mGycm^2$)	32,138.0	8723.0
3DRA fluoroscopy exposure DAP ($mGycm^2$)	10,718.5	5548.5
Segmentation time (min)	6.0	2.0
EnSite Fusion time (min)	21.5	7.0
CT effective dose (mSv)	11.47	1.2
3DRA effective dose (mSv)	2.93	0.6
CT amount of iodine contrast agent (mg)	55,500.0	4500.0
3DRA amount of iodine contrast agent (mg)	31,450.0	0.0

The strategy of conventional mapping combined with the Philips EP Navigator system provides excellent anatomic orientation as the acquired 3D image is overlaid on live fluoroscopy screen. Unlike CT, rotational angiography can be performed at any point of the electrophysiology intervention in the operating room, thus the patient is subjected to a lower dose of radiation and contrast medium. Point Tagging is a very useful additional tool within the EP Navigator, which allows important points of ablation to be tagged such as optimal pace mapping sites, application of RF energy and others into the resulting 3D image, alternating sophisticated electroanatomical mapping systems. Our experience suggests that the most beneficial is a fusion of 3D images from the standard EP Navigator system and electroanatomical mapping system EnSite Velocity, which, in a relatively short amount of time, enables a very accurate electroanatomical model to be achieved with sites of interest that are otherwise very difficult to map (Fig. 3).

Study limitations

Several limitations need to be addressed. First of all, it is a small sample size. The study was designed as a pilot study investigating the feasibility of 3D rotation angiography as a guidance of complex electrophysiology procedures in the left ventricle. For an objective assessment of statistical differences between the two methods (CT and 3DRA), larger randomized trials are required. Another disadvantage is the inability of automated segmentation and reconstruction of acquired 2D images into a 3D volume representation. Such a tool is available in a commercial version of Philips EP Navigator Release 3.5 only as a supplement to a reconstruction of the left atrium. This fact may be highly discouraging for other centers to routinely employ 3D rotational angiography in visualization of additional cardiac and non-cardiac structures. Our configuration of Philips Allura Xper FD10 system might also represent a limitation as the size of the flat detector is only 10 × 10 inches which is not appropriate for patients with higher BMI and results in suboptimal isocentering and

Table 3 3DRA versus CT measurement of aortic bulbus diameter (N = 5)

Characteristic	Spearman corr. coeff.	Wilcoxon test (Z score)	*P* value
Diameter 1	0.9	0.674	0.50
Diameter 2	0.7	0.405	0.69

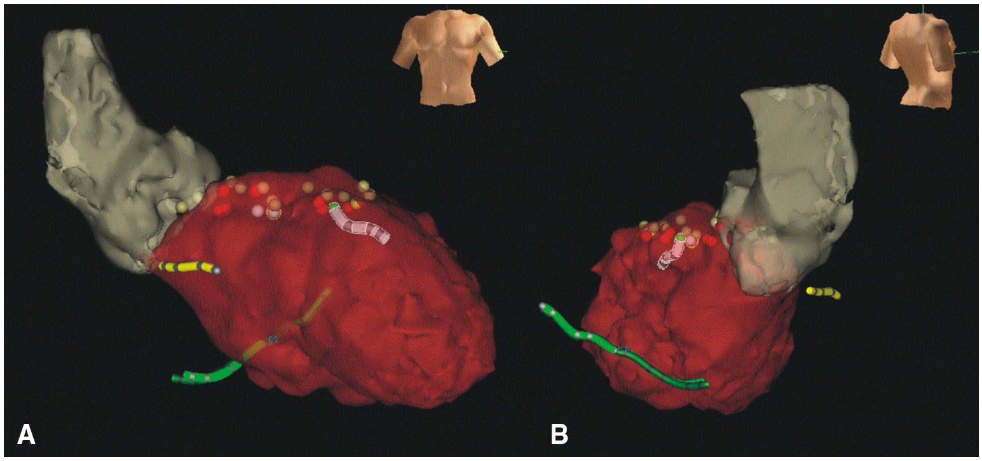

Fig. 3 3DRA fused with EnSite Velocity system in AP view (**a**) and RAO 120° view (**b**). Left ventricle (*red color*), aortic bulbus and a part of the ascending aorta (*grey color*) are depicted. In the lateral part of the LVOT and aortic bulbus, 3D points tracked during the procedure are shown, such as sites of pacemapping and earliest excitement (*white/beige dots*), RF application (*red dots*), and successful line of ablation with arrhythmia elimination (*yellow dot*). Also shown are a decapolar catheter placed into the coronary sinus (*green color*), a quadrupolar catheter positioned at His bundle region (*yellow color*) and an ablation catheter advanced through aorta into the LVOT (*white color*)

image cutoffs, most commonly missing apex. At the time of the study, software for inside volume evaluation of the resulting 3D image was not available to us, therefore we could not assess whether direct injection leads to enlarged and skewed visualization of the left ventricle or not. Furthermore, we suppose that it is impossible to determine the exact contour of endocardium during rapid ventricular pacing since ventricle is contrasted during both systole and diastole.

Future direction

We believe that the main barrier preventing many centers from employing this strategy to other anatomical structures of interest is the inability of automated segmentation of acquired images. With the premise that similar clinical outcomes of CT and 3D rotational angiography would be confirmed in a larger population, and tools for automated reconstruction of structures other than left atrium will be incorporated into the next version of the Philips EP Navigator, this method may be effectively applied to guide catheter ablation for ventricular tachycardias also in other centers. The advantage is an automatic fusion of a reconstructed 3D image with live fluoroscopy which obviates the need for intricate and protracted fusion with CT scans. Furthermore, a substantial reduction in radiation exposure and use of contrast medium is of great benefit not only to the patient. Larger randomized trials are, however, needed for final comparison of these methods. Such a study is under preparation at our center.

Conclusion

Our findings have demonstrated that 3D reconstruction of the left ventricle is feasible, safe and effective. The resulting 3D volumes have been used in several ways to guide VT ablation. The prospect of further refinement of the method as well as development of novel features and software algorithms for visualization of cardiac structures is presumed.

Acknowledgments This work was supported by European Regional Development Fund—Project FNUSA-ICRC (No. CZ.1.05/1.1.00/02.0123).

Conflict of interest None declared.

References

1. Committee Members, Blomstrom-Lundqvist C, Scheinman MM, Aliot EM et al (2003) ACC/AHA/ESC guidelines for the management of patients with supraventricular arrhythmias—

executive summary: a report of the American college of cardiology/American heart association task force on practice guidelines and the European society of cardiology. J Am Coll Cardiol 42(8):1493–1531
2. Cappato R, Calkins H, Chen SA et al (2005) Worldwide survey on the methods, efficacy, and safety of catheter ablation for human atrial fibrillation. Circulation 111:1100–1105
3. Aliot EM, Stevenson WG, Almendral-Garrote JM et al (2009) EHRA/HRS expert consensus on catheter ablation of ventricular arrhythmias: developed in a partnership with the European Heart Rhythm Association (EHRA), a registered branch of the European Society of Cardiology (ESC), and the Heart Rhythm Society (HRS); in collaboration with the American College of Cardiology (ACC) and the American Heart Association (AHA). Heart Rhythm 6(6):886–933
4. Members Committee, Zipes DP, Camm AJ, Borggrefe M et al (2006) ACC/AHA/ESC 2006 guidelines for management of patients with ventricular arrhytmias and the prevention of sudden cardiac death. Europace 8(9):746–837
5. Orlov MV, Ansari MM, Akrivakis ST et al (2011) First experience with rotational angiography of the right ventricle to guide ventricular tachycardia ablation. Heart Rhythm 8:207–211
6. Hilbert S, Dagres N, Hindricks G et al (2011) Rapid ventricular pacing: a fast, reliable, and safe technique for optimization of image acquisition during rotational angiography for catheter ablation of atrial fibrillation. Heart Vessels 26:349–352
7. Tian J, Jeudy J, Smith MF et al (2010) Three-dimensional contrast-enhanced multidetector CT for anatomic, dynamic, and perfusion characterization of abnormal myocardioum to guide ventricular tachycardia ablations. Circ Arrhythm Electrophysiol 3:496–504
8. Andreu D, Berruezo A, Ortiz-Pérez JT et al (2011) Integration of 3D electroanatomic maps and magnetic resonance scar characterization into the navigation system to guide ventricular tachycardia ablation. Circ Arrhythm Electrophysiol 4:674–683
9. Orlov MV, Hoffmeister P, Chaudhry GM et al (2007) Three-dimensional rotational angiography of the left atrium and esophagus—A virtual computed tomography scyn in the electrophysiology lab? Heart Rhythm 4(1):37–43

Feasibility and safety of right and left ventricular three-dimensional rotational angiography for guiding catheter ablation of ventricular arrhythmias

Zdenek Starek, Jiri Wolf, Frantisek Lehar, Jiri Jez, Tomas Kulik, Alena Kulikova

Background. Three-dimensional rotational angiography (3DRA) of the heart is an imaging technique that displays the left atrium and adjacent structures during catheter ablation of atrial fibrillation. The aim is to evaluate the feasibility and safety of 3DRA for imaging the right and left ventricles of patients undergoing catheter ablation of ventricular arrhythmias.
Methods. From 8/2010 to 6/2015, 35 patients underwent 3DRA of the right (20 patients) or left ventricle (15 patients) with a Philips Allura FD 10 X-ray system using a direct protocol. The success rate of the 3D model, as well as the procedure times and complications of 3DRA, was evaluated, and the 3DRA model was compared with ventricular computer tomography (CT).
Results. The overall 3D model success rate was 91.4%. The 3D models were graded as excellent for 65.7% of patients and as useful for 25.7% of patients. The imaging success rate was slightly higher for the right ventricle than for the left ventricle (95%, 86.7%, respectively). The times required to perform 3DRA of the right and left ventricle were 12.5 +/- 2.1 min and 14.7 +/- 2.8 min, respectively. There were no significant differences between 3DRA and ventricular CT.
Conclusion. Ventricular 3DRA allows the easy and safe creation of 3D models of the cardiac ventricles. The success rate is comparable to the success rate of the 3DRA for imaging the left atrium. There was no difference in imaging quality between the two ventricles. 3DRA models of the ventricles are comparable with CT models of the ventricles.

Key words: 3D rotational angiography, left ventricle, right ventricle, catheter ablation of arrhythmias, ventricular arrhythmias, image integration

International Clinical Research Center, 1st Department of Internal Medicine – Cardioangiology, St. Anne's University Hospital Brno, Pekarska 53, 656 91 Brno, Czech Republic
Corresponding author: Zdenek Starek, e-mail: zdenek.starek@fnusa.cz

INTRODUCTION

Catheter ablation guided by 3D electroanatomical mapping[1] (CARTO (Biosense Webster, Diamond Bar, CA) and EnSite Velocity (St Jude Medical, St Paul, MN)) is now the method of choice for treating complex atrial and ventricular arrhythmias[2,3].

The creation of electroanatomical maps based on 3D models of the left atrium or cardiac ventricles developed via computed tomography (CT) to guide ablation procedures is common[4,5].

Three-dimensional rotational angiography (3DRA) of the heart was developed to image the left atrium during catheter ablation of atrial fibrillation[6-8] and represents a new alternative to cardiac CT imaging[9,10]. Models of other cavities and structures, such as the esophagus[11,12] or cardiac ventricles[13,14], can be acquired and used during ablation.

Our objective was to evaluate the feasibility and safety of 3DRA for the creation of models of the left and right ventricle in patients undergoing catheter ablation of ventricular arrhythmias.

MATERIAL AND METHODS

Patient population

This retrospective study enrolled 35 consecutive patients who were referred to our center for catheter ablation of ventricular arrhythmias from August 2010 to June 2015. All patients underwent right or left ventricular 3DRA, and 18 patients also underwent ventricular CT. A study regarding a portion of this group of patients was published previously[14].

Rotational angiography imaging

Imaging was carried out with a Philips Allura Xper FD 10 X-ray system (Philips Medical Systems Inc., Best, the Netherlands) using a protocol described previously[14]. The contrast agent (a total of 85 mL of contrast agent was administered at a velocity of 20 mL/sec) was administered into the right ventricle (RV) or left ventricle (LV), and rotational images were acquired (the C-arm was isocentrically rotated 240° over 4.1 s using an X-ray acquisition speed of 30 frames per second).

Ventricle isocentering was achieved using two X-ray projections with a maximally raised flat panel.

Before rotational angiography, cardiac output was reduced via rapid ventricular stimulation at a frequency of 200–220/min.

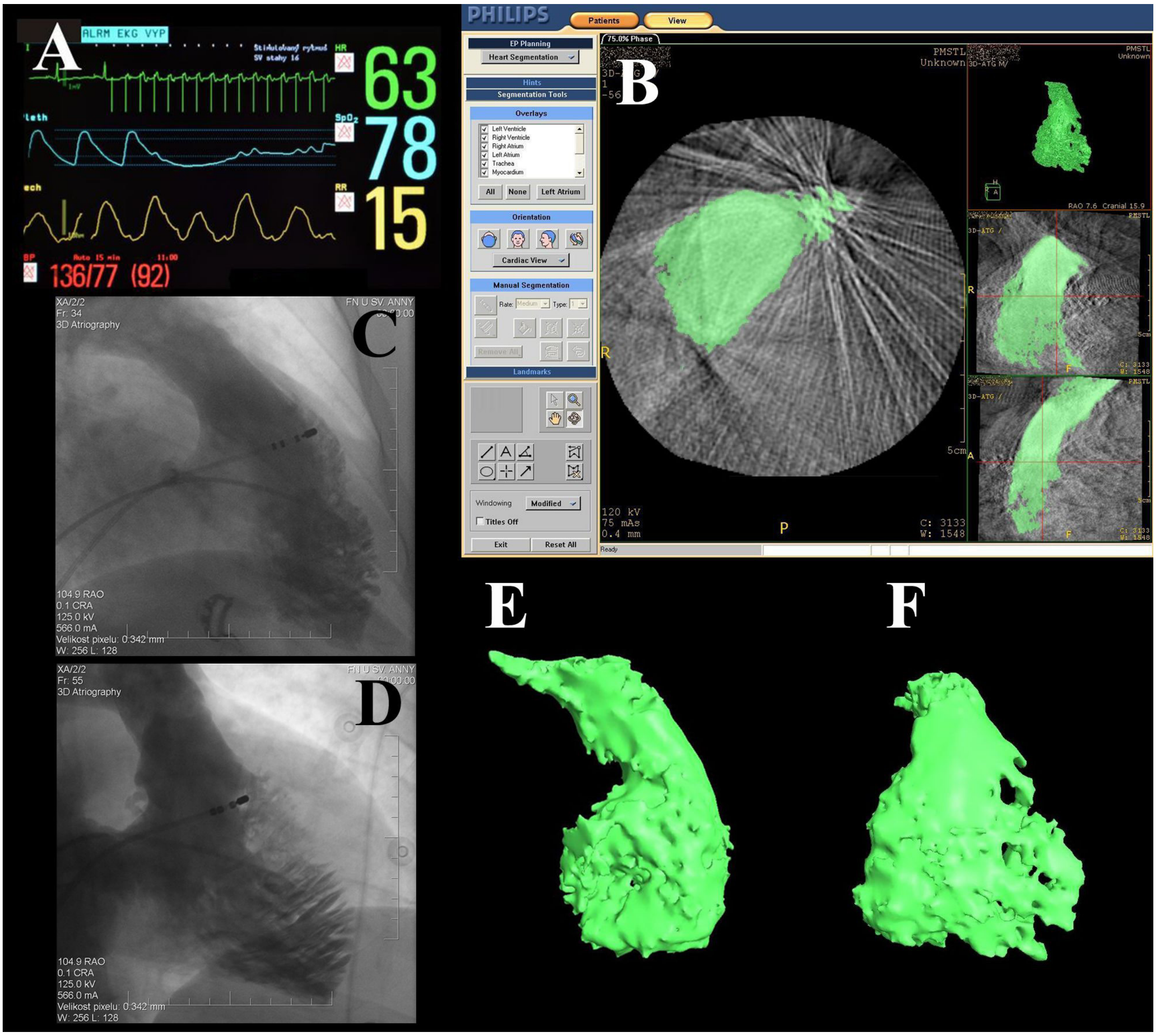

Fig. 1. Data acquisition and right ventricle (RV) 3D model segmentation. (A) Cardiac output via rapid stimulation was documented based on a decrease in saturation, (B) Segmentation of the 3D model using raw data. Shown are the XYZ sections of the 3D rotational angiography data, with the RV colored in green. (C, D) Rotational angiography of the right ventricle, RAO 104 (C), RAO 10 (D). (E, F) The final rendered model of the right ventricle, RAO 100 (E), RAO 40 (F).
LAO - Left oblique view, RAO - Right oblique view

After rotational angiography, data were automatically transmitted from the X-ray system to an EP Navigator workstation (EP Navigator 3.1, Philips Healthcare, Best, the Netherlands), where 3D models of both ventricles were manually segmented, (Fig. 1). These 3DRA models were automatically integrated with live fluoroscopic images (Fig. 2 and 3).

CT imaging

CT imaging was performed using an ECG non-gated protocol on a 64-slice CT scanner (GE Lightspeed VCT, General Electric, Fairfield, USA). The CT parameters were as follows: 120 kV, 800 mA, a collimation of 63x0.625 mm, and a spiral pitch factor of 0.98. Image reconstruction was performed on a 512x512 pixel array. Contrast was administered through a peripheral vessel.

Qualitative and quantitative image analysis

Qualitative analysis. The rotational angiography imaging results were independently assessed by two expert physicians. The rotational angiography results for each patient were assessed in 23 projections (right anterior oblique (RAO) 55° to left anterior oblique (LAO) 55°, in steps of 5°). The images were graded on a scale of 1–3 as follows: (1) not diagnostic, or characterized by indistinguishable ventricular contours, non-identifiable bodies or unrecognizable ventricular outflow tracts (VOTs); (2) useful, or characterized by blurred ventricular contours, missing or unclear ventricular apex, and poorly visible VOT-aortic/pulmonary valve junctions; and (3) excellent, or characterized by clear ventricular contours, easily identifiable ventricular bodies and ventricular outflow tracts, and identifiable aortic or pulmonary valve-ventricular out-

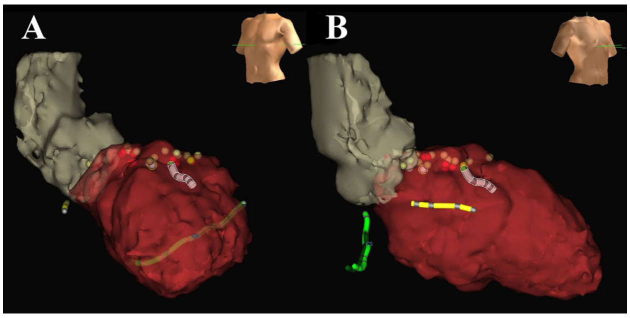

Fig. 2 . Integration of the 3D models of the right (A and B) and left (C and D) ventricle with fluoroscopic images, LAO 30 (A), RAO 39 (B), RAO 39 (C), LAO 41 (D).
RAO - Right anterior oblique projection, LAO - Left anterior oblique projection

flow tract junctions. In the event of disagreement between the two reviewers with respect to angiogram 'grading', the images were re-assessed by both reviewers, and a consensus was reached. This method was modified from that previously described by Tang et al.[15].

Quantitative image analysis. The images of the right and left ventricle that were acquired via 3DRA were compared to those acquired via CT. Using the raw data stored in the EP Navigator workstation, we compared the subvalvular diameters of the outflow tracts and the diameter of the aortic/pulmonary valve bulbus measured via 3DRA with those measured via CT (see Fig 3).

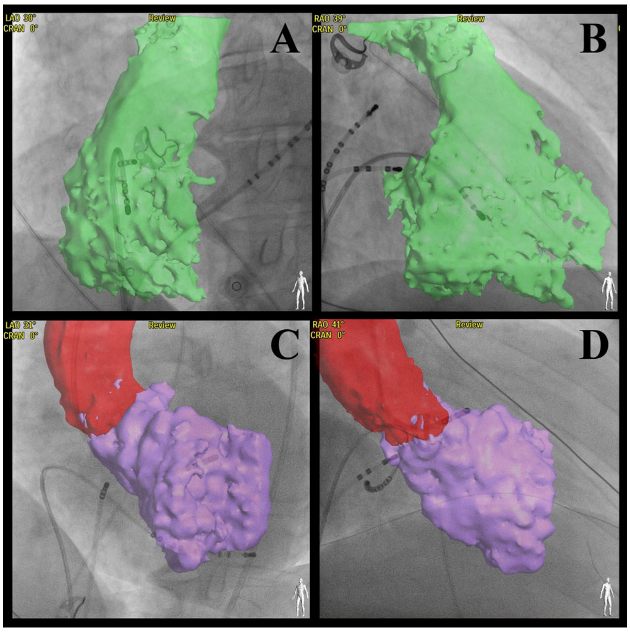

Fig. 3. Comparison of CT and 3DRA raw data measurements. (A, B) Picture of the body of the right ventricle and pulmonary valve, as well as part of the pulmonary artery, A – 3DRA, B – CT, (C, D) Picture of the body of the left ventricle and aortic bulbus, as well as part of the ascending aorta, C – 3DRA, D – CT.
3DRA - 3D rotational angiography, CT – Computed tomography

Image integration and ablation procedures

All ablation procedures were performed with the support of the 3D ventricular models generated via 3DRA, which were merged with live fluoroscopic images.

We supported the ablation procedures using synchronized projections of the 3D X-ray model and the 3D electroanatomical map or by directly merging the 3D X-ray model with the 3D electroanatomical map.

The ablation procedures were performed in a standardized manner. Idiopathic ventricular extrasystoles originating from the right ventricular outflow tract (RVOT) were conventionally ablated with standard 4-mm tip ablation catheters with the support of the 3D models generated via 3DRA, which were integrated live fluoroscopic images. Left ventricular outflow tract (LVOT) arrhythmias and ventricular arrhythmias caused by structural heart disease were treated with irrigated tip catheters with the support of the 3D electroanatomical mapping system EnSite Velocity.

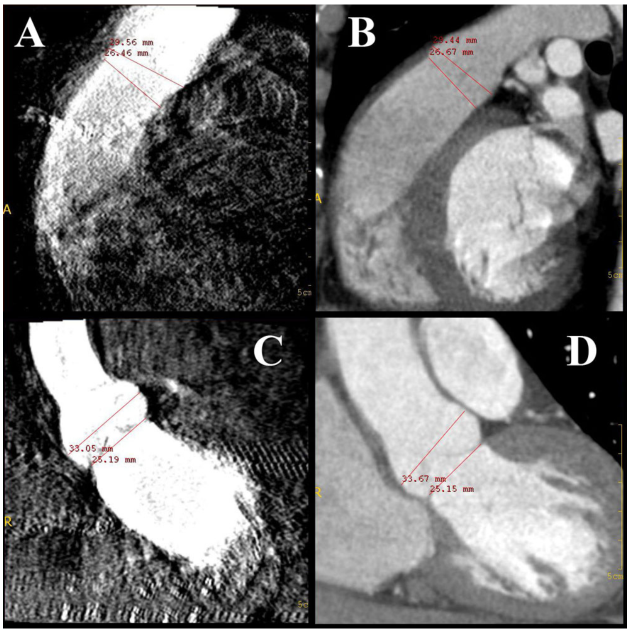

Fig. 4. Integration of the 3D model of the left ventricle and the 3D electroanatomical mapping system EnSite Velocity, with tagged ablation points on the surface of the left ventricular outflow tract (yellow and white dots).
A - Left oblique projection, B - Right oblique projection

Statistical analysis

Statistical analysis was performed using STATISTICA software (data analysis software system), StatSoft, Inc. (2013), version 12, www.statsoft.com. Data were analyzed using descriptive statistics. Differences between the two groups (CT vs. 3DRA) were evaluated by Spearman's rank correlation coefficient, and confidence intervals were reported. The two methods were compared using the Wilcoxon-Mann-Whitney U two-sample rank-sum test. The significance level was set to 0.05.

Table 1. Patient characteristics.

Patient characteristics	3DRA of the right ventricle	3DRA of the left ventricle	Total
Number of patients	20	15	35
Age	52.55 +/- 16.42	65 +/- 16.35	57.89 +/- 16.32
Males	11 (55%)	8 (53.33%)	19 (54.29%)
EF of LV	57.95 +/- 8.22	56.53 +/- 8.22	57.34 +/- 8.11
Body mass index	27.92 +/- 4.48	26.98 +/- 4.6	26.36 +/- 4.48
Structural heart disease	0	2 (13.33%)	2 (5.71%)
Hypertension	7 (35%)	7 (46.67%)	14 (40%)
Idiopathic RVOT arrhythmias	20	N/A	N/A
Idiopathic LVOT arrhythmias	N/A	13	N/A
Structural heart disease arrhythmias	N/A	2	N/A

RVOT - right ventricular outflow tract, LVOT - left ventricular outflow tract

Table 2. Duration of individual 3DRA steps.

Duration of individual 3DRA steps	3DRA of the right ventricle	3DRA of the left ventricle	*P*
Average total time from the introduction of the pigtail to the end of segmentation in EP Navigator (min)	12.5 +/- 2.1	14.7 +/- 2.8	0.036
Average time for data exportation from EP Navigator to the 3D mapping system (min)	NA	4.8 +/- 0.9	
Average total procedure time (min)	131.5 +/- 58.1 †	221.5 +/- 72.2 † (387.0 +/- 43.0*)	†0.002
3DRA share in total procedure time (%)	9.5	6.6 (3.8*)	

* Ablations of ventricular arrhythmias in patients with structural heart disease, n=2
† Ablations of ventricular arrhythmias in patients without structural heart disease, n=33

Table 3. Success rate of 3DRA.

Success rate of 3DRA	3DRA of the right ventricle n=20	3DRA of the left ventricle n=15	3DRA of both ventricles n=35	*P*
Excellent 3DRA	14 (70%%)	9 (60%)	23 (65.7%)*	
Useful 3DRA	5 (25%)	4 (26.7%)	9 (25.7%)	
At least useful (excellent + useful)	19 (95%)*	13 (86.7%)*	32 (91.4%)	*0.048
Not diagnostic 3DRA	1 (5%)	2 (13.3%)	3 (8.6%)	

3DRA - three-dimensional rotational angiography

Table 4. 3DRA versus CT.

Characteristic	N	Spearman corr. coeff.	Wilcoxon test (Z score)	*P*
Aortic bulbus diameter	5	0.9	0.674	0.50
Subvalvular LVOT diameter	5	0.7	0.405	0.69
Pulmonary valve diameter	12	0.874	1.647	0.10
Subvalvular RVOT diameter	12	0.881	1.530	0.09

RESULTS

From August 2010 to June 2015, 35 patients underwent right or left ventricular 3DRA before catheter ablation of ventricular arrhythmias. Twenty patients underwent also underwent cardiac CT.

The average radiation dose for all ventricular 3DRA procedures was 10875.4 +/– 3318.4 mGy/cm^2. The average radiation dose for right ventricular 3DRA was 9638.2 +/– 3318.4 mGy/cm^2, and the average radiation dose for left ventricular 3DRA was 12731.25 +/– 2399.9 mGy/cm^2. The average radiation dose for all catheter ablation procedures was 22200.3 +/– 11488.3 mGy/cm^2. The average radiation dose for right ventricular arrhythmia ablation was 17680.7 +/– 11488.3 mGy/cm^2, the average radiation dose for LVOT arrhythmia ablation was 27675.7 +/- 8905.5 mGy/cm^2, and the average radiation dose for LV structural arrhythmia ablation was 38367.3 +/- 8561.1 mGy/cm^2

Patient characteristics

Of the 35 patients enrolled in this study, 20 underwent 3DRA of the RV, and 15 underwent 3DRA of the LV. Five patients who underwent 3DRA of the LV underwent CT of the LV, and 13 patients who underwent 3DRA of the RV underwent CT of the RV. Most patients were ablated for idiopathic ventricular extrasystoles originating from the RVOT and LVOT. Three patients had diminished EFs, two patients had structural heart disease (ischemic cardiomyopathy after MI), and one patient with idiopathic LVOT extrasystoles had a diminished EF due to arrhythmia-induced cardiomyopathy.

Rotational angiography image acquisition and qualitative and quantitative image assessment

The mean systolic and diastolic blood pressures at the start of rotational ventricular angiography were 132.67 +/- 17.01 mmHg and 78.54 +/- 13.04 mmHg, respectively. The times required to perform right and left ventricular 3DRA were 12.5 +/- 2.1 min and 14.7 +/- 2.8 min, respectively. Given the small number of patients in both groups, this difference appeared to be significant (P=0.036). Total procedure time was significantly longer for ablations involving the left ventricle (P=0.002) than for ablations involving the right ventricle. For details, see Table 2.

Qualitative image assessment. The overall success rate of the protocol (excellent and useful models) was 91.4%. The 3D volume reconstructions were graded as excellent in 65.7% of patients and as useful in 25.7% patients. The vast majority of the models classified as useful were missing the apex of the ventricle, which was cropped due to imperfect isocentering. The examination results were useless in three patients, and a system failure occurred in one patient, as the loss of the connection between the power injector and the pigtail catheter resulted in the ventricle not filling with contrast. The resulting model did not anatomically correspond to the visualized ventricle and therefore could not be used in two patients. The success rate of 3DRA of the RV was slightly higher than the success rate of 3DRA of the LV (95% vs. 86.7%). Given the small number of patients in both groups, this difference appeared to be statistically significant (P=0.048). After excluding the technical error (disconnected connecting tubes in one case of failed 3DRA) the difference between the success rates of right and left ventricular 3DRA was negligible (95% vs. 92.8) (P=0.759). Additional details can be found in Table 3.

Because manual segmentation was performed, the resulting models had somewhat uneven surfaces, but the sizes and shapes of the images completely matched those of the displayed ventricles. Reassessments of anatomical accuracy were performed throughout each procedure, and no discrepancies were reported.

Quantitative image assessment. The datasets of the 3DRA and CT images of the 5 patients who underwent 3DRA of the LV and the 12 patients who underwent 3DRA of the RV (one patient who underwent CT of the RV underwent unsuccessful 3DRA of the RV) were compared. Using the Wilcoxon–Mann–Whitney U two-sample rank-sum test, we failed to reject the null hypothesis that there is no difference between the two groups at the 0.05 significance level (Table 4).

Catheter ablation with the support of 3DRA

All radiofrequency ablations were performed in the standard manner and were without complications. For catheter ablation of idiopathic RVOT arrhythmias, fluoroscopy and the 3D model were the only imaging methods used. For all ablations of LVOT extrasystoles and arrhythmias caused by structural heart disease, we used the 3D electroanatomical mapping system EnSite Velocity and the 3D model of the ventricle generated by 3DRA to create 3D electroanatomical maps.

In two patients, integration of the resulting 3D image of the LV and the electroanatomical map generated using EnSite Velocity was accomplished using the aortic bulbus and coronary ostia as fiducial points (Fig 4).

DISCUSSION

Three-dimensional rotational angiography of the cardiac ventricles proved to be a simple and reliable method of imaging the cardiac ventricles. The success rate of creating an applicable model using the direct protocol was 91.4%. Orlov et al. noted that their success rate for 3DRA of the right ventricle was 87.5% (ref.[13]), which is comparable to the success rates of the direct left atrial protocols used to image the left atrium via 3DRA. Tang et al. reported a success rate of 95.7% using this left atrial protocol[15]. Kriatselis et al. reported a success rate of almost 100% (ref.[16]). The success rate of ventricular 3DRA noted in this study was not significantly different from the success rate noted in our cohort of 238 patients who underwent catheter ablation of atrial fibrillation and were examined via 3DRA of the left atrium using the direct left atrial protocol (91.4% vs. 94.54%, P=0.894) (ref.[12]).

Not diagnostic or useful images were attributed to the learning curve associated with ventricular 3DRA, as it is a new imaging method. Splitting the patients into two groups according to the dates of their procedures showed that the probability of a not diagnostic or useful result was 38.9% (18 patients, 7 suboptimal results) during the first half of the study and 23.5% (17 patients, 4 suboptimal results) during the second half of the study. For example, early in the series, poor isocentering or problems with image cut-offs caused by improper isocentering resulted in the generation of suboptimal images

The main concern associated with the use of 3DRA models of cardiac cavities is imaging quality. As CT models are considered the gold standard for imaging cardiac cavities, the most reliable means of verifying the accuracy of a 3DRA model is to compare it with a model created using CT data. Several studies have compared models of the left atrium generated using 3D rotational angiography to models generated using CT imaging[9,6,15]. Comparisons between these atrial models were based mostly on measurements of the ostia of the pulmonary veins and showed that there was a very strong correlation between the models generated by each modality. Using similar methods in our small group of patients, we noted a very strong correlation between the left ventricular models generated using 3DRA and CT data[14].

An equally important issue is the clinical benefit of using 3D ventricular models. In our cohort of 516 patients who were examined with 3DRA of the left atrium during radiofrequency ablation of atrial fibrillation, the average time from the introduction of the pigtail catheter to the end of segmentation was 8.47 min[12]. Despite the need to use manual segmentation when creating the ventricular model, the total procedure times for each ventricle were only slightly longer (12.5 +/- 2.1 min for right ventricle; 14.7 +/- 2.8 min for left ventricle) than that for the left atrium. The manual segmentation time of the left ventricle was slightly longer than the manual segmentation time of the right ventricle, probably because the former procedure was more complicated due to the presence of the aortic bulb and the coronary artery stems; however, from a practical point of view, the difference between the two manual segmentation times was negligible.

We observed contrasting results when evaluating the impacts of ventricular 3DRA on the total duration of and radiation dose associated with the procedure. For the aforementioned group of patients who were referred for atrial fibrillation ablation[12], 3DRA imaging accounted for only 4.5% of the total procedure time and 33.6% of the total radiation exposure. In the case of 3D models of the left ventricle, the impacts of 3DRA on procedure time and radiation exposure were comparable. In the case of catheter ablation of left ventricular arrhythmias in patients with structural heart disease and patients with idiopathic ventricular extrasystoles originating from the LVOT, 3DRA imaging accounted for 3.8% and 6.6% of the total procedure time and 33.2% and 46% of the radiation exposure, respectively. However, in the case of ventricular arrhythmias originating from the RVOT, the impact of 3DRA was less favorable, as 3DRA imaging accounted for almost 10% of the total procedure time and 54.5% of the total radiation dose. Given the relatively large amount of time required to perform 3DRA and the considerable amount of radiation exposure associated with the procedure, which is comparable to or worse than that associated with 3DRA of the left atrium[6,9,12], the use of this method to support ablation of ventricular arrhythmias should be carefully considered, and the benefits of its use should be weighed against the possible risks of its use. This method may be recommended for guiding catheter ablations, for which CT-generated heart cavity models are commonly used. For ablation of RVOT extrasystoles, however, routine use of this method is questionable.

Study Limitations

Several limitations need to be addressed. First of all, we were unable to automatically segment and reconstruct the 3D models of the ventricles, as automatic segmentation is available only for reconstruction of the left atrium. The 3D models of the ventricles must be manually segmented, which is somewhat time consuming and requires an experienced operator. This limitation may discourage other centers from routinely employing 3D rotational angiography to visualize additional cardiac and non-cardiac structures. Second, the size of the standard cardiology flat detector (10 x 10 inches) is not appropriate for patients with higher BMIs, and the use of this flat detector results in suboptimal isocentering and image cut-offs, which most commonly affect the apex. We also believe that it is impossible to determine the exact contour of the endocardium during rapid ventricular pacing because the contrast-enhanced appearance of the ventricle is the same during both systole and diastole.

CONCLUSION

3D rotational angiography of the ventricles allows the easy and safe periprocedural creation of 3D models of the cardiac ventricles, which are useful for guiding catheter ablation of ventricular arrhythmias. The 3DRA and CT models of the ventricles are comparable. There were no differences in image quality between the right and left ventricle.

Acknowledgement: This study was supported by the project no. LQ1605 from the National Program of Sustainability II.

Author contributions: All authors had full access to all the data in the study and take responsibility for the integrity of the data and the accuracy of the data analysis; ZS, JW: study concept and design, acquisition of data, manuscript drafting; FL, JJ: acquisition of data, critical revision, AK, TK: Data analysis and interpretation, critical revision, statistical analysis.

Conflict of interest statement: The authors state that there are no conflicts of interest regarding the publication of this article.

REFERENCES

1. Gepstein L, Hayam G, Ben-Haim SA. A novel method for nonfluoroscopic catheter-based electroanatomical mapping of the heart. In vitro and in vivo accuracy results. Circulation 1997;95(6):1611-22.
2. Calkins H, Kuck KH, Cappato R, Brugada J, Camm AJ, Chen SA, Crijns HJ, Damiano RJ Jr, Davies DW, DiMarco J, Edgerton J, Ellenbogen K, Ezekowitz MD, Haines DE, Haissaguerre M, Hindricks G, Iesaka Y, Jackman W, Jalife J, Jais P, Kalman J, Keane D, Kim YH, Kirchhof P, Klein G, Kottkamp H, Kumagai K, Lindsay BD, Mansour M, Marchlinski FE, McCarthy PM, Mont JL, Morady F, Nademanee K, Nakagawa H, Natale A, Nattel S, Packer DL, Pappone C, Prystowsky E, Raviele A, Reddy V, Ruskin JN, Shemin RJ, Tsao HM, Wilber D. 2012 HRS/EHRA/ECAS expert consensus statement on catheter and surgical ablation of atrial fibrillation: recommendations for patient selection, procedural techniques, patient management and follow-up, definitions, endpoints, and research trial design. J Interv Card Electrophysiol 2012;33(2):171-257.
3. Aliot EM, Stevenson WG, Almendral-Garrote JM, Bogun F, Calkins CH, Delacretaz E, Della Bella P, Hindricks G, Jaïs P, Josephson ME, Kautzner J, Kay GN, Kuck KH, Lerman BB, Marchlinski F, Reddy V, Schalij MJ, Schilling R, Soejima K, Wilber D. EHRA/HRS Expert Consensus on Catheter Ablation of Ventricular Arrhythmias: developed in a partnership with the European Heart Rhythm Association (EHRA), a Registered Branch of the European Society of Cardiology (ESC), and the Heart Rhythm Society (HRS). Heart Rhythm 2009;6(6):886-933.
4. Malchano ZJ, Neuzil P, Cury RC, Holmvang G, Weichet J, Schmidt EJ, Ruskin JN, Reddy VY. Integration of cardiac CT/MR imaging with

three-dimensional electroanatomical mapping to guide catheter manipulation in the left atrium: implications for catheter ablation of atrial fibrillation. J Cardiovasc Electrophysiol 2006;17(11):1221-9.
5. Yamashita S, Sacher F, Mahida S, Berte B, Lim HS, Komatsu Y Amraoui S, Denis A, Derval N, Laurent F, Sermesant M, Montaudon M, Hocini M, Haïssaguerre M, Jaïs P, Cochet H. Image Integration to Guide Catheter Ablation in Scar-Related Ventricular Tachycardia. J Cardiovasc Electrophysiol 2016;27(6):699-708.
6. Kriatselis C, Tang M, Nedios S, Roser M, Gerds-Li H, Fleck E. Intraprocedural reconstruction of the left atrium and pulmonary veins as a single navigation tool for ablation of atrial fibrillation: a feasibility, efficacy, and safety study. Heart Rhythm 2009;6(6):733-41.
7. Li JH, Haim M, Movassaghi B, Mendel JB, Chaudhry GM, Haffajee CI, Orlov MV. Segmentation and registration of three-dimensional rotational angiogram on live fluoroscopy to guide atrial fibrillation ablation: a new online imaging tool. Heart Rhythm 2009;6(2):231-7.
8. Stárek Z, Lehar F, Jež J, Wolf J, Novák M. 3D X-ray imaging methods in support catheter ablations of cardiac arrhythmias. Int J Cardiovasc Imaging 2014;30(7):1207-23.
9. Thiagalingam A, Manzke R, D'Avila A, Ho I, Locke AH, Ruskin JN, Chan RC, Reddy VY. Intraprocedural volume imaging of the left atrium and pulmonary veins with rotational X-ray angiography: implications for catheter ablation of atrial fibrillation. J Cardiovasc Electrophysiol 2008;19(3):293-300.
10. Lehar F, Starek Z, Jez J, Novak M, Wolf J, Stepanova R, Kruzliak P, Kulik T, Zbankova A, Jancar R, Vitovec J. Comparison of clinical outcomes and safety of catheter ablation for atrial fibrillation supported by data from CT scan or three-dimensional rotational angiogram of left atrium and pulmonary veins. Biomed Pap Med Fac Univ Palacky Olomouc Czech Repub 2015;159(4):622-8.
11. Orlov MV, Hoffmeister P, Chaudhry GM, Almasry I, Gijsbers GH, Swack T, Haffajee CI. Three-dimensional rotational angiography of the left atrium and esophagus - A virtual computed tomography scan in the electrophysiology lab? Heart Rhythm 2007;4(1):37-43.
12. Starek Z, Lehar F, Jez J, Wolf J, Kulik T, Zbankova A, Novak M. Periprocedural 3D imaging of the left atrium and esophagus: comparison of different protocols of 3D rotational angiography of the left atrium and esophagus in group of 547 consecutive patients undergoing catheter ablation of the complex atrial arrhythmias. Int J Cardiovasc Imaging 2016;32(7):1011-9.
13. Orlov MV, Ansari MM, Akrivakis ST, Jadidi A, Nijhof N, Natan SR, Wylie JV, Hicks A, Armstrong J, Jais P. First experience with rotational angiography of the right ventricle to guide ventricular tachycardia ablation. Heart Rhythm 2011;8(2):207-11.
14. Wolf J, Starek Z, Jez J, Lehar F, Lukasova M, Kulik T, Novak M. Rotational angiography of left ventricle to guide ventricular tachycardia ablation. Int J Cardiovasc Imaging 2015;31(5):899-904.
15. Tang M, Kriatselis C, Ye G, Nedios S, Roser M, Solowjowa N, Fleck E, Gerds-Li JH. Reconstructing and registering three-dimensional rotational angiogram of left atrium during ablation of atrial fibrillation. Pacing Clin Electrophysiol 2009;32(11):1407-16.
16. Kriatselis C, Tang M, Roser M, Fleck E, Gerds-Li H. A new approach for contrast-enhanced X-ray imaging of the left atrium and pulmonary veins for atrial fibrillation ablation: rotational angiography during adenosine-induced asystole. Europace 2009;11(1):35-41.

J Interv Card Electrophysiol
DOI 10.1007/s10840-016-0121-x

Long-term mobility of the esophagus in patients undergoing catheter ablation of atrial fibrillation: data from computer tomography and 3D rotational angiography of the left atrium

Zdeněk Stárek [1,2] · František Lehar [1,2] · Jiří Jež [1,2] · Alena Žbánková [1,2] · Tomáš Kulík [1,2] · Jiří Wolf [1,2] · Miroslav Novák [1,2]

Received: 8 December 2015 / Accepted: 23 February 2016

Abstract
Purpose Computed tomography (CT) and 3D rotational angiography (3DRA) of the left atrium (LA) are used to evaluate the esophagus prior to radiofrequency ablation for atrial fibrillation. The aim of this study was to compare preprocedural and periprocedural views of the esophagus and the left atrium.
Methods From September 2011 to August 2012, 3DRA and CT of the LA were performed on 56 patients before they underwent catheter ablation of atrial fibrillation. The 3DRA was performed periprocedurally, and the CT was performed an average of 20 days prior to the procedure. 3D models of the LA and the esophagus were then segmented on the EP Navigator V 3.1 workstation. Five positions of the esophagus, A–E, in order from left to right, were evaluated.
Results The most common position of the esophagus was behind the left part of the LA (CT, position B ($n = 26$)) and behind the central part of the LA (3DRA, position C ($n = 21$)). The maximum shift of the esophagus was three positions, and the average shift was 0.857 ± 0.766 of a position. There was a shift of one position in 44.6 % of the patients, two positions in 17.9 %, and three positions in 1.8 %. A statistically significant difference was found between the positions of the esophagus when the 3DRA and CT evaluations were compared.
Conclusions The most common position of the esophagus was behind the middle and left part of the LA. The outpatient views of the esophagus obtained before ablation did not reflect the position of the esophagus at the beginning of the procedure.

Keywords Computer tomography of the heart · 3D rotational angiography of the left atrium · Esophagus imaging · Atrial fibrillation · Catheter ablation of arrhythmias · Atrioesophageal fistula

1 Introduction

In the early twenty-first century, catheter ablation for atrial fibrillation has become a recognized form of treatment for patients with drug refractory atrial fibrillation [1]. The basis for catheter ablation is the isolation of the pulmonary veins by creating circular radiofrequency lesions around the ostia [2]; additional ablations are often required in patients with persistent atrial fibrillation and involve linear lesions in the left atrium [3]. A very serious but rare procedural complication is the development of an atrioesophageal fistula [4]. Atrioesophageal fistulas comprise less than 0.1 % of all

✉ Zdeněk Stárek
zdenek.starek@fnusa.cz

František Lehar
frantisek.lehar@gmail.com

Jiří Jež
jiri.jez@fnusa.cz

Alena Žbánková
alena.zbankova@fnusa.cz

Tomáš Kulík
tomas.kulik@fnusa.cz

Jiří Wolf
jiri.wolf@fnusa.cz

Miroslav Novák
miroslav.novak@fnusa.cz

1 International Clinical Research Center, 1st Department of Internal Medicine—Cardioangiology, St. Anne's University Hospital Brno, Pekařská 53, 656 91 Brno, Czech Republic

2 Faculty of Medicine, Masaryk University, Kamenice 5, 625 00 Brno, Czech Republic

Published online: 12 March 2016

complications [5] but are fatal in 70 to 80 % of cases [6] and are the cause of 16 % of overall deaths related to the catheter ablation of atrial fibrillation [4]. An atrioesophageal fistula can be caused by the application of radiofrequency energy on the posterior wall of the left atrium, causing damage to the esophagus, which is in close contact with this area [7, 8]. Identifying the exact position of the esophagus during catheter ablation may help reduce the risk of damage to the esophagus. The standard imaging method currently used during catheter ablation of atrial fibrillation is contrast enhanced computed tomography (CT) of the heart [9]. A new imaging method equivalent to CT is 3D rotational angiography (3DRA) of the left atrium [10]. Both methods make it possible to determine the position of the esophagus in relationship to the left atrium. Previous studies on the utility of a preprocedural CT view of the position of the esophagus have yielded contradictory results. Some studies showed a relatively stable position of the esophagus in the long term [11–14]. Conversely, other studies, such as the work of Daoud et al. [15] and Nolker et al. [16], found a poor correlation between the preprocedural view of the esophagus using CT and its actual position during the ablation procedure. Our aims in this work were to demonstrate the accuracy of the preprocedural view of the esophagus using CT of the heart for predicting the position of the esophagus during catheter ablation and to evaluate the effect of the time delay between the CT scan and the ablation.

2 Methods

2.1 Group of patients

This retrospective study evaluated a group of 56 patients referred for catheter ablation of atrial fibrillation who underwent a multislice CT of the heart and thorax along with 3D rotational angiography (3DRA) of the left atrium and esophagus when they participated in a prior, prospective study comparing this two imaging techniques. The prior study was approved by the institutional review board, and written informed consent was obtained from all the patients [17]. This current retrospective study was also approved by the ethics committee of our institution.

2.2 CT Imaging

A CT scan was performed using the ECG nongated protocol on a 64-slice unit (GE Lightspeed VCT, General Electric, Fairfield, USA). CT parameters were as follows: 120 KV, 800 mAs, collimation of 63×0.625 mm, and a spiral pitch factor of 0.98. Image reconstruction was performed on a 512×512 pixel array. A total of 100–150 ml of contrast agent was administered through a peripheral vein (Ultravist 370, Bayer Pharma AG, Berlin, Germany). During the procedure, the patients held their arms aloft while holding their breath. The data were burned onto a CD-ROM, and a 3D reconstruction of the left atrium and esophagus was created from the acquired data using a workstation EP Navigator (EP Navigator 3.1, Philips Healthcare, Best, The Netherlands). The spatial resolution of CT data was so high that it allowed both the segmentation of the left atrium visualized with a contrast agent and the segmentation of the native esophagus without the use of a contrast agent.

2.3 Rotational angiography imaging

3DRA of the left atrium and esophagus was performed at the beginning of the procedure immediately after transseptal puncture. Imaging was carried out using the Allura Xper FD 10 X-ray system (Philips Medical Systems Inc., Best, The Netherlands) with the left atrial protocol. For the 3DRA, a contrast agent was injected into the atrium and a rotational image was acquired. After opacification of the left atrium and pulmonary veins, the C-arm was isocentrically rotated 240° (120° right anterior oblique to 120° left anterior oblique) over 4.1 s with an X-ray acquisition speed of 30 frames per second. During the rotational imaging, the patients were breathing normally and in a recumbent position with the natural position of the arms alongside the body.

The isocentering of the left atrium was achieved from an anteroposterior and left lateral X-ray view. The contrast agent was injected using a standard power injector (Mark V, Medrad Inc., Indianola, PA, USA) [18] via a pigtail catheter which was introduced through a transseptal sheath (Agilis NxT 8.5F) into the left atrium. After reducing the cardiac output by rapid stimulation of the ventricles (frequency 230/min), the contrast agent was injected, and after a delay of 2 s, the rotation of the C-arm commenced [19]. In total, 60 ml of the contrast agent was injected at a rate of 15 ml/s.

The esophagus was visualized following the oral administration of 20–30 ml of a barium sulfate contrast agent (Micropaque, Guerbet, Roissy, France) during the rotational angiography of the left atrium [10].

The 3DRA model of the left atrium was reconstructed offline on the workstation EP Navigator (EP Navigator 3.1, Philips Healthcare, Best, The Netherlands). Automatic segmentation was supplemented where necessary by manual segmentation. The 3D model of the esophagus was segmented manually on the same workstation.

2.4 Qualitative image analysis

To determine the position of the esophagus in relation to the atrium for both modalities, we used a modified method devised by Kottkamp et al. [13] We divided the posterior wall of the left atrium and the adjacent pulmonary veins into five vertical columns, A–E, from left to right. Columns A and E were arranged laterally behind the ostia of the pulmonary veins, column C was in the middle of the left atrial posterior wall, and columns B and D were in intermediate positions. The position of the esophagus behind the left atrium was described according to these columns. In the case of an oblique position of the esophagus across multiple columns, we determined the position according to the column which contained the largest part of the esophagus.

For the CT models, we measured the width of the posterior wall of the left atrium in the transverse plane at the level of the inferior pulmonary veins. We calculated the average width of one column A–E from the measured average width of the posterior wall of the left atrium and that allowed us to quantitatively express the shift of the esophagus position in millimeters.

For both modalities, we measured the width of the esophagus at three levels—at the level of the LA roof, the LA bottom, and at the midpoint between those two landmarks (see Fig. 1).

Two experienced investigators conducted a blinded, independent evaluation of all the patients and determined the position of the esophagus in relationship to the left atrium. A statistical evaluation of the distribution of esophageal positions for both modalities and a comparison of the difference in the position of the esophagus for each patient were subsequently performed from the CT and 3DRA models.

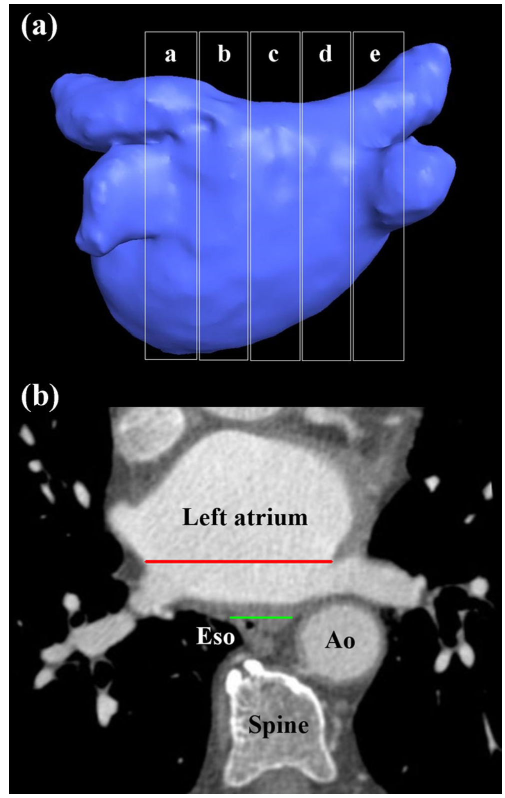

Fig. 1 **a** Methodology of the assessment of the esophageal position. The posterior wall of the left atrium and adjacent ostia of the pulmonary veins (PVs) are divided into five columns *a–e* in the direction from the left-sided PVs to the right-sided PVs. The position of the esophagus in the region behind the left atrium is evaluated and described according to the column in which the bulk of the esophagus lies. **b** Methodology for measuring the width of the posterior wall of the left atrium and the esophagus. In the transverse view of the LA, the diameter of the posterior wall of the LA was defined as the distance between the midpoints of the right and left inferior PVs (*red line*). The *green line* illustrates the measurement of the width of the esophagus. *LSPV* left superior pulmonary vein, *LIPV* left inferior pulmonary vein, *RSPV* right superior pulmonary vein, *RIPV* right inferior pulmonary vein, *Eso* esophagus, *Ao* aorta

3 Statistical analysis

The position of the esophagus in each group (3DRA vs. CT) was analyzed by the Wilcoxon matched pairs test. The null hypothesis H0 ($\alpha = 0.05$) assumed that there was no statistically significant difference between the esophagus positions in the CT group and 3DRA group. Finally, an analysis was carried out to determine whether the shift of the esophagus position depended on the time interval between the CT and 3DRA examination. The analysis was performed using a Mann–Whitney *U* test.

4 Results

In the period from September 2011 to August 2012, sequential examinations using CT of the heart and 3D rotational angiography of the left atrium were carried out on 56 patients undergoing catheter ablation of atrial fibrillation. The majority of the patients were male with a mean age of 60 years with normal left ventricle function and slightly enlarged LA; most of them had no structural heart disease (89 %). Most of the patients were ablated for paroxysmal atrial fibrillation (see Table 1).

The average width of the posterior wall of the left atrium was 56.1 ± 7.0 mm. The average width of one esophageal position (columns A–E) was 11.2 ± 1.4 mm. The average width of the esophagus from CT and 3DRA data was 15.89 ± 4.03 and 17.13 ± 4.3 mm, respectively (for details, see Table 2).

Statistically, the most frequent position of the esophagus in the CT models was B ($n = 26$, 46.4 %), and in the 3DRA models, the most frequent position was C ($n = 21$, 37.5 %). Statistically, the least frequent position in the CT and 3DRA models was E ($n = 1$, 1.8 %, $n = 3$, 5.4 %, respectively) (see Fig. 2).

Comparing CT and 3DRA models for each patient revealed a maximum shift of the esophagus of three positions (from B to E, 33.6 mm), and the average shift of the esophagus was 0.857 ± 0.766 of the position (9.6 mm). A shift of the

Table 1 Patient characteristics

Patient characteristics	
Number of patients	56
Age	59.80 ± 9.59
Male	44 (78.57 %)
Ejection fraction of left ventricle	57.12 ± 7.95 %
Size of the left atrium (from transthoracic ultrasound of the heart)	45.20 ± 6.00 mm
Body mass index	29.15 ± 4.33
Structural heart disease	6 (10.71 %)
Hypertension	27 (48.21 %)
Paroxysmal atrial fibrillation	30 (53.57 %)
Persistent atrial fibrillation	25 (44.64 %)
Long standing persistent atrial fibrillation	1 (1.79 %)

esophagus between the CT and 3DRA model of one position (11.2 mm) was detected in 44.6 % of patients; there was a shift of the esophagus of two positions (22.4 mm) in 17.9 % of the patients and a shift of the esophagus of three positions (33.6 mm) in 1.8 % of patients. For examples of esophageal displacement, see Fig. 3. A statistical comparison of the position of the esophagus to the left atrium in 3DRA and CT models for each individual patient found a statistically significant difference ($p = 0.001$). The time interval between the 3DRA and CT examinations averaged 20 ± 26 days (from 1 to 132 days, median of 7.5 days). In eight patients (14.3 %), CT was performed the day before the catheter ablation, and in this subset of patients, the average interval from CT to ablation was 22 h and 3 min. The average shift of the esophagus in this group of patients was 0.875 ± 0.78 of the position; there was a shift of the esophagus of one position in 37.5 % of the patients and two positions in 25 % of patients. In this group of patients, there was no statistically significant difference between the positions of the esophagus in CT and 3D rotational angiography.

The acquisition of data went without major complications. The average duration of rapid ventricle stimulation was 7.4 s. Hypotension during rapid ventricle stimulation was tolerated very well without subjective or objective problems, probably due to the preserved ejection fraction. No patient developed ventricular fibrillation or another malignant arrhythmia as a consequence of rapid ventricular stimulation. Direct left atrial contrast agent injection has no complications. No patient had aspiration of oral contrast agents or other complications associated with the use of contrast agents dosed orally. No patient developed an atrioesophageal fistula or other esophageal complication.

Table 2 Average width of the esophagus from CT and 3DRA

Position of measurement	Average width of esophagus from CT (mm)	Average width of esophagus from 3DRA (mm)
Superior	15.23 ± 3.74	15.11 ± 5.42
Mid	15.70 ± 4.14	15.45 ± 4.90
Inferior	15.89 ± 4.20	14.41 ± 2.58
Average 1–3	15.61 ± 4.03	14.99 ± 4.3

5 Discussion

The results of our work confirmed the findings of previous studies that determined that the esophagus is typically located behind the left side of the left atrium [7, 13]. The most notable finding of our study was the statistically significant difference between the position of the esophagus in the preprocedural view using CT and the position at the beginning of the ablation as measured by 3DRA. In only 35.7 % of patients was the esophagus in the same location at 3DRA during ablation as it had been in the preprocedural CT. A change of location of the esophagus of at least one position (more than 11 mm) was shown in the rest of the patients. We tried to verify whether a smaller interval of time between CT examination and ablation contributed to a better prediction of the position of the esophagus. For an average interval of just 22 h and 3 min between CT examination and actual ablation in a subgroup of eight patients, the results were comparable—an average shift of 0.875 ± 0.78 of the position, a shift of one position in 37.5 % of patients, and shift of two positions in 25 % of patients. Given the small number of patients in this group ($n = 8$), this difference did not prove to be statistically significant, but its absolute value was entirely comparable with the findings for the entire group of patients (average shift of 0.857 ± 0,77, shift of one position in 44.6 % and two positions in 17.9 % of patients, $n = 56$).

Our findings confirm the results of the work of Daoud et al. [15], which showed a significant shift of the esophagus in 13 % of patients. For the remaining patients, CT was able to correctly predict the position of the esophagus defined into three groups as “left, middle, and right.” However, a shift of the esophagus of more than half its width was detected in 44 % of these patients, which seemed clinically significant. This group accounts for 44.6 % of patients with a shift in the esophagus of one position in our work. Additionally, the work of Nolker et al. [16] demonstrated a poor correlation between preprocedural CT of the heart and periprocedural 3DRA of the left atrium and esophagus in a relatively small sample of patients ($n = 14$). The last study showing significant movement of the esophagus was the work of Kobza et al. [20]. The authors found in small cohort of patients ($n = 18$) that reliance on CT images, even if acquired within 24 h before ablation, does not ensure adequate intraprocedural localization of the

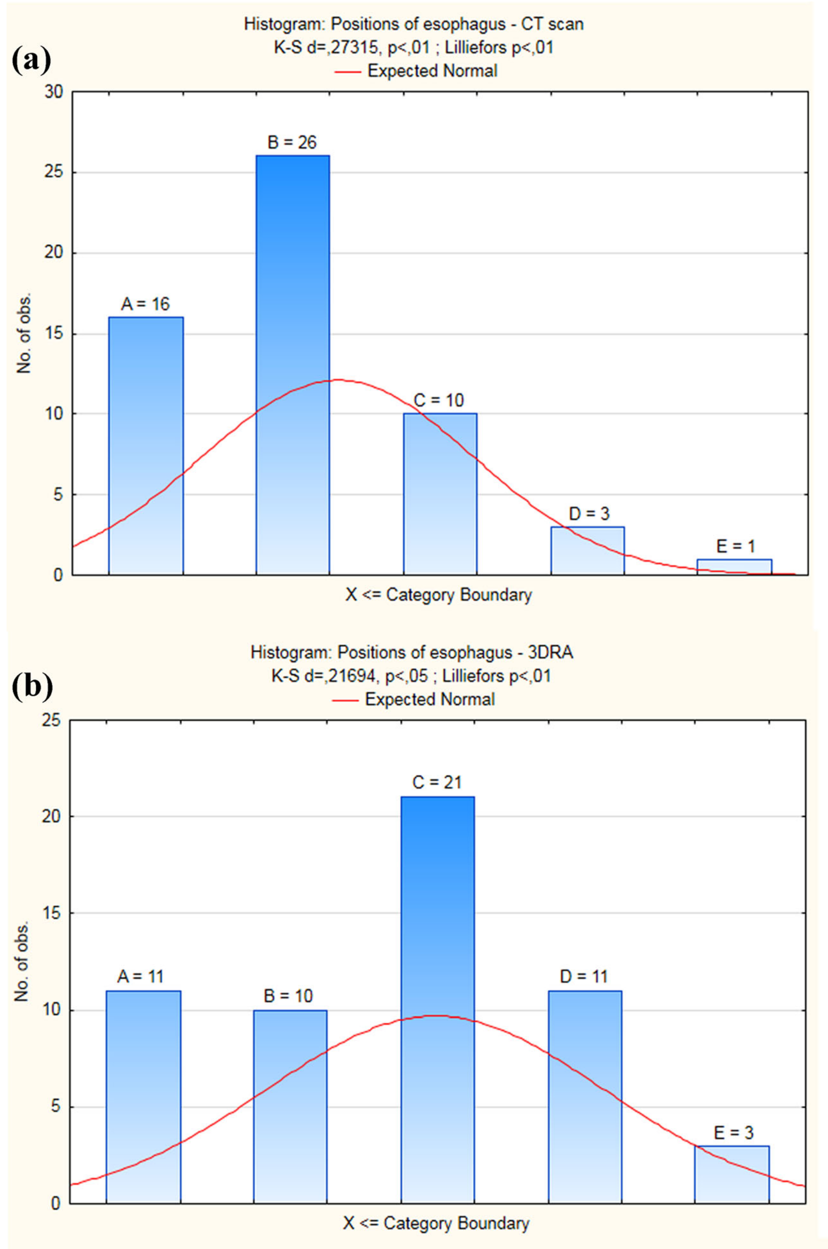

Fig. 2 Graph **a** shows the distribution of esophagus positions from the CT of the heart. Graph **b** shows the distribution of esophagus positions from the 3DRA of the left atrium and esophagus

esophagus. Sixty-six percent of patients had an average shift of the esophagus greater than 10 mm.

Several previous studies have shown a relatively stable long-term position of the esophagus [11–13]. For these studies, determining the position of the esophagus during ablation was performed by introducing an electrophysiological catheter or naso-gastric tube that did not capture the entire lumen of the esophagus. Consistent with the results of our work and those of Daoud et al. [15], this work demonstrated "disconcordance," i.e., a significant change in the position of the esophagus, between the preprocedural and periprocedural view in approximately 10 % of cases. The work of Kennedy et al. [14] demonstrated a significant shift in the position of the esophagus over 7 months in 17 % of their sample. The remainder of patients demonstrated no shift in the position of the esophagus. The apparent discrepancy between the results of the work of Kennedy et al. and our work is, in our opinion, due to the more precise determination of the positions of the esophagus behind the posterior wall of the left atrium. In our work, we had five positions A–E, whereas Kennedy evaluated only three positions—left, center, and right. The percentage of patients with an esophageal shift of two or more positions in our study was 19.7 %, which corresponds to a 17 % esophageal shift of at least ≥1 cm in Kennedy's work.

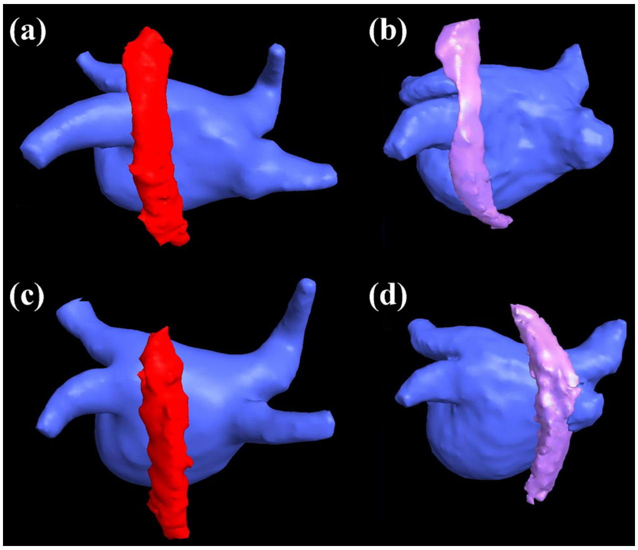

Fig. 3 Examples of the shift of the esophagus between CT and 3DRA models, posteroanterior view. **a** Minimum shift of the esophagus (CT model, column B), **b** minimum shift of the esophagus (3DRA model, column B), **c** maximum shift of the esophagus (CT model, column B), and **d** maximum shift of the esophagus (3DRA model, column E)

3DRA oh the left atrium is simple and safe method for imaging of the esophagus. Despite the fact that the patients were in light sedation, no complications were noted. No instances of aspiration of oral contrast were observed.

A limitation of our study is that we compared the whole esophagus as shown in the CT of the heart with the contrast-imaged lumen of the esophagus in 3DRA; thus, we compared a static structure with a recording of the swallowing of a contrast agent. However, the difference measured between the width of the esophagus in CT and 3DRA was negligible (average width 15.89 ± 4.03 and 17.13 ± 4.3 mm, respectively). Swallowing the contrast agent for 3DRA "compensates" to a certain extent for the thickness of the muscle of the esophagus (which is usually <5 mm [8]), and the resulting rotational esophagogram approximates the actual width of the esophagus in CT.

Another limitation is the possibility that swallowing a barium oral contrast agent can stimulate motility of the esophagus and increase its mobility. However, routine examinations of esophageal motility have failed to demonstrate this effect [21]. We also did not find any increase of the mobility of the esophagus after repeated swallowing of a contrast agent. This result is based on several esophagograms performed during catheter ablation of atrial fibrillation within our unpublished project called "Short-term mobility of the esophagus."

The question is how much the data are useful and necessary in case of the mobility of the esophagus during EP procedure. Available published data are confusing and still not clear. Sherzer et al. [22] demonstrated the stable position of the esophagus with minimal displacement during the procedure. Contrarily, Daoud et al. and Good et al. [15, 23] show significant mobility of the esophagus during the procedure. Our unpublished data (mentioned above) show only minimal nonsignificant movement of the esophagus during ablation. We hope that periprocedural imaging of the esophagus can contribute to the safety of the procedure.

The investigators cannot exclude the possibility that differences in the procedures used to determine the position of the esophagus did not affect the observations, e.g., CT versus 3DRA, different arm positions, medications, post-absorptive state, etc. However, according to our knowledge, we believe that these factors could not be relevant.

6 Conclusion

The position of the esophagus in relationship to the left atrium is variable. The most common position of the esophagus is behind the middle and to the left side of the posterior wall of left atrium; the least common position is behind the right-sided pulmonary veins. A timescale of several days to weeks resulted in a significant change in the position of the esophagus in relationship to LA. A preprocedural view of the esophagus obtained more than 22 h before ablation did not reflect the actual position of the esophagus during the procedure.

Acknowledgments This work was supported by the Grant of the European Regional Development Fund—Project FNUSA-ICRC (No. CZ.1.05/1.1.00/02.0123).

Compliance with ethical standards The study received the approval from the ethics committee of our institution.

Competing interests The authors declare that they have no conflicts of interest.

References

1. Calkins, H., Kuck, K. H., Cappato, R., Brugada, J., Camm, A. J., Chen, S. A., et al. (2012). 2012 HRS/EHRA/ECAS expert consensus statement on catheter and surgical ablation of atrial fibrillation: recommendations for patient selection, procedural techniques, patient management and follow-up, definitions, endpoints, and research trial design. *Journal of Interventional Cardiac Electrophysiology, 33*(4), 171–257.
2. Haïssaguerre, M., Jaïs, P., Shah, D. C., Takahashi, A., Hocini, M., Quiniou, G., et al. (1998). Spontaneous initiation of atrial fibrillation by ectopic beats originating in the pulmonary veins. *New England Journal of Medicine, 339*(10), 659–666.
3. Haïssaguerre, M., Jaïs, P., Shah, D. C., Gencel, L., Pradeau, V., Garrigues, S., et al. (1996). Right and left atrial radiofrequency catheter therapy of paroxysmal atrial fibrillation. *Journal of Cardiovascular Electrophysiology, 7*(12), 1132–1144.
4. Cappato, R., Calkins, H., Chen, S. A., Davies, W., Iesaka, Y., Kalman, J., et al. (2009). Prevalence and causes of fatal outcome

in catheter ablation of atrial fibrillation. *Journal of the American College of Cardiology, 53*(19), 1798–1803.

5. Cappato, R., Calkins, H., Chen, S. A., Davies, W., Iesaka, Y., Kalman, J., et al. (2010). Updated worldwide survey on the methods, efficacy, and safety of catheter ablation for human atrial fibrillation. *Circulation. Arrhythmia and Electrophysiology, 3*(1), 32–38.
6. Ghia, K. K., Chugh, A., Good, E., Pelosi, F., Jongnarangsin, K., Bogun, F., et al. (2009). A nationwide survey on the prevalence of atrioesophageal fistula after left atrial radiofrequency catheter ablation. *Journal of Interventional Cardiac Electrophysiology, 24*(1), 33–36.
7. Cury, R. C., Abbara, S., Schmidt, S., Malchano, Z. J., Neuzil, P., Weichet, J., et al. (2005). Relationship of the oesophagus and aorta to the left atrium and pulmonary veins: implications for catheter ablation of atrial fibrillation. *Heart Rhythm, 2*(12), 1317–1323.
8. Lemola, K., Sneider, M., Desjardins, B., Case, I., Han, J., Good, E., et al. (2004). Computed tomographic analysis of the anatomy of the left atrium and the oesophagus: implications for left atrial catheter ablation. *Circulation, 110*(24), 3655–3660.
9. Ejima, K., Shoda, M., Yagishita, D., Futagawa, K., Yashiro, B., Sato, T., et al. (2010). Image integration of three-dimensional cone-beam computed tomography angiogram into electroanatomical mapping system to guide catheter ablation of atrial fibrillation. *Europace, 12*(1), 45–51.
10. Orlov, M. V., Hoffmeister, P., Chaudhry, G. M., Almasry, I., Gijsbers, G. H., Swack, T., et al. (2007). Three-dimensional rotational angiography of the left atrium and oesophagus—a virtual computed tomography scan in the electrophysiology lab? *Heart Rhythm, 4*(1), 37–43.
11. Kobza, R., Auf der Maur, C., Kurtz, C., Hoffmann, A., Allgayer, B., & Erne, P. (2007). Oesophagus imaging for radiofrequency ablation of atrial fibrillation using a dual-source computed tomography system: preliminary observations. *Journal of Interventional Cardiac Electrophysiology, 19*(3), 167–170.
12. Piorkowski, C., Hindricks, G., Schreiber, D., Tanner, H., Weise, W., Koch, A., et al. (2006). Electroanatomic reconstruction of the left atrium, pulmonary veins, and oesophagus compared with the "true anatomy" on multislice computed tomography in patients undergoing catheter ablation of atrial fibrillation. *Heart Rhythm, 3*(3), 317–327.
13. Kottkamp, H., Piorkowski, C., Tanner, H., Kobza, R., Dorszewski, A., Schirdewahn, P., et al. (2005). Topographic variability of the oesophageal left atrial relation influencing ablation lines in patients with atrial fibrillation. *Journal of Cardiovascular Electrophysiology, 16*(2), 146–150.
14. Kennedy, R., Good, E., Oral, H., Huether, E., Bogun, F., Pelosi, F., et al. (2008). Temporal stability of the location of the oesophagus in patients undergoing a repeat left atrial ablation procedure for atrial fibrillation or flutter. *Journal of Cardiovascular Electrophysiology, 19*(4), 351–355.
15. Daoud, E. G., Hummel, J. D., Houmsse, M., Hart, D. T., Weiss, R., Liu, Z., et al. (2008). Comparison of computed tomography imaging with intraprocedural contrast oesophagram: implications for catheter ablation of atrial fibrillation. *Heart Rhythm, 5*(7), 975–980.
16. Nölker, G., Gutleben, K. J., Marschang, H., Ritscher, G., Asbach, S., Marrouche, N., et al. (2008). Three-dimensional left atrial and oesophagus reconstruction using cardiac C-arm computed tomography with image integration into fluoroscopic views for ablation of atrial fibrillation: accuracy of a novel modality in comparison with multislice computed tomography. *Heart Rhythm, 5*(12), 1651–1657.
17. Lehar, F., Starek, Z., Jez, J., Novak, M., Wolf, J., Kruzliak, P., et al. (2013). Rotational atriography of left atrium—a new imaging technique used to support left atrial radiofrequency ablation. *Interv Akut Kardiol, 12*(4), 184–189.
18. Li, J. H., Haim, M., Movassaghi, B., Mendel, J. B., Chaudhry, G. M., Haffajee, C. I., et al. (2009). Segmentation and registration of three-dimensional rotational angiogram on live fluoroscopy to guide atrial fibrillation ablation: a new online imaging tool. *Heart Rhythm, 6*(2), 231–237.
19. Thiagalingam, A., Manzke, R., D'Avila, A., Ho, I., Locke, A. H., Ruskin, J. N., et al. (2008). Intraprocedural volume imaging of the left atrium and pulmonary veins with rotational X-ray angiography: implications for catheter ablation of atrial fibrillation. *Journal of Cardiovascular Electrophysiology, 19*(3), 293–300.
20. Kobza, R., Schoenenberger, A. W., & Erne, P. (2009). Esophagus imaging for catheter ablation of atrial fibrillation: comparison of two methods with showing of esophageal movement. *Journal of Interventional Cardiac Electrophysiology, 26*(3), 159–164.
21. Summerton, S. L. (2005). Radiographic evaluation of oesophageal function. *Gastrointestinal Endoscopy Clinics of North America, 15*(2), 231–242.
22. Sherzer, A. I., Feigenblum, D. Y., Kulkarni, S., Pina, J. W., Casey, J. L., Salka, K. A., et al. (2007). Continuous nonfluoroscopic localization of the esophagus during radiofrequency catheter ablation of atrial fibrillation. *Journal of Cardiovascular Electrophysiology, 18*(2), 157–160.
23. Good, E., Oral, H., Lemola, K., Han, J., Tamirisa, K., Igic, P., et al. (2005). Movement of the esophagus during left atrial catheter ablation for atrial fibrillation. *Journal of the American College of Cardiology, 46*(11), 2107–2110.

ESC European Society of Cardiology

Europace (2017) **19**, 1310–1316
doi:10.1093/europace/euw187

CLINICAL RESEARCH
Ablation for atrial fibrillation

Three-dimensional rotational angiography of the left atrium and the oesophagus: the short-term mobility of the oesophagus and the stability of the fused three-dimensional model of the left atrium and the oesophagus during catheter ablation for atrial fibrillation

Zdenek Starek[1,2]*, Frantisek Lehar[1,2], Jiri Jez[1,2], Martin Scurek[1,2], Jiri Wolf[1,2], Tomas Kulik[1,2], Alena Zbankova[1,2], and Miroslav Novak[1,2]

[1]International Clinical Research Center, 1st Department of Internal Medicine—Cardioangiology, St. Anne's University Hospital Brno, Pekařská 53, 656 91 Brno, Czech Republic; and [2]Faculty of Medicine, Masaryk University, Kamenice 5, 625 00 Brno, Czech Republic

Received 29 February 2016; accepted after revision 28 May 2016; online publish-ahead-of-print 2 December 2016

Aims The objective of this study was to evaluate the mobility of the oesophagus and the stability of the three-dimensional (3D) model of the oesophagus using 3D rotational angiography (3DRA) of the left atrium (LA) and the oesophagus, fused with live fluoroscopy during catheter ablation for atrial fibrillation.

Methods and results From March 2015 to September 2015, 3DRA of the LA and the oesophagus was performed in 33 patients before catheter ablation for atrial fibrillation. Control contrast oesophagography was performed every 30 min. The positions of the oesophagograms and the 3D model of the LA and the oesophagus were repeatedly measured and compared with the spine. The average shift of the oesophagus ranged from 2.7 ± 2.2 to 5.0 ± 3.5 mm. The average real-time oesophageal shift ranged from 2.7 ± 2.2 to 3.8 ± 3.4 mm. No significant shift was detected until the 90th minute of the procedure. The average shift of the 3D model of the LA and the oesophagus ranged from 1.4 ± 1.8 to 3.3 ± 3.0 mm (right–left direction) and from 0.9 ± 1.2 to 2.2 ± 1.3 mm (craniocaudal direction). During the 2 h procedure, there were no significant shifts of the model.

Conclusion During catheter ablation for atrial fibrillation, there is no significant change in the position of the oesophagus until the 90th minute of the procedure and no significant shift in the 3D model of the LA and the oesophagus. The 3D model of the oesophagus reliably depicts the position of the oesophagus during the entire procedure.

Keywords 3D Rotational angiography of the left atrium and oesophagus • Image integration • Catheter ablation of atrial fibrillation • Mobility of the oesophagus • Atrioesophageal fistula

Introduction

Radiofrequency ablation for atrial fibrillation is a recognized treatment for patients with drug refractory atrial fibrillation.[1] Catheter ablation involves the isolation of the pulmonary vein by placing circular radiofrequency lesions around the ostium of the pulmonary veins[2] in patients with persistent atrial fibrillation; these lesions can be supplemented by additional ablations, such as linear lesions in the left atrium (LA)[3] or ablation of the fractionated atrial potentials.[4] The emergence of an atrioesophageal fistula is a rare, but very

* Corresponding author. Tel: +420543182187; fax: +420543182205. *E-mail address*: zdenek.starek@fnusa.cz

What's new?

- During catheter ablation for atrial fibrillation, there is no significant change in the position of the oesophagus up to 90th minute of the procedure.
- During procedure lasting up to 120 min, the average shift of the oesophagus is up to 5 mm.
- There is no significant shift in the 3D model of the left atrium and the oesophagus during the 2 h procedure.
- Three-dimensional model of the oesophagus created at the beginning of the catheter ablation for atrial fibrillation reliably reflected the position of the oesophagus during the entire procedure.

serious complication.[5] Atrioesophageal fistulas comprise <0.1% of all complications[6] but are fatal in 70–80% of cases[7] and are the cause of 16% of deaths associated with catheter ablation for atrial fibrillation.[5] Atrioesophageal fistulas are caused by the application of radiofrequency energy along the posterior left atrial wall, leading to damage of the oesophagus, which is in close contact with this area.[8,9]

The visualization of the relative position of the oesophagus and LA can contribute to a reduced risk of oesophageal damage. The mapping of the LA guided by 3D X-ray models of the LA provides objective information about the existing anatomy of the LA and the oesophagus.[10] Contrast-enhanced computed tomography (CT) is a standard method used for the 3D imaging of the LA and the oesophagus.[11] The 3D rotational angiography (3DRA) of the LA is a new method equivalent to CT.[12–15] The results of the studies involving the preprocedural imaging of the position of the oesophagus by CT indicated that the oesophagus is a mobile structure, and preprocedural imaging of the position of the oesophagus, in many cases, does not reflect the position of the oesophagus during ablation.[16,17] A single image of the oesophagus obtained at the beginning of the ablation procedure may not be valid for the duration of the procedure, and the position of the oesophagus relative to the LA can vary significantly during an ablation procedure that lasts several hours.[16,18] The aim of our work was to verify the applicability of the periprocedural 3DRA of the LA and the oesophagus for imaging of the oesophagus during catheter ablation for atrial fibrillation. We sought to verify the short-term mobility of the oesophagus and the stability of the 3D model of the oesophagus fused with live fluoroscopy during catheter ablation for atrial fibrillation.

Methods

Patient population

This prospective study enrolled a group of 33 consecutive patients who were referred for catheter ablation for atrial fibrillation. In all patients, the ablation was carried out with the support of the 3DRA of the LA with contrasting imaging of the oesophagus. Patients with a history of iodine allergy or with impaired renal function [glomerular filtration rate <45 mL/s/1.73 m^2, as estimated using the Modification of Diet in Renal Disease (MDRD) formula] were excluded from the study. The institutional review board approved the study protocol, and written informed consent was obtained from all patients.

Rotational angiography imaging

Imaging was carried out using the Allura Xper FD 10 X-ray system (Philips Medical Systems, Inc., Best, The Netherlands) according to a left atrial protocol. The basic method of 3DRA involves the injection of contrast into the LA and the acquisition of the rotational image. After the opacification of the LA and the pulmonary veins, the C-arm was isocentrically rotated over 240° (120° right anterior oblique to 120° left anterior oblique) over 4.1 s with an X-ray acquisition speed of 30 frames per second. During rotational imaging, the patients were placed in a supine position with their arms in a natural position along the body, and a normal breathing was maintained.

Isocentring of the LA was obtained from the anteroposterior (AP) and left lateral X-ray views. The injection of contrast agent was carried out using a standard power injector (Mark V, Medrad, Inc., Indianola, PA, USA).[19] A pigtail catheter was introduced through the transseptal sheath (Agilis NxT 8.5F, St. Jude Medical, St. Paul, MN, USA) into the LA. After the reduction of the cardiac output via rapid stimulation of the ventricles (frequency 230/min), the application of the contrast agent was initiated, and after a delay of 2 s, we commenced the rotation of the C-arm.[20] In total, 60 mL of contrast agent was injected at an injection velocity of 15 mL/s.

The oesophagus was visualized using the oral administration of 20–30 mL of barium sulphate contrast agent (Micropaque, Guerbet, Roissy, France) during the 3DRA of the LA.[12]

The 3DRA model of the LA was reconstructed offline using the EP Navigator workstation (EP Navigator 3.0, Philips Healthcare, Best, The Netherlands). Automatic segmentation was supplemented with manual segmentation when necessary. The 3D model of the oesophagus was manually segmented using the same workstation. The 3D model of the LA and the oesophagus was automatically registered using live fluoroscopy and was used for the navigation of the catheters during the entire procedure.

Current imaging of the position of the oesophagus

To verify the position of the oesophagus during the procedure, contrast oesophagography was performed approximately every 30 min. The oesophagus was opacified using the oral administration of 20–30 mL of barium sulphate contrast agent, and the localization of the oesophagus was recorded on an X-ray screen with the 3D model of the LA and the oesophagus (*Figure 1*).

Quantitative imaging analysis

For the purpose of our current study, we set a shift of the analysed structure of <5 mm as negligible. According to our experience, a shift of <5 mm is not significant to the operator during atrial fibrillation ablation. Data were evaluated offline by two experienced investigators. In an independent blinded manner, these investigators determined the positions of the oesophagus relative to the LA and measured the positions of the oesophagus and the LA. Interindividual variability was calculated.

At the beginning of the procedure, the positions of the 3D model of the oesophagus and the LA were determined in all patients immediately following the 3DRA and the fusion of the 3D models with live fluoroscopy. The positions of the oesophagus during contrast oesophagography were then determined. The position of the 3D model of the LA and the oesophagus was determined every 30 min during oesophagography. Measurements were performed using GIMP (a free program

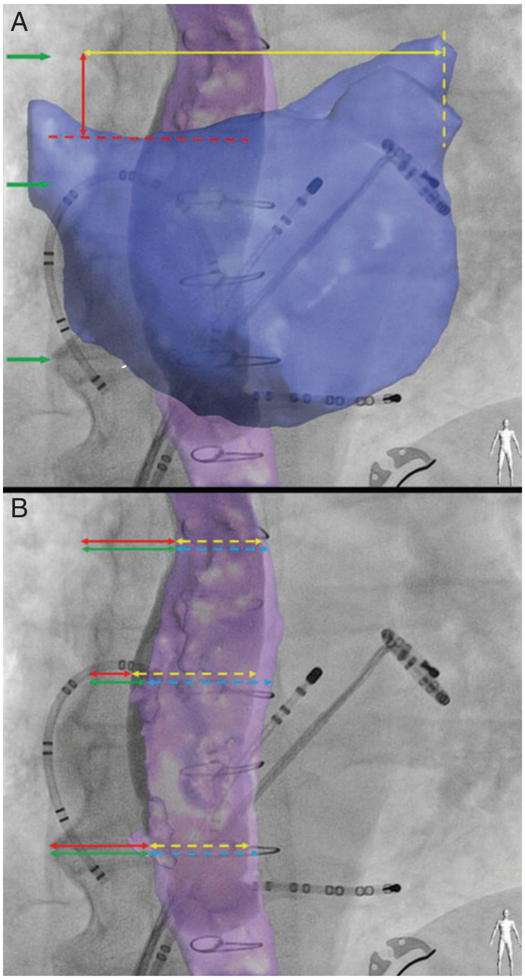

Figure 1 Methodology of the measurements. (*A*) A complex image of the live fluoroscopy screen showing the X-ray image of the heart and the chest in an AP projection with a fused model of the LA and the oesophagus. The green arrows indicate the locations of the relevant vertebra against which each measurement of the position of the oesophagus was carried out. The yellow arrow indicates the measurement of the position of the 3D model of the LA from the nearest vertebra in the right–left direction. The red arrow indicates the measurement of the position of the 3D model of the LA in the craniocaudal direction. (*B*) The measurement of the position of the oesophagograms and the 3D model of the oesophagus. Red arrows indicate the measurement of the position of the oesophagus (oesophagograms) relative to the nearest vertebra. Green arrows indicate the measurement of the position of the 3D model of the oesophagus relative to the nearest vertebra. Yellow arrows indicate the measurement of the width of the oesophagus (oesophagogram). Blue arrows indicate the measurement of the width of a 3D model of the oesophagus. Measurements were carried out at three levels (see *A*). The 3D model of the LA is hidden in *B* for greater clarity. (*B*) The minimum shift of the oesophagus after 60 min by 2.3 mm at the top position, by 1.4 mm at the central position, and by 0.7 mm at the lower position. We observed a very high correlation between the actual position of the oesophagus displayed on the oesophagogram and the initial position of the oesophagus displayed on the 3D model of the oesophagus from 3DRA registered using live fluoroscopy.

that enables measurements of JPG images, version 2.8.14, http://www.gimp.org/). The positions of both the 3D model of the oesophagus and the contrast oesophagograms were measured in the superior, middle, and inferior segments of the oesophagus; the spine served as a stationary reference structure. The superior segment of the oesophagus corresponded to the highest level of the 3D model of the LA, the inferior segment corresponded to the bottom level of the LA model, and the middle segment corresponded to the level between the upper and lower segments. The three vertebrae that were closest to the LA model created using the 3DRA were identified. The upper segment of the oesophagus was measured at the level of the upper corner of the lateral edge of the upper vertebra, the middle segment of the oesophagus was measured at the middle of the lateral edge of the middle vertebra, and the lower segment was measured at the level of the lower corner of the lateral edge of the lower vertebra. If the model of the oesophagus was not optimally depicted and oesophageal contours were not shown throughout the entire course of the oesophagus, we manually refilled the contours of the oesophagus before performing measurements. We measured the distances from the vertebrae to the lateral wall of the oesophagus and the width of the oesophagus in all segments, which allowed us to calculate the position of the centre of the oesophagus in every segment. Furthermore, the position of the 3D model of the LA and the oesophagus, relative to the closest vertebrae in the AP projection, was measured. We calculated the right–left shift of the model as the distance between the lateral upper corner of the first vertebra visible above the 3D model of the atrium and the point at which the left superior pulmonary vein and the LA auricle contour intersected. We measured the craniocaudal movement of the 3D model as the distance between the lateral upper corner of the first vertebra visible above the 3D model and the lowest point of the roof of the LA. For detailed measurements, see *Figure 1*.

Each measurement was repeated three times to reduce intra-individual variability, and the result was the average of these three measurements. The average of the two results measured by the two investigators was used for statistical analysis. In this way, the resulting distances between the oesophagus and the 3D model of the LA from the spine were recalculated into the actual distances in millimetres using a constant obtained by recalculating the known size of the ablation catheter with a diameter of 7 French.

Initially, we evaluated the oesophageal shift or the short-term mobility of the oesophagus during ablation [the shift of the current position of the oesophagus (actual contrast oesophagograms) in the right–left direction towards the input position]. The position of the 3D model of the oesophagus at the first measurement immediately after the fusion with live fluoroscopy was considered to be the entry position of the oesophagus.

Secondly, we calculated the real-time oesophageal shift—the shift of the oesophagus relative to the 3D oesophagus model in real time (the difference between the actual position of the oesophagus obtained by the contrast oesophagogram and the position of the 3D model of the oesophagus fused with live fluoroscopy during a specific measurement, which reflects any possible deviation of the position of the 3D model from the optimally registered model at the beginning of the examination).

Furthermore, the shift of the 3D model of the LA and the oesophagus was evaluated (the stability of the fused 3D model during ablation). The position of the 3D model during the first measurement immediately after the fusion with live fluoroscopy was taken as the input position of the correctly fused model. The right–left and craniocaudal movements of the model of the LA were evaluated, and the change in the position of the 3D model between individual measurements during the procedure was recorded. For details, see *Table 2*.

Catheter ablation

Ablation procedures were performed in a standard manner under light sedation (boluses of i.v. fentanyl and i.v. diazepam) using an irrigated tip catheter guided by the 3D electroanatomical mapping system EnSite Velocity (St. Jude Medical). Circumferential PV isolation confirmed using the 20-pole circumferential mapping catheter provided the basis for all procedures involving paroxysmal atrial fibrillation. Additional roof and mitral isthmus lines and coronary sinus ablations were performed in cases of persistent atrial fibrillation. Oesophageal imaging was taken into account for the creation of ablation lines in the posterior wall of the LA.

Ethics

This study complies with the Declaration of Helsinki. The research protocol was approved by the locally appointed ethics committee. The informed consent of the subjects has been obtained.

Statistical analysis

The baseline characteristics of the patients, the shift of the oesophagus, and the 3D oesophagus model in real time were analysed descriptively. Continuous variables are presented as the arithmetic means with standard deviations, and categorical variables are presented as the number (%) of patients. A one-sample *t*-test or its nonparametric alternative (Wilcoxon signed rank test), based on the distribution of data, was used to test whether a shift was significantly lower than 5 mm in each position and at each time point of measurement (30, 60, 90, and 120 min into the procedure). The results with *P*-values <0.05 were considered statistically significant.

Results

From March 2015 to September 2015, 33 patients undergoing catheter ablation of the LA were examined using 3DRA of the LA and the oesophagus. The majority of patients were males with an average age of 60 years who presented with no structural heart disease, a normal left ventricle function, and a slightly enlarged LA (see *Table 1*).

The average duration of catheter ablation was 112 ± 43 min, and an average of three contrasting oesophagograms were performed (range: 1–4). On average, contrasting oesophagograms were performed every 33 ± 10 min. The total execution time of the 3DRA of the LA and the oesophagus including the manual segmentation of the oesophagus was 9.92 min.

All measurements were not performed in all patients. Unfortunately, not all of the dimensions were measurable (unclear outline of the vertebra, oesophagus model non-segmented up to the level of the vertebra, overlap of the oesophagus model and vertebra). The number of measured values decreases with the increasing time of the procedure because some procedures had a shorter duration and were already complete at the time of some measurements (e.g. 120 min). A total of 13% of the values were unmeasurable during the study; for results of measured values, see *Table 2*.

Interobserver variability was 1.8 ± 1.5 mm. Intraobserver variability was 1.5 ± 1.3 mm.

The average width of the oesophagus was 18.8 ± 5.8 mm at the superior position, 19.5 ± 6.1 mm at the medium position, and 16.9 ± 4.6 mm at the inferior position.

The average shift of the position of the oesophagus during catheter ablation (average shift of the contrast oesophagograms during the individual measurements for superior, medium, and inferior positions of the measurement) ranged from 2.7 ± 2.2 to 5.0 ± 3.5 mm. The maximum shift of the oesophagus was 11.9 mm, and the minimum shift was 0.1 mm. A ≥3 mm shift of the oesophagus was present in 44.8% of patients, and a shift of the oesophagus ≥8 mm was present in 5% of the patients. The shift of the oesophagus during the procedure was significantly lower than 5 mm for measurements at 30, 60, and 90 min.

The average real-time oesophageal shift (shift of the virtual model of the oesophagus fused with live fluoroscopy at a given time in relation to the actual position of the oesophagus at the same measurement for the superior, medium, and inferior positions of the measurement) ranged from 2.7 ± 2.2 to 3.8 ± 3.4 mm. The real-time oesophageal shift was significantly lower than 5 mm for all measurements at 30, 60, 90, and 120 min with the exception of the measurement at 120 min in the inferior position.

The average shift of the 3D model of the LA and the oesophagus in the right–left direction ranged from 1.4 ± 1.8 to 3.3 ± 3.0 mm, and the shift in the craniocaudal direction ranged from 0.9 ± 1.2 to 2.2 ± 1.3 mm. The maximum shift of the 3D model was 11 mm in the right–left direction and 6.1 mm in the craniocaudal direction, and the minimum shift was 0 mm in both directions. A shift of the 3D model in the right–left direction ≥3 mm was present in 28.7% of patients, and a shift of ≥8 mm was present in 4% of patients. A shift of the 3D model in the craniocaudal direction ≥3 mm was present in 11.9% of patients, and a shift of ≥8 mm was not detected in any patient. The shift of the 3D model during the procedure was significantly lower than 5 mm for all measurements.

Details of the measurements are summarized in *Table 2*. For examples of the movement of the oesophagus and the 3D model of the LA and the oesophagus, see *Figures 1* and *2*.

Table 1 Patient characteristics

Patient characteristics	
Number of patients	33
Age	61.73 ± 8.02
Male	25 (75.76%)
Ejection fraction of left ventricle	57.09 ± 8.57
Size of LA	42.59 ± 5.74
Body mass index	27.46 ± 3.37
Structural heart disease	6 (18.18%)
Hypertension	14 (42.42%)
Paroxysmal atrial fibrillation	24 (75.00%)
Persistent atrial fibrillation	8 (25.00%)
Long-standing, persistent atrial fibrillation	1 (3.03%)

Discussion

Our work yielded three major results. The first finding was that the oesophagus is a relatively stable structure within a few hours of the ablation procedure; its position in the posterior mediastinum relative to the heart does not significantly change. The non-significant results of the measurements at 120 min are probably due to the

Table 2 **Oesophageal shift, real-time oesophageal shift, and 3D model shift**

Oesophageal shift, position superior (mm)	30 min N = 31	3.5 ± 2.3 (P = 0.001)	60 min N = 29	2.7 ± 2.2 (P < 0.001)	90 min N = 26	3.2 ± 2.3 (P < 0.001)	120 min N = 13	4.2 ± 2.4 (P = 0.119)
Oesophageal shift, position medium (mm)	N = 32	3.2 ± 2.2 (P < 0.001)	N = 30	3.1 ± 1.7 (P < 0.001)	N = 27	3.4 ± 2.4 (P = 0.001)	N = 13	4.2 ± 2.3 (P = 0.107)
Oesophageal shift, position inferior (mm)	N = 29	2.9 ± 2.2 (P < 0.001)	N = 26	3.5 ± 2.4 (P = 0.002)	N = 23	3.6 ± 2.9 (P = 0.018)	N = 11	5.0 ± 3.5 (P = 0.497)
Real-time oesophageal shift, position superior (mm)	N = 31	3.2 ± 2.4 (P < 0.001)	N = 30	3.5 ± 2.7 (P = 0.003)	N = 27	3.8 ± 3.4 (P = 0.039)	N = 13	3.4 ± 2.5 (P = 0.019)
Real-time oesophageal shift, position medium (mm)	N = 32	3.2 ± 2.5 (P < 0.001)	N = 30	2.7 ± 2.2 (P < 0.001)	N = 27	3.1 ± 2.3 (P < 0.001)	N = 14	3.2 ± 2.4 (P = 0.007)
Real-time oesophageal shift, position inferior (mm)	N = 29	3.0 ± 2.3 (P < 0.001)	N = 26	3.0 ± 1.9 (P < 0.001)	N = 23	3.3 ± 2.3 (P = 0.001)	N = 12	3.5 ± 3.0 (P = 0.057)
3D model shift, craniocaudal direction (mm)	N = 31	0.9 ± 1.2 (P < 0.001)	N = 30	1.6 ± 1.0 (P < 0.001)	N = 27	2.0 ± 1.5 (P < 0.001)	N = 13	2.2 ± 1.3 (P < 0.001)
3D model shift, left–right direction (mm)	N = 31	1.4 ± 1.8 (P < 0.001)	N = 30	2.3 ± 2.1 (P < 0.001)	N = 27	3.3 ± 3.0 (P = 0.003)	N = 13	3.2 ± 2.8 (P = 0.019)

Oesophageal shift—shift of actual contrasting oesophagogram relative to the oesophageal position at the beginning of the procedure.
Real-time oesophageal shift—shift of the actual oesophageal position (contrasting oesophagogram) relative to the actual position of the 3D model of the oesophagus.
3D model shift—shift of the 3D model of the LA and oesophagus during procedure.
P-value of one-sample *t*-test to test whether the change is lower than 5 mm.

movement of the oesophagus after 2 h of surgery, as well as the small number of patients in this group (a range of 12–13 patients). With a small patient population, the average shifts ranged from 3.5 ± 3.0 to 5.0 ± 3.5 mm, which did not reach statistical significance. These results confirm the conclusions of Sherzer *et al.*,[21] who reported the stable position of the oesophagus with minimal displacement in a group of 33 patients ablated under general anaesthesia for atrial fibrillation. Our results suggest that the oesophagus behaves similarly in patients ablated under light sedation. Our study did not confirm the results of Good *et al.* or Daoud *et al.*,[18,22] which described significant mobility of the oesophagus during these procedures. The cause of this inconsistency is not clear as both works compared two contrasting oesophagograms acquired during catheter ablation for atrial fibrillation conducted under light sedation.

A second notable finding was that when the actual mobility of the oesophagus and the shift of the model of the LA and the oesophagus during the ablation procedure were evaluated, the resulting shift was virtually identical to the displacement of the oesophagus and was not statistically significant. We conclude that the 3D model of the oesophagus reliably reflected the position of the oesophagus during a 2 h procedure.

The third chief result was that the automatic fusion of the 3D model of the LA and the oesophagus resulting from rotational angiography was reliable throughout the procedure, and there was no significant shift of the model towards the patient's heart, even after more than 2 h. The reliability of the fusion of the model with live fluoroscopy was dependent on a number of factors affected by the patient's cooperation during the procedure. The cooperation of patients in whom we performed ablation under light sedation was generally very good. We can conclude that the model of the LA and the oesophagus fused with live fluoroscopy reflects the position of these structures throughout the procedure with great precision. To achieve this reliability, it is not necessary to carry out the procedure under general anaesthesia. To the best of our knowledge, no previous studies have supported this conclusion.

The total execution time of the 3DRA of the LA and the oesophagus was virtually the same as in conventional clinical procedures performed at our department.[23] Three-dimensional rotational angiography constituted 8.8% of the total catheter ablation time.

Our findings are limited by the fact that we measured the lumen of the oesophagus, not the actual oesophagus, during oesophagography. According to our data of the long-term mobility of the oesophagus[16] compared with the preprocedural CT of the heart and the oesophagus (static imaging of the oesophagus) and the periprocedural 3DRA of the LA and the oesophagus (dynamic imaging of the oesophagus during oesophagography), there were no significant differences between the oesophagogram and the CT imaging of the oesophagus. The measured difference between the width of the oesophagus during CT and 3DRA was minimal (average widths of 15.89 ± 4.03 and 17.13 ± 4.3 mm, respectively). This width was in the range of the widths of the oesophagus reported in studies of the detailed anatomy of the oesophagus and the LA using CT data (from 11 to 24 mm).[8,9,24] Swallowing the contrast agent in 3DRA appears to compensate for the thickness of the oesophageal muscle (which is usually <5 mm[8]), and the resulting oesophagogram approximates the actual oesophagus displayed by CT.

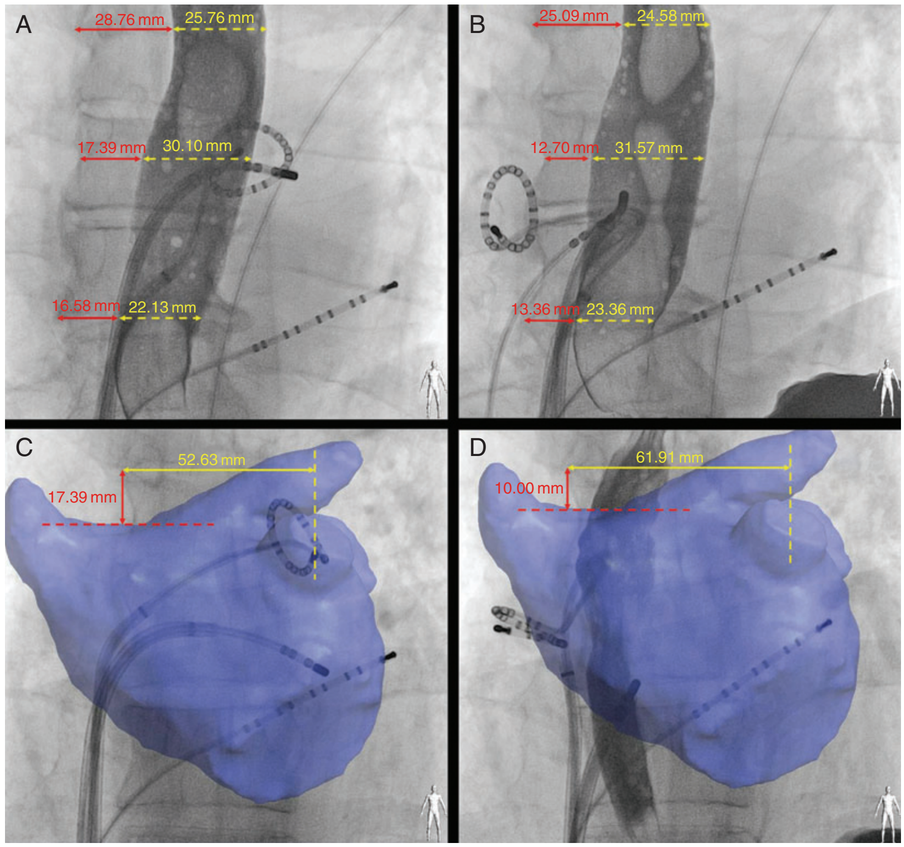

Figure 2 Examples of the shift of the position of the oesophagus and the 3D model of the LA. (*A* and *B*) The shift of the position of the oesophagus. (*A*) The position of the oesophagus *j* after 30 min of the procedure. (*B*) The position of the oesophagus after 90 min; a shift in the position of the actual oesophagus by 3.67 mm in the upper position, by 4.69 mm in the middle position, and by 3.22 mm in the lower position. (*C* and *D*) An example of the shift of the 3D model of the LA. (*C*) The 3D model at the beginning of the examination. (*D*) The 3D model after 60 min with a shift of 9.28 mm in the right–left direction and a shift of 7.39 mm in the craniocaudal direction.

The next limitation is the relatively small number of measured values in the group of 120 min measurements and the relatively large portion of unmeasurable values during the oesophagus and LA model measurements. Despite that 13% of the values of the 90 min group were unmeasurable, the results of this group are statistically significant. The combination of a small number of procedures longer than 2 h and the presence of unmeasurable values led to non-significant results in the group of patients measured at 120 min. It appears that after 120 min, the oesophagus is more mobile, but the measured values are only slightly larger and do not exceed 5 mm on average.

The imaging of the oesophagus using barium sulphate contrast agent proceeded without complications. However, the use of barium is not without risk in a possibly injured oesophageal wall, and water-soluble contrast agents such as Gastrografine (meglumine diatrizoate) could be a safer alternative if available.

The final limitation of this study is the possibility that swallowing the barium contrast agent could stimulate the motility of the oesophagus and increase its mobility. However, this effect has not been demonstrated during the routine investigations of oesophageal mobility,[25] and our results did not indicate an increased mobility of the oesophagus due to the repeated swallowing of the contrast agent.

Conclusion

There was no significant change in the position of the oesophagus during the ablation procedure lasting up to 90 min. During procedures lasting up to 120 min, the average shift of the oesophagus was up to 5 mm. During the entire procedure, there was no significant shift in the 3D model of the LA and the oesophagus created using 3DRA, which was automatically fused with live fluoroscopy at the beginning of the procedure. The 3D model of the LA and the oesophagus fused with live fluoroscopy was very stable during the procedure. The 3D model of the oesophagus created at the beginning of the catheter ablation for atrial fibrillation reliably reflected the position of the oesophagus during the entire procedure and enabled us to monitor the position of the oesophagus behind the LA throughout the entire process.

Funding

This work was supported by Project No. LQ1605 from the National Program of Sustainability II and by Masaryk University specific research project MUNI/A/1270/2015 and by Masaryk University, Faculty of Medicine, Kamenice 5, 625 00 Brno, Czech Republic.

Conflict of interest: none declared.

References

1. Calkins H, Kuck KH, Cappato R, Brugada J, Camm AJ, Chen SA *et al*. 2012 HRS/EHRA/ECAS expert consensus statement on catheter and surgical ablation of atrial fibrillation: recommendations for patient selection, procedural techniques, patient management and follow-up, definitions, endpoints, and research trial design. *Europace* 2012;**14**:528–606.
2. Haïssaguerre M, Jaïs P, Shah DC, Takahashi A, Hocini M, Quiniou G *et al*. Spontaneous initiation of atrial fibrillation by ectopic beats originating in the pulmonary veins. *N Engl J Med* 1998;**339**:659–66.
3. Haïssaguerre M, Jaïs P, Shah DC, Gencel L, Pradeau V, Garrigues S *et al*. Right and left atrial radiofrequency catheter therapy of paroxysmal atrial fibrillation. *J Cardiovasc Electrophysiol* 1996;**7**:1132–44.
4. Nademanee K, McKenzie J, Kosar E, Schwab M, Sunsaneewitayakul B, Vasavakul T *et al*. A new approach for catheter ablation of atrial fibrillation: mapping of the electrophysiologic substrate. *J Am Coll Cardiol* 2004;**43**:2044–53.
5. Cappato R, Calkins H, Chen SA, Davies W, Iesaka Y, Kalman J *et al*. Prevalence and causes of fatal outcome in catheter ablation of atrial fibrillation. *J Am Coll Cardiol* 2009;**53**:1798–803.
6. Cappato R, Calkins H, Chen SA, Davies W, Iesaka Y, Kalman J *et al*. Updated worldwide survey on the methods, efficacy, and safety of catheter ablation for human atrial fibrillation. *Circ Arrhythm Electrophysiol* 2010;**3**:32–8.
7. Ghia KK, Chugh A, Good E, Pelosi F, Jongnarangsin K, Bogun F *et al*. A nationwide survey on the prevalence of atrioesophageal fistula after left atrial radiofrequency catheter ablation. *J Interv Card Electrophysiol* 2009;**24**:33–6.
8. Lemola K, Sneider M, Desjardins B, Case I, Han J, Good E *et al*. Computed tomographic analysis of the anatomy of the left atrium and the esophagus: implications for left atrial catheter ablation. *Circulation* 2004;**110**:3655–60.
9. Wang SL, Ooi CG, Siu CW, Yiu MW, Pang C, Lau CP *et al*. Endocardial visualization of esophageal-left atrial anatomic relationship by three-dimensional multidetector computed tomography "navigator imaging". *Pacing Clin Electrophysiol* 2006;**29**:502–8.
10. Starek Z, Lehar F, Jez J, Wolf J, Novák M. 3D X-ray imaging methods in support catheter ablations of cardiac arrhythmias. *Int J Cardiovasc Imaging* 2014;**30**:1207–23.
11. Malchano ZJ, Neuzil P, Cury RC, Holmvang G, Weichet J, Schmidt EJ *et al*. Integration of cardiac CT/MR imaging with three-dimensional electroanatomical mapping to guide catheter manipulation in the left atrium: implications for catheter ablation of atrial fibrillation. *J Cardiovasc Electrophysiol* 2006;**17**:1221–9.
12. Orlov MV, Hoffmeister P, Chaudhry GM, Almasry I, Gijsbers GH, Swack T *et al*. Three-dimensional rotational angiography of the left atrium and esophagus—a virtual computed tomography scan in the electrophysiology lab? *Heart Rhythm* 2007;**4**:37–43.
13. Lehar F, Starek Z, Jez J, Novak M, Wolf J, Stepanova R *et al*. Comparison of clinical outcomes and safety of catheter ablation for atrial fibrillation supported by data from CT scan or three-dimensional rotational angiogram of left atrium and pulmonary veins. *Biomed Pap Med Fac Univ Palacky Olomouc Czech Repub* 2015;**159**:622–8.
14. Nölker G, Gutleben KJ, Asbach S, Vogt J, Heintze J, Brachmann J *et al*. Intracardiac echocardiography for registration of rotational angiography-based left atrial reconstructions: a novel approach integrating two intraprocedural three-dimensional imaging techniques in atrial fibrillation ablation. *Europace* 2011;**13**:492–8.
15. De Buck S, Alzand BS, Wielandts JY, Garweg C, Phlips T, Ector J *et al*. Cardiac three-dimensional rotational angiography can be performed with low radiation dose while preserving image quality. *Europace* 2013;**15**:1718–24.
16. Starek Z, Lehar F, Jez J, Zbankova A, Kulik T, Wolf J *et al*. Long-term mobility of the esophagus in patients undergoing catheter ablation of atrial fibrillation: data from computer tomography and 3D rotational angiography of the left atrium. *J Interv Card Electrophysiol* 2016 Mar 12. [Epub ahead of print].
17. Nölker G, Gutleben KJ, Marschang H, Ritscher G, Asbach S, Marrouche N *et al*. Three-dimensional left atrial and esophagus reconstruction using cardiac C-arm computed tomography with image integration into fluoroscopic views for ablation of atrial fibrillation: accuracy of a novel modality in comparison with multislice computed tomography. *Heart Rhythm* 2008;**5**:1651–7.
18. Good E, Oral H, Lemola K, Han J, Tamirisa K, Igic P *et al*. Movement of the esophagus during left atrial catheter ablation for atrial fibrillation. *J Am Coll Cardiol* 2005;**46**:2107–10.
19. Li JH, Haim M, Movassaghi B, Mendel JB, Chaudhry GM, Haffajee CI *et al*. Segmentation and registration of three-dimensional rotational angiogram on live fluoroscopy to guide atrial fibrillation ablation: a new online imaging tool. *Heart Rhythm* 2009;**6**:231–7.
20. Thiagalingam A, Manzke R, D'Avila A, Ho I, Locke AH, Ruskin JN *et al*. Intraprocedural volume imaging of the left atrium and pulmonary veins with rotational X-ray angiography: implications for catheter ablation of atrial fibrillation. *J Cardiovasc Electrophysiol* 2008;**19**:293–300.
21. Sherzer AI, Feigenblum DY, Kulkarni S, Pina JW, Casey JL, Salka KA *et al*. Continuous nonfluoroscopic localization of the esophagus during radiofrequency catheter ablation of atrial fibrillation. *J Cardiovasc Electrophysiol* 2007;**18**:157–60.
22. Daoud EG, Hummel JD, Houmsse M, Hart DT, Weiss R, Liu Z *et al*. Comparison of computed tomography imaging with intraprocedural contrast esophagram: implications for catheter ablation of atrial fibrillation. *Heart Rhythm* 2008;**5**:975–80.
23. Starek Z, Lehar F, Jez J, Zbankova A, Kulik T, Wolf J *et al*. Periprocedural 3D imaging of the left atrium and oesophagus: comparison of different protocols of 3D rotational angiography of the left atrium and oesophagus in group of 547 consecutive patients undergoing catheter ablation of the complex atrial arrhythmias. *Int J Cardiovasc Imaging* 2016 Apr 26. [Epub ahead of print].
24. Cury RC, Abbara S, Schmidt S, Malchano ZJ, Neuzil P, Weichet J *et al*. Relationship of the esophagus and aorta to the left atrium and pulmonary veins: implications for catheter ablation of atrial fibrillation. *Heart Rhythm* 2005;**2**:1317–23.
25. Summerton SL. Radiographic evaluation of esophageal function. *Gastrointest Endosc Clin N Am* 2005;**15**:231–42.

5 SOUHRN

V práci byly zkoumány různé aspekty použití 3D RTG zobrazovacích metod v podpoře katétrových ablací srdečních arytmií pomocí. K vizualizaci srdečních oddílů jsme používali multidetektorové angio CT srdce a 3D rotační angiografii srdce.

V několika článcích jsme hodnotili detailní anatomii levé síně a přiléhajících struktur, zejména jícnu. Z CT dat jsme statisticky vyhodnotili detailní vztah mezi jícnem a zadní stěnou levé síně, která je důležitá z hlediska rizika poškození jícnu při ablaci v levé síni. Z 3DRA dat jsme na velkém počtu pacientů ověřili nejčastější polohu jícnu ve vztahu k zadní stěně levé síně.

Zabývali jsme se též významem 3D rotační angiografie srdce v podoře katétrových ablací arytmií. Vzhledem k nejasnostem okolo optimálního akvizičního protokolu jsme na velkém souboru pacientů ověřili optimální protokol s maximální spolehlivostí a optimálním zobrazení levé síně a efekt jeho použití při katétrové ablaci fibrilace síní. V několika publikacích jsme srovnali 3D modely levé síně vytvořené pomocí 3DRA levé síně a CT srdce. Výsledné modely levé síně ani efektivita jejich použití při katétrové ablaci se signifikantně nelišily. Dle našich výsledků klinický výstup a bezpečnost katétrové ablace fibrilace síní s podporou 3D modelů z CT a z 3DRA dat byly srovnatelné.

Vzhledem k velmi přesnému a relativně jednoduchému zobrazení polohy jícnu jsme se zabývali možnostmi ochrany jícnu pomocí jeho vizualizace 3D RTG zobrazovacími metodami. Prokázali jsme, že preprocedurální zobrazení polohy jícnu vůči levé síni pomocí CT srdce v horizontu dnů a týdnů před ablačním výkonem je nepoužitelné ke spolehlivému zobrazení polohy jícnu při výkonu. Dlouhodobá mobilita jícnu je natolik vysoká, že nelze statisticky signifikantně předpovědět aktuální polohu jícnu při výkonu. Naše další práce, studující krátkodobou mobilitu jícnu během několikahodinové ablace v levé síni nezjistila statisticky významný rozdíl mezi polohou jícnu na počátku výkonu, během výkonu a na jeho konci. Zobrazení jícnu na počátku ablace nám umožnuje spolehlivě lokalizovat tuto strukturu během celého výkonu. Zároveň jsme prokázali, že fúze 3D modelu levé síně vytvořeného pomocí 3DRA s live fluoroskopií je velmi stabilní a dlouhodobě přesná. I po několikahodinovém výkonu zůstává model ve správné poloze s rozdílem jen několik milimetrů.

Vzhledem k velmi dobrým zkušenostem s 3DRA levé síně jsme v několika publikacích ověřili použití této metody k vytvoření 3D modelů srdečních komor použitých k podpoře katétrové ablace komorových arytmií. Prokázali jsme, že 3DRA levé i pravé komory je metoda bezpečná, proveditelná a plně použitelná při katétrové ablaci komorových arytmií. 3D modely pravé i levé komory vytvořené pomocí 3DRA srdce jsou srovnatelné s modely z CT dat

Vzhledem k nezanedbatelným rizikům plynoucím z použití RTG záření při tvorbě výše zmiňovaných modelů jsme se zaměřili i na srovnání dávek RTG záření pro jednotlivé metody a protokoly. Ukázalo se, že při 3D zobrazení levé síně byla dávka při použití starších modelů CT přístrojů několikanásobně vyšší než u 3DRA srdce. S nástupem nových generací CT přístrojů se tento rozdíl zmenšuje nicméně rizika zůstávají. Proto jsme dle našich zkušeností vytvořili nový akviziční protokol pro angio CT levé síně umožňující signifikantně snížit dávku RTG záření u pacientů podstupující toto vyšetření při zachování kvality umožňující efektivní použití těchto modelů při katétrové ablaci fibrilace síní.

6 ZÁVĚR

3D RTG zobrazovací metody srdce zaznamenaly v posledních desetiletích významný rozvoj a významnou měrou se podílely na zvýšení účinnosti a bezpečnosti katétrových ablací arytmií. Vzhledem k naprosto převažující ablaci fibrilace síní je nejčastěji zobrazovanou strukturou levá síň. Angio CT srdce nám umožnilo jedinečný pohled na komplexnost a variabilitu anatomické stavby srdce a okolních struktur, a to zejména levé síně a jícnu. 3DRA levé síně a jícnu nám umožnila jednoduché a bezpečné periprocedurální zobrazení těchto struktur v rámci podpory katétrových ablací fibrilace síní. Při ablacích komorových arytmií 3D CT modely srdečních komor přinášejí informace nejen o anatomii těchto dutin, ale i funkční data zobrazující fibrózu a jizvení komorového myokardu. CT srdce s pozdní perfúzí a analýzou ztenčení stěny levé komory či kombinace CT srdce a dalších zobrazovacích metod se blíží funkčním datům z magnetické rezonance srdce. 3DRA je s limitovaným profitem použitelná i v podpoře katétrových ablací komorových arytmií. Dobře zobrazuje anatomii těchto dutin, nicméně funkční data popisující kvalitu komorového myokardu tato modalita nepopisuje. Do budoucna se dá předpokládat další rozvoj těchto metod, a to zejména v segmentu CT srdce, kde nástup nové generace spektrálních CT umožní další zvýšení kvality zobrazení, přesnější zobrazení patologických změn myokardu a v neposlední řadě i snížení dávky RTG záření, kterému je vystaven pacient.